DISTILLATION OF A BINARY MIXTURE IN THE CENTRIFUGAL MOLECULAR STILL

by

Adnan Mohammed Ahmad Murad
B.Sc. (Wales)

Thesis submitted to the C.N.A.A.
in partial fulfilment of the requirements
for the
Degree of PHILOSOPHIAE DOCTOR

The collaborating establishment was

Dow Corning Ltd.

Department of Chemical Engineering
The Polytechnic of Wales

JUNE 1982

To my Wife, Afrah

CERTIFICATE OF RESEARCH

This is to certify that, except where specific reference is made, the work described in this thesis is the result of the investigation by the candidate.

.....
Candidate

.....
Director of Studies

Dated: June 1982

DECLARATION

This is to certify that neither this thesis nor any part of it has been presented or is being concurrently submitted in candidature for any other degrees.

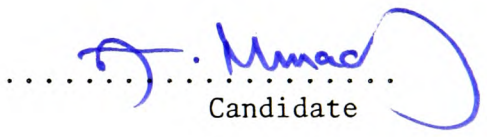

.....
Candidate

Dated: June 1982

ACKNOWLEDGEMENTS

I wish to express my gratitude to my Director of Studies, Dr.G.J.Rees, for his guidance, encouragement, and valuable supervision throughout the investigation.

I am particularly indebted to Dr.D.B.Scully for his assistance, advice, and stimulating comments at the various stages of the investigation. Sincere appreciation is also extended to Dr.G.Roberts of the Science Department for designing the electronic switch.

My thanks are due to those members of the Technical Staff of this Department who assisted in the modification and maintenance of the experimental apparatus.

Appreciation is also tendered to Dow Corning Ltd. for supplying some of the test materials which were used in this study.

Sincere thanks are especially extended to my Parents, for without their sacrifice, patience, and financial support this work could not have been accomplished.

Finally, I would like to thank Mrs.E.Phillips for undertaking the difficult task of typing the thesis.

DISTILLATION OF A BINARY MIXTURE IN THE CENTRIFUGAL MOLECULAR STILL

Adnan M.A. Murad

ABSTRACT

This thesis describes an investigation of the transport phenomena of a binary mixture over a rotating disk and under conditions of molecular distillation. These phenomena were studied using a modified version of the commercially designed centrifugal molecular still, CMS-5.

A mathematical model was developed which relates the equations of maximum evaporation rate, heat and mass transfer of the transport behaviour of fluid on a rotating disk to such parameters as mass flow rate, composition, film thickness, mean velocity, Reynolds number, surface temperature, and relative volatility.

Numerical techniques have been used in solving the model, and from the computed and the experimentally measured values, it was possible to evaluate the performance of the still in terms of the theoretical molecular plate.

The mathematical model is also capable of predicting the mean distillation rate and composition of distillate. Reasonable agreement was obtained between the measured and calculated values.

In order to solve the mathematical model, it was also necessary to evaluate experimentally some physical property data of the binary mixture.

Mean rates of distillation and compositions of distillate of the binary mixture (di-2-ethylhexyl phthalate - di-2-ethylhexyl sebacate) were measured for a set of feed compositions over a range of temperatures and feed rates. The overall performance of the centrifugal still and the binary mixture were evaluated.

CONTENTS

CHAPTER I

INTRODUCTION

The ever increasing demand for highly pure compounds such as vitamins, anhydrous enzymes, and diffusion oils requires more than often the process of molecular distillation, which is the only method for the separation of heat-sensitive, high molecular weight and low volatility materials by distillation.

In this process the material is heated in an environment of high vacuum such that the distance travelled by the evaporating molecules before being condensed is comparable to the mean free path of the vapour molecules in the residual gas. The use of high vacuum thus provides the escaping molecules with an unobstructed path of travel between the evaporating and condensing surfaces, and consequently the vanishing of the dynamic equilibrium between the liquid and the vapour phases; i.e. there is no boiling phenomenon and distillation proceeds at any temperature as long as there is a temperature difference between the evaporating and condensing surfaces.

Operating at such reduced pressure and without the state of equilibrium limits the applicability of the vast documentation related to conventional distillation. However, at the turn of the century theories were put forward where the interfacial resistance and maximum evaporation rate became the controlling factors during the process of molecular distillation.

The maximum evaporation rate theory offers molecular distillation a unique advantage over the conventional equilibrium distillation, where materials having similar vapour pressures can be separated providing that their molecular weights are different. Unfortunately, in practice this advantage has not been realised. Factors like the geometry of the system, collisions between molecules, orientation of molecules, surface depletion, torpidity effect, and many others were thought to be the contributors to this deficiency.

Since these factors are not inter-related, the low efficiency of only one affects very extensively the performance of the distillation process, if not the whole chemical plant. Subsequently, a race was under way among chemists, designers, and chemical engineers to overcome some of the factors involved and to offer the most efficient equipment in terms of performance, cost, and versatility. One of the most successful equipment was the centrifugal molecular still and, despite its high cost, its excellent separating power made it the outstanding molecular distillation equipment for decades, and up to the present day.

In essence, this still consists of a heated rotating disk which distributes the fluid in the form of a thin film across its surface utilizing the centrifugal force, and a nearby cooler surface for collecting the vapourized molecules. The entire system is enclosed in a highly evacuated container.

In recent years, a significant increase in commercial applications has been noted. However, only limited studies relating to

the basic principles of distillation under high vacuum conditions have been carried out; also it seems that the basic knowledge of the fundamental mechanisms of heat, mass, and momentum transfer underlying the phenomena has not been used in describing this process. In addition, despite the number of theoretical and experimental research papers published over the years, little effort has been directed to date towards evaluating quantitatively the distillation rate and relative volatility under conditions of high vacuum, molecular distillation in the centrifugal molecular still.

Due to the fact that the present chemical, petrochemical, and food industries involve more high molecular weights and thermally-sensitive materials, and despite the relatively high capital cost of the centrifugal molecular still which may now be justified if high value and thermally-sensitive products are recovered, it is felt that a renewed appoach along experimental and theoretical lines would be of significant importance in aiding the understanding of the molecular distillation process. Therefore, in view of continued interest in this field, the aims of this investigation were :

(1) To develop a qualitative and quantitative understanding of mass and heat transfer mechanisms in the centrifugal molecular still.

(2) To develop a mathematical model in which the equations of heat and mass transfer of the transport behaviour of fluid on a rotating disk are related to such parameters as mass flow rate, composition, film thickness, mean velocity, Reynolds number, surface temperature, and relative volatility; thus providing a basis of interpreting and correlating the experimental results.

(3) To ascertain the effect of each of the parameters listed below on the operating characteristics of the still :

(a) Temperature of distilland

(b) Temperature of feed

(c) Temperature of condensing surface

(d) Rate of feed to rotor

(e) Composition of feed

(4) To identify the true temperature of distillation.

(5) To study theoretically and experimentally the separation efficiency of the still.

CHAPTER II

LITERATURE SURVEY

2.1 THE CONCEPT OF MOLECULAR DISTILLATION

Hickman [46] states that: "The process of free transfer under high vacuum from evaporator to condenser is known as unobstructed-path distillation; when the distance of transfer is comparable with the mean free path [59] of the vapour molecules in the residual gas, it is known as molecular distillation".

In other words, molecular distillation means the transfer of vapour from the warmer surface of a liquid to the cooler surface of a nearby condenser, the space between the two being evacuated sufficiently to prevent any obstruction of the vapour and, consequently, there is no dynamic equilibrium between phases.

Carman [22] has discussed the relationship between molecular distillation and other methods of distillation. He points out that the formation and transfer of vapour is achieved by three different mechanisms :

(1) Distillation by boiling - where bubbles of vapour are produced throughout the liquid at the rate necessary to consume the heat supplied. The rate of distillation is controlled by the rate of heat transfer, and the latter is usually set by the requirements that the liquid should boil quietly and without super-heating. The condenser must usually be well separated from the boiling liquid to avoid splashing.

(2) Normal evaporative distillation - in which the rate of evaporation is controlled by the rate of mass transfer between evaporating and condensing surfaces, not by the rate of heat transfer. If the rate of heat transfer is increased, the liquid rises in temperature until the increase in saturation vapour pressure of the liquid produces a corresponding increase in rate of mass transfer.

(3) Molecular evaporative distillation - shortly, molecular distillation, which can be looked at as a form of evaporative distillation in which the rate is governed solely by the absolute rate of molecular escape from the liquid surface; that is, there is essentially no return of molecules from the vapour to the liquid, and the temperature and corresponding escaping rate attained by the liquid are determined by the heat input, and are unaffected by the vapour space conditions, except that the pressure must be very low.

Since the boiling point of a substance is defined as the temperature at which the pressure of the vapour overcomes that of the surrounding gas, and since in the molecular still, theoretically, there is no surrounding gas and hence no boiling point, distillation occurs at almost any temperature as long as there is a difference in temperature between the evaporating and condensing surfaces.

2.2 MEAN FREE PATH

Free path is a term given to the distance traversed by a molecule of a gas between two successive collisions with neighbouring

molecules. The average distance traversed by all molecules between collisions is called the "mean free path".

This distance, which is of fundamental importance in molecular distillation, can be computed for a gas or a mixture of gases on the basis of kinetic theory.

Clausius [24] evaluated the mean free path of a molecule by assuming all molecules to be stationary, with the exception of one, and arrived at the following formula :

$$\lambda = \frac{1}{\pi N \sigma^2} \qquad \ldots 2.1$$

where

λ = mean free path (cm) ;

N = number of molecules in 1 cm^3 ;

σ = diameter of the molecule (cm).

In the case where not one molecule only is in motion while all the others are at rest - but where all molecules move with equal velocity - the mean free path becomes :

$$\lambda = \frac{1}{\frac{4}{3} \pi N \sigma^2} \qquad \ldots 2.2$$

Maxwell [75], by introducing the real law of distribution where he takes into account the relationship between relative velocities and actual velocities when a number of molecules all in motion are present, deduced the following expression for the

mean free path :

$$\lambda = \frac{1}{\sqrt{2}\ \pi\ N\ \sigma^2} \qquad \ldots 2.3$$

By taking the average over the time, instead of in space, Tait [12] found, instead of the numerical factor $\sqrt{2}$, the factor 1.477 and the formula becomes :

$$\lambda = \frac{1}{1.477\ \pi\ N\ \sigma^2} \qquad \ldots 2.4$$

If it is assumed that the perfect gas laws apply then, for example, Maxwell's equation may be otherwise expressed [17] :

$$\lambda = \frac{2.331 \times 10^{-20}\ T}{P\ \sigma^2} \qquad \ldots 2.5$$

where

T = absolute temperature (^{o}K) ;

P = pressure (mm Hg).

It is evident from the above equation that molecules at atmospheric pressure travel very small distances between successive collisions, but these distances will increase considerably at low pressure.

The above-mentioned expressions for the evaluation of the mean free path apply only to one molecular species of the gas. However, in molecular distillation, there is always present a mixture of gases comprised of the distilling molecules and the

residual air molecules. Normally, the materials which require the conditions of molecular distillation are of high molecular weight, and therefore the molecules of the vapour are much heavier than those of residual air molecules. The probability that the large vapour molecules collide with the relatively small molecules of the residual air moving about at random is much higher than that of the collisions of the latter with one another. The corrected mean free path for large molecules of diameter σ_2 traversing randomly distributed air molecules, is given by Loeb [69] as :

$$\lambda = \frac{1}{\sqrt{2}\ \pi\ N_2\ \sigma_2^2 + \pi\ N_1 \sigma_1^2 \sqrt{\overline{C}_1^2 + \overline{C}_2^2} \Big/ \overline{C}_2} \qquad \ldots 2.6$$

where

N_1 = number of air molecules ;

N_2 = number of vapour molecules ;

$\overline{C}_1$ = R.M.S. velocity of air molecules ;

$\overline{C}_2$ = R.M.S. velocity of vapour molecules ;

σ_1 = diameter of air molecule ;

σ_2 = diameter of vapour molecule.

Loeb's relationship can be arranged into a more convenient form based on the kinetic theory :

$$\lambda = \frac{1}{\pi \left(\frac{\sigma_1 + \sigma_2}{2} \right)^2 N \left(1 + \frac{M_1\ T_2}{M_2\ T_1} \right)^{1/2}} \qquad \ldots 2.7$$

where

M_1 = molecular weight of air ;

M_2 = molecular weight of vapour ;

T_1 = kinetic temperature associated with air ;

T_2 = kinetic temperature associated with vapour ;

N = number of molecules in 1 cm^3.

In our consideration of the mean free path, it is not the question to determine exactly its numerical value, but merely to obtain an approximate notion of its magnitude, and hence the exact knowledge of where the discrepancies lie in the above-mentioned theories is not necessary. Furthermore, Hickman [46] showed that distillation is less hindered by residual air molecules than is predicted by theory. He states: "The residual molecules are not an independent maze through which the vapour must wander, but a movable barrier readily disturbed by distillation".

Jacobs et al. [58] conducted experiments on the trajectories of vapour molecules and measured the undeflected paths of oil molecules and, surprisingly, found that these paths are considerably greater than the mean free path calculated by the theory. Table 2.1 shows Jacobs' results.

Jacobs' findings are of particular interest to the designer of the molecular still, because they release him from the restriction of making the length of the gap between the evaporating and condensing surfaces of the same order of magnitude as that of the mean free path.

Table 2.1 : Comparison of free paths and undeflected paths for high boiling organic esters.

Ester	Undeflected Path (cm)	Free Path (cm)	Ratio
Di-n-amyl phthalate	5.60	0.601	9.3
Di-n-amyl sebacate	4.41	0.474	9.3
Di-2-ethylhexyl phthalate	3.97	0.482	8.2

2.3 RATE OF DISTILLATION

Hertz [42], from the theoretical analysis of his experiments, arrives at the following fundamental conclusions : There exists for every substance a maximum rate of evaporation, which depends only on the temperature of the surface and on the specific properties of the substance. The maximum rate of evaporation of a substance can never be larger than the number of vapour molecules that strike the surface of the condenser under equilibrium conditions.

Consequently, the upper limit of the maximum rate of evaporation is given by a relationship developed by Meyer [76]. This relationship gives the number of molecules of a gas at rest as a whole, that strike unit area per unit time :

$$i = \frac{1}{4} \nu n_s \quad [\text{molecules cm}^{-2} \text{ sec}^{-1}] \qquad \ldots 2.8$$

where

ν = mean gas kinetic velocity [cm sec^{-1}] ;

n_s = equilibrium concentration of the vapour [molecules cm^{-3}].

The mass rate of vaporization, w, is obtained by substitution of ν and n_s [31] :

$$w = P_{\mu b} \left(\frac{M}{2 \pi R T} \right)^{1/2} \qquad \ldots 2.9$$

$$= 5.833 \times 10^{-2} \times P_{mm} \left(\frac{M}{T} \right)^{1/2} \quad (gm\ cm^{-2}\ sec^{-1}) \qquad \ldots 2.10$$

where

$P_{\mu b}$ = gas pressure (millibar) ;

P_{mm} = gas pressure (torr) ;

M = molecular weight ;

T = absolute temperature (^oK) ;

R = gas constant = 8.3143 (J $mole^{-1}\ {}^oK^{-1}$).

Accordingly, knowing the vapour pressure, the theoretical rate is deduced at once from equation (2.10).

Experimentally, Hertz obtained roughly 10 percent of the maximum rate according to equation (2.10), and that was mainly due to lack of accuracy when measuring surface temperature.

Knudsen [65] carried out the first really unambiguous measurements on mercury. The rate of evaporation was found to be the maximum. However, this applied only to carefully purified

mercury; the rate of evaporation of impure mercury was slower by up to three orders of magnitude.

Langmuir [67] was the first to employ the above equation for the determination of vapour pressure of tungsten. Brönsted and Hevesy [11], in applying molecular distillation to separate partially the isotopes of mercury, found that the rate of molecular distillation of the components is inversely proportional to the square-root of the molecular weights of these components, as indicated by the equation. Washburn et al. [110] found that the equation held for solutions if no recondensation occurred on the evaporating surface. The actual rate of evaporation will be less than the theoretical, because of some reflection of molecules from the condensing surface. Langmuir [68] found that, under the worst conditions, reflection from the condenser will not be greater than 90 percent.

However, as any practical data can only approach the maximum value stated by the equation, some factor is normally obtained from the ratio of the practical to the theoretical rate, which is the degree of departure from this theoretical.

Knudsen's [65] theoretical work was specially significant because he introduced the concept of α, the coefficient of evaporation, defined as :

$$\alpha = \frac{\text{Actual rate of evaporation}}{\text{Theoretical maximum rate of vaporization}}$$

The coefficient of evaporation (later also denoted as condensation coefficient [99]) should not be confused with the accommodation coefficient [64] which was defined by Knudsen as a parameter characterizing the exchange of energy between gases and solid or liquid surfaces.

Burch and Van Dijck [15] postulated that if the residual gas pressure be made sufficiently low, that molecular distillation occurred, then further reduction of pressure would produce no change in distilling speed. Fawcett [34] verified this statement by experimentation with a falling film still. He found that variation of the gap between the evaporating and condensing surfaces over wide limits did not produce any very noticeable variation in still performance, provided the gap did not become much larger than the molecular mean free path. A rate of distillation of between 70 and 90 percent of the theoretical was realized, and the discrepancy is probably due to collisions of distillate molecules with each other or with residual air molecules.

Other workers [1, 3] have studied evaporation rates of many liquids and have concluded that water [2] and other polar liquids [3] have low coefficients; while symmetrical molecules [3, 4] evaporate at the maximum rate. Hickman [51], believing that previous workers' measurements had been made with ultra-simple apparatus - the means had perhaps been inadequate for the task - led him to the design of the falling-stream tensimeter, where he studied the evaporation coefficient of di-2-ethylhexyl phthalate

and di-2-ethylhexyl sebacate and concluded that the two liquids examined do evaporate with a coefficient of unity from clean, new surfaces, and that kind of assurance was much needed for his work.

Hickman's [48] studies of the surface structure of liquids under vacuum in the pot still led him to the discovery of a new phenomenon, called torpidity, which is the blocking of the evaporating surface by contaminants, and hence reducing the area of effective evaporation. This phenomenon was also investigated by Kajiura and Yoshikawa [109]. As the molecular weight and viscosity of the distilland is increased, replenishment of the desired component in the surface layer becomes a major concern. Hickman [46] has indicated that it is imperative to keep the layer of distilling liquid, or distilland, as thin as possible for this reason, and also to reduce the risk of thermal decomposition.

Thermal decomposition (Hazard) is also thought to be a contributory factor to the evaporation coefficient and has been studied by Embree [49].

The influence of the geometry of the evaporator on the extent of evaporation was also studied by Hickman and Trevoy [51] where they found that the number of molecules returning to the evaporator is much lower during evaporation from cylindrical or spherical surfaces than in the case where evaporation and condensation proceed between two flat plates.

There could be other factors which may or may not have a direct influence on the coefficient of evaporation; yet this coefficient is only a factor, though it may well be suited to the study and presentation of data referring to a single effect. It is little more than an uncertainty factor when it is used to represent the whole process of distillation.

2.4 MATHEMATICAL APPROACH TO THE THEORY OF EVAPORATION

Despite the number of experimental papers published over the first four decades of the century concerning the evaporation of liquids under vacuum, little agreement was found in relation to the values of the evaporation coefficient, even for the same materials and under similar conditions. A consequence has been a resort to mathematical theory.

Herzfeld [43], Polanyi and Wigner[90], and Newmann [78] solved the problem of how long it would take on the average until a molecule leaves its potential trough, where it is bound with an energy λ, the energy of evaporation,by a statistical approach. On this basis, they could derive equation (2.10) but had to make the additional assumption that all molecules on the surface have a binding energy, λ, and that all of them have an equal chance to evaporate.

Polanyi and Wigner [90] first gave a rough estimate of the evaporation possibility by assuming that the surface molecules

oscillate isotropically about their equilibrium positions, and that these oscillations are independent of the oscillations of neighbouring molecules. If the frequency of the harmonic oscillations is ν, the number of energy fluctuations per second $\geq \lambda$ in one direction of oscillation is $\nu \cdot e^{-\lambda/kT}$. If one assumes that any fluctuation $\geq \lambda$ leads to evaporation, then the evaporation probability of a molecule in the surface is :

$$f \approx \nu \cdot e^{-\lambda/kT} \qquad [sec^{-1}] \qquad ...2.11$$

The above relationship does not take into account the interaction between the molecules, and hence it leads to low probability values. Polanyi and Wigner calculated these interactions by using an array of oscillating points as a model and arrived at a final expression for the evaporation probability :

$$f \approx \frac{2\lambda}{kT} \cdot \nu \cdot e^{-\lambda/kT} \qquad ...2.12$$

An entirely different approach was followed by Herzfeld, Pelzer and Neumann in their attempt to calculate the evaporation probability. They based their method on the following consideration: The state of any molecule on the surface can be described by two distribution functions - the Maxwell energy distribution, and the distribution of their centres of gravity in space. If the molecule is situated at the periphery of the attraction sphere, no activation energy is required for its evaporation since it possesses already a potential energy equal to the heat of evaporation. The evaporation

probability of a surface molecule is consequently

$$f = A \int_0^{\infty} \rho(\vec{r}_o) \cdot f(w) \cdot dw \qquad \ldots 2.13$$

where

A = the surface area ;

$\rho(\vec{r}_o)$ = the mean density of the molecule ;

r_o = radius of the attraction sphere ;

$f(w)$ = Maxwell distribution of gas velocities perpendicular to the surface.

Upon integration, the above equation yields :

$$f = A \left(\frac{kT}{2\pi m} \right)^{1/2} \cdot \rho(\vec{r}_o) \qquad (sec^{-1}) \qquad \ldots 2.14$$

The mean density $\rho(\vec{r}_o)$ is determined by the distribution function to :

$$\rho(\vec{r}_o) = \frac{e^{-\lambda/kT}}{\int_0^{\tau} e^{-\varepsilon(\vec{r})/kT} \cdot d\tau} \qquad \ldots 2.15$$

with an integration over the whole attraction sphere τ, where $\varepsilon(\vec{r})$ is the potential energy which is the outcome of the deviation $\vec{r} = (r, y, z)$ from the equilibrium position. This fact characterizes the spacial distribution $\rho(x, y, z) = \rho(\vec{r})$.

The above integral represents the volume contribution of the partition function Q^k of the condensate. The complete partition function contains, in addition, the momentum contribution, which is :

$$h^{-3} \cdot \int\int\int_{-\infty}^{\infty} e^{-(P_x^2 + P_y^2 + P_z^2) / 2 m kT} \cdot d P_x \cdot d P_y \, d P_z$$

...2.16

$$= \left(\frac{2 \pi m kT}{h} \right)^{3/2} = Q^{\nu},$$

which is at the same time equal to the partition function Q^{ν} of the unit volume of the ideal gas. Hence, the evaporation probability can be written as :

$$f = A \left(\frac{kT}{2 \pi m} \right)^{1/2} \frac{Q^{\nu}}{Q^{k}} e^{-\lambda/kT} = A \cdot \frac{\nu}{4} n_s \quad (sec^{-1}) \quad ...2.17$$

This is actually the maximum rate of evaporation according to equation (2.10), because

$$\frac{Q^{\nu}}{Q^{k}} \cdot e^{-\lambda/kT} = n_s \quad ...2.18$$

is the statistical expression of the mass-action law.

Knack and Stranski [23] indicated that equations (2.13,2.17) reduce to Wigner and Polanyi equations for the special case of Einstein solid where :

$$\varepsilon(r) = 2 \pi^2 \nu^2 m r^2 \quad ...2.19$$

$$\rho(r_o) = \frac{e^{-\lambda/kT}}{\int_0^{r_o} e^{-\varepsilon(r)/kT} \cdot 4 \pi r^2 \cdot dr} \quad ...2.20$$

where r is now the radius and not the radius vector $\vec{r}$.

Penner [82 , 83 , 84 , 85] treatment of the evaporation theory is based on two different approaches :

(i) Evaporation rate based on classical reaction kinetics - where it was supposed that the rate of loss of molecules $- dn_{v/dt}$ from a given volume V is proportional to the number of molecules n_s exposed at the surface, i.e.

$$- \frac{dn_v}{dt} = j_e \; n_s \quad , \qquad \ldots(2.21)$$

where j_e is a rate constant for evaporation and according to the chemical reaction kinetics consideration

$$j_e = B \; \exp \left(- \Delta E_v / R \, T\right) \quad , \qquad \ldots(2.22)$$

where ΔE_v is the molar activation energy for evaporation and B is a frequency factor.

By relating the heat of evaporation ΔH_v to ΔE_v [36], the evaporation constant becomes :

$$j_e = e \; B \; \exp \left(- \Delta H_v / RT \right) \qquad \ldots(2.23)$$

Since the frequency factor represents some sort of an upper limit for the collision frequency, i.e.

$$B = \frac{\left(2 \; \Delta H_v / M\right)^{1/2}}{\nu_f^{1/2}} \qquad \ldots(2.24)$$

where M is the molecular weight and ν_f is the free volume per

molecule in the condensed state.

Introducing equations (2.23, 2.24) to equation (2.21), and rearranging, the evaporation rate is given by :

$$w = e\,\rho\left[(2\,\Delta H_v/M)^{1/2} \Big/ \nu_f^{1/3}\; n^{1/3}\right] \exp\left(-\Delta H_{v/RT}\right) \quad \ldots 2.25$$

where n is the number of molecules per unit volume and, according to Kincaid and Eyring [63],

$$\nu_f = \nu(1/U)^3\,(R\,T\,\gamma/M)^{3/2} \quad \ldots 2.26$$

where

ν = volume per molecule in the liquid state ;

U = sound velocity in the liquid ;

γ = ratio of specific heat at constant pressure to the specific heat at constant volume.

Penner found good agreement between the values calculated for CCl_4, $CHCl_3$, C_6H_6, etc., for which the free volume model is a satisfactory description of the liquid state and that of equation (2.10), but poor agreement for associated liquids such as water or alcohol.

(ii) Evaporation rate based on the theory of absolute reaction rate - where the evaporation constant j_e is given by [36]

$$j_e = K\left(\frac{kT}{h}\right)\frac{Q^*}{Q}\exp\left(-\Delta E_v/R\,T\right) \quad \ldots 2.27$$

where

K = transmission coefficient ;

k = Boltzmann's constant ;

h = Planck's constant ;

Q^* = partition function of the activated state ;

Q = complete partition function.

By substituting equation (2.27) into equation (2.21) and using suitable transformations, the evaporation rate, w, is then given by:

$$w = e\, K\, p\, (m/2\pi kT)^{1/2} \qquad ...2.28$$

where m is the mass per molecule. Penner concluded that results calculated from equation (2.28) with $e\,K = 1$, should be identical with results calculated from equation (2.10) with the evaporation coefficient = 1.

Penner realised that equation (2.28) should be modified further to take into account liquids with hindered rotation, as was emphasized by Kincaid and Eyring [63], and hence the rate equation becomes :

$$w = K\, \phi\, p\, (m/2\pi kT)^{1/2} \qquad ...2.29$$

where ϕ represents the free-angle ratio, i.e. the ratio of the rotational partition function in the liquid to the rotational partition function in the gas.

Kincaid and Eyring [63], Hirschfelder, Stevenson and Eyring [54] have developed an account of liquid structure in which the partition function for the translatory motions of the molecules is expressed in terms of a free volume which can be estimated from the velocity of sound in the liquid. From the estimated free volume and the observed vapour pressure, Kincaid and Eyring evaluate the 'free-angle ratio', i.e. the ratio of the partition function for rotation of the molecules in the liquid to that for the molecules in the vapour, on the assumption that the partition function of internal vibration of a molecule is unaltered by the transition from the liquid to the vapour phase.

There is a surprisingly close agreement between the values of evaporation coefficient and free-angle ratio for benzene, carbon tetrachloride, and liquids which are associated by hydrogen bonds. This agreement fails for chloroform which, in spite of its high dipole moment, does not form hydrogen bonds.

The theory of evaporation was also studied by Wyllie [114]. He used a model of the liquid surface consisting of a compact ordered layer with a mobile adsorbed layer of molecules above it. On the assumption that evaporating and condensing molecules pass through the adsorbed condition, it was shown that the evaporation coefficient is determined by rate of exchange between substrate and adsorbed layer, and adsorbed layer and vapour, respectively. In particular, a coefficient of evaporation near unity results if the rate of exchange between substrate and mobile layer is very

much greater than that between mobile layer and vapour. The above assumption did not give satisfactory explanation of the equality of the evaporation coefficient and free-angle ratio defined by Kincaid and Eyring [63] for alcohol molecules. With a stagnant liquid surface, Wyllie reported a value of the evaporation coefficient of glycerol equal to 0.05. Subsequently, Trevoy [108] studied evaporation of glycerol from a fast flowing jet and concluded that the evaporation coefficient was equal to unity. The low value of α found by Wyllie might then be attributed to a contamination of the surface. Greenberg [38], using renewable liquid film, found the value of α for glycerol approaches 0.88 as the feed rate increases. Another criticism of Wyllie's work has been raised by Burrows [18] : the geometry of the system was such that an important fraction of evaporating molecules might have been reflected back to the interface, thus lowering the evaporation coefficient to almost ten times its value.

Heideger and Boudart [41] describe a method that concerns the increase in the concentration of molecules when vaporization occurs in a vessel which is first evacuated and then isolated. The theory assumes implicitly that the vaporized molecules are instantaneously distributed throughout the space occupied to form an increasing but uniform concentration of molecules, which is maintained in completely random motion according to the kinetic theory. Burrows [20] extensively criticized the method of Heideger and Boudart, although they justified the correctness of their method since they found a value of 0.05 for the evaporation coefficient of glycerol which is similar to that of Wyliie's. Burrows states :

"The readings of pressure on which Heideger and Boudart rely bear no direct relationship to the kinetic equations which they use".

Burrows [17, 19] in his statistical treatment of the evaporation coefficient, supposes that molecules evaporate with a cosine distribution without re-evaporation from the condenser. The summary of the theory is as follows :

The probability that a molecule travels a distance r without collision is

$$e^{-\frac{r}{\lambda}},$$

where λ is the mean free path. $\frac{r}{\lambda}$ for a given set of conditions may be expressed as

$$\frac{d}{k \cdot \lambda_E}$$

where d is the length of the gap between evaporator and condenser; k is a suitable factor; and λ_E is the mean free path in equilibrium vapour. If $\frac{d}{k\,\lambda_E} = K$ then

$e^{-\frac{r}{\lambda}}$ becomes e^{-K}, when related to the average conditions in the gap. These conditions may happen in the following way :

(i) The fraction of molecules that reach the condenser without collision is e^{-K}

(ii) The fraction of molecules that collide is $(1 - e^{-K})$

(iii) The fraction of colliding molecules that reach the condenser is $(1 - e^{-K})\ e^{-K}$

(iv) The probability that a molecule reaches the condenser after multiple collisions is the value of a factor F which expresses the ratio of the condensing area to the total area. Therefore the fraction of such molecules which reaches the condenser is given by $F\ (1 - e^{-K})^2$

The evaporation coefficient, α , is equal to the number of molecules reaching the condenser to the number of evaporated molecules :

$$\alpha = F + (1 - F)\left(2\,e^{-K} - e^{-2K}\right) \qquad \ldots 2.30$$

Table 2.2 lists the evaporation coefficient for different values of K and F. These data are graphically presented in Figure 2.1.

Table 2.2 : The variation of evaporation coefficient for different values of K and F.

K	F = 0.5	F = 0.7	F = 0.8
0.25	0.98	0.99	0.99
0.50	0.92	0.95	0.97
1.00	0.80	0.88	0.92
2.00	0.63	0.77	0.85
4.00	0.52	0.71	0.81

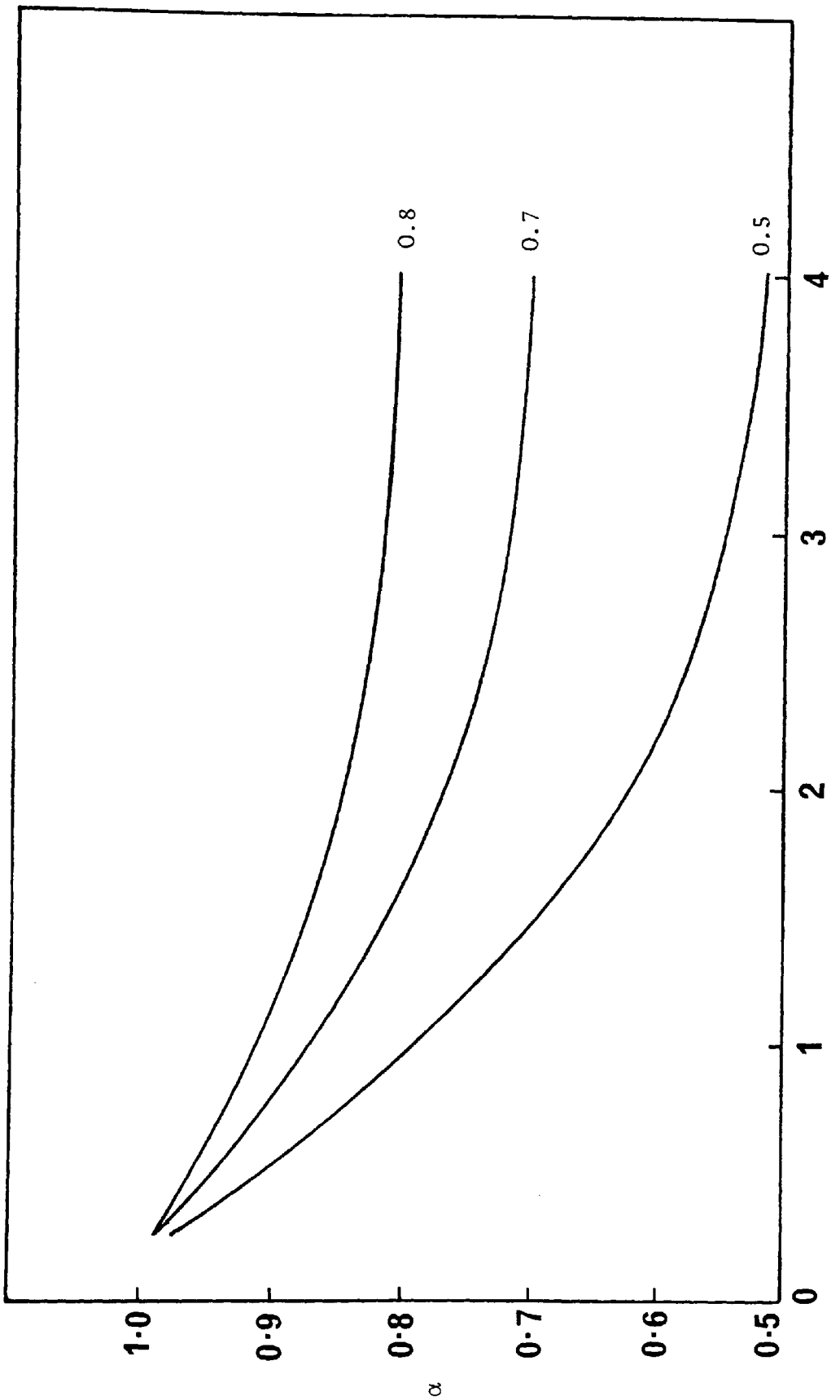

Figure 2.1 : Variation of evaporation coefficient, α, with K for different values of F.

Burrows found that if a value of 30 is chosen for K then the calculated evaporation coefficient fits the data of Hickman and Trevoy [51] reasonably well for both di-2-ethylhexyl phthalate and di-2-ethylhexyl sebacate.

Also of interest is the theoretical work of Toei [106] who treats the problem of mass transfer under vacuum by analyzing the Boltzmann equation with the two-sided Maxwellian velocity distribution function of molecules.

By assuming that the system is isothermal, the integral form of one-dimensional Boltzmann equation was used to obtain the following final equations :

$$P_e - P_c = \frac{2 - \alpha}{\alpha} \gamma + P_r \left(1 - e^{-\xi \gamma L}\right) \qquad \ldots 2.31$$

$$\xi = \frac{1}{2 P_t D} \left(\frac{2 kT}{\pi m}\right)^{1/2} \qquad \ldots 2.32$$

$$w = \left(\frac{m}{2 \pi kT}\right)^{1/2} \gamma \qquad \ldots 2.33$$

where

P_e = saturated vapour pressure at the evaporator ;

P_c = saturated vapour pressure at the condenser ;

P_r = residual air pressure ;

P_t = total pressure ;

α = evaporation coefficient ;

γ = integral constant ;

L = length of the gap ;

ξ = defined by equation (2.32) ;

D = diffusion coefficient ;

k = Boltzmann's constant ;

T = absolute temperature ;

m = mass of a molecule.

The evaporation rate can be calculated under various driving forces and partial pressure of the residual air by solving equation (2.31) for γ and substituting the value into equation (2.33).

A series-resistance model was also suggested by Toei. In this model, there are three resistances for the mass transfer : (a) the resistance of evaporation; (b) the resistance of diffusion between the evaporating and condensing surfaces; (c) the resistance of condensation.

Equation (2.10) is considered for the evaporation and condensation rates, and the usual diffusion equation is considered for the diffusion through the residual air, i.e.

$$w = \frac{M P_t D}{RTL} \ln \frac{P_{rc}}{P_{re}} \qquad \ldots 2.34$$

where

M = molecular weight ;

P_{rc} = pressure of the residual air at the condenser ;

P_{re} = pressure of the residual air at the evaporator.

Using equations (2.10,2.34), a similar equation to (2.31) was obtained.

The calculated evaporation rate according to Toei's equations seems to agree fairly well with that given by equation (2.10), but for a material with evaporation coefficient of unity. Unfortunately, the author gives no comments concerning polar liquids or non-ideal or orientated materials.

Table 2.3 lists values of evaporation coefficient for selected compounds, calculated according to some of the theories just mentioned, together with the reported experimental values.

It is clear that there is disagreement among workers concerning these values. However, it seems that although the mathematical theory could take into account factors like the geometry of the system, collisions between molecules and, even to some extent, the orientation of molecules. There are other factors yet to be physically understood before they could be encountered by the mathematical theory. Such factors are vapour phase interactions, steric and surface structure considerations, surface energy distribution, depletion and surface cooling, and may be others which might not have been explored yet.

Table 2.3 : Comparison between experimental and theoretical evaporation coefficients.

Liquid	Temp. (°C)	Evaporation coefficient			Ref.
		Free-angle ratio	Equation (2.12)	Experimental	
Benzene	6	>0.85	0.078	0.90	[4]
Carbon tetrachloride	0	1.0	0.79	1.0	[4]
Chloroform	2	0.54	0.086	0.16	[4]
Dibutyl phthalate	20	$\sim 7\times10^{-4}$	0.052	1.0	[9]
Diethyl adipate	0	0.05	0.54	0.177	[100]
Di-2-ethylhexyl phthalate	100	$\sim 6\times10^{-5}$	0.042	1.0	[51]
Di-2-ethylhexyl sebacate	136	$\sim 5\times10^{-7}$	0.040	1.0	[51]
Ethyl alcohol	0	0.018	0.2	0.024	[4,13]
Glycerol	19	0.046	0.06	0.05	[41,114]
Glycerol	18-70	0.046	0.06	1.0	[108]
Methyl alcohol	0	0.048	0.3	0.045	[4]
Water	20	0.04	0.033	0.042	[27]
Water	43	0.04	0.033	0.027	[27]
Water	7-50	0.04	0.033	0.35-1.0	[77]
Water	10-30	0.04	0.033	0.036-0.04	[1]

2.5 DISTILLATION OF A BINARY MIXTURE

To be of a practical value, molecular distillation should apply to mixtures as well as to the evaporation of pure substances. The following paragraphs will indicate the theoretical and experimental aspects achieved so far in this field.

2.5.1 Theoretical Considerations

Assuming the validity of Raoult's Law, the relative volatility in equilibrium distillation for an ideal binary mixture is given by :

$$\alpha_e = \frac{y\,(1-x)}{x\,(1-y)} = \frac{P_1}{P_2} \qquad \ldots 2.35$$

where

y = the concentration of the more volatile component in the vapour phase ;

x = the concentration of the more volatile component in the liquid phase ;

P_1 = vapour pressure of component 1 ;

P_2 = vapour pressure of component 2 .

For real mixtures,

$$\alpha_{er} = \frac{P_1}{P_2}\,\frac{\gamma_1}{\gamma_2} \qquad \ldots 2.36$$

where γ_1 and γ_2 are the activity coefficients of the components.

According to Sunier [103] and Washburn [110], the evaporation of components of a mixture under the conditions of molecular distillation should proceed according to the following expression :

$$\frac{w_1}{w_2} = \frac{P_1}{P_2}\sqrt{\frac{M_2}{M_1}} \qquad \ldots 2.37$$

This expression represents the ratio of the rate of distillation of one component to that of another component at constant temperature. This ratio is actually the relative volatility in molecular distillation under ideal conditions, i.e.

$$\alpha_m = \frac{P_1}{P_2}\sqrt{\frac{M_2}{M_1}} \qquad \ldots 2.38$$

α_m, also, can be easily derived from equations (2.10), and hence the relative volatility for real mixtures may be expressed as :

$$\alpha_{mr} = \frac{\gamma_1 P_1}{\gamma_2 P_2}\sqrt{\frac{M_2}{M_1}} \qquad \ldots 2.39$$

It can be seen that the relative volatility under molecular distillation differs by a factor of $\sqrt{\frac{M_2}{M_1}}$ from that under conventional equilibrium distillation, i.e.

$$\frac{\alpha_m}{\alpha_e} = \frac{\alpha_{mr}}{\alpha_{er}} = \sqrt{\frac{M_2}{M_1}} \qquad \ldots 2.40$$

This factor, theoretically, gives molecular distillation a unique property; that is, the ability to separate components of the same vapour pressure but different molecular weights.

Burrows [17] derives expressions for relative volatility as follows :

Let Q_1 be the initial weight of component 1 in the distilland; w_1 the weight evaporated in time t, and W_1 the weight left behind in the distilland after a time t.

Then,

$$w_1 = Q_1 - W_1 \qquad \ldots 2.41$$

The mole fraction of component 1 in the distilland is

$$\left(\frac{W_1}{M_1}\right) \Big/ \left(\frac{W_1}{M_1} + \frac{W_2}{M_2}\right)$$

Combining equation (2.10) with the above expression, the rate of distillation of component 1 becomes :

$$-\frac{dW_1}{dt} = 5.833 \times 10^{-2}\, \chi \left[\left(\frac{W_1}{M_1}\right) \Big/ \left(\frac{W_1}{M_1} + \frac{W_2}{M_2}\right) \right] P_1 \sqrt{\frac{M_1}{T}}\; A \quad \text{gm/sec.} \qquad \ldots 2.42$$

where A is the area of evaporation;

and, similarly, for the second component :

$$-\frac{dW_2}{dt} = 5.833 \times 10^{-2} \times \left[\left(\frac{W_2}{M_2}\right) \Big/ \left(\frac{W_2}{M_2} + \frac{W_1}{M_1}\right) \right] P_2 \sqrt{\frac{M_2}{T}}\; A \quad \text{gm/sec.} \qquad \ldots 2.43$$

Dividing equation (2.42) by equation (2.43), gives :

$$\frac{d W_1}{d W_2} = \frac{P_1}{P_2} \frac{W_1}{W_2} \sqrt{\frac{M_2}{M_1}} \qquad \ldots 2.44$$

Integrating between the limits Q and W for the two components, and assuming that the temperature is constant,

$$\log \frac{W_1}{Q_1} = \frac{P_1}{P_2} \sqrt{\frac{M_2}{M_1}} \log \frac{W_2}{Q_2} \qquad \ldots 2.45a$$

Another way of expressing equation (2.45a) is :

$$\frac{W_1}{Q_1} = \left(\frac{W_2}{Q_2} \right)^{\alpha_m} \qquad \ldots 2.45b$$

Assuming that all deviations from Raoult's Law are covered by an activity coefficient γ for each component, then equation (2.44) takes the form :

$$\frac{d W_1}{d W_2} = \frac{\gamma_1 P_1}{\gamma_2 P_2} \sqrt{\frac{M_2}{M_1}} \frac{W_1}{W_2} \qquad \ldots 2.46$$

In this instance, it is not justified to integrate the above equation, even though distillation occurs at constant temperature, unless the ratio $\frac{\gamma_1}{\gamma_2}$ is known to be constant over the range considered. Upon such circumstances, equation (2.46) becomes :

$$\frac{W_1}{Q_1} = \left(\frac{W_2}{Q_2} \right)^{\alpha_{mr}} \qquad \ldots 2.47$$

The real relative volatility α_{mr} can be determined with a knowledge of $\frac{W_1}{Q_1}$ and $\frac{W_2}{Q_2}$. The values of W and Q can be determined from the relationship between composition and refractive index.

Burrows also defines the separation efficiency factor f_s for binary mixtures to replace the evaporation coefficient where only one specie is involved,

$$f_s = \frac{\alpha_{mr}}{\alpha_m} = \frac{\gamma_1}{\gamma_2} \qquad \ldots 2.48$$

Also of equal importance is the application of the Rayleigh equation [94] to the process of molecular distillation. Although the equation has been developed for differential distillation, it can also be used for the process of continuous distillation for the film evaporator. Dieter [28] proved its validity at normal pressure and also at reduced pressure.

The integrated form of the equation is

$$\ln \frac{S}{S_o} = \int_{x_o}^{x} \frac{dx}{y - x} \qquad \ldots 2.49$$

where

S_o = initial number of moles of the distilland ;

S = final number of moles of the distilland ;

x_o = initial composition of the more volatile component ;

x = final composition of the more volatile component ;

y = composition of the more volatile component in vapour.

If the relative volatility may be assumed constant over the range considered, then :

$$y = \frac{\alpha \quad x}{1 + (\alpha - 1)\, x} \qquad \ldots 2.50$$

Substituting in equation (2.49), then the solution will be :

$$\ln \frac{S}{S_o} = \frac{1}{\alpha - 1} \ln \left[\frac{x(1 - x_o)}{x_o(1 - x)} \right] + \ln \frac{1 - x_o}{1 - x} \qquad \ldots 2.51$$

Upon re-arrangement, the above equation yields :

$$\alpha_w = 1 + \frac{\ln \dfrac{x(1 - x_o)}{x_o(1 - x)}}{\ln \dfrac{S}{S_o} \dfrac{(1 - x)}{(1 - x_o)}} \qquad \ldots 2.52$$

which is the actual controlling factor of separation of a binary mixture during its molecular distillation.

2.5.2 Experimental Considerations

It should be emphasized here that the factors which inhibit the rate of distillation from attaining its maximum possible value during evaporation of single-component liquids do apply equally well in the case of binary distillation of mixtures. At the same time, these factors could have different effects towards each component separately. Therefore the deviation from Raoult's Law

is not the only one which influences the separation efficiency factor.

During the process of evaporation, the mean free path decreases with rising temperature, so in binary distillation the more volatile component at the vapour phase will collide more frequently at higher than at lower temperatures, and its probability of returning to the evaporation surface increases. This will undoubtedly reduce the separation efficiency factor; but, at the same time, it could be deduced that distillation at low temperature will produce better separation, but lower rate. Also of interest is the rate of thermal decomposition which could have a different degree of effect in each component. Figure 2.2, which is extracted from Ishii's work [57] concerning the distillation of a model mixture, shows that the rate of thermal decomposition of di-2-ethylhexyl phthalate is equivalent to 3 ~ 4 of that of di-2-ethylhexyl sebacate at each optimum working temperature.

For those reasons, and may be others, the importance of the ratio $\sqrt{\frac{M_2}{M_1}}$ which gives molecular distillation its unique advantage over conventional equilibrium distillation, has not been realized in practice. The fact that Brönsted and Hevesey [11] successfully isolated the isotopes of mercury by molecular distillation attests to the validity of the ratio. Since the isotopes are assumed to have 'equal' vapour pressure, the separation achieved must have been due to difference in molecular weights.

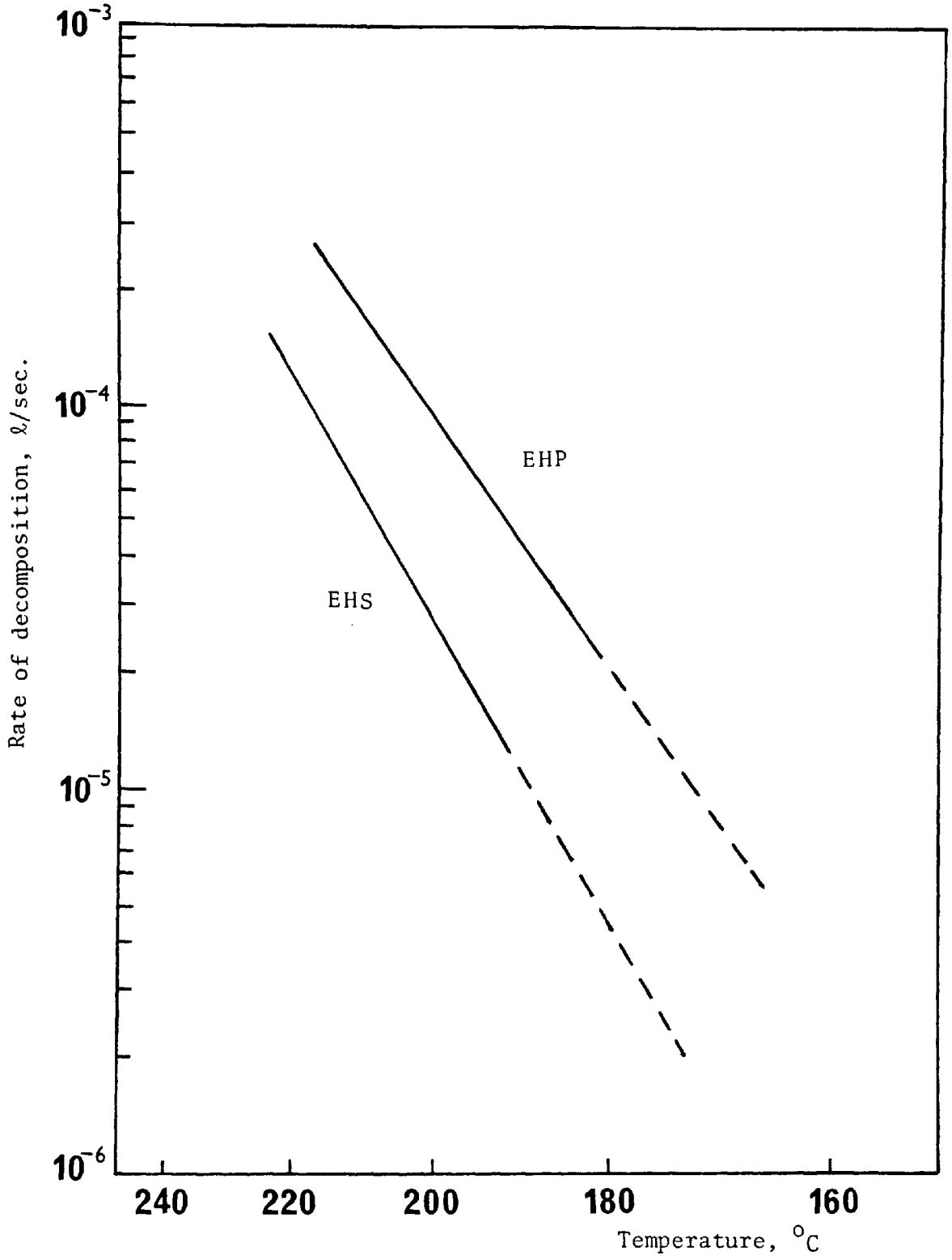

Figure 2.2 : Rate of thermal decomposition of di-2-ethylhexyl phthalate and di-2-ethylhexyl sebacate.

Perry and Fuguitt [88] studied the separation of the components of the system di-2-ethylhexyl phthalate - di-2-ethylhexyl sebacate (EHP-EHS) using an unstirred pot still, and found a value for the experimental relative volatility of 2.85 over a wide range of distillation rates (0.0001 to 0.0050) gm/sec/cm^2. The value of the relative volatility did not improve even at low temperature. Followed by Hickman and Trevoy [52] with a magnetically stirred pot still, excellent improvement on the value of relative volatility was obtained at low temperature.

The system EHP-EHS was also studied by Trevoy [107] in his attempts to compare the relative volatility under conventional and molecular distillation. According to his data (Figure 2.3), the values of the relative volatility in conventional and molecular distillation almost coincide at temperatures below 120^{o}C, while above 120^{o}C α_{er} is greater than α_{mr}, which is contrary to theory (since $(M_2/M_1)^{1/2} = 1.045$); i.e. better separation was achieved under equilibrium conditions, where the process is controlled by P_1/P_2 than for molecular distillation, which is governed by $\frac{P_1}{P_2}\sqrt{\frac{M_2}{M_1}}$. One would expect that α_{mr} should be greater than α_{er} at low temperatures, and that the two would tend to be equal at higher temperatures as, upon increase of temperature non-equilibrium evaporation should pass into an equilibrium process as a result of increased molecular collisions. Trevoy suggests that there are unknown factors in his experimental work which overshadowed the importance of the $\sqrt{\frac{M_2}{M_1}}$ ratio.

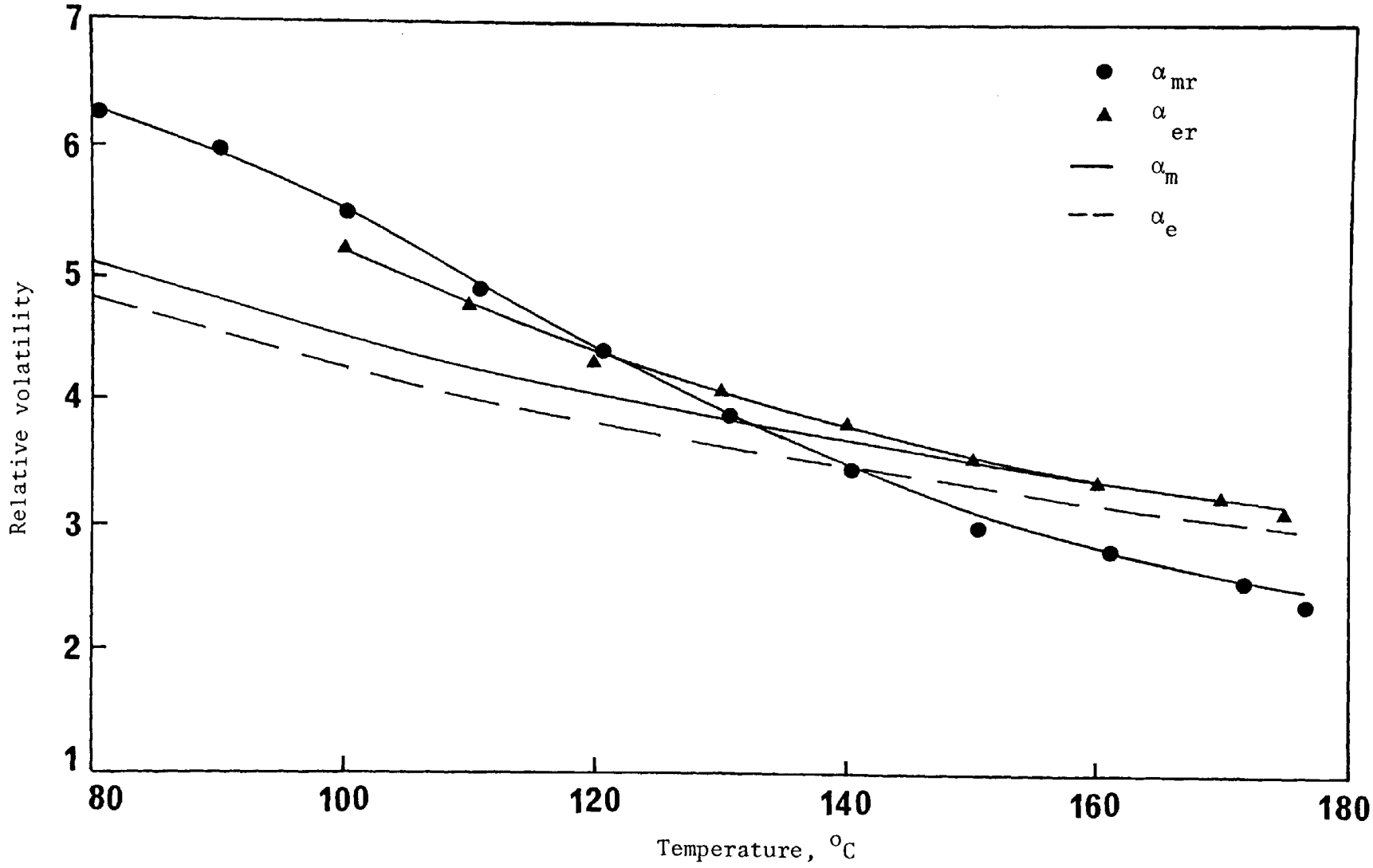

Figure 2.3 : Variation of relative volatility with temperature for the system di-2-ethylhexyl phthalate-di-2-ethylhexyl sebacate.

Burrows [17], using a circulating batch molecular still on the system EHP-EHS, found the values of the experimental relative volatility varied between 2.50 and 2.83 at 130°C; the theoretical relative volatility α_m at 130°C is 3.94.

Malyusov and Mala'feev [72] carried out similar experiments to that of Trevoy. Figure 2.4 shows their results. It is interesting to note that the ratio $\left(\frac{M_2}{M_1}\right)^{1/2}$ is greater than unity at low temperatures and tends to unity with increase of temperature. However, their data confirm the validity of the ratio $\sqrt{\frac{M_2}{M_1}}$ but only at low temperatures.

Kawala [61], using the tensimeter construction proposed by Hickman and Trevoy [51], conducted experiments concerning the relative volatility of the system dibutyl phthalate-dibutyl sebacate (DBP-DBS) and the system EHP-EHS. Figures 2.5 and 2.6 show his results. It was also confirmed that the relative volatility α_{mr} of both systems is virtually independent of the composition of the mixture.

One important factor which contributes to the deficiency of the separation during molecular distillation of mixtures should not be overlooked, and can be explained as follows: Since molecular distillation is a surface phenomenon, as soon as it commences, the more volatile component will evaporate at a relatively greater rate than the less volatile component, leaving the surface of the liquid richer with the less volatile component, and unless this richness is decreased by the diffusion of the

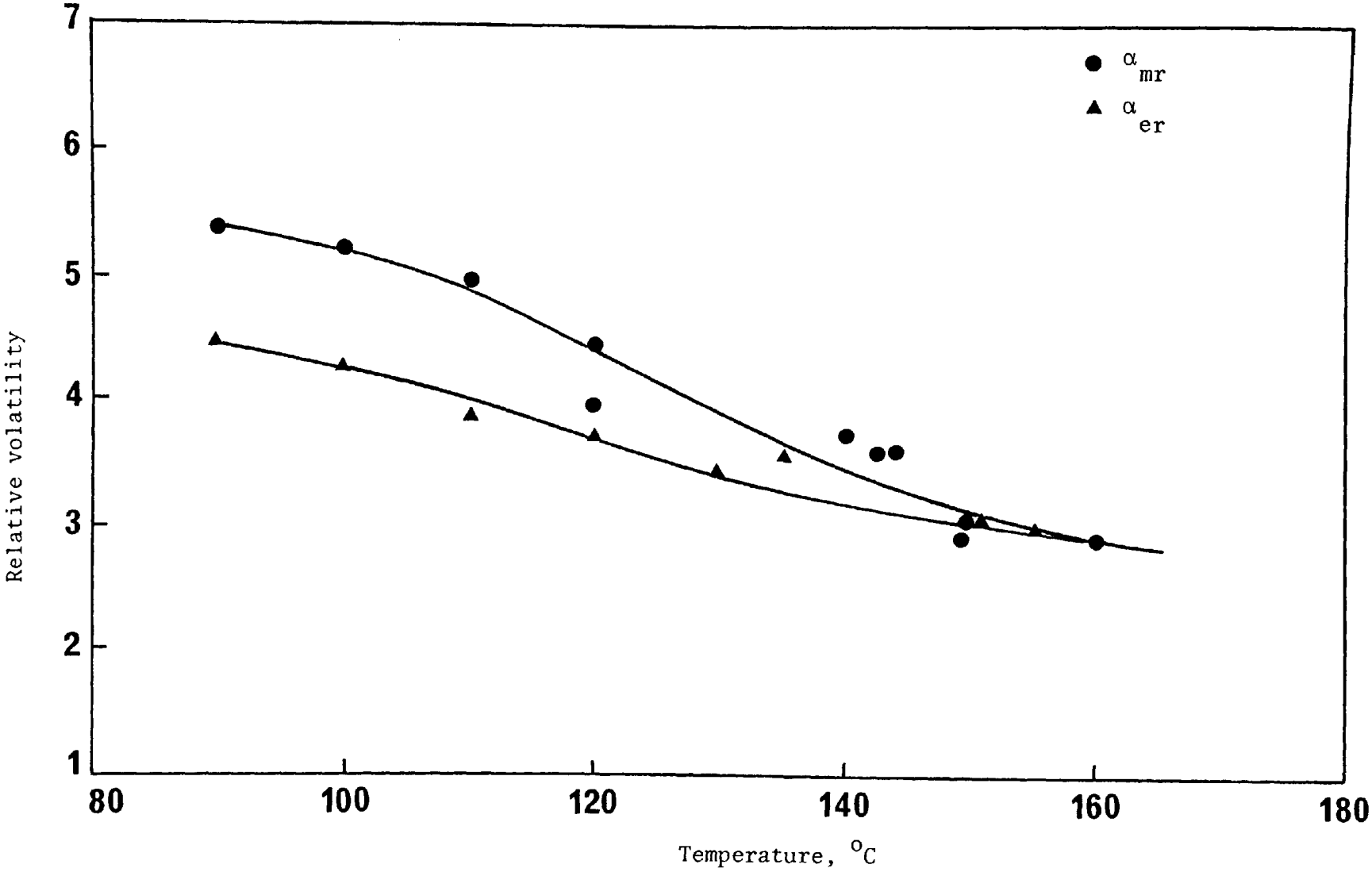

Figure 2.4 : Variation of relative volatility with temperature for the system di-2-ethylhexyl phthalate-di-2-ethylhexyl sebacate.

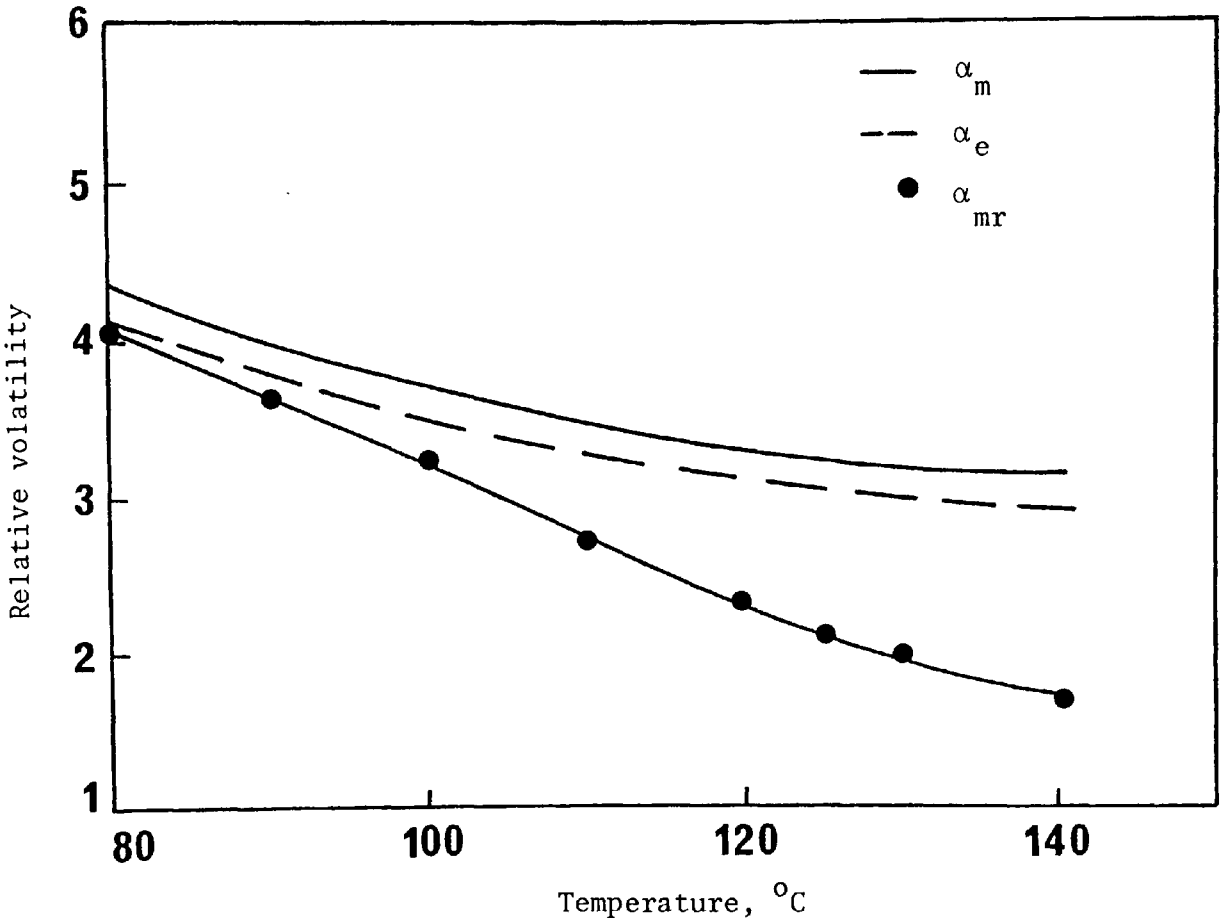

Figure 2.5 : Variation of relative volatility with temperature for the system dibutyl phthalate-dibutyl sebacate.

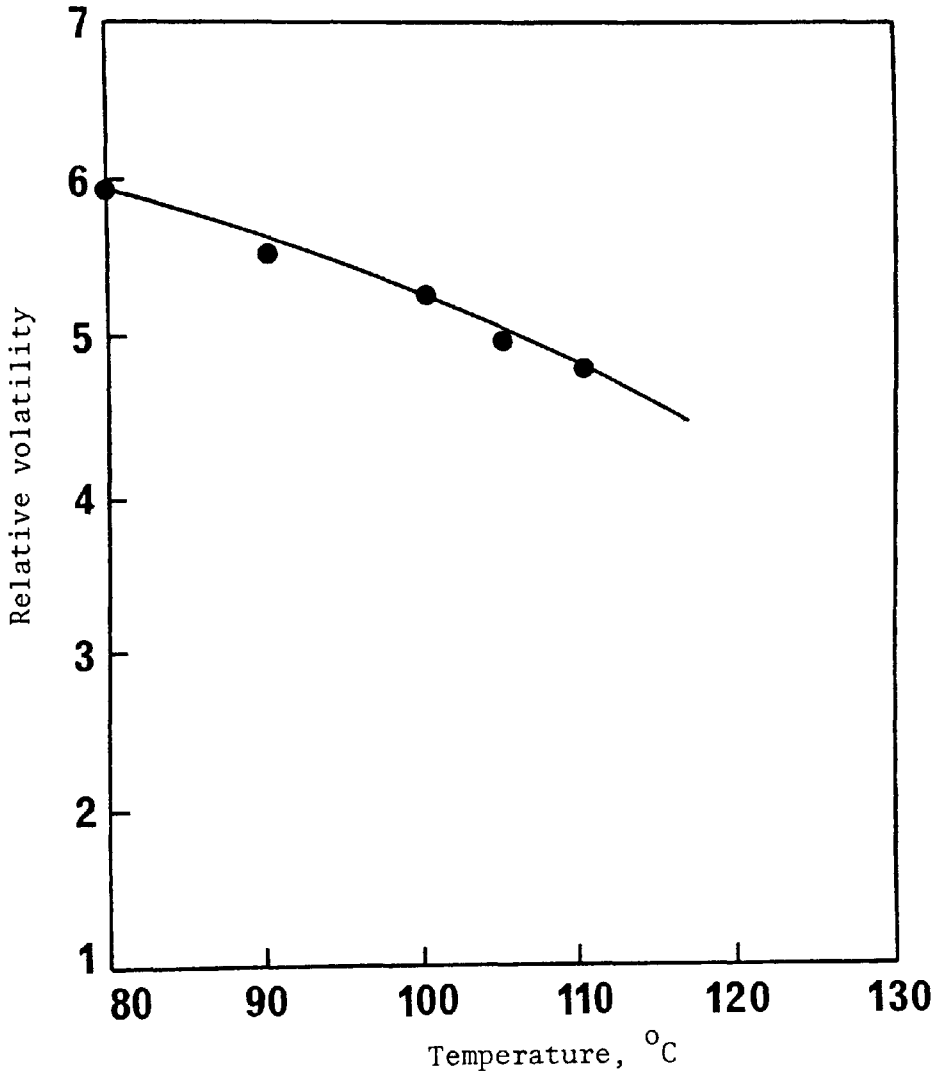

Figure 2.6 : Variation of relative volatility with temperature for the system di-2-ethylhexyl phthalate-di-2-ethyl-hexyl sebacate.

more volatile component from the bulk of liquid, no further similar rate of evaporation of the more volatile component is attained. The application of continuous and intensive agitation will rejuvenate the evaporating surface and ensure that the rate of diffusion is balancing the rate of evaporation of a given component. However, a theoretical treatment of the combined effects of the diffusion flow of a component through a vertically falling film and the rate of evaporation of that component, assuming that Raoult's Law applies, has been attempted by Rukenshtein [97], who postulated a constant liquid temperature.

2.6 MOLECULAR STILLS

In order that a molecular still may perform a particular separation process under conditions of molecular distillation, the following design features should be observed :

(1) Residual gas pressure should be lower than 1 micron Hg., and this has to be maintained during the whole course of distillation. The monographs of Dushman [31] and Yarwood [116] deal with the theoretical and experimental problems associated with the various types of pumps and auxiliary equipments that are required to obtain and maintain such high vacuum.

(2) The distance between the evaporation and condensation surfaces should be of the same order of magnitude as the mean free path of the molecules.

(3) Radiation losses are normally caused due to the small length of the gap between the hot evaporator and the cold condenser. This may result in a low thermal efficiency and, at the same time, cause some molecules to re-evaporate from the surface of the condenser with a consequential reduction of the effective distillation rate. These losses may be offset to some extent if the temperature of the condensation surface is kept at a minimum of 50°C and a maximum of 100°C lower than that of the evaporation surface.

(4) The still should be capable of producing a thin renewable film of distilland with uniformity of area, thickness, and rate of feed. The production of thin films can be achieved by gravity [44], or centrifugal forces imparted to the distilland by rotating the evaporator [45]. When liquids are distributed in the form of a thin film, complete surface wetting should be maintained,as the imperfect covering reduces the effective area of evaporation leading to the formation of hot spots and, consequently, a reduction in the value of evaporation coefficient. Norman and Binns [80] have discussed the problems of minimum wetting rates in wetted rod columns. The keeping of distilland in the form of thin film will ensure that diffusion takes place rapidly enough to make the surface composition representative of the liquid beneath, reduce the time of exposure of heat-sensitive materials and hence reducing the thermal hazard, reduce if not eliminate the torpidity effect, increase the rate of heat flow from the surface of the evaporator to the surface of the distilland, and aid in the degassing of the distilland and hence reduce splashing or bubbling of the distilland.

(5) Since the material has to be degassed prior to molecular distillation, some sort of degassing arrangement has to be incorporated in the design. Watt [111] and Taylor [104] treated in detail the degassing systems and their constructional problems.

(6) Also, the still has to be capable of providing controllable heat supply to the evaporator, and be equipped with reliable temperature and pressure reading facilities.

In view of the above requirements, many stills have appeared during the last six decades. These stills are of two general types :

(a) Pot-type stills ;

(b) Flowing film stills.

A brief description of some of the stills which have been developed will be presented in this section. Full details concerning the construction and operation of these stills can be found in the monographs of Watt [111] and Hollo [55].

2.6.1 Pot Stills

These stills are the earliest developed, and are simple in construction; evaporation takes place from a stagnant surface of a pool of distilland to a nearby air-cooled or water-cooled condenser. Bronsted's [11] and Burch's [14] stills are of this type.

2.6.2 Falling-Film Stills

Hickman [46,49] developed this still in order to overcome some of the factors contributing to the relatively poor performance of pot stills. The distilland is degassed in one or two stages and then allowed to pass over the walls of an upright standing metal cylinder situated within a concentric-cooled condensing cylinder. The distilland flows down the walls in the form of thin film by the action of gravity.

2.6.3 Wiped-Film Stills

These can be considered as special versions of the falling-film stills in which better film formation is ensured mechanically by means of various aids. The latest version of this type of still was developed recently by Tkac [105].

2.6.4 Centrifugal Stills

In these stills, the distilland is fed to the centre of a rotating evaporator, thus utilizing a force many times greater than that of gravity, to spread the distilland in the form of a very thin film, hence reducing exposure time to a minimum. Table 2.4 shows that the film thickness was reduced from that in the falling-film still by a factor of approximately 10, while time of exposure to heat was reduced by a factor of 200. Hickman [45] was the first to construct a centrifugal molecular still.

Table 2.4 : Transition from pot still to centrifugal still [46]

Approx. Date	Still	Pressure (mm Hg)	Approximate Distilland Thickness (mm)	Approximate Time of Exposure (sec.)
1922	Lab. pot still	0.1	10 - 50	3600-18000
1928	Lab. tray still	0.1	1 - 10	300 - 3600
1935	Ind. falling-film	0.001	1 - 3	120 - 600
1930	Lab. falling-film	0.001	0.1 -0.3	10 - 50
1940	Ind. centrifugal	0.001	0.03 -0.06	0.1 - 1
1936	Lab. centrifugal	0.001	0.01 -0.02	0.04-0.08

2.7 SEPARATORY POWER OF THE MOLECULAR STILL

The ability to separate constituents from a mixed distilland is a fundamental property of any particular still. Since the molecular distillation process is a non-equilibrium one, therefore a molecular still may only represent one distillation unit and, as such, one theoretical molecular plate (TMP) [47] as the maximum under ideal conditions. The concept of TMP is somewhat analogous to the theoretical plate in equilibrium distillation, but in the case of flowing-film molecular stills is rather complicated, because succeeding areas of the film during evaporation cannot be identical in composition except at infinite ratio of evaporation to throughput.

The number of TMP, n, can be calculated using an equation analogous to the Fenske equation :

$$n = \frac{\log \frac{x_n(1 - x_o)}{x_o(1 - x_n)}}{\log \alpha} \qquad \ldots 2.53$$

where

x_o = mole fraction of the more volatile component in the distilland;

x_n = mole fraction of the more volatile component in the distillate ;

α = relative volatility calculated from the equilibrium data.

Malyusov [73] also proposed that :

$$\alpha_w = \alpha^n \qquad \ldots 2.54$$

The variation of TMP with the constructional property of the molecular still is shown in Table 2.5.

Table 2.5 : TMP values for different molecular stills

Molecular Still	TMP
Pot stills	0.3 - 0.4
Falling-film stills	0.8
Centrifugal stills	0.8 - 0.95

However, it was suggested by Biehler [7] that the separatory power of the molecular still can exceed one TMP at very low rates of distillation (Fig.2.7). This is due to the fact that, on a flat cone, the film expands mechanically towards the edge of the funnel, and this increases the separatory power. This observation was also confirmed by Hickman [52] in experiments in a push-pull tensimeter.

2.8 APPLICATIONS OF MOLECULAR DISTILLATION

It was shown in the preceding sections that molecular distillation represents a means of vaporization at low pressures and corresponding low temperatures; and with the utilization of thin-film techniques, it becomes the only method suitable for the separation of heat-sensitive, high molecular weight and low volatility materials by distillation, by which thermal decomposition can be avoided or reduced to a minimum.

It would be impractical to give a list of all materials which have been treated by the process of molecular distillation. Hollo [55] gives references of over 300 substances which have been treated by this process since 1920. The most recent applications might be classified under the following headings [70] :

Dimer acids
Fatty amides and fatty amines
Monoglycerides
Sugar esters
Halogenated hydrocarbons
Anhydrous lanolin
Epoxy resins
Lubricants and greases
Vitamins

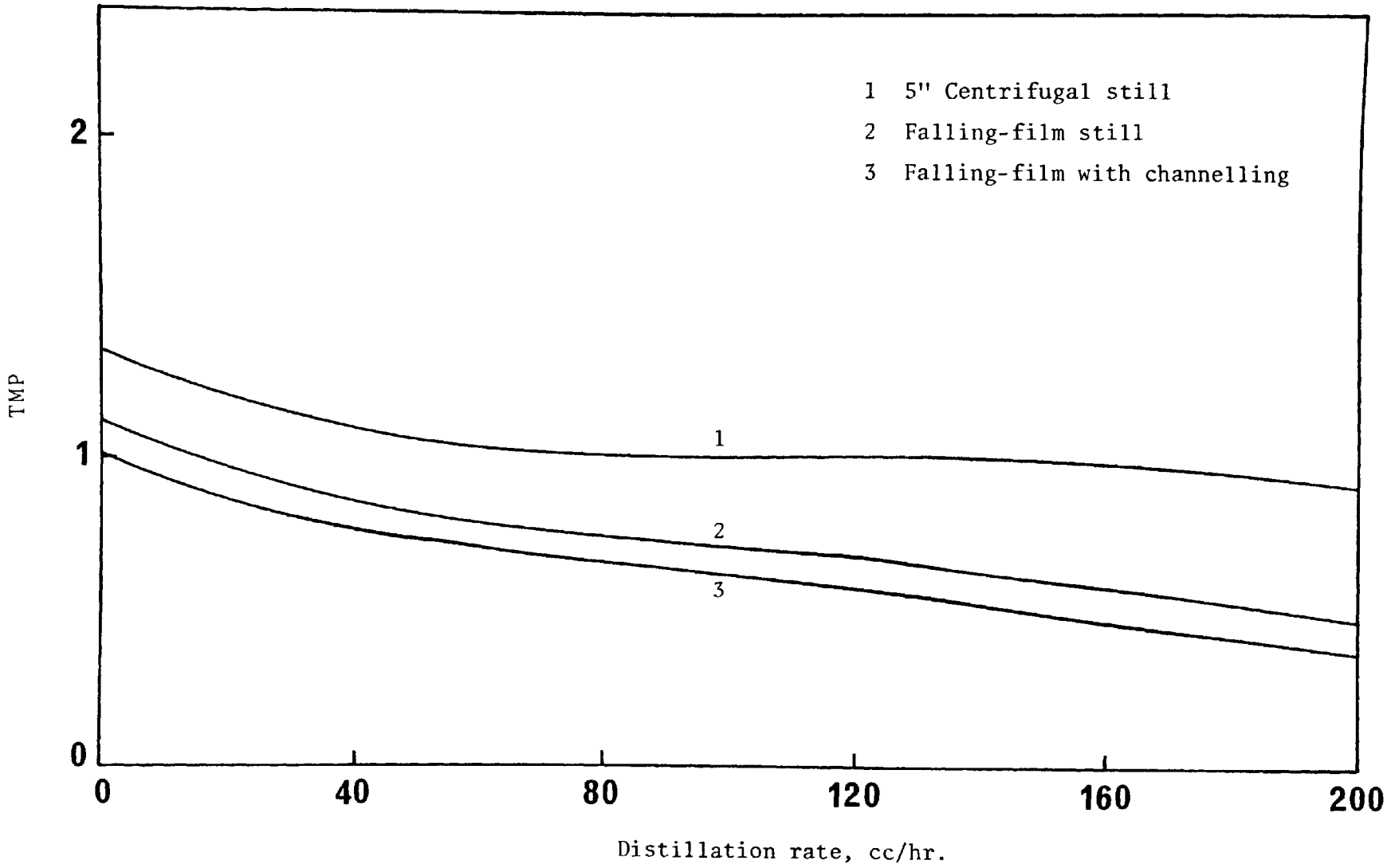

Figure 2.7 : Performance curves for centrifugal and falling film stills.

CHAPTER III

EXPERIMENTAL ASPECTS

3.1 BRIEF DESCRIPTION OF THE COMMERCIAL CENTRIFUGAL MOLECULAR STILL

"Consolidated Vacuum Corporation, Rochester, New York", manufactures a wide range of centrifugal molecular stills, the smallest of these, the CMS-5, was used during the experimental phase of the present investigation.

Figures 3.1, 3.2, and 3.3. show schematic diagrams of the general features of the equipment. The horizontal base plate supports beneath it the concave electrically-heated evaporator rotor, the drive mechanism of the rotor, the feed pump, and the distilland receiver. These items are housed in the removable bell jar which acts as a vacuum chamber, its dome-shaped face as a condenser facing the evaporator rotor and, in addition, its lower portion serves as a reservoir for the feed liquid charge. The drive motor and feed pump worm gears are mounted on top of the base-plate.

The vacuum is attained by means of a mechanical fore-pump backed up by an oil diffusion pump. These are connected to the vacuum chamber by a large manifold passing through the base-plate. The control items are housed in the side panel, which also supports the base-plate.

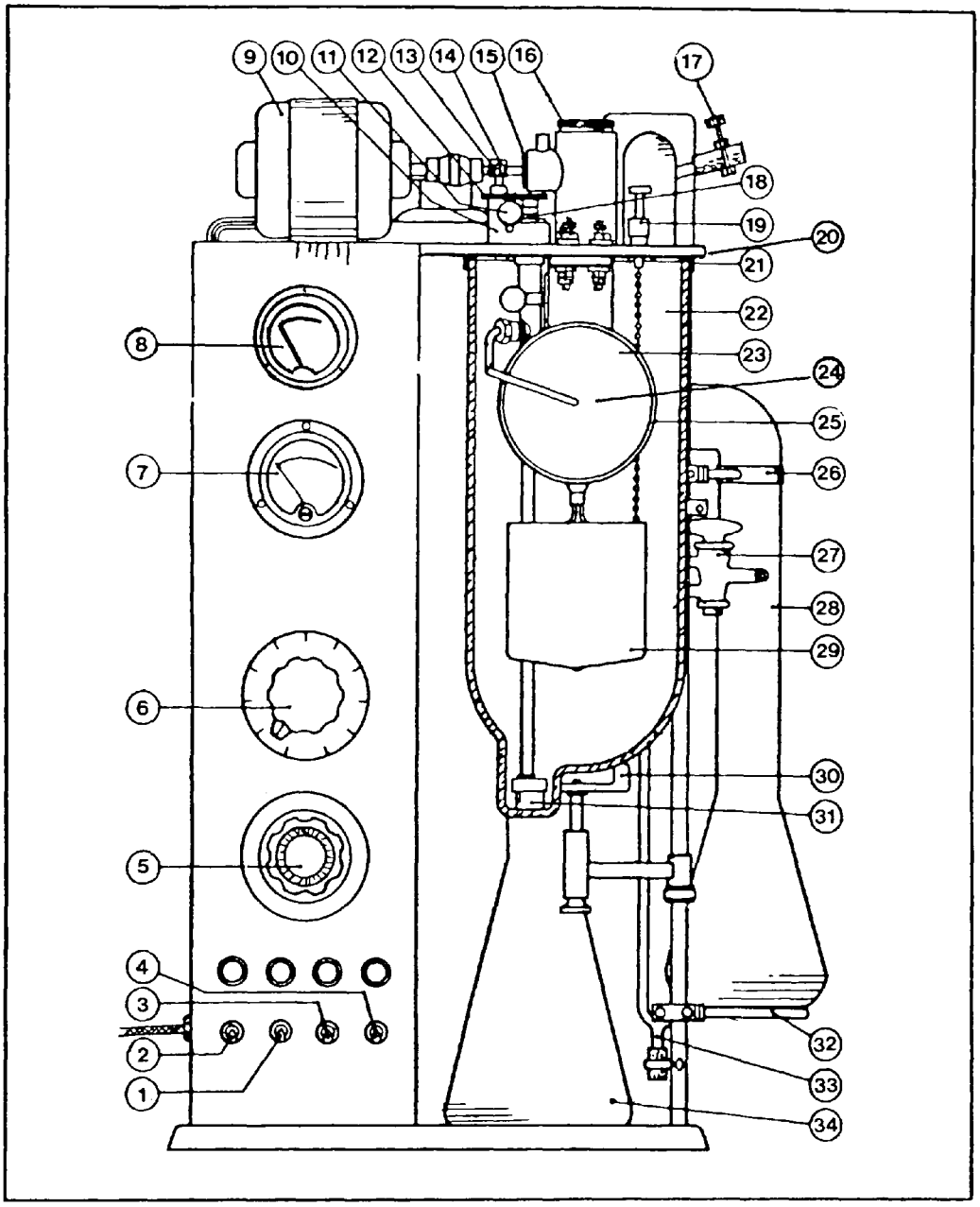

Figure 3.1 : Schematic diagram of the CMS-5 (front view).

1. Switch-Diffusion Pump
2. Switch-Mechanical Pump
3. Switch-Drive Motor
4. Switch-Rotor Heater
5. Auto-Transformer (Rotor Heater)
6. Auto-Transformer (Diffusion Pump)
7. Thermocouple Meter
8. Heater Current Meter
9. Drive Motor
10. Gear Mount
11. Thumb Nut
12. Drive Gears
13. Worm Gear
14. Spur Gear
15. Main Drive Shaft
16. Rotor Chain Cap
17. Bleed Tube Pinch Clamp
18. Feed Pump Drive Shaft
19. Distilland Receiver Ball Valve Shaft
20. Base Plate
21. L-Gasket
22. Bell Jar
23. Rotor
24. Feed Tube
25. Collecting Gutter
26. Clamp
27. Stopcock
28. Diffusion Pump
29. Distilland Receiver
30. Support Clamp
31. Feed Pump
32. Support Ring
33. Drain Tube
34. Ballast Flask

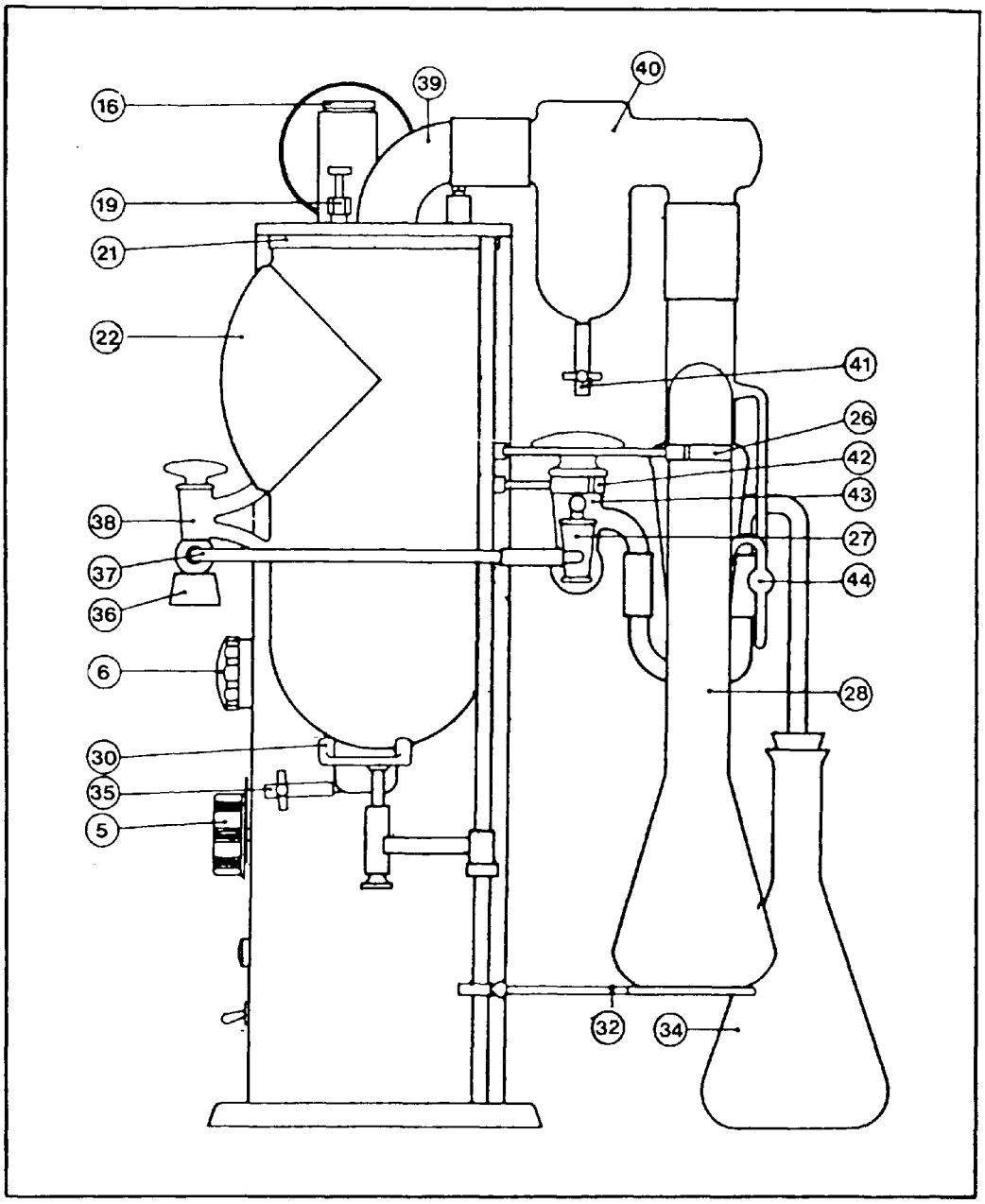

Figure 3.2 : Schematic diagram of the CMS-5 (side view).

5. Auto-Transformer (Rotor Heater)
35. Drain Pinch Clamp
30. Support Clamp
6. Auto-Transformer (Diffusion Pump)
36. Rubber Stopper
37. Aluminium Tube
38. Withdrawal Stopcock
22. Bell Jar
21. L-Gasket
19. Distilland Receiver Ball Valve Shaft
16. Rotor Chain Cap
39. Exhaust Manifold
40. Cold Trap
41. Drain Pinch Clamp
26. Clamp
42. Clamp
43. Stopcock
27. Stopcock
44. Manometer
28. Diffusion Pump
34. Ballast Flask
32. Support Ring

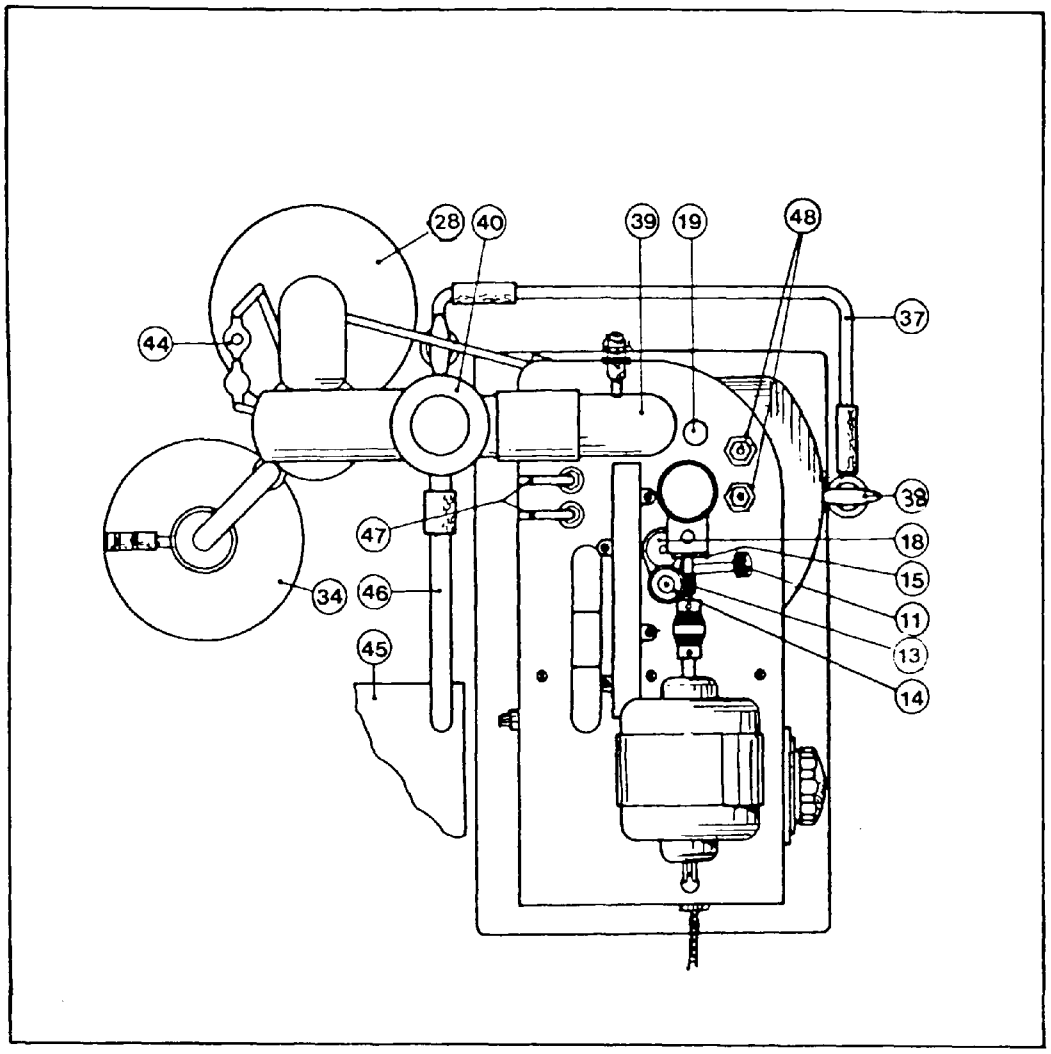

Figure 3.3 : Schematic diagram of the CMS-5 (top view).

45. Mechanical Fore-pump
46. Tubing
47. Bearing Cooling Tubes
34. Ballast Flask
44. Manometer
28. Diffusion Pump
40. Cold Trap
39. Exhaust Manifold
19. Distilland Receiver Ball Valve Shaft
48. Leads
37. Aluminium Tube
38. Withdrawal Stopcock
18. Feed Pump Drive Shaft
15. Main Drive Shaft
11. Thumb Nut
13. Worm Gear
14. Spur Gear

Distilland is fed at the base of the rotor and caused, by centrifugal action, to form a thin film over the entire surface of the evaporator. The evaporated vapour is condensed on the inside face of the bell jar, where it can be extracted via the withdrawal stopcock. The unvaporized residue slides off the rotor and into the distilland receiver.

However, detailed description and operation techniques are readily available [25]. The main characteristics and specifications of this still are listed in Table 3.1.

Table 3.1 : Characteristics and specifications of the CMS-5

Bell Jar	Pyrex
Rotor	Aluminium, No.108 Alloy
Rotor Feed Tube	Spun Aluminium
Rotor Gutter	304 Stainless Steel
Feed Pump Housing	Meehanite
Feed Pump Gears	Steel
Feed Pump Shaft	Drill Rod Steel
Rotor Outside Diameter*	11.43 cm
Rotor Centre Flat	2.2225 cm
Rotor Centre Dimple	0.9525 cm
Rotor Slant Height	5.08 cm
Rotor Face Angle	15^{o}
Rotor Speed	1330-1340 rpm
Rotor Heat Input	0-500 Watts
Distilling Area	100 cm^2 (Effective)
Throughput	10-35 cm^3 /min
Charge	100-1500 cm^3
Operating Pressure	1-10 microns Hg

*There is an additional 0.3175 cm flat on periphery.

3.2 MODIFICATION OF THE COMMERCIAL STILL

Since the CMS-5 has been designed for commercial uses only, and in order to carry out the experimental phase of the present investigation, several modifications were made.

3.2.1 Condensation Surface

The inside face of the dome serves as the condensation surface of the CMS-5. This is neither an aerofoil nor water-cooled condenser, and also lacks a temperature measuring device. The absence of a proper condenser adds a limitation to this still from the point of view of efficiency; although what concerns the present investigation is that the condenser temperature is such that re-evaporation is negligible.

It should be emphasized that any attempt to refabricate the dome of the bell jar is an extremely delicate task, as this could deform the upper neck or the withdrawal stopcock, and hence makes it impossible to attain the required vacuum.

Therefore a condenser, Plate 3.1, was fabricated from 12 cm diameter glass tube. This is a simple water-cooled condenser with an inlet connected to a water supply and an outlet connected first to a flowmeter and then to a discharge sink. It is also provided with a thermometer pocket. The condenser was fixed to the outside face of the dome opposite the evaporator with an adhesive material (Araldite). As an extra precaution, the condenser was fitted with a metal clamp to hold it in place in

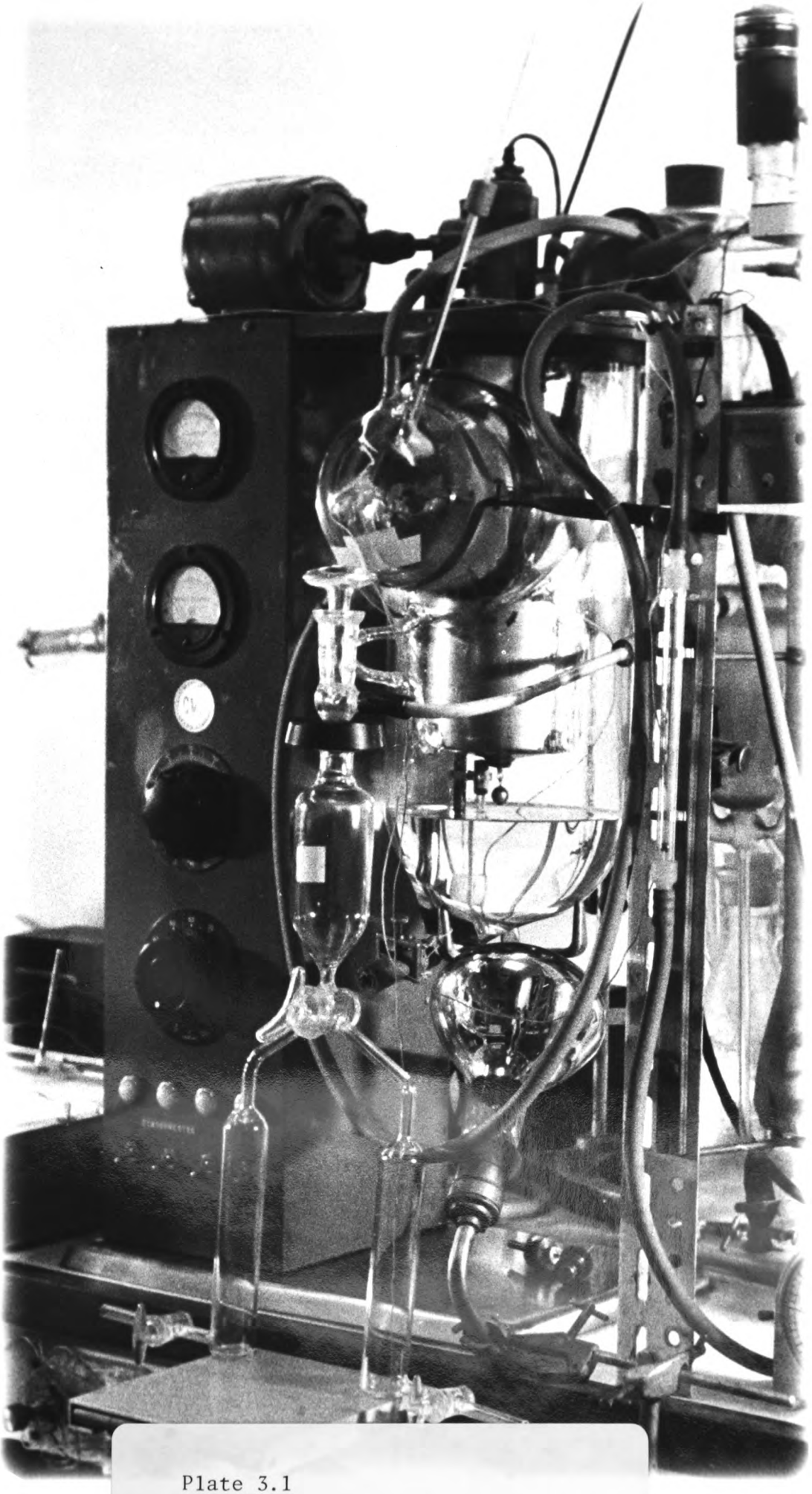

Plate 3.1

Illustration of the water-cooled condenser and distillate receiver

case the adhesive material failed due to excessive heat. The fixing of the condenser had also involved the extension of the withdrawal stopcock tubes. This task was performed on the bell jar, which was then annealed for a period of four hours at 600^{o}C and left overnight in the warm oven, to cool down. The alignment of the glass molecules was examined with the aid of the strainviewer,and the bell jar was then tested for vacuum tightness.

3.2.2 Distillate Receiver

A distillate receiver, Plate 3.1, was fabricated from 3-5 cm diameter glass tubes. It consists of three separate bottles, triangularly welded to a three-way stopcock. The top bottle has a conical base and a lipped neck wide enough to surround the outlet of the withdrawal stopcock and sits perfectly on the O-shape rubber stopper. The other two bottles have cylindrical shapes with a stopcock in each of the discharge lines.

With this arrangement, the receiver is capable of holding three separate samples during any experimental run, and hence the rate of distillation could be checked and double-checked during constant operating conditions. Also, it has an operational advantage which can be explained as follows: Suppose the distillation is taking place at constant temperature and pressure and the distillate is being collected in a one-bottle distillate receiver ; any sudden departure from the working temperature and pressure will alter the rate and composition of the distillate and make the whole experimental run void; whereas if the three-bottle

receiver was used, only the first sample becomes void, and distillation may carry on while restoring the operating conditions. As soon as these conditions are realised, distillate collection may proceed in the second bottle.

3.2.3 Distilland Receiver

The distilland receiver is normally equipped with a ball valve situated inside the receiver which can be operated externally by the vertical movement of the ball valve shaft. When this valve is open, the distilland can be circulated back to the feed. Unfortunately, this valve is badly designed, since it does not make a tight closure due to metal-to-metal contact, i.e. it allows a continuous dripping of the distilland into the feed, and hence contaminating and changing its composition.

Therefore an arrangement was made whereby an O-ring rubber gasket was fixed around the opening beneath the receiver and the ball valve was suspended through the opening outside the receiver. This proved to give a satisfactory close contact and the dripping behaviour was completely eliminated.

In order to prevent the accidental overflow of the distilland, a glass tube was fabricated and fixed to the side of the receiver, serving as a level indicator. Plate 3.2 shows the modified distilland receiver, while Figures 3.4 a & b show schematic diagrams of the receiver before and after modification, respectively.

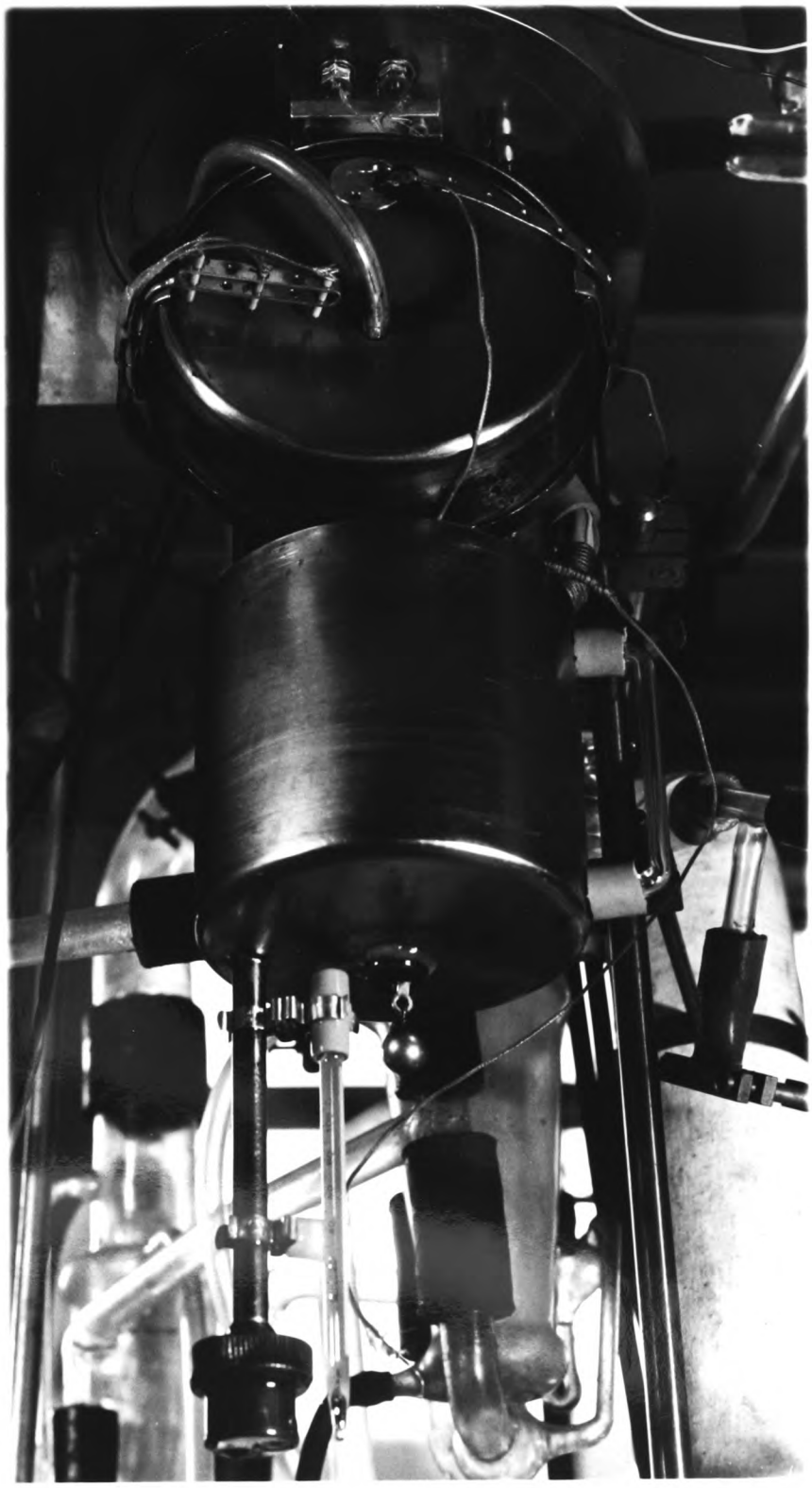

Plate 3.2

Illustration of the modified distilland receiver, thermocouples, and feed thermometer.

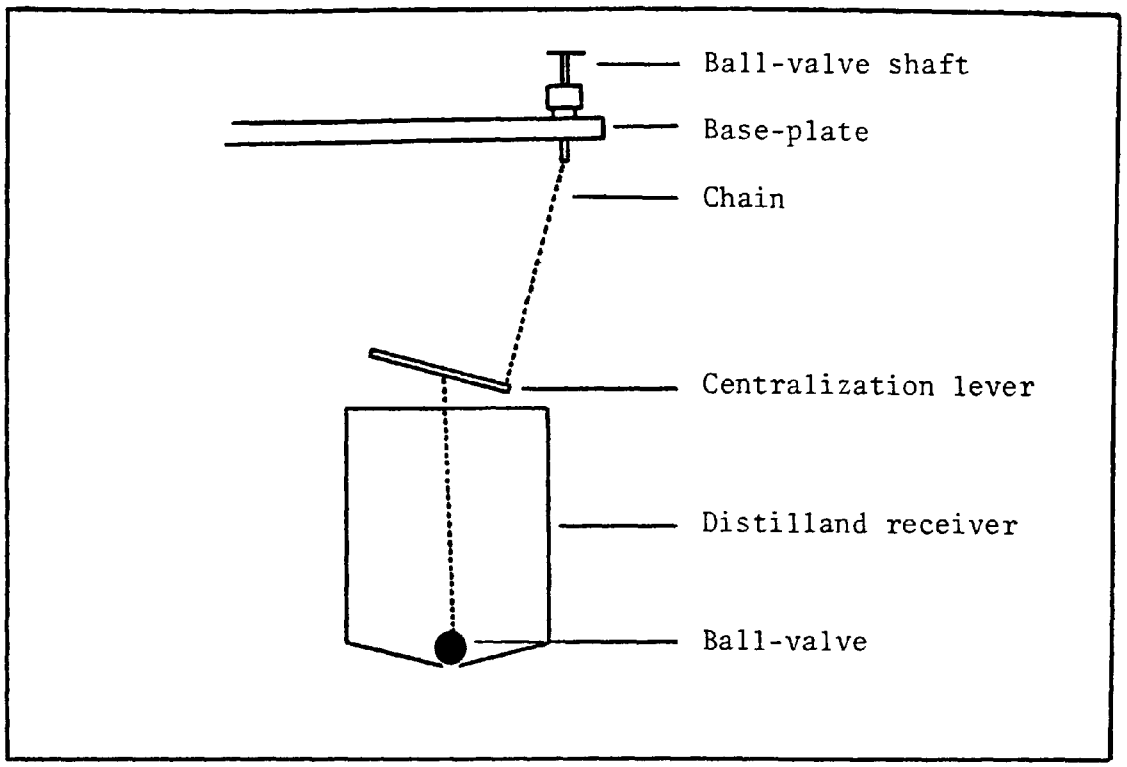

Figure 3.4a : Schematic diagram of distilland receiver before modification.

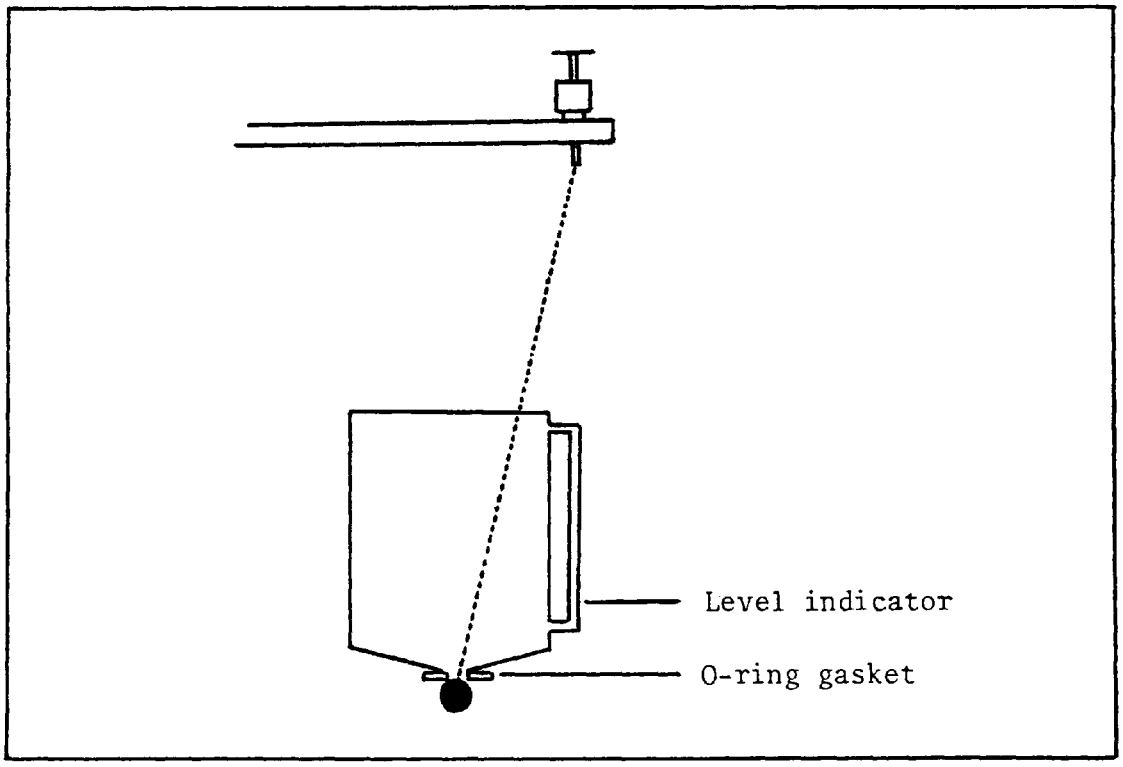

Figure 3.4b : Schematic diagram of distilland receiver after modification.

3.2.4 Vacuum System

In order to increase the mean free path of the evaporating molecules, the vacuum pumping capacity of the still was increased by the addition of a second two-stage, glass, oil diffusion pump, type GB-25. The two pumps were coupled in parallel across the vapour line between the still and the mechanical forepump. The pump heaters were connected in series and operated from a single variable auto-transformer. With this arrangement, the possible originally attained vacuum was improved by more than one order of magnitude. Plate 3.3 shows the vacuum achieved during a typical experimental run.

The vacuum attained by the system is normally measured by a single thermistor-type gauge. This gauge is installed in the branch line that tapped into the bell jar chamber through the base plate. It is a dual scale instrument, capable of reading the pressure to 1 micron Hg. Since the vacuum pumping capacity was increased, a second gauge, Penning type, was installed in a short line just off the main manifold. The scale of this gauge extends to 10^{-7} torr.

Two cold traps were added to the system; one between the second oil diffusion pump and the still, and the other between the mechanical forepump and the still. These will eliminate the contamination of the fluid in the pumps, indicate whether evaporating molecules are escaping from the vacuum chamber, and increase the rate of evacuation of the system. Plate 3.4 shows the second diffusion pump and its cold trap.

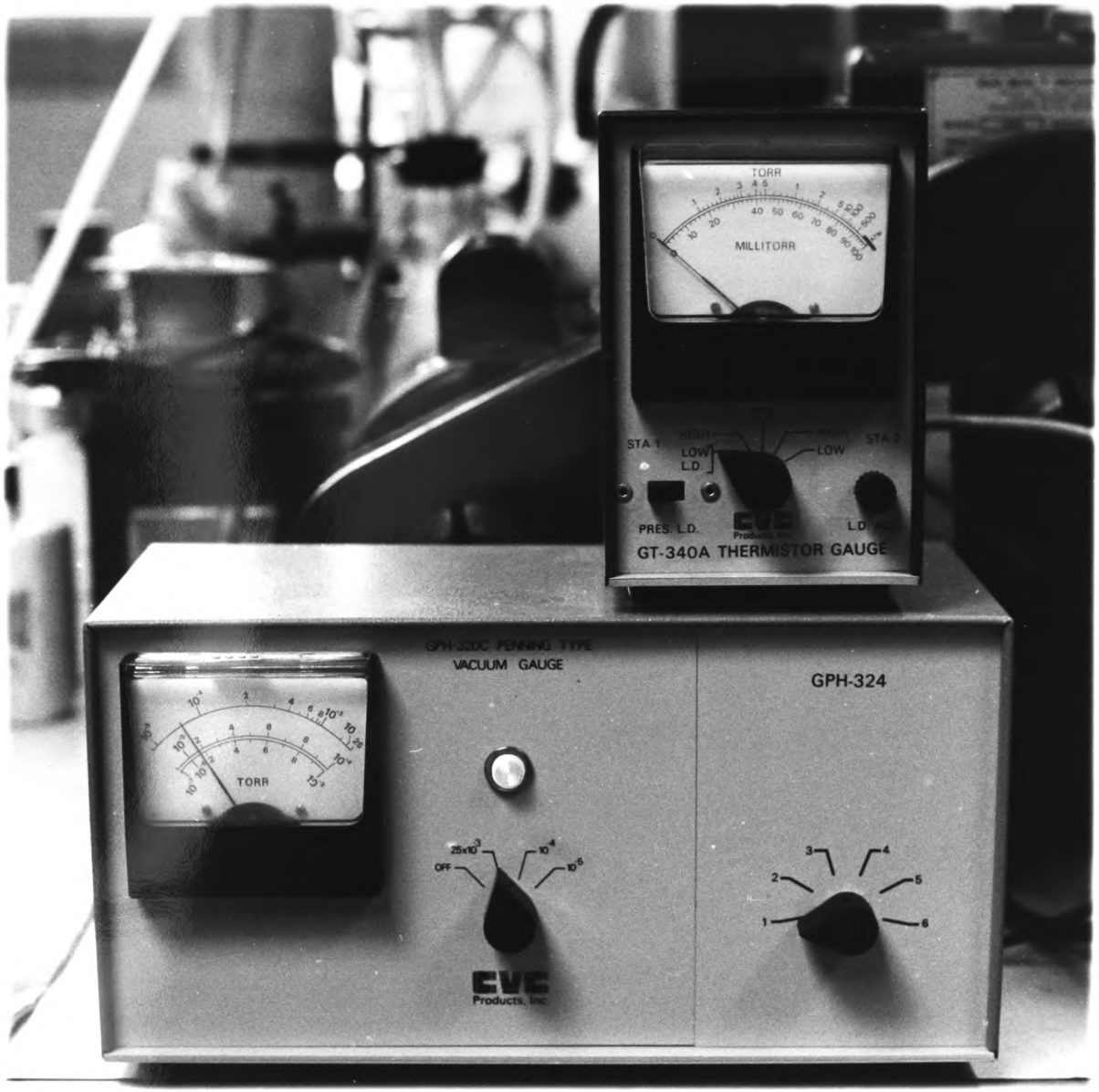

Plate 3.3

Vacuum gauges : Thermistor gauge pointing at 10^{-3} mm Hg and Penning gauge pointing at $\simeq 5 \times 10^{-5}$ mm Hg

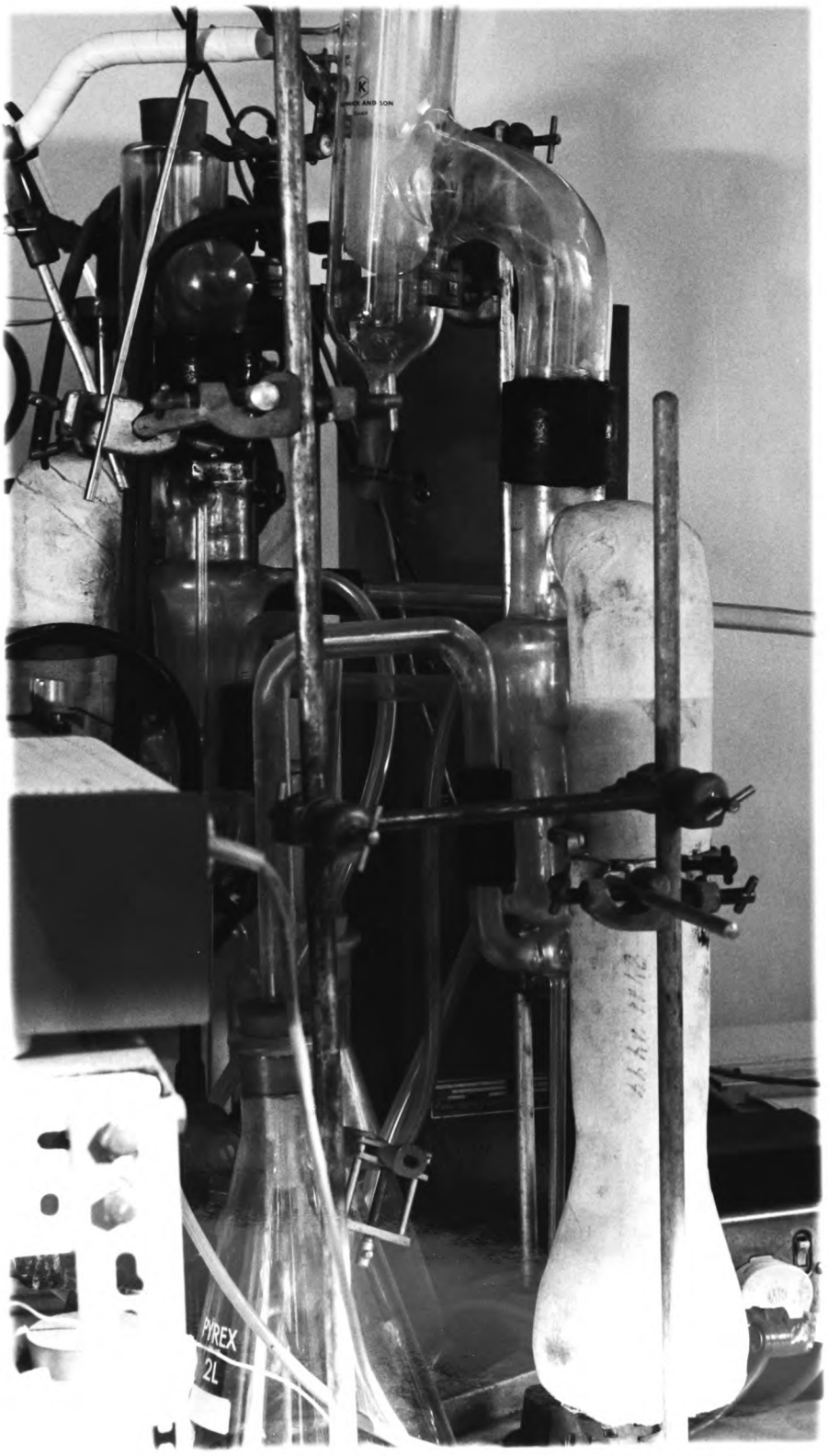

Plate 3.4

Illustration of the second diffusion pump and its cold trap at the rear of the still

3.2.5 Temperature Measurement

The distillation temperature is normally provided by a single iron-constantan thermocouple located in a groove on the rear face of the rim at the periphery of the rotor. The sketch in Figure 3.5 shows the point where the thermocouple probe meets the distilland residue.

It will be shown in Chapter V that temperature gradients exist in the liquid film in such a way that the surface temperature does not remain constant but increases in a certain manner, traversing across the film from vertex to periphery. This implies that the thermocouple, where it is located, does not give the true temperature of distillation, although its location is the most practical from a design standpoint.

For many organic materials, an error of 1^{o} C in the temperature measurement will produce an error of 8 -10% in the vapour pressure, and subsequently, a corresponding error in the rate of vaporization when the material is subjected to a molecular distillation treatment. Therefore in order to correlate theory with experiment it is necessary to determine as accurately as possible the temperature of the evaporating liquid surface. Although this is desirable, it is by no means an easy task with the problem in hand since the liquid film is so thin (0.01 -0.1 mm) and moving in a rotational way (from a stationary observer point of view), and consequently it becomes impractical to measure its variable surface temperature by means of conventional devices. However, the following approach was adopted:

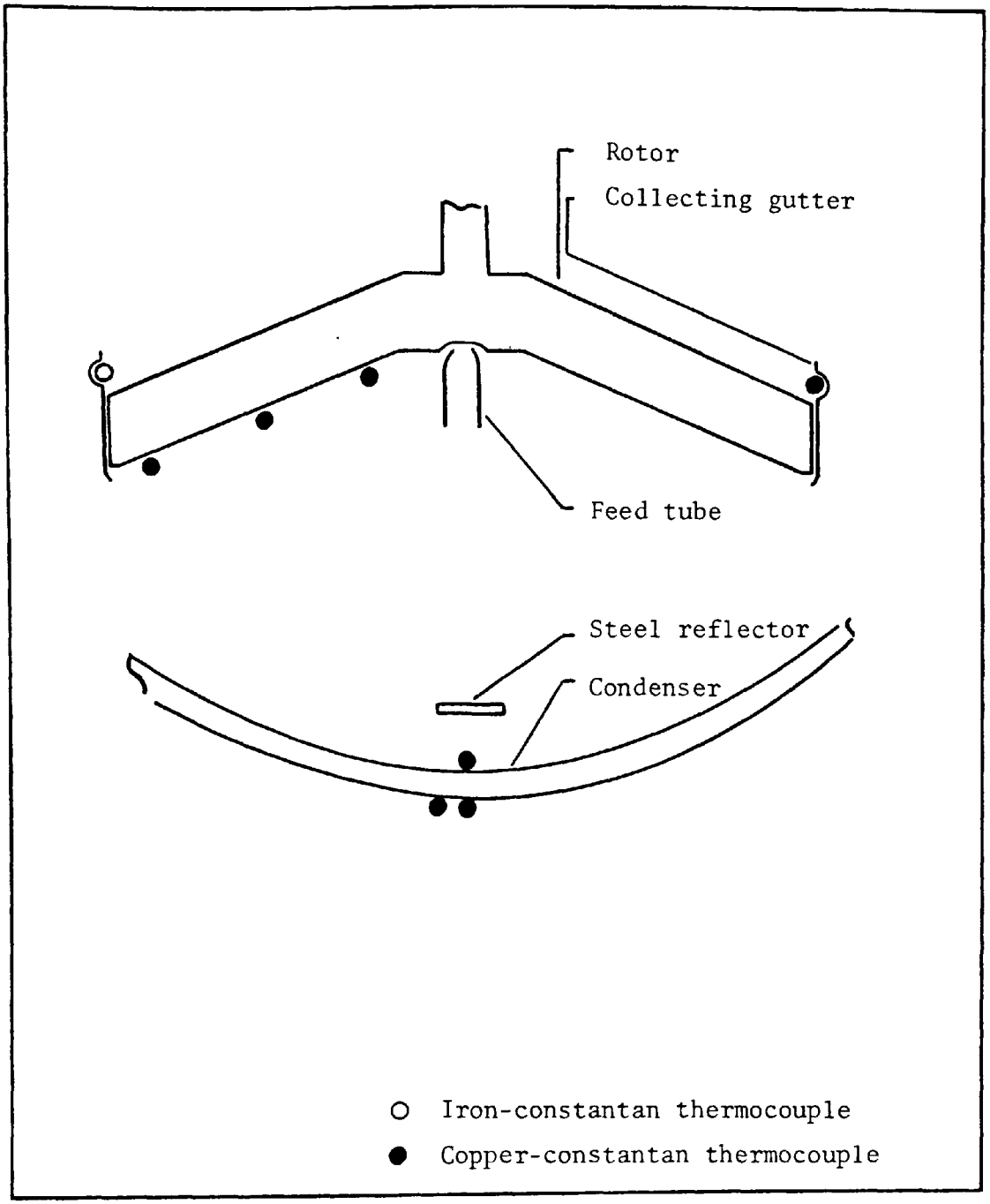

Figure 3.5 : Schematic diagram of thermocouples locations (top view).

A thermocouple junction made from very fine (0.3 mm diameter) copper-constantan wires was installed opposite the present iron-constantan thermocouple, as shown in Figure 3.5. The average temperature of these thermocouples is considered as the mean bulk temperature of the distilland residue at the point where it leaves the rotor surface.

Although there is a radial temperature gradient at the liquid surface, the temperature of each point remains constant during steady operating conditions and, to ensure this,three copper-constantan thermocouples were constructed and installed in a frame facing the evaporating surface. Their probes are so near, but do not touch, the liquid surface. It is not expected from these thermocouples to give the temperatures of the liquid surface but, as stated above, to ensure that the temperature of the points they face remains constant. This arrangement is shown schematically in Figure 3.5, while Plate 3.2 shows the actual set-up.

In order to measure the temperature drop across the condenser, two thermocouples were constructed of the same material. One was fixed on the centre of the outside face of the dome before fixing the water-cooled condenser with an extra thermocouple as standby. The other was fixed on a spring-loaded clamp where it could touch the centre of the inside face of the dome. This is shielded from the direct path of vapour by a steel reflector. The arrangement is shown in Figure 3.5.

Plate 3.2 shows one more thermocouple and a thermometer located in the feed reservoir by the feed pump. These were used to measure the temperature of the feed.

The problem of connecting the output of these thermocouples to a pen recorder was solved in two stages:

(1) In order to take the thermocouple's output out of the vacuum chamber, it was thought impractical to tamper with the base plate, as this could damage this important item and put the whole still at risk. Therefore a T-shaped container was fabricated from glass (Figure 3.6). One end was connected by a rubber sleeve to the vapour line between the second diffusion pump and the still. The other two ends were fitted with rubber stoppers. Four electrical connectors were fitted in each stopper. All wires, including two standby, were passed through the main manifold and through a side opening to the vapour line. The copper parts of the wires were connected to the internal ends of seven of the connectors, and the constantan parts to the internal end of the eighth common connector. The whole assembly was then tested regarding vacuum tightness.

(2) In order to reduce the number of pen recorders, an electronic circuit was designed. It mainly comprises of a clock, 4-bit binary adder, and 16 analogue switches. The circuit is capable of closing the open circuits of 16 thermocouple (7 were used) in sequential pre-set short (0 - 70 sec) equal time intervals. Simultaneously, the output of each thermocouple, in turn, is recorded on the chart of one pen recorder, and the whole cycle is repeated soon after the

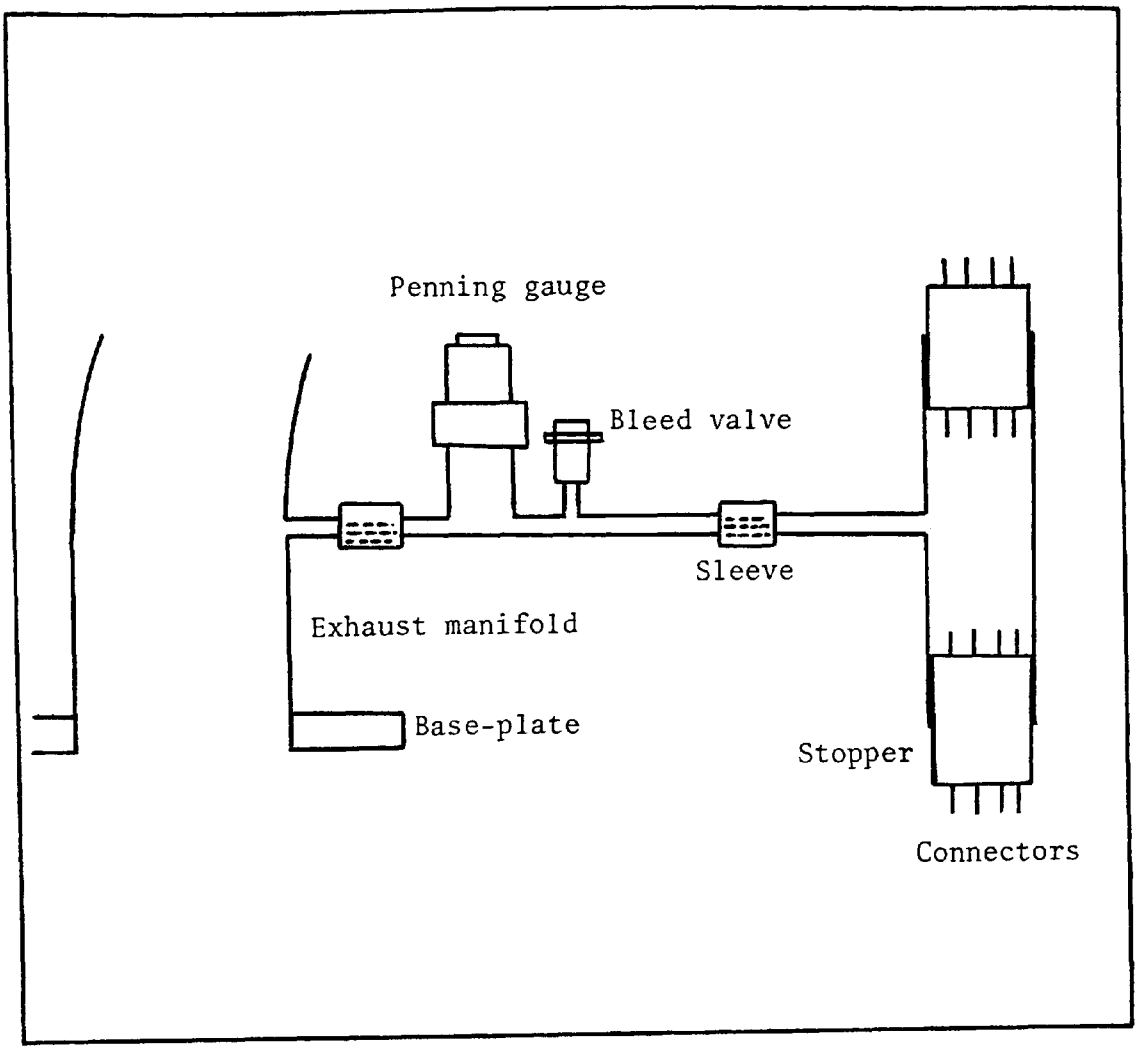

Figure 3.6 : Schematic diagram of the T-shaped container, attached to the vacuum system.

output of the last thermocouple has been recorded. Figure 3.7 shows a block diagram of the circuit.

The output of the installed thermocouple at the periphery is also connected independently to a second pen recorder. This offers a continuous monitoring of its temperature to ensure steady operating conditions.

All thermocouple probes were made by silver-soldering and calibrated individually. The common cold junction was maintained at a constant temperature in a mixture of ice and water.

3.3 TEST MATERIALS

The materials used during the experimental phase of the present investigation were :

(1) Di-2-ethylhexyl phthalate

(2) Di-2-ethylhexyl sebacate

Full details on the choice and properties of these materials are given in Chapter IV.

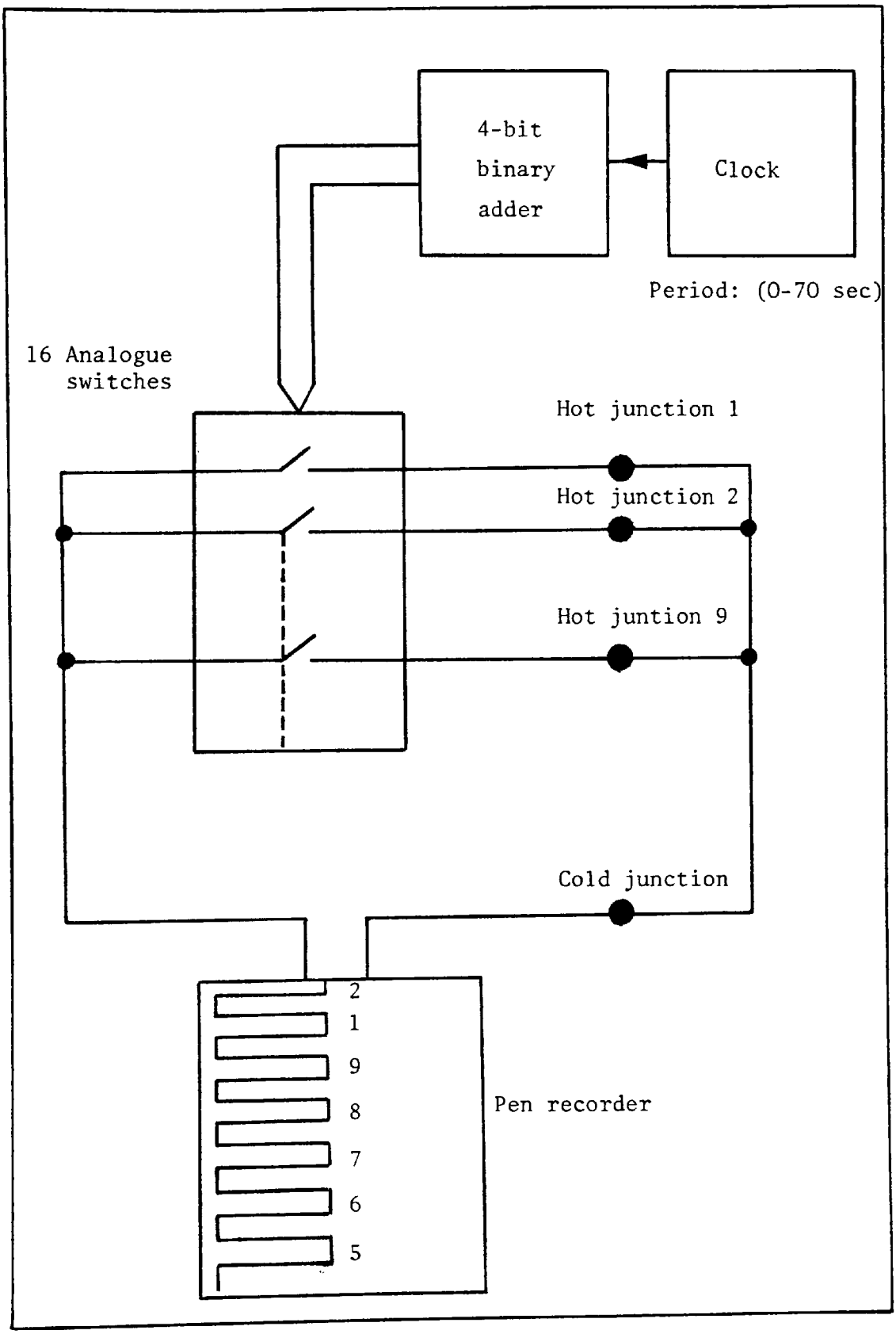

Figure 3.7 : Block diagram of the electronic switch.

3.4 RATE OF FEED DETERMINATION

The CMS-5 is normally equipped with a constant volume, vane-type, rotary pump. It operates totally submerged in the liquid feed at the lower portion of the bell jar. The drive shaft of the pump passes vertically through a hollow discharge tube and through a rotary shaft seal in the base-plate. It is then coupled to the shaft of the drive motor by means of gear transmission. The feed tube to the rotor is nut-connected to a threaded opening near the top of the discharge tube. The speed of the drive shaft, i.e. the pumping capacity, depends on the size of gear engaged in the transmission. Four sizes are available: 30, 40, 50, and 80 teeth.

In order to carry out the rate studies, it was important to determine exactly the pumping capacity of the pump for each gear. After a few test trials, it quickly became apparent that the pumping capacity depends considerably on the viscosity of the feed as well as on the size of gear used. It was at first considered that it would be desirable to obtain a calibration curve of pumping capacity as a function of gear size and viscosity. This calibration was not obtained, however, due to the wear and tear which no doubt would take place in the pump during the course of the experimental investigation, which would definitely reduce its efficiency. Since at each stage of the experimental investigation different composition of the test material was used, therefore the rate of feed of that composition at that time was determined using 30, 40, and 50 teeth gears for a set of probable feed temperatures. The procedure was as follows :

The bell jar and distilland receiver ball valve were removed. One end of plastic tubing was attached to the distilland discharge opening, and the other end to a calibrated cylinder, as shown in Plate 3.5. The pump was submerged in a 400 ml beaker which is situated in a crucible-shape, variable input heater. The liquid was heated to the required temperature and one of the gears was engaged to start the pumping. For each gear, and over a range of temperatures, the rate of collection of five 100 cc samples was measured and averaged. Reproducibility of these runs was excellent ; all measurements were well within 1.5% of the mean.

The results of these tests are plotted in Figures 3.8, 3.9, 3.10, 3.11, 3.12, 3.13, and 3.14 as mass rates versus temperature for the spur gears (30, 40, and 50 teeth).

3.5 PHOTOGRAPHIC STUDIES OF THE LIQUID FILM

The stroboscopic photographs, Plates 3.6 to 3.10, were taken of the rotor with and without the loading of liquid film. All spur gears were used and the feed temperature was $17^{o}C$ and $120^{o}C$.

High-speed film was also taken of the rotor tracking a particle of the liquid film from the moment of impinging on the centre of the rotor to the moment of departure at the periphery.

By the aid of the stroboscope, the rotational speed of the rotor was confirmed to be 1330 rpm, which was also proven to be

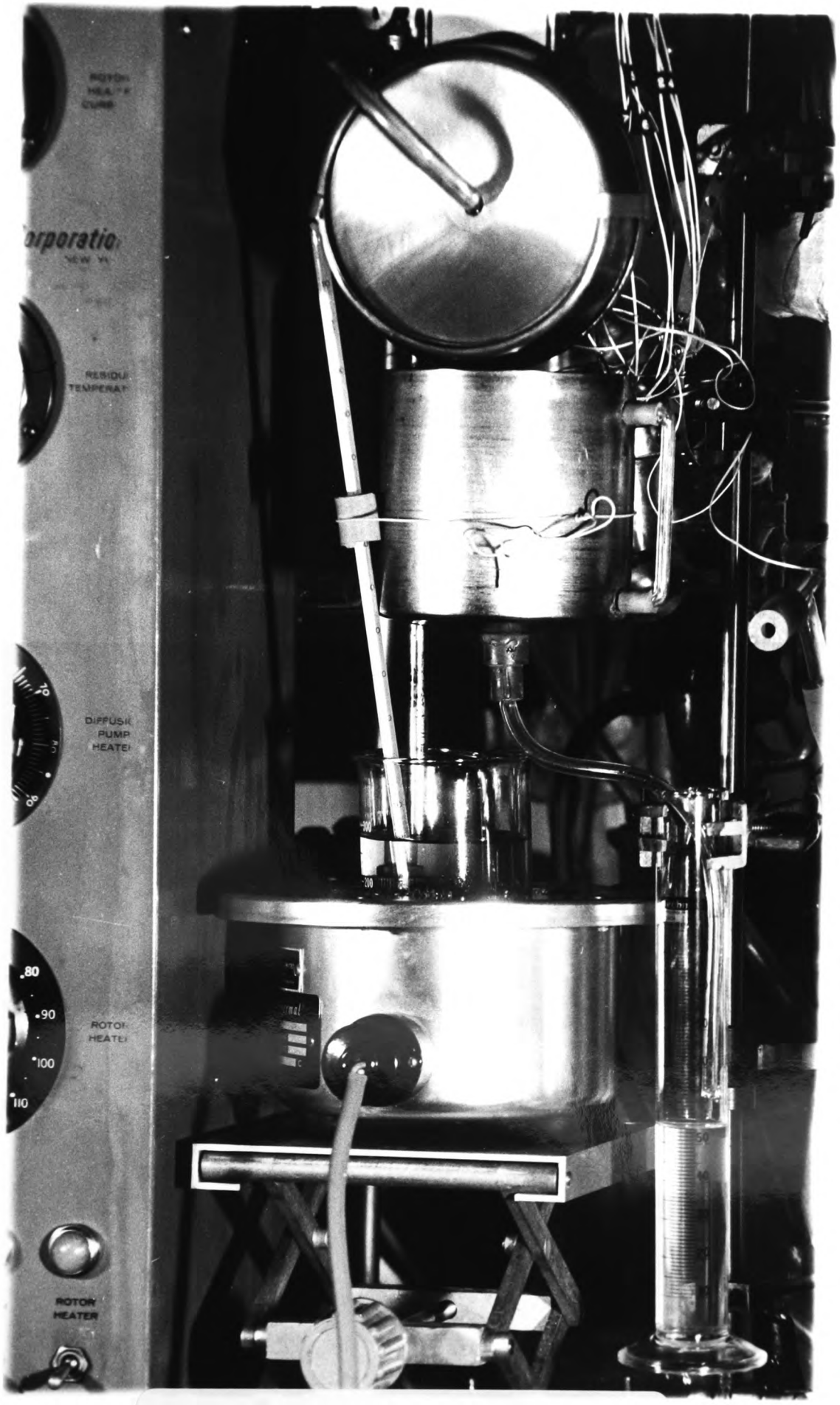

Plate 3.5

Illustration of the arrangement
for determining rate of feed

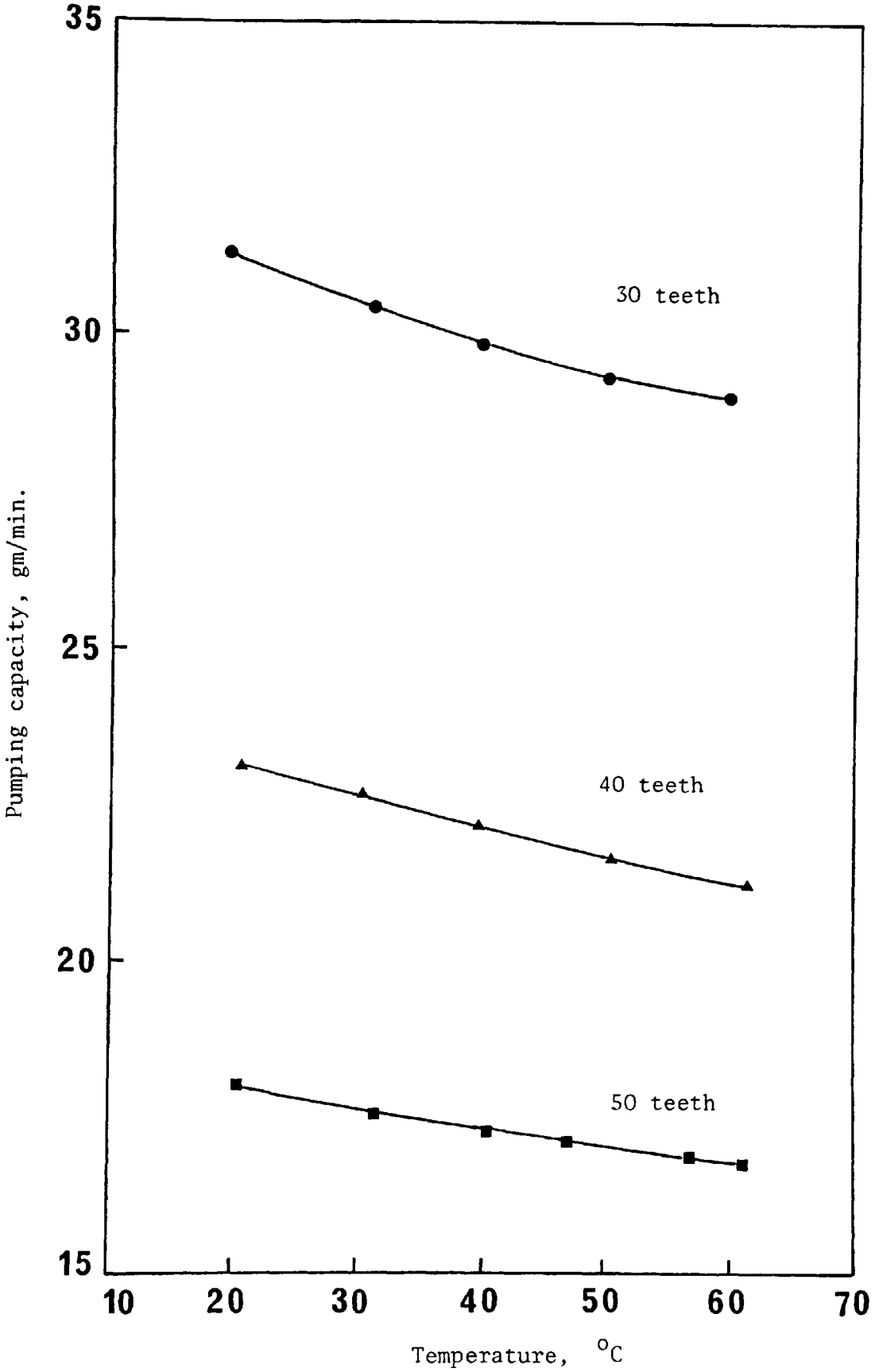

Figure 3.8 : Feed pump calibration, EHS (pure).

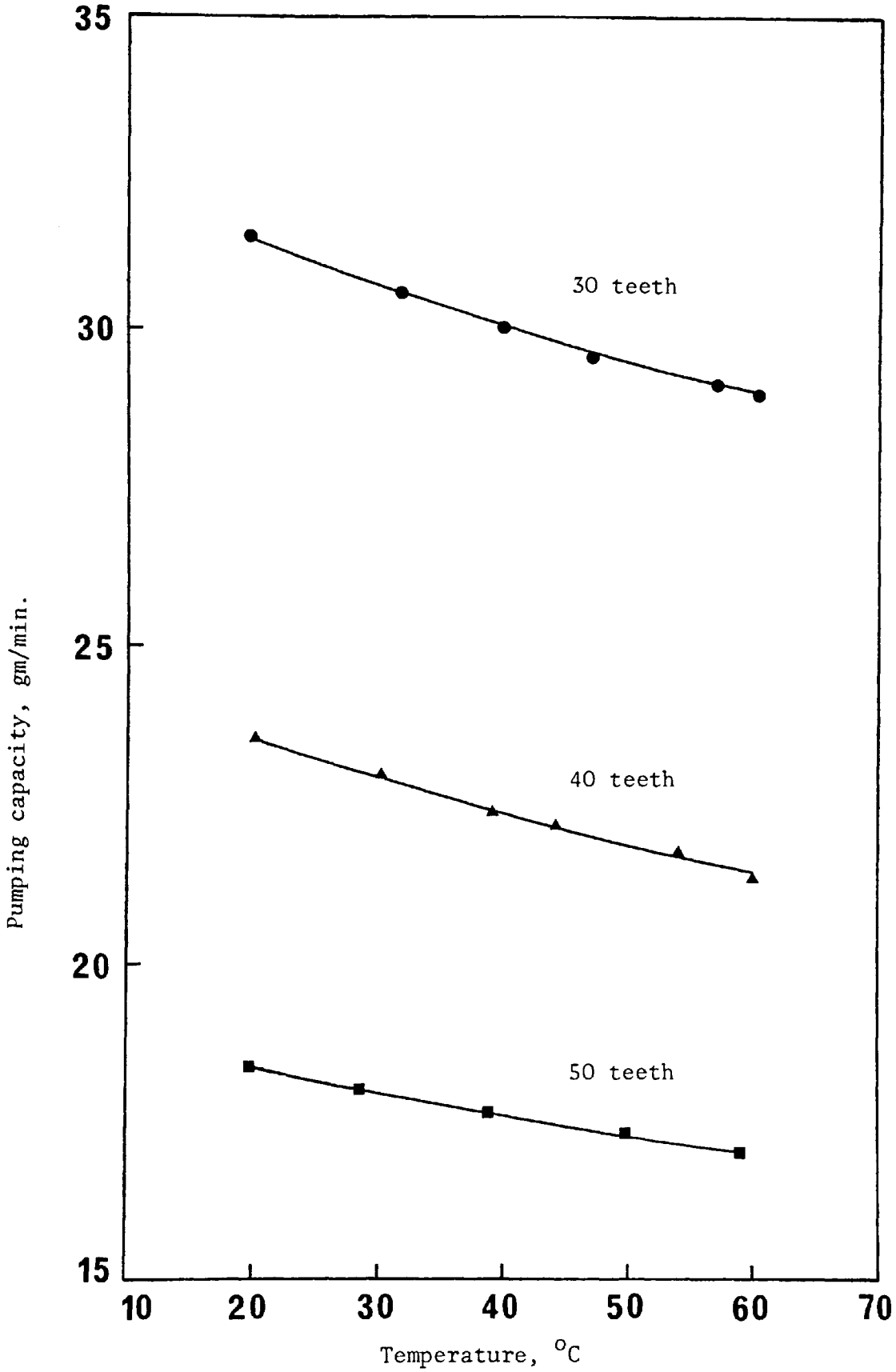

Figure 3.9 : Feed pump calibration, 0.1122 EHP mole fraction.

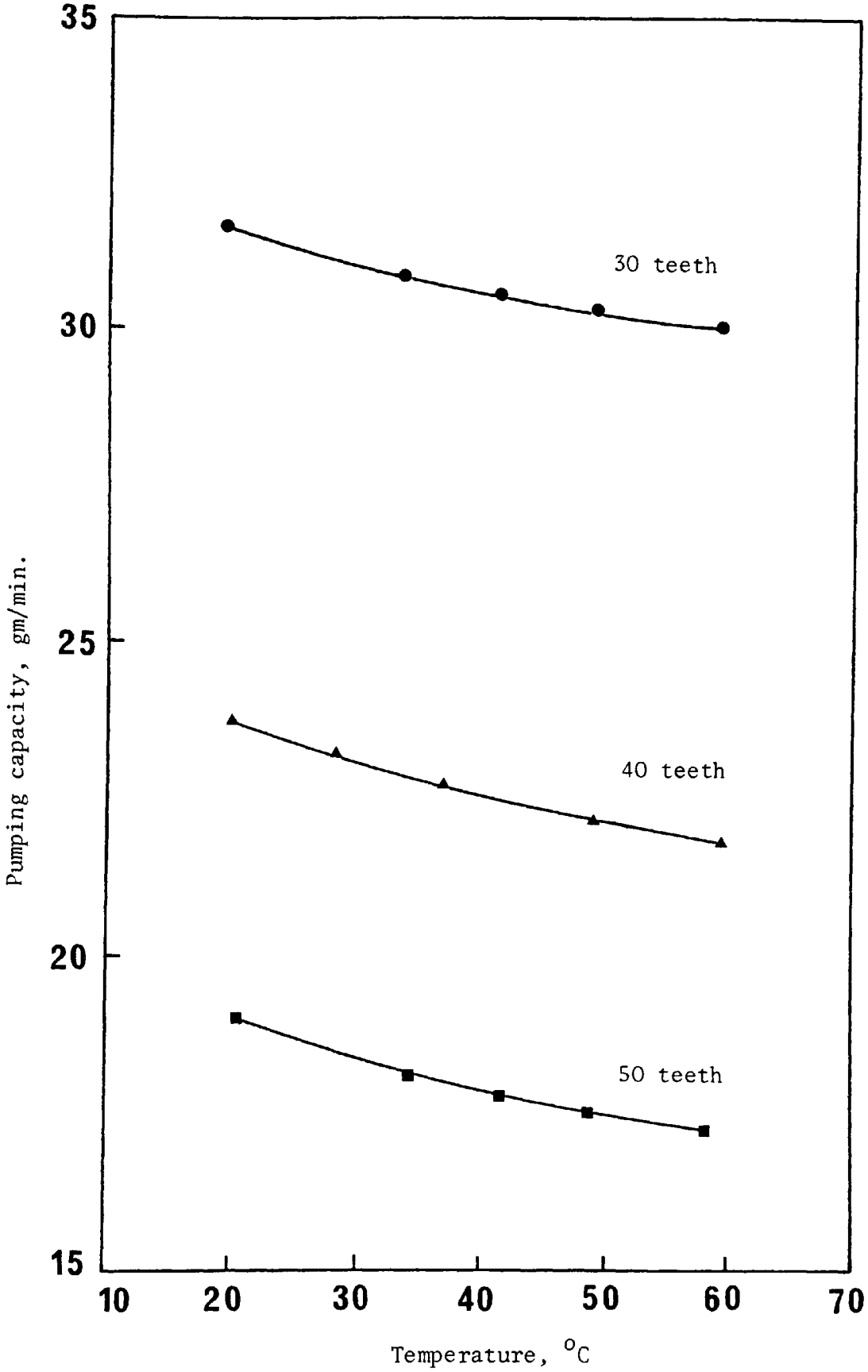

Figure 3.10 : Feed pump calibration, 0.3179 EHP mole fraction.

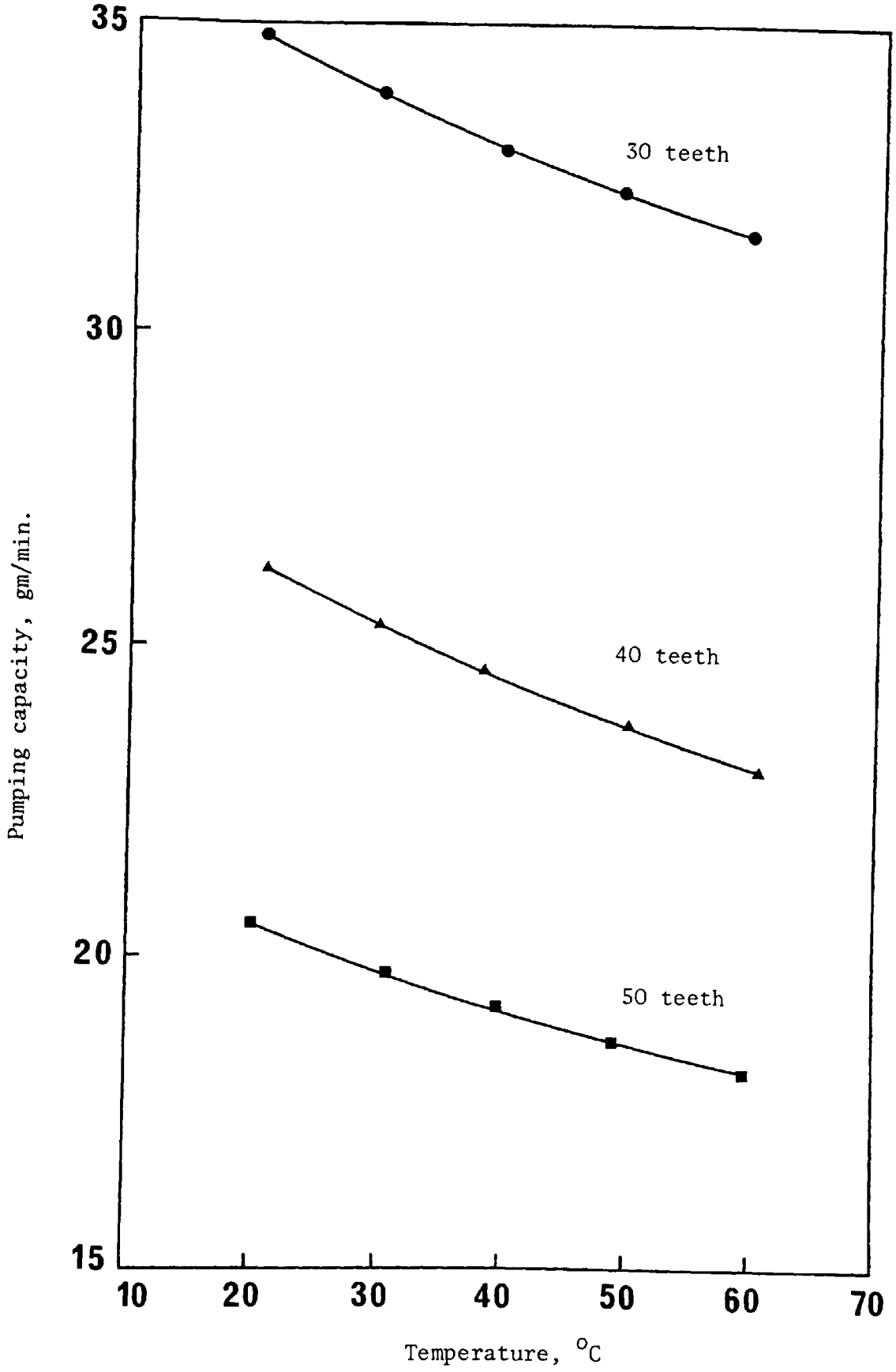

Figure 3.11 : Feed pump calibration, 0.5234 EHP mole fraction.

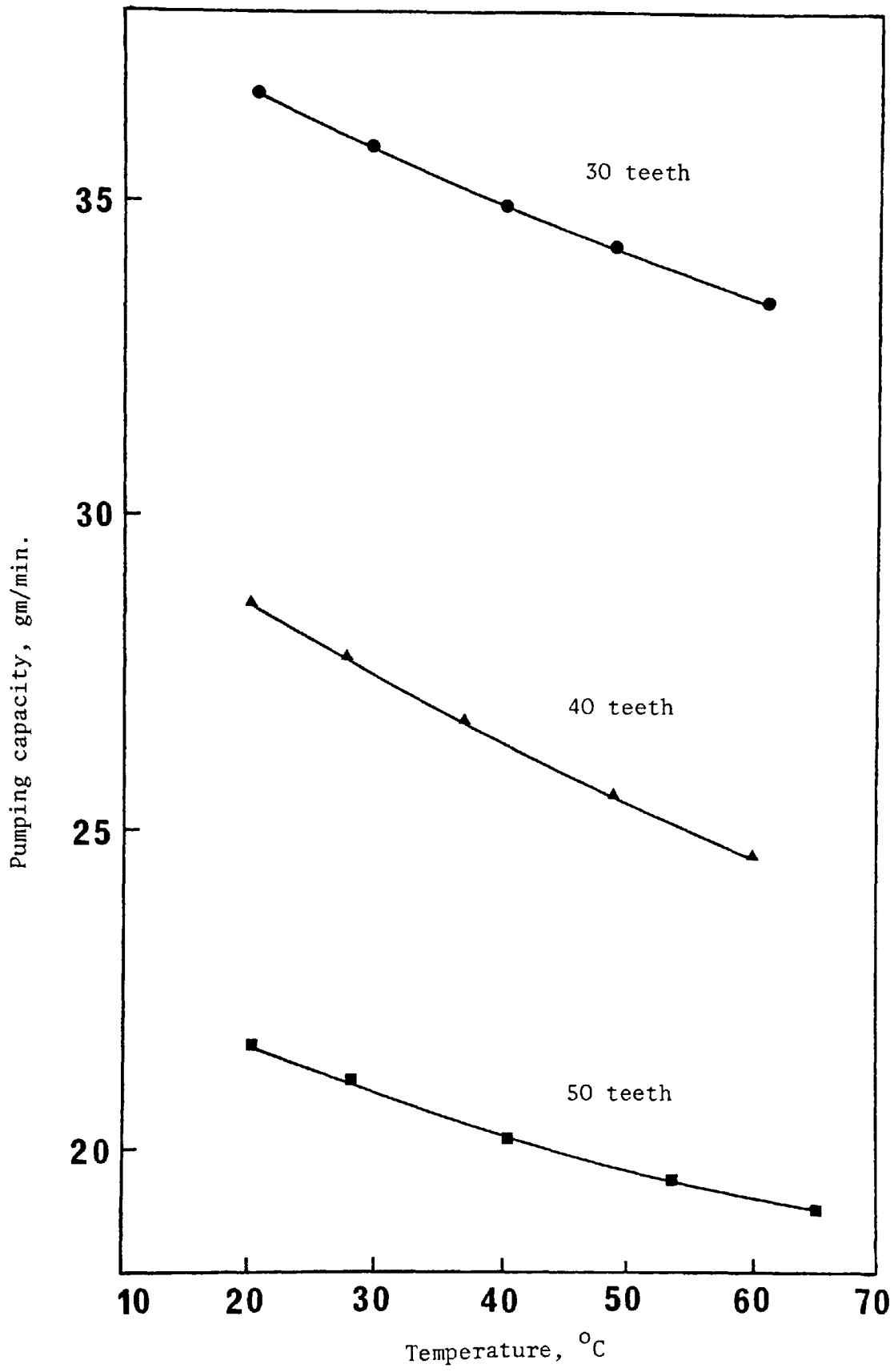

Figure 3.12 : Feed pump calibration, 0.7340 EHP mole fraction.

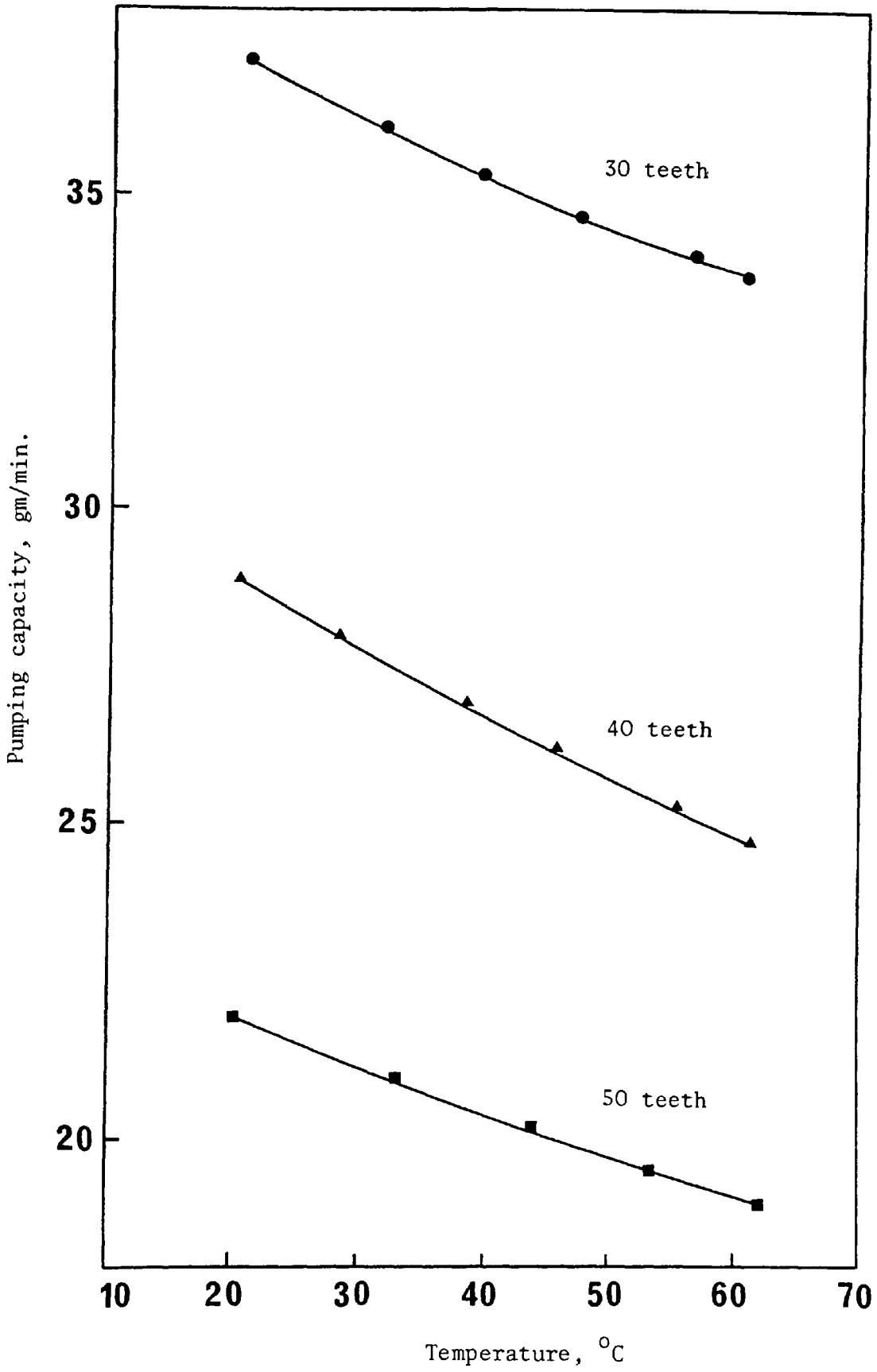

Figure 3.13 : Feed pump calibration, 0.9013 EHP mole fraction.

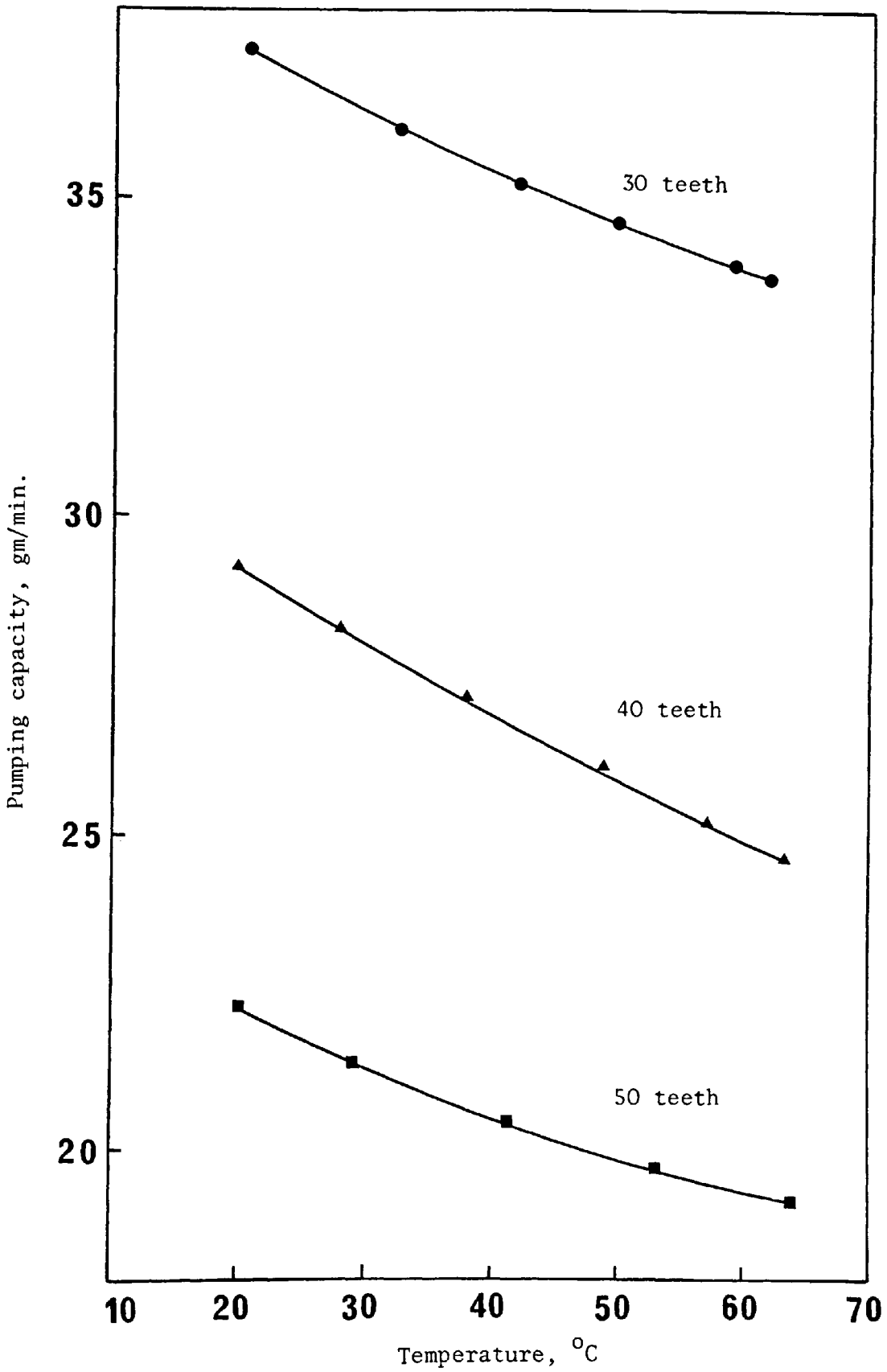

Figure 3.14 : Feed pump calibration, EHP (pure).

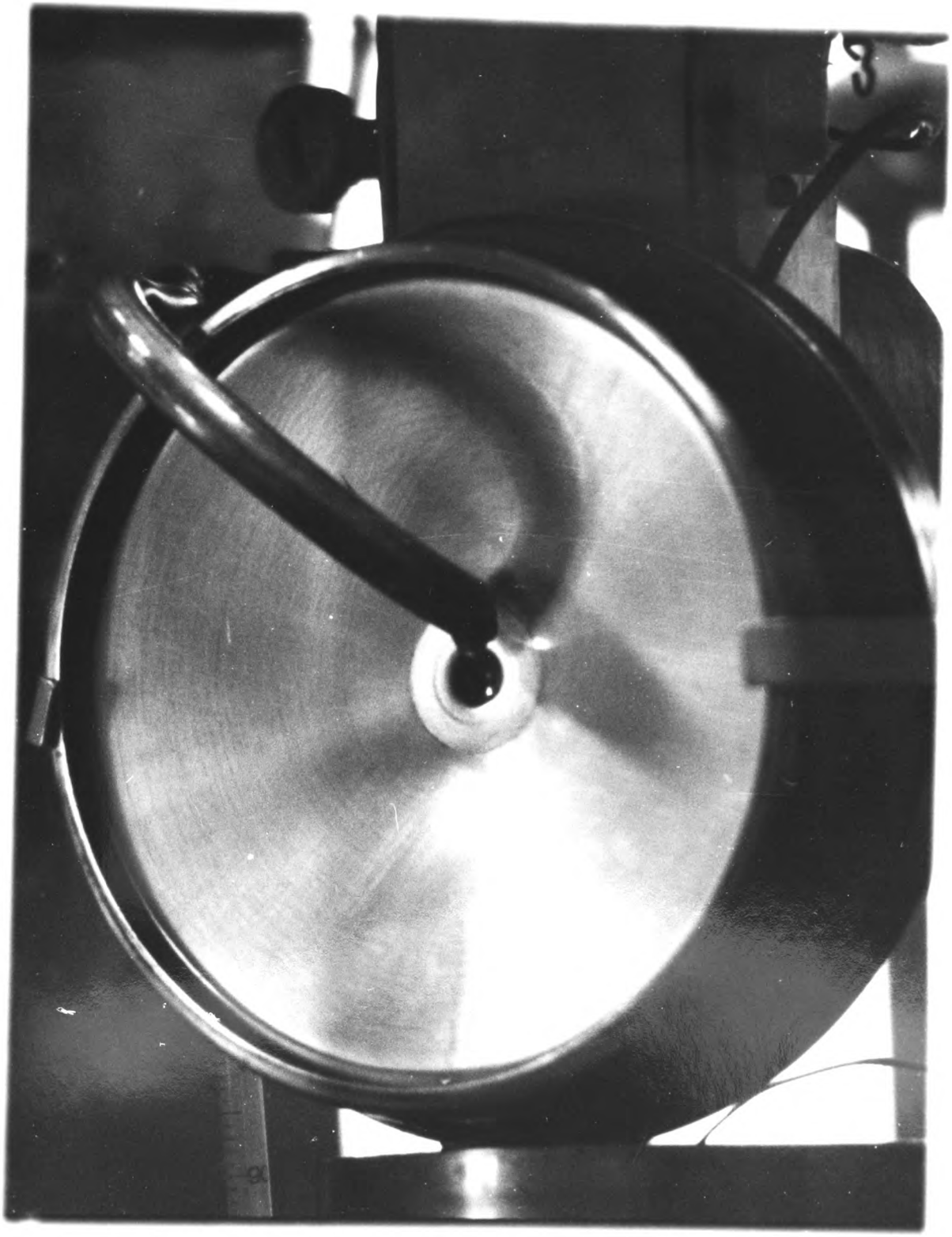

Plate 3.6

Stroboscopic photograph of the rotor without liquid loading

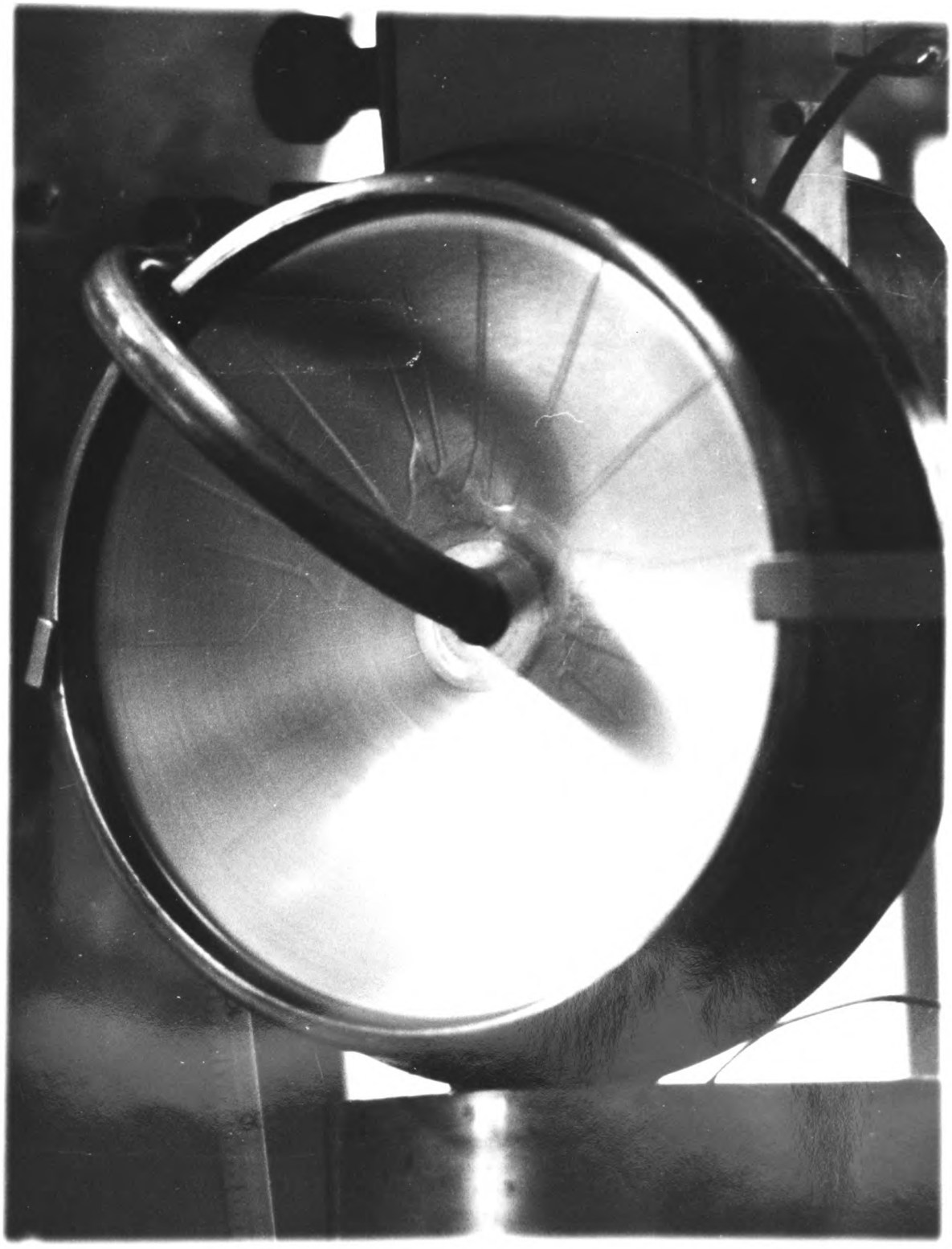

Plate 3.7

Stroboscopic photograph of EHP impinging on the rotor surface at 17^{o}C using low feeding rate

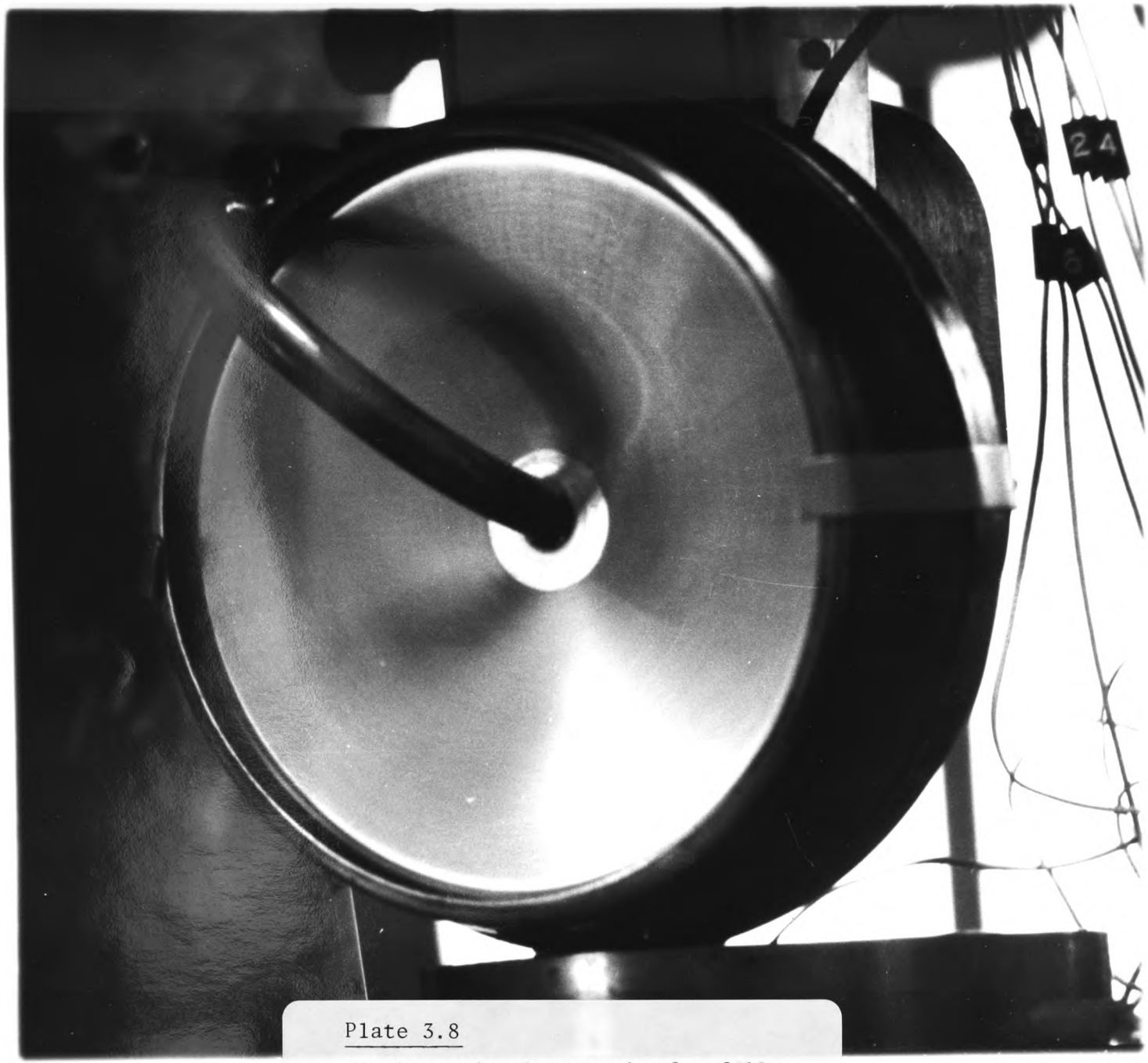

Plate 3.8

Stroboscopic photograph of a fully-developed liquid film on the rotor surface at 17°C using low feeding rate

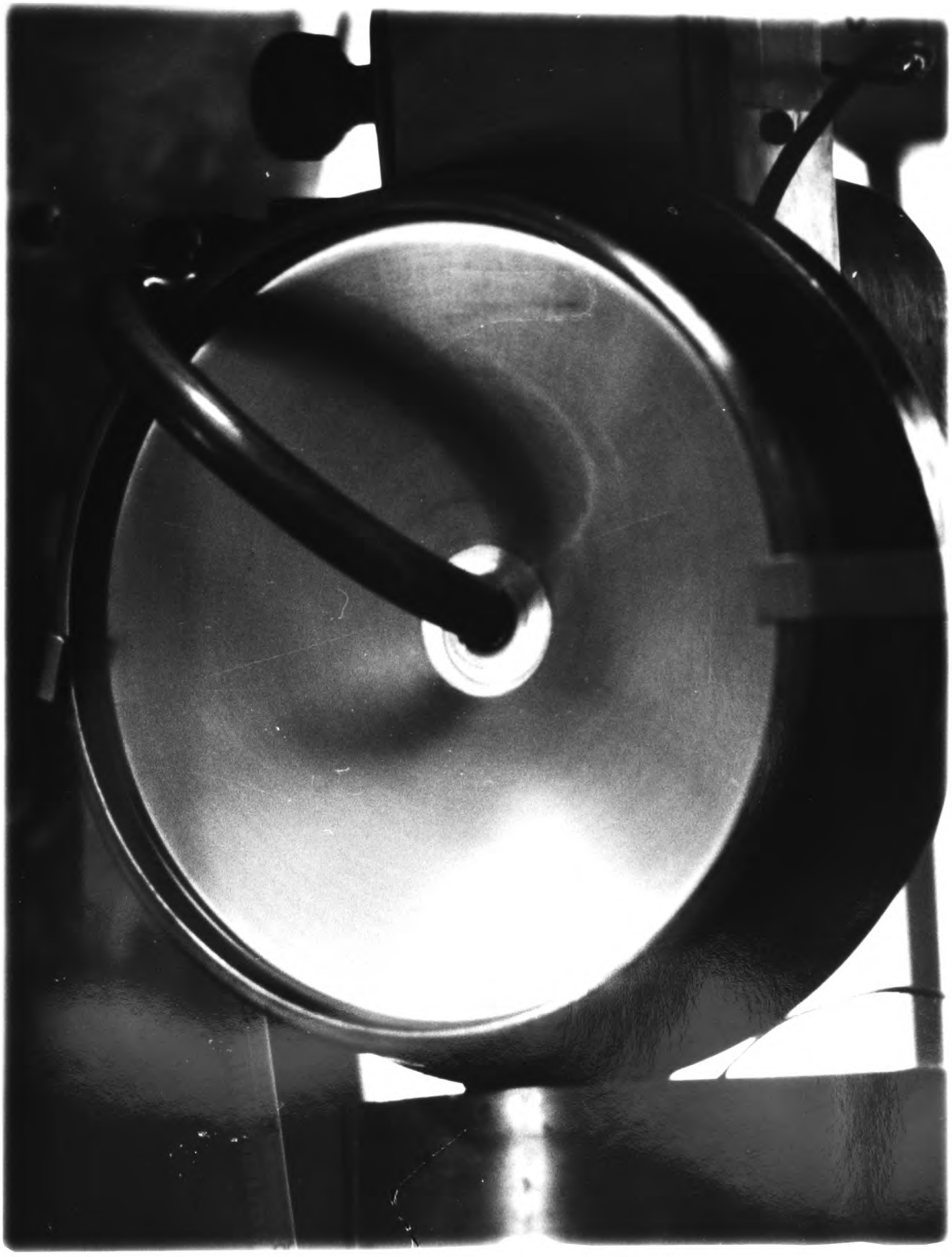

Plate 3.9

Stroboscopic photograph of EHS on the rotor surface, fed at 120°C using high feeding rate

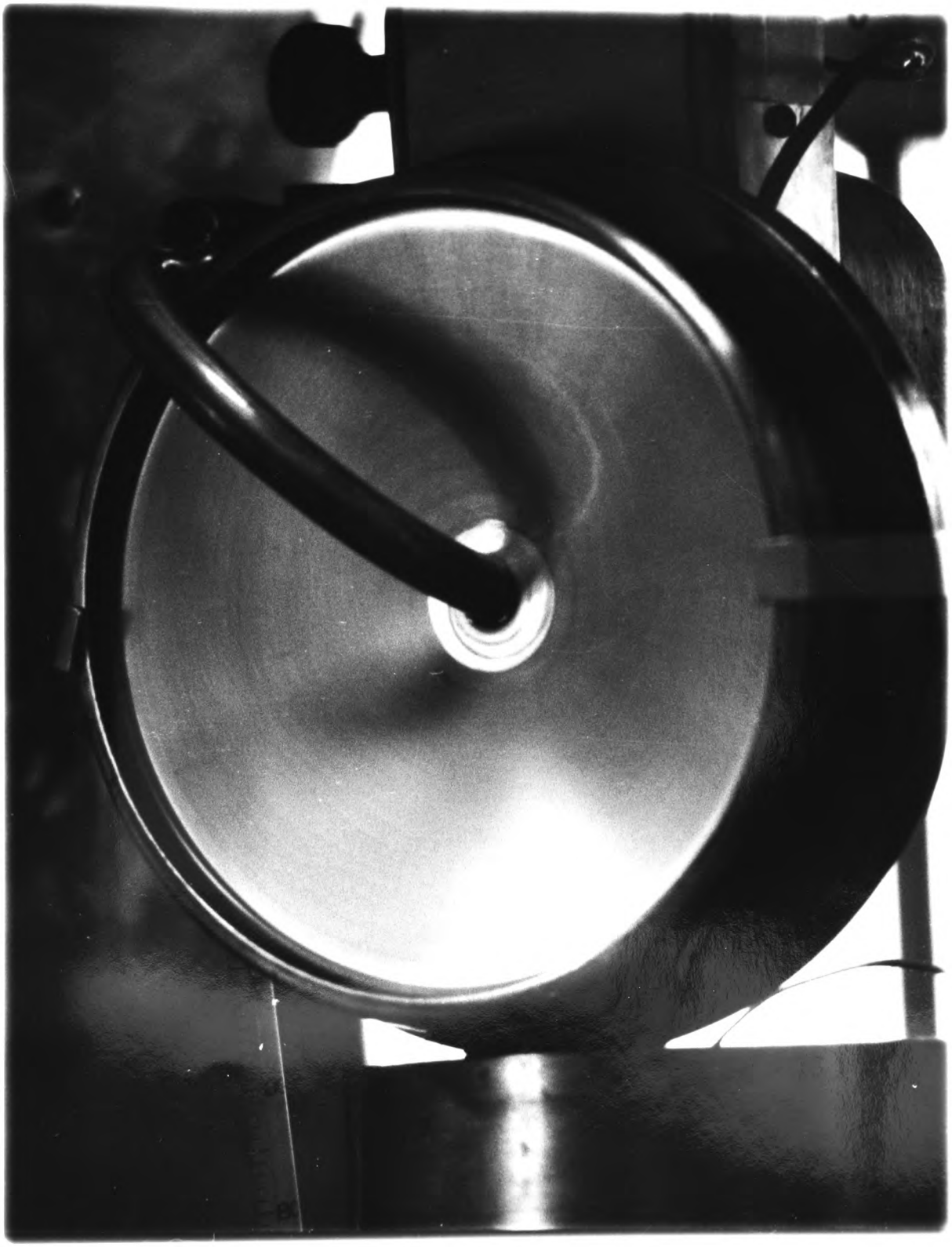

Plate 3.10

Stroboscopic photograph of EHP on the rotor surface, fed at 120°C using high feeding rate

unaffected by the various experimental liquid loadings on the rotor. This speed was checked frequently throughout the experimental investigation.

3.6 LIMITING TEMPERATURE OF MATERIALS

The degasification process, which is a preliminary stage during the process of molecular distillation, is normally speeded up by increasing the temperature of the distilland, but this could increase the thermal hazard [49] of the material, which is contrary to one of the main advantages of the centrifugal molecular still. Therefore a safe degasification temperature was determined using the following simple procedure :

Approximately 100 ml of the pure material was contained in a 200 ml beaker. This was placed in a thermostatically controlled water-bath for a period of four hours. The sample was then taken out, allowed to cool down to room temperature, and its physical properties were examined.

The procedure was carried out on fresh samples of di-2-ethylhexyl phthalate and di-2-ethylhexyl sebacate covering the temperature range $20^{o}C$ to $80^{o}C$ in $10^{o}C$ intervals.

3.7 DISTILLATION PROCESS

3.7.1 Plan of Investigation

3.7.1.1 *Pre-modification of the CMS-5*

A number of preliminary runs concerning the separation of glycerides, silicone oils, aliphatic hydrocarbons, butyl phthalate, and di-2-ethylhexyl phthalate were carried out in order to give good practice in the operation of the molecular still, to test its reliability and limitations, and to open the way to the areas which need modifications.

In addition, evaporation rate studies were conducted on EHP and EHS using three different feed rates.

3.7.1.2 *Post-modification of the CMS-5*

The modified still offered the following controllable parameters:

(1) Rate of cooling water to condenser.

(2) Temperature of feed.

(3) Rate of feed to rotor.

(4) Mean distilland temperature at the periphery.

(5) Composition of feed.

An optimum value of rate of cooling water to condenser was determined using the pure components and employing the highest feed

rate together with a set of mean distilland temperatures ranging from 100°C to 160°C in approximately 10°C intervals. This optimum was kept during all experimental runs.

In order not to expose the material to high temperatures, particularly during the degasification process, the feed temperature was kept fairly low (40 - 60°C) during all experimental runs.

Rate of distillation and composition of distillate measurements were obtained by conducting experimental runs on the pure components and binary mixtures ranging from 10 to 90 mole % in approximately 20% intervals, employing the three available spur gears, and a set of temperatures ranging from 100°C to 200°C in approximately 15°C intervals. The rate of cooling water to condenser and the temperature of feed were not treated as parameters.

3.7.2 Still Preparation

In preparing the still, the following procedure was used prior to every experimental run :

(1) The rotor assembly, feed pump, discharge and feed tubes, base-plate, distilland receiver, distillate receiver, and the bell jar, were cleaned thoroughly with xylene, then with acetone, and dried using hot air.

(2) All thermocouple probes were inspected for location, cleanness, and cracks.

(3) Worm gear and rotor ball-bearing were lubricated.

(4) Rubber connections throughout the system were inspected for cracks.

(5) The bell jar L-gasket, withdrawal stopcock, and distillate receiver stopcocks and lipped neck were greased, using a thin film of high vacuum heavy celvacene grease.

(6) Distilled water-ice mixture was placed in the thermos containing the thermocouples cold junction.

(7) The availability of cooling water, power, and liquid nitrogen supplies were ascertained.

(8) The proper working order of all items was checked.

In addition, full service of the still and the vacuum system was carried out frequently according to procedures outlined in the CVC Instruction Bulletin 3-5-A.

3.7.3 Test Sample Preparation

To achieve the accurate rate measurements aimed at in the present investigation, the commercial di-2-ethylhexyl phthalate and di-2-ethylhexyl sebacate were initially distilled separately under conditions of high vacuum molecular distillation, using the present still. With this process, it was possible to obtain pure materials with physico-chemical properties matching the properties reported

in the literature [19] for the pure compounds. The procedure will be outlined in Section 3.7.4.

In order to prepare a test mixture, a total of 4000 gm of the pure compounds making the required composition was prepared in a large beaker. Although the two compounds are soluble in each other, the mixture was mixed thoroughly for a period of two hours, using a magnetic stirrer. The composition of the mixture was then confirmed by the refractometric method. The 4000 gm mixture was then divided into seven small batches, to be used individually during the experimental runs.

3.7.4 Experimental Runs

The physical set-up of the experimental apparatus during a typical experimental run is shown in Plate 3.11.

The ready-clean still was first flushed throughout with a small quantity of the test sample to be distilled, which was rejected after the flushing process. 500 gms of the test sample was introduced to the feed reservoir. Degasification was started by pumping the feed to the rotor surface and circulating it back to the feed reservoir, at the same time engaging the mechanical forepump. This degasification process lasts normally about one hour and, at the end of this period, the pressure falls to about 200 micron Hg and the frothing and bubbling in the liquid stops. Also during this period, the distillate receiver bottles were evacuated, in turn, by opening the three-way valve from one to the other.

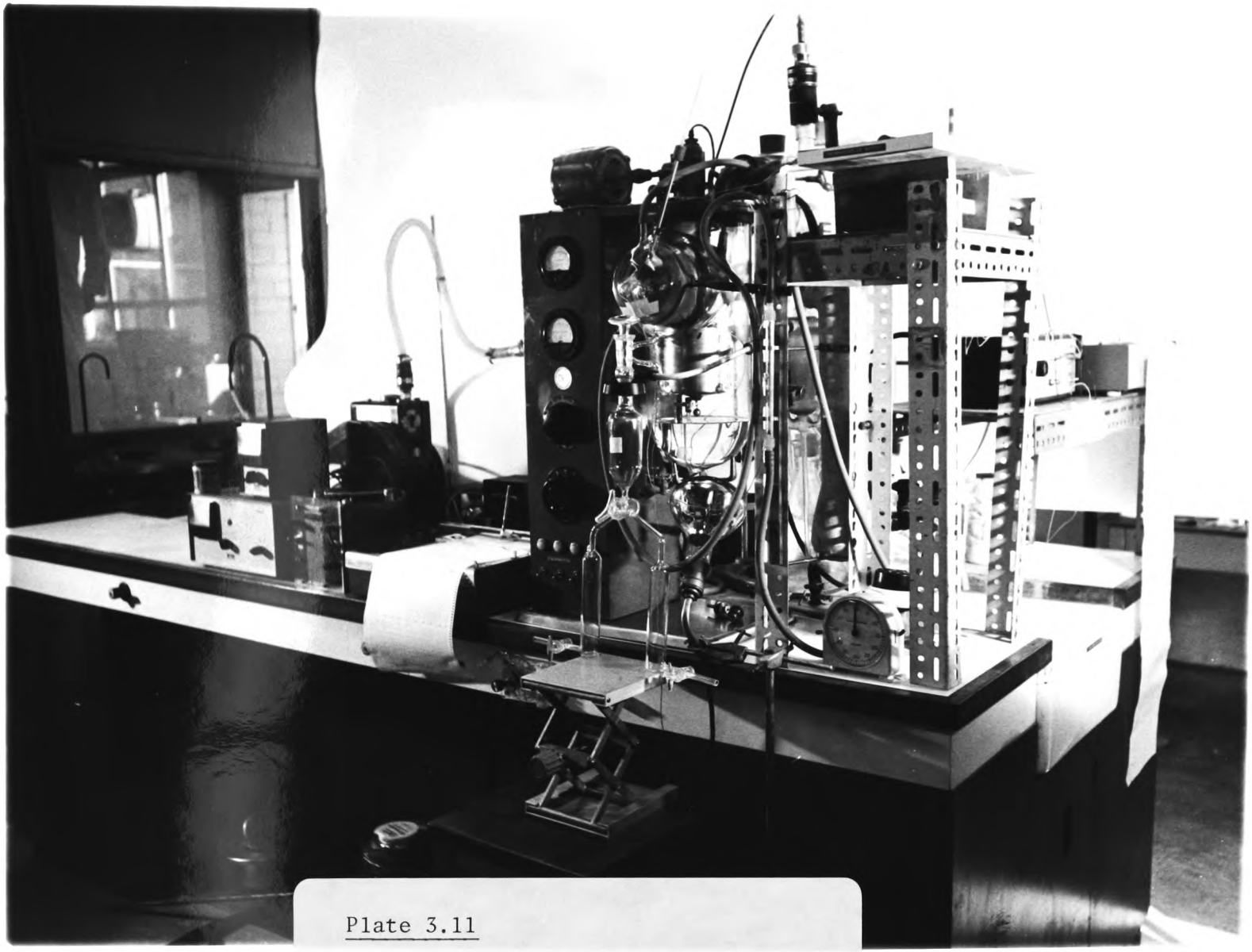

Plate 3.11

Illustration of the modified CMS-5
during a typical experimental run

When assured by this pressure that the system was leak-tight, the following steps were carried out :

(1) The withdrawal stopcock was turned to the circulating position.

(2) The condenser cooling water was supplied.

(3) The oil diffusion pumps were engaged by raising their heat input gradually and, ten minutes later, their cooling water was supplied.

(4) The three cold traps were filled with liquid nitrogen.

(5) The independent pen recorder was engaged.

(6) The heat input to the rotor was supplied and increased gradually until the required temperature of the distilland at the periphery was reached. At the same time, the cooling water to the rotor was supplied.

As soon as the pressure falls below 10 microns Hg, fine drops of distillate start accumulating on the inside face of the dome. As the pressure falls further, a thin film of distillate develops and starts flowing down by gravity to the withdrawal stopcock. This distillate was allowed to return back to the feed until the pressure fell below 10^{-4} mm Hg. The system normally reaches the required steady temperature and pressure in about 2.5 hours.

Prior to distillate collection, the distillate receiver bottles were evacuated to the same pressure as that of the still. The electronic switch and the pen recorder were switched on.

When assured that all temperatures and pressures were steady, the distilland ball valve was closed and, at the same time, the 3-way withdrawal stopcock was turned 180^{o} for distillate collection.

In each bottle of the distillate receiver, the same quantity of distillate was collected and the duration of each was recorded. If any pattern of increasing or decreasing duration was observed the entire run was repeated; otherwise the still was shut down.

3.8 MEASUREMENT OF COMPOSITION

Initially, a composition-refractive index curve was constructed. This was carried out by measuring the refractive indices of known compositions of the EHP-EHS system made up to an accuracy of 0.1% from the pure components. The instrument used was the Abbe-60-Refractometer which employs the critical angle effect. Details of the operations and principles of this refractometer is available from the manufacturer [6].

The refractive index measuring procedure was as follows: The surface of the prism of the refractometer was cleaned and kept at a constant temperature (25^{o}C) by circulating water from a thermostatically-controlled bath. Two drops of the test sample were placed on the prism surface and the hinged box was closed over the drops. While observing the field of view in the field

telescope, the control knob was rotated until the borderline appeared. By means of the control wheel, the borderline was placed on the crosswire intersection. By observing the scale reading in the scale telescope, the refractive index was read off.

The refractive indices of distillates and feeds during the course of the experimental investigation were measured using the above procedure and the corresponding value of mole fraction was obtained from the equation of the curve.

The refractometer readings are subject to a minimum error of $\pm$ 0.0001; this results in a limit of error for each observed composition of at least $\pm$ 0.002 mole fraction.

3.9 MEASUREMENT OF VISCOSITY

The Rotovisco Model RV2 was used to determine the viscosity of the pure components and a set of compositions over a range of temperatures. This viscometer employs a large set of sensors, each designed to provide a specified range of shear rate and shear stress. Therefore the viscosity range is also defined for each sensor.

Preliminary tests with various sensors proved that the NV viscosity sensor system was the most suitable for the present investigation. This sensor system consists of a cup and a bell-shaped rotor, both of which are mathematically defined and used with a tempering

vessel. The tempering vessel and cup are connected to the fitting of a thermostatically-controlled water circulator.

The technique is based on placing approximately 9 cc of the sample in the annular space, between the rotor and the fixed cup, and allowing the water to circulate until the required temperature has been reached. The rotor is driven by an electrically-controlled motor at a defined r.p.m. The torque produced by the sample under test is measured by the measuring head and transformed into an electrical value by means of a high precision potentiometer. The voltage output, S, of the potentiometer is linear to the angular displacement of the spring inside the measuring head, and is indicated on the control console.

The viscosity of the sample can then be calculated from the following equation :

$$\mu = \frac{G \cdot S}{n} \qquad \text{(centipoise)}$$

where

G = instrument factor, depending on type of measuring head and sensor system;

G = 300.557 (cps/scale grad.min) for the NV sensor system, using measuring head MK 500 ;

n = test speed (rpm).

The viscosity of each sample was found to be the same for each n/S relationship. Thus, the material exhibits Newtonian behaviour. The reproducibility of the measurement on the same sample

was within 3%. This was attributed to frictional effects.

Specific details of the Rotovisco construction and operation are available in the Rotovisco RV2 instruction manual which is obtainable from the manufacturer [37].

3.10 MEASUREMENT OF SPECIFIC HEAT

Specific heats have been obtained using a differential scanning calorimeter, model Perkin-Elmer DSC-2, coupled with a Tektronix 31 programmable calculator system via a Perkin-Elmer calculator interface.

The DSC-2 instrument is of the power-compensator type; the sample and reference material being contained in separate furnaces and supplied with separate heaters. The two furnaces are maintained normally at the same temperature by a servo system, operated by platinum resistance thermometers which control the amount of heat supplied to each furnace.

When an endothermic or exothermic reaction takes place in the sample, the change in power required to maintain the sample holder at the same temperature as the reference holder - that is, its programmed temperature - during the reaction is recorded as a peak on a strip chart recorder. The chart abscissae indicates the temperature range at which the reaction takes place and the total peak area indicates the total energy transfer to or from the sample.

If no reaction takes place in the sample over the given temperature range, the displacement of the position of the instrument baseline with the sample in the sample holder, from the position of the baseline with the sample holder empty at any temperature within that range, is directly proportional to the heat capacity of the sample.

The procedure was to link the calculator to the DSC-2 and obtain a baseline over the required temperature range with the sample and reference holder containing empty aluminium sample pans; and then the baseline was obtained with the sample in the sample pan.

The sample weight, temperature range, heating rate, and sensitivity were entered into the calculator SPECIFIC HEAT PROGRAM at the beginning of the test. At the end of the test, the calculator provided a printout of the specific heat of the sample at regular temperature intervals across the temperature range used.

Details of the DSC-2 are available from the manufacturer [86].

CHAPTER IV

THE BINARY MIXTURE

4.1 THE CRITERIA REQUIRED FOR A TEST MIXTURE

For a test mixture to be capable of characterising a certain type of molecular still, Rees et al [95] give a list of requirements which should be observed when choosing a pair of liquids. A summary of the main points of that list which each liquid should have is given below :

(1) To have a vapour pressure in the range 1×10^{-2} mm to 1×10^{-4} mm at operating temperatures.

(2) To conform, as closely as possible, to ideal mixing and solution behaviour.

(3) To be capable of making a mixture whose relative volatility does not depend considerably on temperature.

(4) To be well characterised as to physical properties.

One other important criterion which should not be overlooked is that the relative volatility of the mixture should also be composition-independent. However, extensive search through the literature resulted in only a few binary mixtures which relatively conform to the necessary requirements. The most suitable of these mixtures are the following :

(1) dibutyl phthalate and dibutyl azelate [74,113];

(2) di-2-ethylhexyl phthalate and dibutyl azelate [71] ;

(3) di-n-octyl phthalate and di-2-ethylhexyl sebacate [87] ;

(4) dibutyl phthalate and di-2-ethylhexyl sebacate [95] ;

(5) dibutyl phthalate and dibutyl sebacate [61] ;

(6) di-2-ethylhexyl phthalate and di-2-ethylhexyl sebacate [26,95];

The first three of these systems are characterised by a noticeably temperature-dependent relative volatility. The fourth system has a high relative volatility, giving it the advantage when evaluating low efficiency molecular stills. The fifth system has a relative volatility which is virtually independent of composition but with appreciable temperature-dependence. The last system seems to be the most suitable for evaluating the centrifugal molecular still, since its relative volatility is independent of composition and its temperature-dependency is lower than that of the fifth system.

As a consequence of the above analysis, the system di-2-ethylhexyl phthalate-di-2-ethylhexyl sebacate (EHP-EHS) was chosen as the binary mixture for the evaluation and characterisation of the centrifugal molecular still during the experimental phase of the present investigation.

4.2 MATERIALS

The two components of the binary mixture were supplied by Koch-Light Laboratories Ltd., Colnbrook, Buckinghamshire, England.

These are organic esters and are mainly used as plasticizers [21] and diffusion oils [57] due to their low vapour pressure and high resistance to air and water vapour.

(1) Di-2-ethylhexyl phthalate (EHP)

Structural formula:

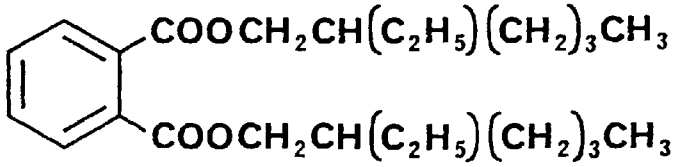

Molecular formula : $C_{24}H_{38}O_4$

Molecular weight : 390.57

Purity on delivery from suppliers : > 99%

Refractive index n_D^{20} on delivery from suppliers: 1.4872

Solubility : in water < 0.01% at 20°C and miscible with most organic solvents.

Colour : pale yellow.

(2) Di-2-ethylhexyl sebacate (EHS)

Structural formula :

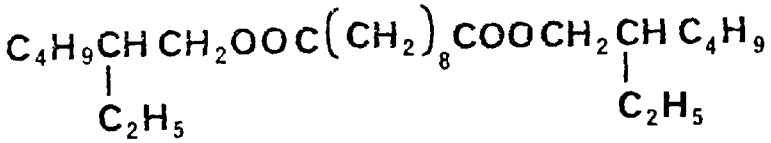

Molecular formula : $C_{26} H_{50} O_4$

Molecular weight : 426.68

Purity on delivery from suppliers : ~ 93%

Refractive index n_D^{20} on delivery from suppliers: 1.4504

Solubility : in water < 0.025% and soluble in ethanol, acetone, and benzene.

Colour : Colourless.

4.2.1 Hazards and Handling of Materials

Experiments [66] indicate that under the normal conditions of industrial use, di-2-ethylhexyl phthalate should present no toxic hazard.

Fumes from the heated material may cause irritation of the eyes and respiratory system. It is a combustible liquid at elevated temperature, flash point 225°C (open cup).

The toxicity of di-2-ethylhexyl sebacate is still unknown. Goggles and gloves were used during the preparation of test samples, and a respirator when the materials were exposed openly to heat.

4.3 PHYSICAL PROPERTY DATA

4.3.1 Vapour Pressure

The lack of vapour pressure data reported in the literature on the EHP and EHS is surprising. However, some data are available

but with large discrepancies. Most of these data have been found to fit the Clausius-Clapeyron equation,

$$\log P = -\frac{A}{T} + B$$

where

P = vapour pressure mm or micron ;

T = temperature ^{o}K ;

A, B = constants.

Table 4.1 illustrates the variation in the values of the constants A and B for both EHP and EHS; it also gives calculated values of vapour pressure of these compounds for two different temperatures, using the related constants. It is, however, impractical to check experimentally the accuracy of these values, and it seems reasonable to choose the most widely used data, i.e. the data of Perry and Weber [89]. Hence, the vapour pressure equations of both compounds become :

$$P_{EHP} = 10^{(14.62 - \frac{5440}{T})} \quad \text{micron}$$

$$P_{EHS} = 10^{(14.90 - \frac{5780}{T})} \quad \text{micron}$$

The variation of vapour pressure with temperature for both components is shown in Figure 4.1.

Table 4.1 : Vapour pressure constants of EHP and EHS.

Compound	A	B	Vapour pressure at 390°K	Vapour pressure at 420°K	Ref.
EHP	5590	15.116	6.06271 μ	64.04367 μ	[50]
	5205	14.15	6.36570 μ	57.16667 μ	[31]
	4870	13.00	3.25702 μ	25.39580 μ	[60]
	5440	14.62	4.69118 μ	46.51778 μ	[89]
	5590	12.12	0.006119 mm	0.064636 mm	[5]
	5757	12.47	0.005111 mm	0.057924 mm	[5]
	5368.71	11.489	0.005285 mm	0.050858 mm	[16]
	5822	12.729	0.006322 mm	0.073637 mm	[93]
	3811	12.639	0.004535 μ	48.91294 μ	[112]*
EHS	5514	14.26	1.32293 μ	13.53407 μ	[31]
	6434	16.54	1.10297 μ	16.63230 μ	[31]
	5780	14.90	1.20085 μ	13.74343 μ	[89]
	5934	12.25	0.001083 mm	0.013226 mm	[102]
	5953.5	12.374	0.001284 mm	0.015813 mm	[16]

* The values of vapour pressure were evaluated using Antoine equation, where the third constant, C = 201.2.

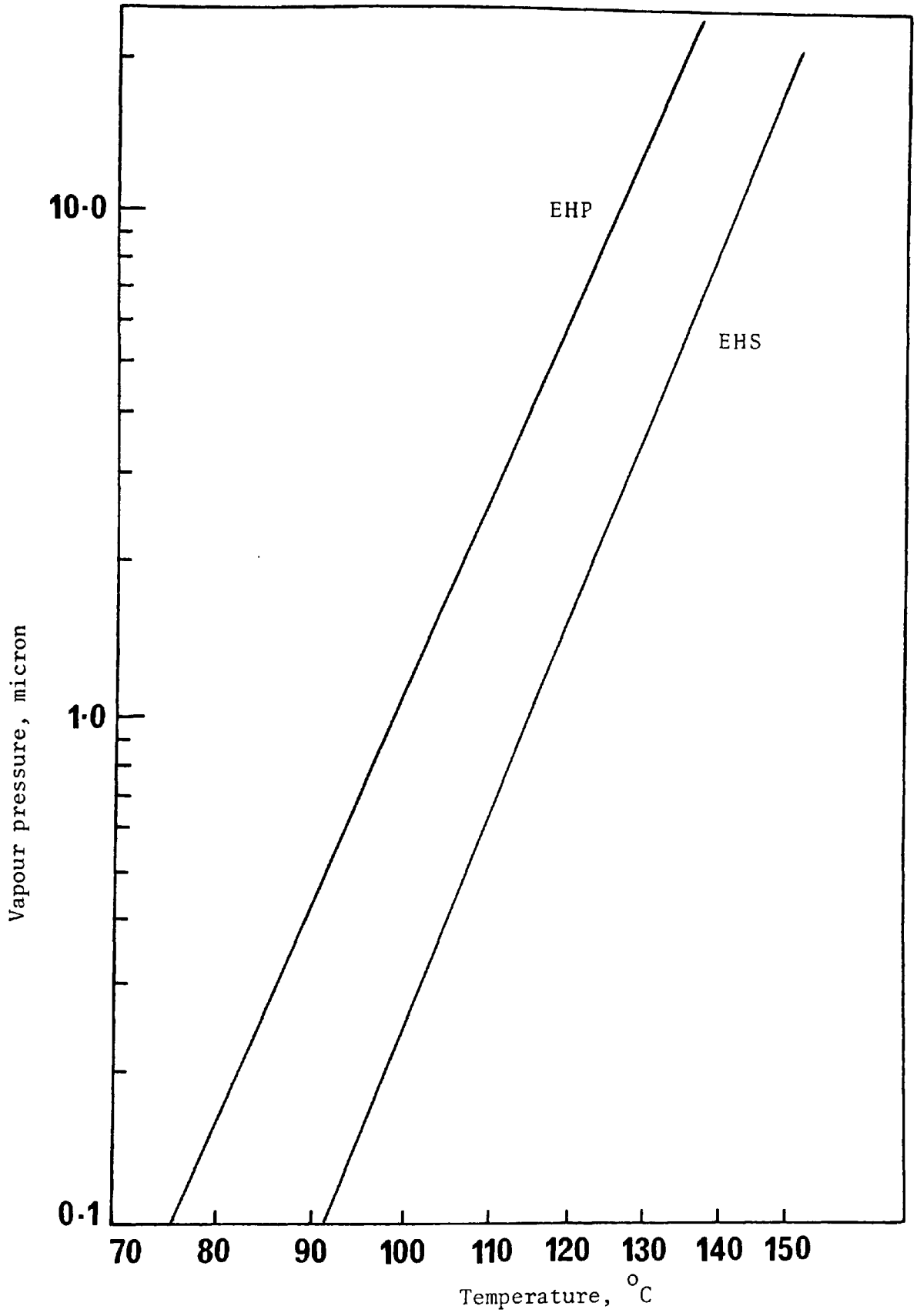

Figure 4.1 : Vapour pressure of EHP and EHS as a function of temperature.

4.3.1.1 *Theoretical Relative Volatility*

It can be recalled from Chapter II that the theoretical relative volatility of a binary mixture under conditions of molecular distillation is given by :

$$\alpha_m = \frac{P_1}{P_2}\sqrt{\frac{M_2}{M_1}}$$

Using the data given in the previous section, the variation of theoretical relative volatility with temperature has been calculated and the results are shown in Figure 4.2.

4.3.1.2 *Experimental Relative Volatility*

The problems associated with the experimental relative volatility under conditions of molecular distillation have been discussed in Chapter II. Figure 4.2 shows the results obtained by various investigators when studying the EHP-EHS system.

An investigation has been carried out by Ziolkowski [117] regarding the limiting temperatures of EHP and EHS. The results are presented in Table 4.2 and these can explain why the experimental relative volatility starts falling in the vicinity of and above the temperature of 114°C.

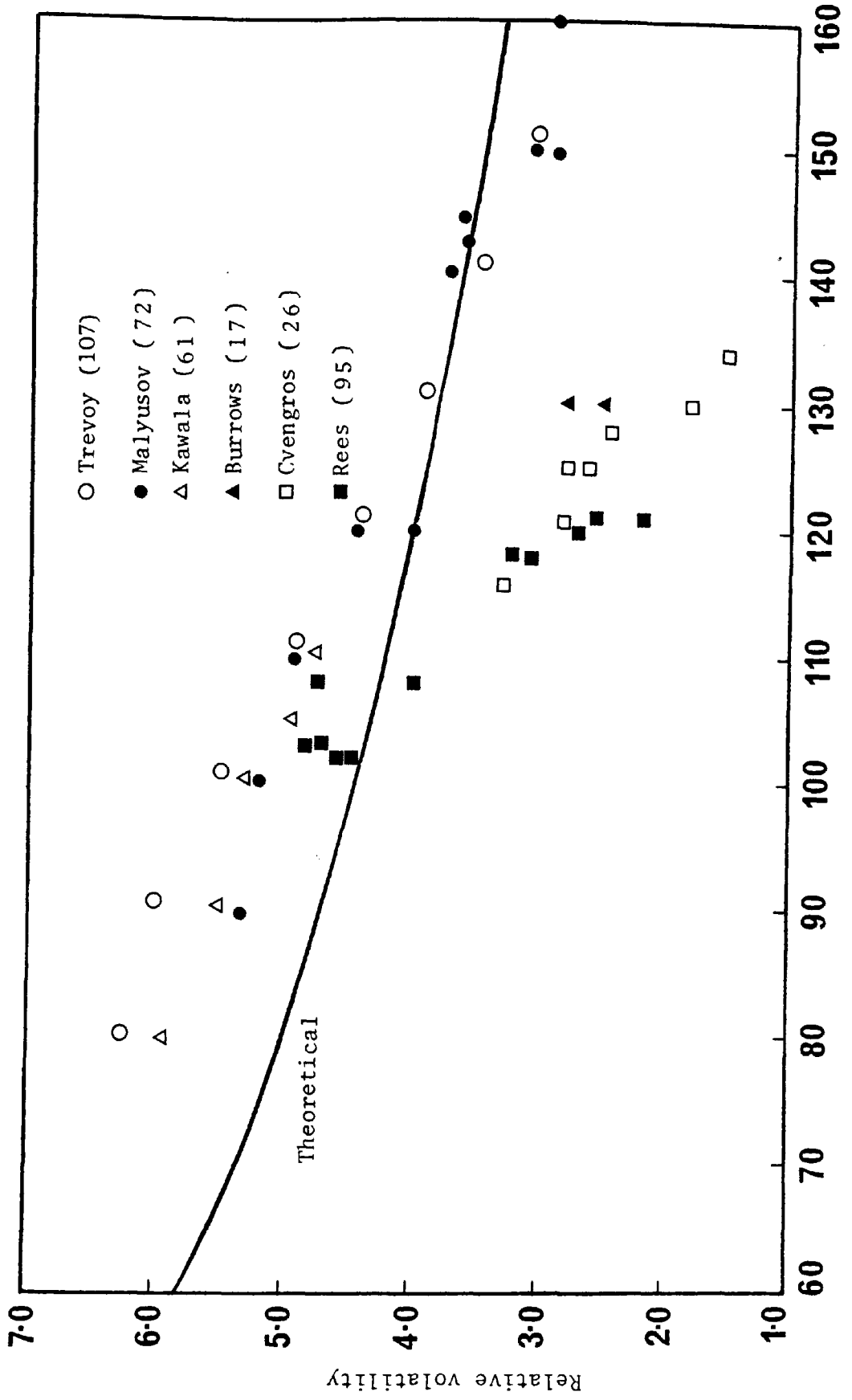

Figure 4.2: Theoretical and experimental relative volatility as a function of temperature.

Table 4.2 : Limiting temperatures of EHP and EHS.

Kind of vaporization	EHP	EHS
Molecular	$t < 114^{o}C$	$t < 132^{o}C$
Intermediate	$114^{o}C < t < 152^{o}C$	$132^{o}C < t < 170^{o}C$
Equilibrium	$t > 152^{o}C$	$t > 170^{o}$

4.3.2 Thermo-Physical Properties

4.3.2.1 *Thermal Conductivity*

Experimental measurements have been performed by Poltz [91] regarding the thermal conductivity of some dialkylphthalate compounds, including EHP. It was found that the thermal conductivity changes linearly with temperature and has very little dependence on the thickness of the liquid layer.

Table 4.3 contains extracted values from Poltz's work. These values have been converted from SI units to cgs units.

Figure 4.3 shows the variation of thermal conductivity with temperature for different layer thicknesses. The extrapolations of

Table 4.3 : Thermal conductivity of EHP as a function of temperature for different layer thicknesses.

Liquid layer thickness (mm)	Thermal conductivity × 10^4 (cal sec^{-1} cm^{-1} $^oC^{-1}$)					
	10°C	25°C	40°C	55°C	70°C	85°C
0.458	3.245698	3.197897	3.166826	3.126195	3.095124	3.059273
0.958	3.250478	3.217017	3.183556	3.135755	3.116635	
1.930	3.262428	3.221797	3.193117	3.157266	3.133365	

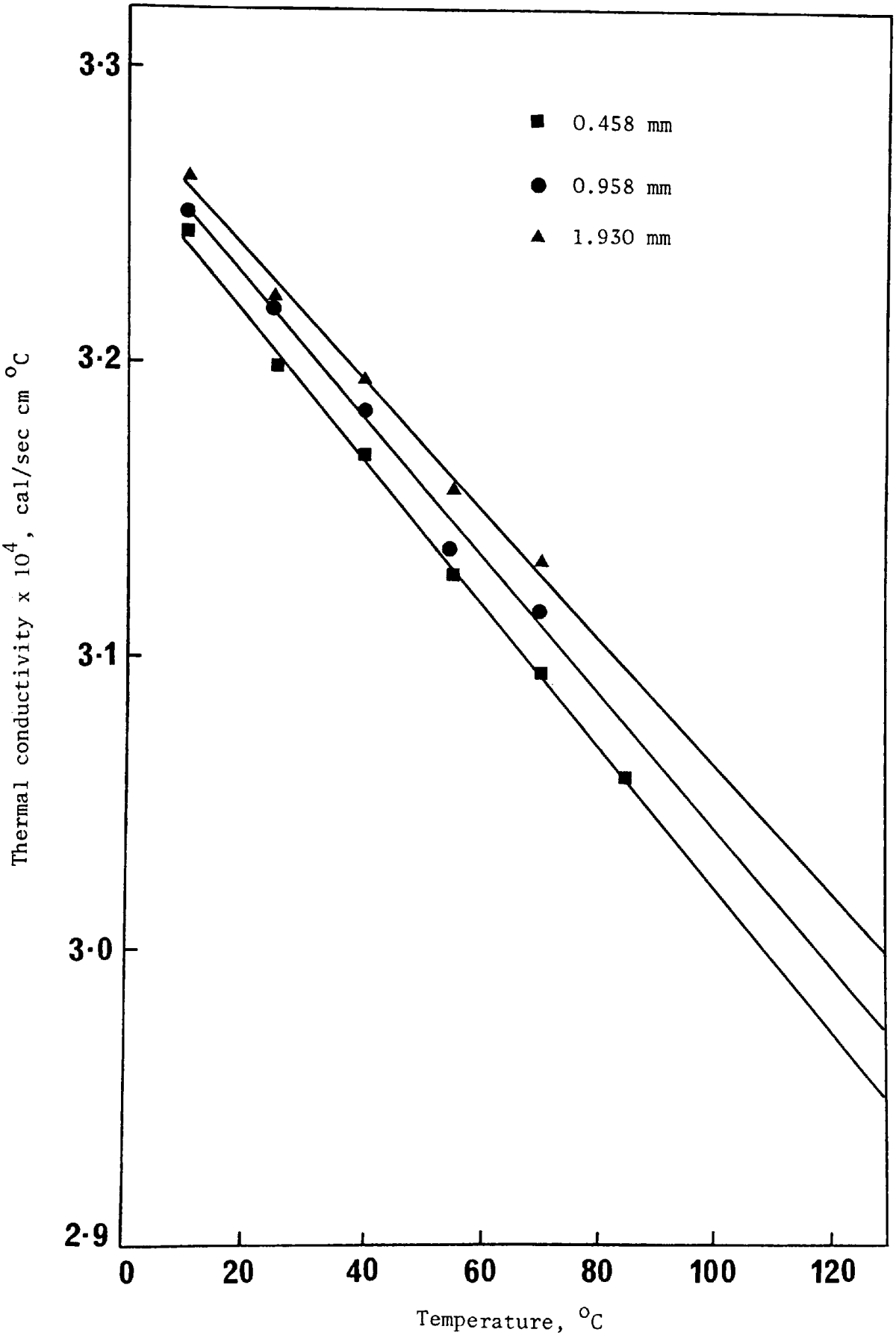

Figure 4.3 : Variation of thermal conductivity of EHP with temperature for different layer thicknesses.

the curves seem to be justifiable since EHP has a high boiling point. The 0.458 mm layer thickness values are thought to be the most suitable for the present investigation since the experimental layer thickness is not likely to be higher than 0.458 mm.

Using a least-squares linear regression program, the thermal conductivity, k, of EHP may be expressed by the following equation :

$$k = 3.264409 \times 10^{-4} - 2.44 \times 10^{-7}\, t$$

(cal/sec $cm^{o}C$)

where

t = temperature (^{o}C).

Unfortunately, data on thermal conductivity of EHS has not been found, despite a thorough search throughout the chemical and physical literature. Although numerous prediction techniques are available [96], it is wisely thought to back-calculate the thermal conductivity using information extracted and manipulated from Greenberg's [38] investigation on the same compound. The method is as follows :

Mean temperature of sample	=	$120^{o}C$
Mean temperature drop, ΔT	=	$0.042^{o}C$
Mean layer thickness,	=	0.0023 cm
Area, A	=	100 cm^2
Mean evaporation rate	=	0.00009 gm cm^{-2} sec^{-1}

and the latent heat of vaporization of EHS as given by Perry and Weber [89] is 61.87 cal gm^{-1}.

Since it has been assumed by Greenberg that the heat flux, q, through the liquid layer is equal to the heat supplied for evaporation, therefore

$$q = 0.00009 \times 61.87$$

$$= 0.0055683 \text{ cal } cm^{-2} sec^{-1}.$$

For heat conduction through liquid films, the simple form of Fourier's Law is :

$$q = k \; A \; \frac{\Delta T}{\delta}$$

Substituting the above values in Fourier's equation, the thermal condutivity is readily found :

$$k = 3.04931 \times 10^{-4} \text{ cal } sec^{-1} \; cm^{-1} \; {}^{o}C^{-1}$$

This seems to fall in the same range of thermal conductivity of EHP, and since the problem under investigation is an engineering one, it is reasonable to adopt the available EHP data for EHS.

4.3.2.2 *Specific Heat*

Since specific heat data on these compounds are not available, the Differential Scanning Calorimeter was used to evaluate the variation of specific heat with temperature for a set of compositions and pure components. Only selected values are shown in Table 4.4, and it may be seen from Figure 4.4 that the specific heat changes linearly with temperature, and also illustrates that the specific heat of the mixture conforms closely to the molal average law.

The straight lines of Figure 4.4 are obtained by using a least-squares linear regression program, and the correlation formula for each one is :

$$C_{EHS} = 8.467394 \times 10^{-4}\, t + 0.4393$$

$$C_{0.1122} = 8.094061 \times 10^{-4}\, t + 0.4399$$

$$C_{0.3179} = 7.823493 \times 10^{-4}\, t + 0.4356$$

$$C_{0.5234} = 7.552297 \times 10^{-4}\, t + 0.4302$$

$$C_{0.7340} = 7.627153 \times 10^{-4}\, t + 0.4192$$

$$C_{0.9013} = 7.185627 \times 10^{-4}\, t + 0.419974$$

$$C_{EHP} = 7.241453 \times 10^{-4}\, t + 0.41406$$

Table 4.4 : Specific heat of a set of mole fractions of EHP as a function of temperature.

EHP mole fraction / Temp. (^{o}C)	0.0000	0.1122	0.3179	0.5234	0.7340	0.9013	1.0000
	Specific heat (cal gm^{-1} $^{o}C^{-1}$)						
78.719	0.5060	0.5036	0.4985	0.4921	0.4820	0.4778	0.4711
88.069	0.5139	0.5112	0.5049	0.4973	0.4874	0.4841	0.4778
97.419	0.5218	0.5187	0.5116	0.5030	0.4927	0.4904	0.4846
108.638	0.5313	0.5278	0.5197	0.5099	0.4994	0.4971	0.4927
117.988	0.5392	0.5354	0.5272	0.5179	0.5079	0.5035	0.4995
127.337	0.5471	0.5429	0.5349	0.5257	0.5136	0.5097	0.5063
138.557	0.5566	0.5520	0.5408	0.5348	0.5240	0.5177	0.5144
147.906	0.5646	0.5596	0.5543	0.5424	0.5360	0.5262	0.5212
157.256	0.5725	0.5672	0.5594	0.5507	0.5397	0.5363	0.5279

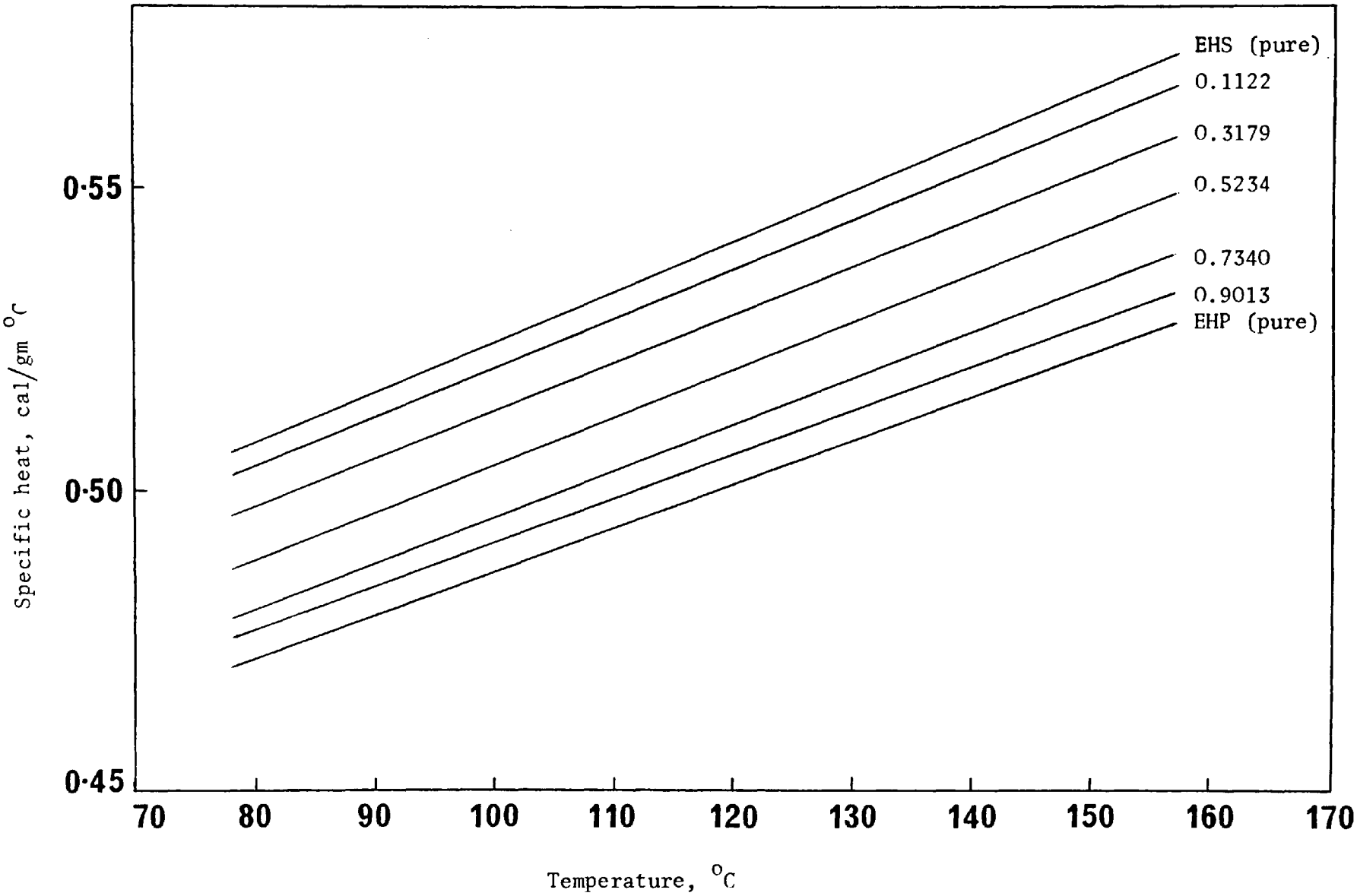

Figure 4.4: Variation of specific heat with temperature for different values of EHP mole fraction.

4.3.3 Rheological Data

Very few investigators [21,38,56,81] give rheological data on these compounds, and even these are only single-point values; but these values, however, offer a basis for comparison with the experimental results obtained here.

The Rotovisco viscometer was used to show that these compounds exhibit Newtonian behaviour; that is, strict proportionality between shear stress and rate of strain, and also to determine the viscosity of the pure compounds and a set of compositions over a range of temperatures up to 97°C. The results are presented in Table 4.5, and the variations are shown in Figure 4.5. Table 4.6 illustrates some of the results obtained here, and those published in the literature. It may be seen that the experimental results are within the practical limits.

Above the temperature of 50°C, the experimental results of EHP and EHS are approximated by the following equations :

$$\mu_{EHP} = 10^{(-1.21731\ t^{0.25} + 4.47608)} \quad \text{(centipoise)}$$

$$\mu_{EHS} = 10^{(44.86476\ t^{-1} + 0.037355)} \quad \text{(centipoise)}$$

with maximum error of 1.73% for the viscosity of EHP and 2.42% for the viscosity of EHS.

Table 4.5 : Viscosity of a set of mole fractions of EHP as a function of temperature.

EHP mole fraction / Temp. (^{o}C)	0.0000	0.1122	0.3179	0.5234	0.734	0.9013	1.0000
	Viscosity (centipoise)						
20	21.10	24.45	33.92	47.20	61.03	74.14	81.17
25	18.00	20.27	26.09	34.83	42.97	51.28	55.31
30	15.29	17.02	21.14	26.59	32.78	38.45	41.40
40	11.19	12.97	15.25	18.09	21.71	24.27	26.35
50	8.40	9.20	10.60	12.43	14.61	16.09	17.19
60	6.38	7.00	7.98	9.23	10.57	11.74	12.37
70	4.77	5.20	5.87	6.74	7.64	8.47	8.88
80	3.86	4.19	4.71	5.40	6.13	6.73	7.05
90	3.43	3.68	3.94	4.34	4.79	5.15	5.34
97	3.18	3.30	3.57	3.82	4.06	4.29	4.45

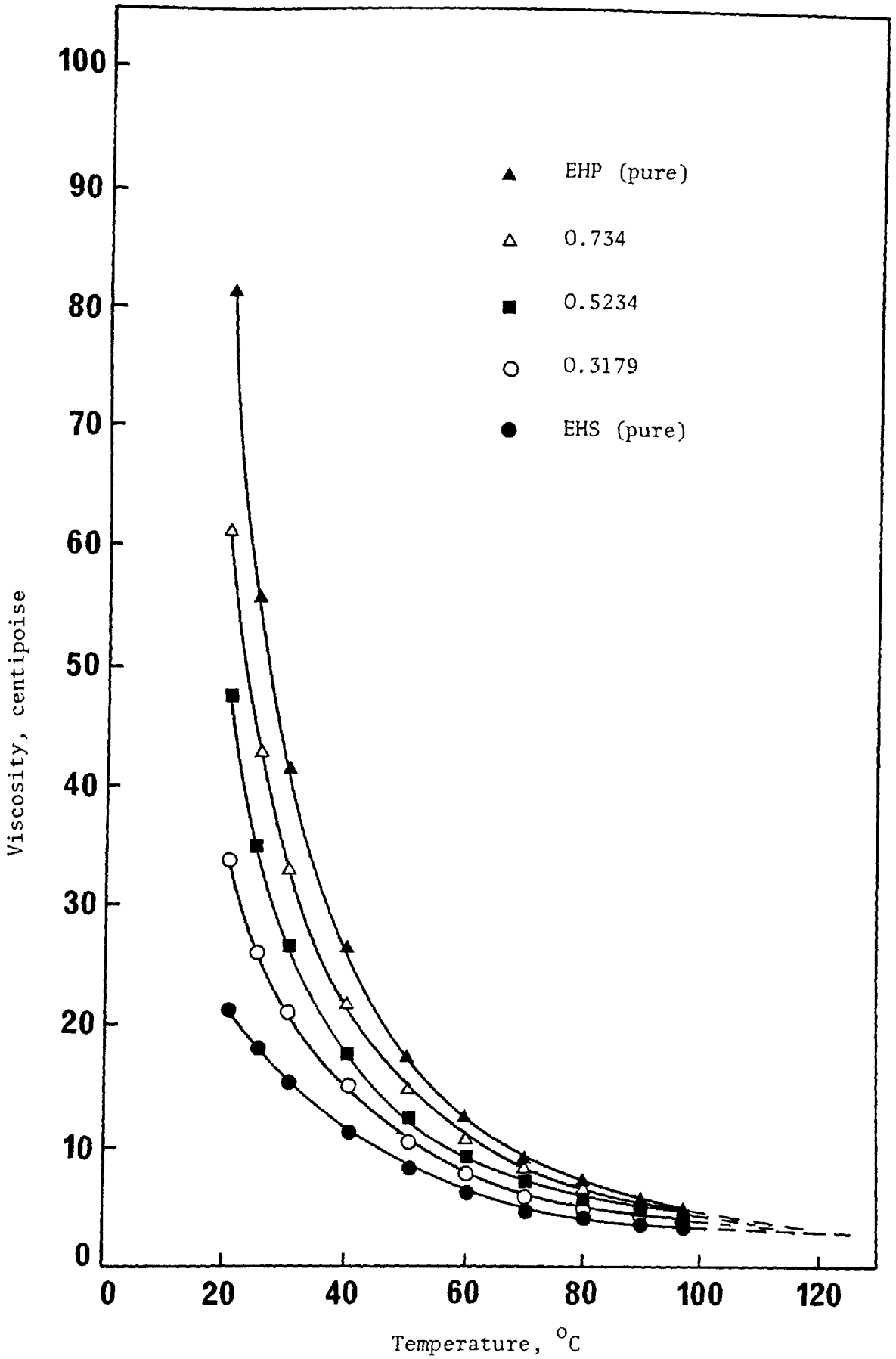

Figure 4.5 : Variation of viscosity with temperature for different values of EHP mole fraction.

Table 4.6 : Viscosity of EHP and EHS : Experimental and reported values.

Temperature (^{o}C)	Viscosity			
	EHP	Ref.	EHS	Ref.
20	81.4 cps	[21]	17.94 cps	[21]
	81.17 cps	*	21.10 cps	*
25			17.85 cps	[81]
			18.00 cps	*
30	43.40 cps	[56]		
	41.40 cps	*		
80			4.04 cst	[21]
			3.86 cps	*
120	2.81 cst	[38]		
	2.80 cps	**		

* Present experimental investigation.

** Extrapolated from the experimental results.

4.3.4 Optical Data

The refractive indices of the EHP-EHS system were determined with an Abbe Refractometer. Figure 4.6 illustrates the variation between the refractive index and the composition at 25°C. The relationship can be expressed by the following second-order equation :

$$n_D^{25} = 1.4488 + 0.02999\ x + 0.00561\ x^2$$

where

n_D^{25} = refractive index at 25°C ,

x = mole fraction of EHP .

The experimental data fit this equation with a maximum deviation of 0.0002.

Neglecting the negative root, this equation has the following solution :

$$x = 13.35115 \sqrt{0.04008 - (1.4488 - n_D^{25})} - 2.6729$$

so that direct results of mole fractions are readily calculated for any value of the refractive index.

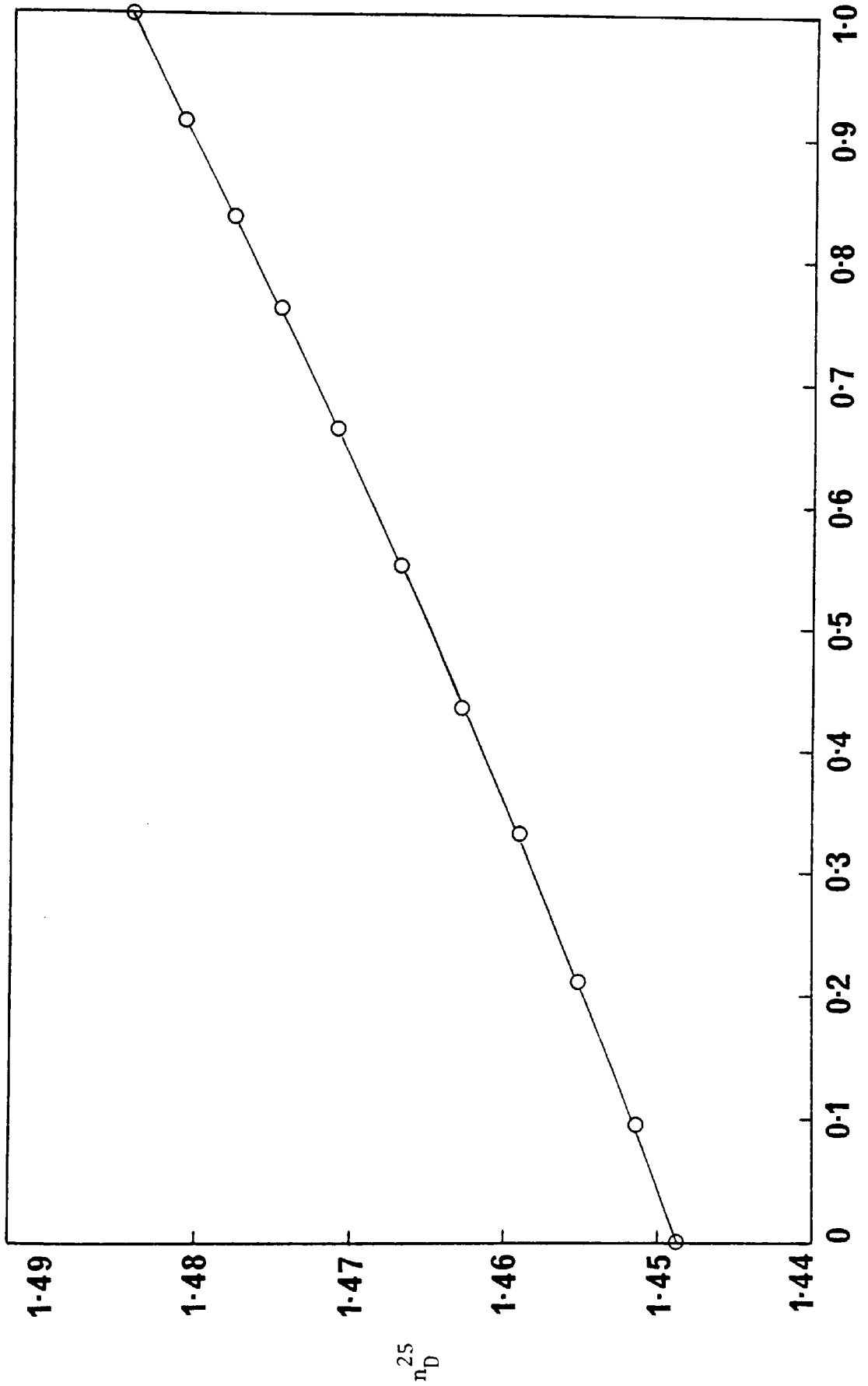

Figure 4.6: Refractive index of EHP - EHS mixtures.

CHAPTER V

THE MATHEMATICAL INTERPRETATION OF THE TRANSPORT PHENOMENA ON A ROTATING DISK

5.1. INTRODUCTION

In summary, a centrifugal molecular still uses low pressure to achieve zero pressure drop and evaporation may take place at any temperature. It employs a renewable thin film developed by centrifugation to attain a high surface to volume ratio and subsequently good heat transfer, and at the same time minimum exposure to the heating surface. These factors combine to reduce the effect of torpidity and minimise the thermal hazard, and hence utilizing the molecular distillation principle to its fullest capability!

The present chapter is intended to provide an approximate mathematical model quantitatively coupling the evaporation rate under vacuum of a binary mixture with the equations of energy and motion, thus relating it to such parameters as composition, film thickness, mean velocity, Reynolds number, and surface temperature, thus providing a basis of interpreting and correlating the experimental results.

5.2 FLUID FLOW

The experimental rotor in relation to the coordinate system is shown schematically in Fig.5.1. The liquid is brought up by the feed tube to the inner part of the rotor surface at a radius r_o. The

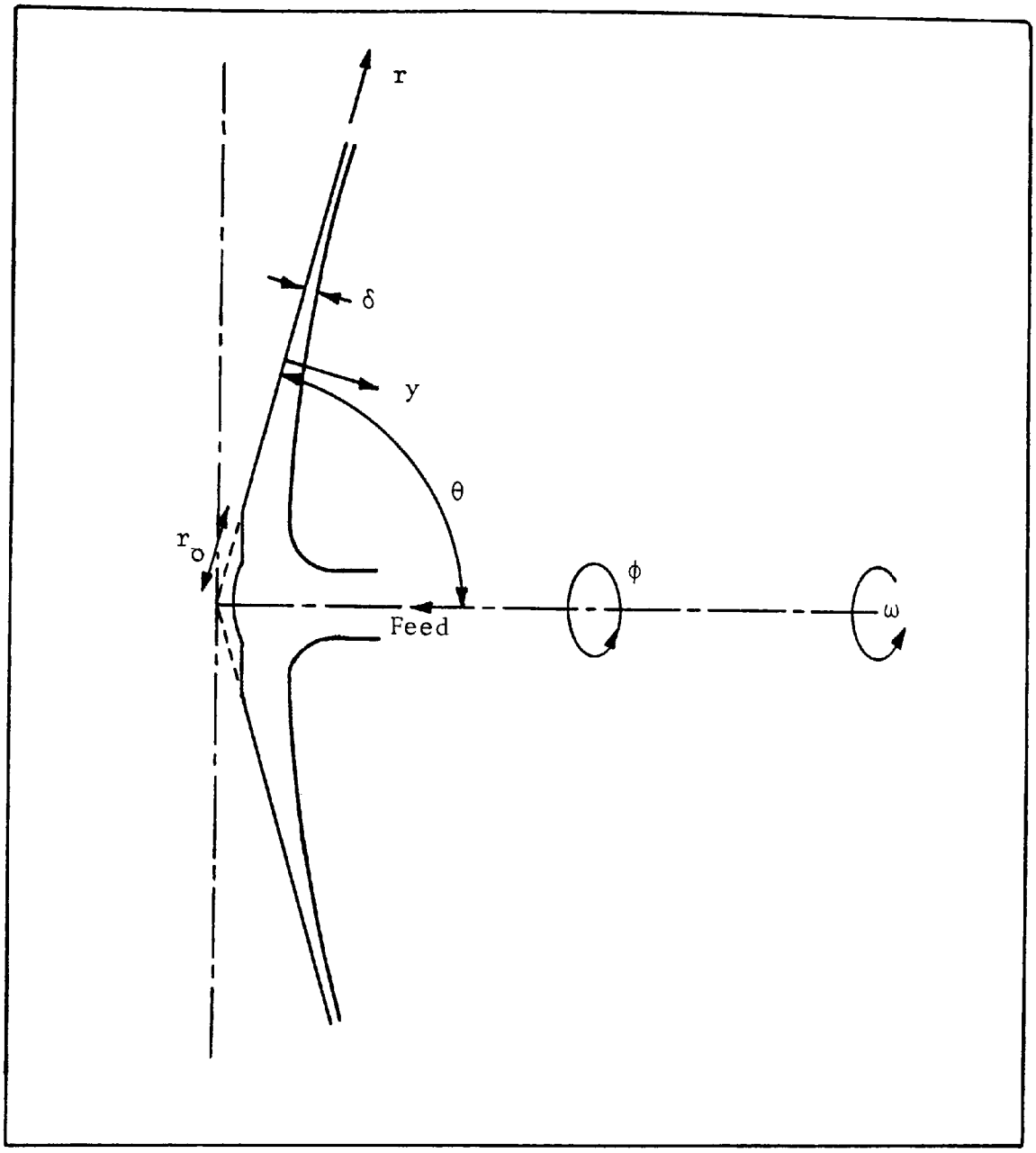

Figure 5.1 : Schematic diagram of the coordinate system of the rotor.

rotational motion of the rotor with an angular velocity of ω radians per second will impart centrifugal forces to the liquid, causing it to flow in a continuous renewable thin film over the entire surface starting at r_o and moving away towards the rim. Thus the case is seen to be one of three-dimensional flow, i.e. there exist velocity components in the radial direction, r, the circumferential direction, ϕ, and the meridional direction, θ. These velocities will be denoted respectively by V_r, V_ϕ, and V_θ.

Many workers [10,29,32,39,53] have assumed that the liquid attains the same rotational speed as that of the rotor, thus ignoring the so-called Coriolis effect [98], while experiments [62,79] show that there may be a difference between the angular velocity of the liquid and the rate of rotation of the rotor. At first the calculation will be performed, taking an account of that difference.

The fluid flow will be considered in terms of spherical coordinates, r, ϕ, θ, as shown in Fig.5.1.

Prior to introducing the equations of motion [8] to this case, the following assumptions are made :

(1) Newtonian laminar flow on the rotor surface.

(2) The effects of the residual gas on the flow are negligible [35].

(3) Surface tension effects are neglected.

(4) The flow is approximately rotationally symmetric.

(5) The thickness of the liquid film is small compared with the rotor radius.

(6) The static pressure is practically constant over the liquid film.

Assumption (5) implies that the meridional velocity is very small when compared with either the radial velocity or the circumferential velocity. If the liquid does not attain the same rotational speed as that of the rotor, then its circumferential velocity relative to the rotor will be given by *:

$$U_\phi = \omega r \sin\theta - V_\phi \qquad \ldots 5.1$$

Hence, by taking into account the above assumptions when comparing the order of magnitudes of the various terms governing the three dimensional flow, the equations of motion and continuity reduce to :

$$V_r \frac{\partial V_r}{\partial r} + \frac{V_\theta}{r} \frac{\partial V_r}{\partial \theta} - \omega^2 r \sin^2\theta + 2\omega U_\phi \sin\theta - \frac{U_\phi^2}{r}$$

$$= \frac{\nu}{r^2} \frac{\partial^2 V_r}{\partial \theta^2} - g \sin\phi \sin\theta \qquad \ldots 5.2\,a$$

$$U_\phi^2 \frac{\cot\theta}{r} - 2\omega U_\phi \cos\theta + \omega^2 r \sin\theta \cos\theta$$

$$= \frac{1}{\rho r} \frac{\partial P}{\partial \theta} + g \sin\phi \cos\theta \qquad \ldots 5.2\,b$$

$$V_r \frac{\partial U_\phi}{\partial r} + \frac{V_\theta}{r} \frac{\partial U_\phi}{\partial \theta} + \frac{V_r U_\phi}{r} - 2\omega V_r \sin\theta$$

$$= \frac{\nu}{r^2} \frac{\partial^2 U_\phi}{\partial \theta^2} + g \cos\phi \qquad \ldots 5.2\,c$$

$$\frac{\partial V_r}{\partial r} + 2\frac{V_r}{r} + \frac{1}{r} \frac{\partial V_\theta}{\partial \theta} = 0 \qquad \ldots 5.2\,d$$

---

*The nomenclature is given in Appendix I.

Introducing the coordinate y defined as :

$$\frac{dy}{d\theta} = - r \qquad \ldots 5.3$$

In order to integrate the system of equations (5.2) it is convenient to introduce a dimensionless distance from the surface of the rotor :

$$\xi = y \cdot \sqrt{\frac{\omega}{\nu}} \qquad \ldots 5.4$$

and a dimensionless radial distance :

$$R = \frac{r}{r_o} \qquad \ldots 5.5$$

Further, the following dimensionless parameters are defined for the velocity components and the pressure :

$$U = \frac{U_\phi}{\omega\, r\, \sin\theta} \qquad \ldots 5.6$$

$$V = \frac{V_r}{\omega\, r\, \sin\theta} \qquad \ldots 5.7$$

$$W = \frac{V_\theta}{\sqrt{\omega\nu}} \qquad \ldots 5.8$$

$$F = \frac{P - P_o}{\rho\sqrt{\omega\nu}\ \omega\, r\, \sin\theta} \qquad \ldots 5.9$$

Inserting these equations into equations (5.2) to obtain :

$$R\,V\frac{\partial V}{\partial R} + V^2 - \frac{W}{\sin\theta}\,\frac{\partial V}{\partial \xi} - 1 + 2\,U - U^2 = \frac{1}{\sin\theta}\,\frac{\partial^2 V}{\partial \xi^2} - \frac{g\sin\phi}{\omega^2\, r\sin\theta} \qquad \ldots 5.10\,a$$

$$U^2 - 2U + 1 = -\frac{1}{\cos\theta}\,\frac{\partial F}{\partial \xi} + \frac{g\sin\phi}{\omega^2 r\sin\theta} \qquad \ldots 5.10\,b$$

$$R\,V\frac{\partial U}{\partial R} + 2\,VU - \frac{W}{\sin\theta}\,\frac{\partial U}{\partial \xi} - 2\,V = \frac{1}{\sin\theta}\,\frac{\partial^2 U}{\partial \xi^2} + \frac{g\cos\phi}{\omega^2 r\sin^2\theta} \qquad \ldots 5.10\,c$$

$$R\,\frac{\partial V}{\partial R} + 3V - \frac{1}{\sin\theta}\,\frac{\partial W}{\partial \xi} = 0 \qquad \ldots 5.10\,d$$

Further simplifications can be made to the above equations by introducing the dimensionless parameter η defined as :

$$\eta = \frac{r_o\,\omega\sin\theta}{V_{r_o}} \qquad \ldots 5.11$$

and redefining the velocity components :

$$U^* = \frac{U_\phi}{V_{r_o}} \qquad \ldots 5.12$$

$$V^* = \frac{V_r}{V_{r_o}} \qquad \ldots 5.13$$

$$W^* = \frac{V_\theta}{V_{r_o}} \qquad \ldots 5.14$$

Rearranging and introducing equations (5.11, 5.12, 5.13 and 5.14) into equations (5.10) to obtain :

$$R^2\, V^* \frac{\partial\left(\frac{V^*}{R}\right)}{\partial R} + V^{*2} - \frac{r_o\, R W^*}{\sqrt{\frac{\nu}{\omega}}} \frac{\partial V^*}{\partial \xi} - R^2\,\eta^2 + 2\,R\,\eta\,U^* - U^{*2}$$

$$= \frac{R\eta}{\sin\theta} \frac{\partial^2 V^*}{\partial \xi^2} - R^2\,\eta^2 \frac{g\,\sin\phi}{\omega^2\, r\,\sin\theta} \qquad \ldots 5.15\ a$$

$$U^{*2} - 2\,R\,\eta\,U^* + R^2\,\eta^2$$

$$= -\frac{R^2\,\eta^2}{\cos\theta} \frac{\partial F}{\partial \xi} + R^2\,\eta^2 \frac{g\,\sin\phi}{\omega^2\, r\,\sin\theta} \qquad \ldots 5.15\ b$$

$$R^2\, V^* \frac{\partial\left(\frac{U^*}{R}\right)}{\partial R} + 2\,U^*\,V^* - \frac{r_o\, R\, W^*}{\sqrt{\frac{\nu}{\omega}}} \frac{\partial U^*}{\partial \xi} - 2\,R\,\eta\,V^*$$

$$= \frac{R\,\eta}{\sin\theta} \frac{\partial^2 U^*}{\partial\,\xi^2} + R^2\,\eta^2 \frac{g\,\cos\phi}{\omega^2\, r\,\sin^2\theta} \qquad \ldots 5.15\ c$$

$$R^2 \frac{\partial\left(\frac{V^*}{R}\right)}{\partial R} + 3\,V^* - \frac{r_o\, R}{\sqrt{\frac{\nu}{\omega}}} \frac{\partial W^*}{\partial \xi} = 0 \qquad \ldots 5.15\ d$$

If $\eta^2 >> \eta$, all terms on the left-hand side of equations (5.15 a,b) which do not possess the parameter η^2 can be neglected, but in equation 5.15 c, the η term on the left-hand side will tend to dominate. Thus, the equations reduce to :

$$-R\,\eta = \frac{1}{\sin\theta} \frac{\partial^2 V^*}{\partial \xi^2} - R\,\eta \frac{g\,\sin\phi}{\omega^2\, r\,\sin\theta} \qquad \ldots 5.16\ a$$

$$1 = -\frac{1}{\cos\Theta} \frac{\partial F}{\partial \xi} + \frac{g\,\sin\phi}{\omega^2\, r\,\sin\Theta} \qquad \ldots 5.16\ b$$

$$-2\,V^* = \frac{1}{\sin\theta} \frac{\partial^2 U^*}{\partial \xi^2} + R\eta \frac{g\,\cos\phi}{\omega^2 r\,\sin^2\theta} \qquad \ldots 5.16\ c$$

$$2V^* = \frac{r_o\, R}{\sqrt{\frac{\nu}{\omega}}} \frac{\partial W^*}{\partial \xi} \qquad \ldots 5.16\ d$$

Upon re-transformation, the above equations become :

$$\frac{\partial^2 V}{\partial \xi^2} = \frac{g \sin\phi}{\omega^2 r} - \sin\theta \qquad \ldots 5.17\ a$$

$$\frac{\partial F}{\partial \xi} = \frac{g \sin\phi \cot\theta}{\omega^2 r} - \cos\theta \qquad \ldots 5.17\ b$$

$$\frac{\partial^2 U}{\partial \xi^2} = -2 \sin\theta\ V - \frac{g \cos\phi}{\omega^2 r \sin\theta} \qquad \ldots 5.17\ c$$

$$\frac{\partial W}{\partial \xi} = 2 V \sin\theta \qquad \ldots 5.17\ d$$

Defining a dimensionless parameter δ^* for the film thickness as :

$$\delta^* = \delta \cdot \sqrt{\frac{\omega}{\nu}} \qquad \ldots 5.18$$

The no-slip condition at the surface of the rotor gives the following boundary conditions :

$$\xi = 0 \quad : \quad U = 0 \ , \ V = 0 \ , \ W = 0$$

and at the free surface of the liquid film, the boundary conditions are :

$$\xi = \delta^* \quad : \quad \frac{\partial U}{\partial \xi} = 0 \ , \ \frac{\partial V}{\partial \xi} = 0 \ , \ F = 0$$

The solutions of the differential equations (5.17) which satisfy the boundary conditions are :

$$V = \frac{1}{2}\left[\sin\theta - \frac{g \sin\phi}{\omega^2 r}\right]\left[2\,\delta^* \xi - \xi^2\right] \qquad \ldots 5.19\ a$$

$$F = \left[\cos\theta - \frac{g \sin\phi \cot\theta}{\omega^2 r}\right]\left[\delta^* - \xi\right] \qquad \ldots 5.19\ b$$

$$U = -\frac{1}{3}\sin\theta\left[\sin\theta - \frac{g \sin\phi}{\omega^2 r}\right]\left[\delta^* \xi^3 - \frac{\xi^4}{4} - 2\,\delta^{*3}\xi\right]$$

$$+ \frac{g \cos\phi}{2\,\omega^2\, r \sin\theta}\left[2\,\delta^* \xi - \xi^2\right] \qquad \ldots 5.19\ c$$

$$W = \sin\theta\left[\sin\theta - \frac{g \sin\phi}{\omega^2 r}\right]\left[\delta^* \xi^2 - \frac{\xi^3}{3}\right] \qquad \ldots 5.19\ d$$

The distributions of these velocities and the pressure are sketched in Figure 5.2.

If the following condition applies :

$$\frac{\text{gravitational force}}{\text{centrifugal force}} \ll 1 \quad ,$$

then, for example, equation (5.19a) reduces to :

$$V = \frac{1}{2}\sin\theta\left[2\,\delta^* \xi - \xi^2\right] \qquad \ldots 5.20$$

i.e.

$$V_r = \frac{\omega^2 r \sin^2\theta}{2\,\nu}\left[2\,\delta y - y^2\right] \qquad \ldots 5.21$$

Many workers [10,39,53], have derived equation (5.21) when studying a similar problem, but assuming a one-dimensional flow. Their conclusions, however, assert the validity of the method adopted here.

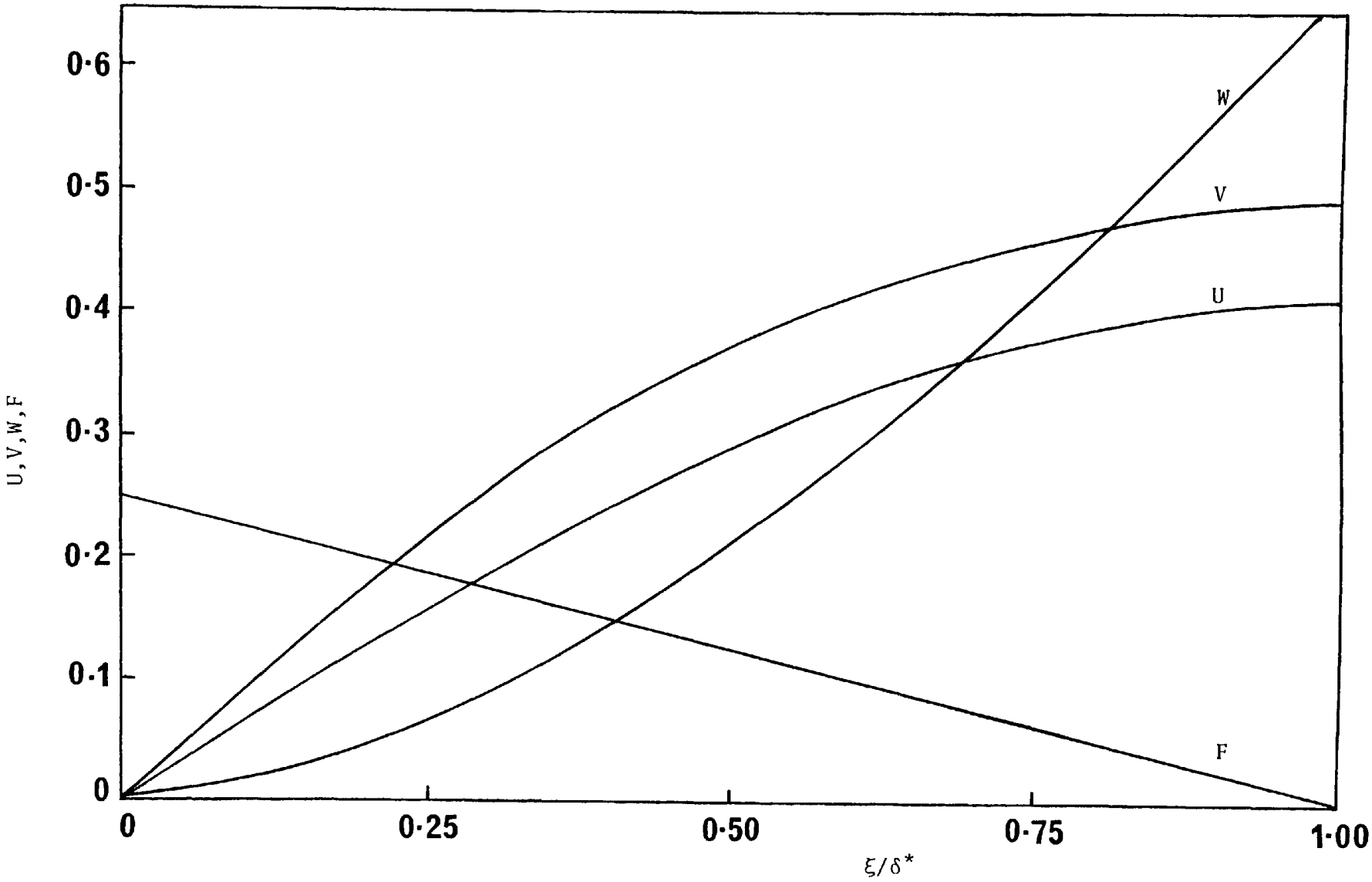

Figure 5.2 : Profiles of dimensionless velocities and pressure.

The volumetric flow rate at any radial position r is given by:

$$Q = 2\pi r \sin\theta \, \delta \, \overline{V}_r$$

$$= \int_0^{\delta} 2\pi r \sin\theta \, V_r \, dy \qquad \ldots 5.22$$

Substituting for V_r from equation (5.21) and integrating, the mean radial velocity becomes :

$$\overline{V}_r = \frac{1}{3} \frac{\omega^2 r \sin^2\theta}{\nu} \delta^2 \qquad \ldots 5.23$$

and the maximum radial velocity is :

$$(V_r)_{mx} = \frac{1}{2} \frac{\omega^2 r \sin^2\theta}{\nu} \delta^2 \qquad \ldots 5.24$$

The mass flow rate at any radial position r is given by :

$$G = 2\pi r \sin\theta \, \rho \, \delta \, \overline{V}_r$$

$$= \frac{2}{3} \pi \rho \frac{\sin^3\theta}{\nu} \omega^2 r^2 \delta^3 \qquad \ldots 5.25$$

The mean $(V_r)_{mx}$ with respect to radial position may be expressed as :

$$(\overline{V}_r)_{mx} = \frac{1}{r - r_o} \int_{r_o}^{r} \frac{1}{2} \frac{\omega^2 r \sin^2\theta}{\nu} \delta^2 dr \qquad \ldots 5.26$$

From equation (5.25) :

$$\delta^2 = \left[\frac{3\nu G}{2\pi \rho \sin^3\theta \, \omega^2} \right]^{2/3} r^{-\frac{4}{3}} \qquad \ldots 5.27$$

Substituting equation (5.27) into equation (5.26) and integrating to obtain :

$$(\bar{V}_r)_{mx} = C\ G^{2/3} \left[\frac{r^{2/3} - r_o^{2/3}}{r - r_o} \right] \qquad \ldots 5.28$$

where

$$C = \frac{3^{5/3}\ \omega^{2/3}}{2^{8/3}\ \pi^{2/3}\ \nu^{1/3}\ \rho^{2/3}}$$

The residence time for a particle at the surface of the liquid film is given by :

$$t = \frac{r - r_o}{(\bar{V}_r)_{mx}}$$

$$= \frac{1}{C\ G^{2/3}} \frac{[r - r_o]^2}{r^{2/3} - r_o^{2/3}} \qquad \ldots 5.29$$

In order to predict whether the flow across the rotor surface is laminar or turbulent, Reynolds number is defined as :

$$Re = \frac{\rho\ \bar{V}_r\ D}{\mu} \qquad \ldots 5.30$$

where

$$D = 4 \times \frac{\text{cross-sectional area of flow}}{\text{wetted perimeter}}$$

For the rotor, $D = 4\delta$, taking the rotor circumference to be infinitely large in comparison to film thickness. Hence,

$$Re = \frac{4 \delta \bar{V}_r}{\nu} \qquad \ldots 5.31$$

Substitute for $\bar{V}_r$ to obtain :

$$Re = \frac{4}{3} \frac{\omega^2 \, Sin^2 \theta}{\nu^2} r \, \delta^3 \qquad \ldots 5.32$$

and for δ to obtain :

$$Re = \frac{2 G}{\pi \mu \, Sin \theta \, r} \qquad \ldots 5.33$$

where it is understood that the Reynolds number is evaluated at radial position, r. Quantitative information concerning the type of flow that can be expected under a given set of physical conditions seems to be only fragmentary. For falling liquid films, the following information may be given [33,40,101]:

laminar flow without rippling:	$Re < 4$ to 25
laminar flow with rippling :	4 to 25 $< Re <$ 1000 to 2000
turbulent flow:	$Re >$ 1000 to 2000

and for films formed by centrifugation, Yamada et al [115] gives :

laminar flow without rippling:	$10 < Re < 140$

However, visual observation by the aid of a stroboscope is highly recommended to detect any rippling or rupture phenomena in the film.

Further useful groupings can be formulated by defining the following dimensionless parameters :

$$G^* = \frac{G}{G_o} \qquad \ldots 5.34$$

$$V_r^* = \frac{\overline{V}_r}{\overline{V}r_o} \qquad \ldots 5.35$$

$$\Delta = \frac{\delta}{\delta_o} \qquad \ldots 5.36$$

Equation (5.25) gives :

$$G_o = \frac{2}{3} \pi \rho \frac{\mathrm{Sin}^3\theta}{\nu} \omega^2 r_o^2 \delta_o^3 \qquad \ldots 5.37$$

Dividing equation (5.25) by equation (5.37) to obtain :

$$G^* = R^2 \Delta^3 \qquad \ldots 5.38$$

and equation (5.23) gives :

$$\overline{V}_{r_o} = \frac{1}{3} \omega^2 \mathrm{Sin}^2\theta \; r_o \; \delta_o^2 \qquad \ldots 5.39$$

Dividing equation (5.23) by equation (5.39) to obtain :

$$V_r^* = R \Delta^2 \qquad \ldots 5.40$$

also equation (5.32) gives :

$$Re_o = \frac{4}{3} \frac{\omega^2 \mathrm{Sin}^2\theta}{\nu^2} r_o \delta_o^3 \qquad \ldots 5.41$$

Dividing equation (5.32) by equation (5.41) to obtain :

$$Re^* = R \Delta^3 \qquad \ldots 5.42$$

Upon re-arrangement of equations (5.38, 5.40, and 5.42), the following are obtained :

$$\Delta = G^{*1/3} R^{-2/3} \quad \ldots 5.43$$

$$V_r^* = G^{*2/3} R^{-1/3} \quad \ldots 5.44$$

$$V_r^* = G^{*1/2} \Delta^{1/2} \quad \ldots 5.45$$

$$Re^* = G^{*1/2} \Delta^{3/2} \quad \ldots 5.46$$

$$Re^* = \frac{G^*}{R} \quad \ldots 5.47$$

The distributions of these parameters are illustrated in Figures 5.3 and 5.4 for $G^* = 1$, i.e. there is no evaporation.

5.2.1 Fluid Flow During the Evaporation Process

In the preceding section, many relationships were derived concerning the fluid flow. In those relationships the mass flow rate across the rotor surface was considered to be constant, i.e. $G^* = 1$. However, for an evaporation to take place, G^* can no longer stay constant. Also, during the distillation of a binary mixture, the composition of the distilland will be changing across the rotor surface. Therefore, new relationships have to be formulated.

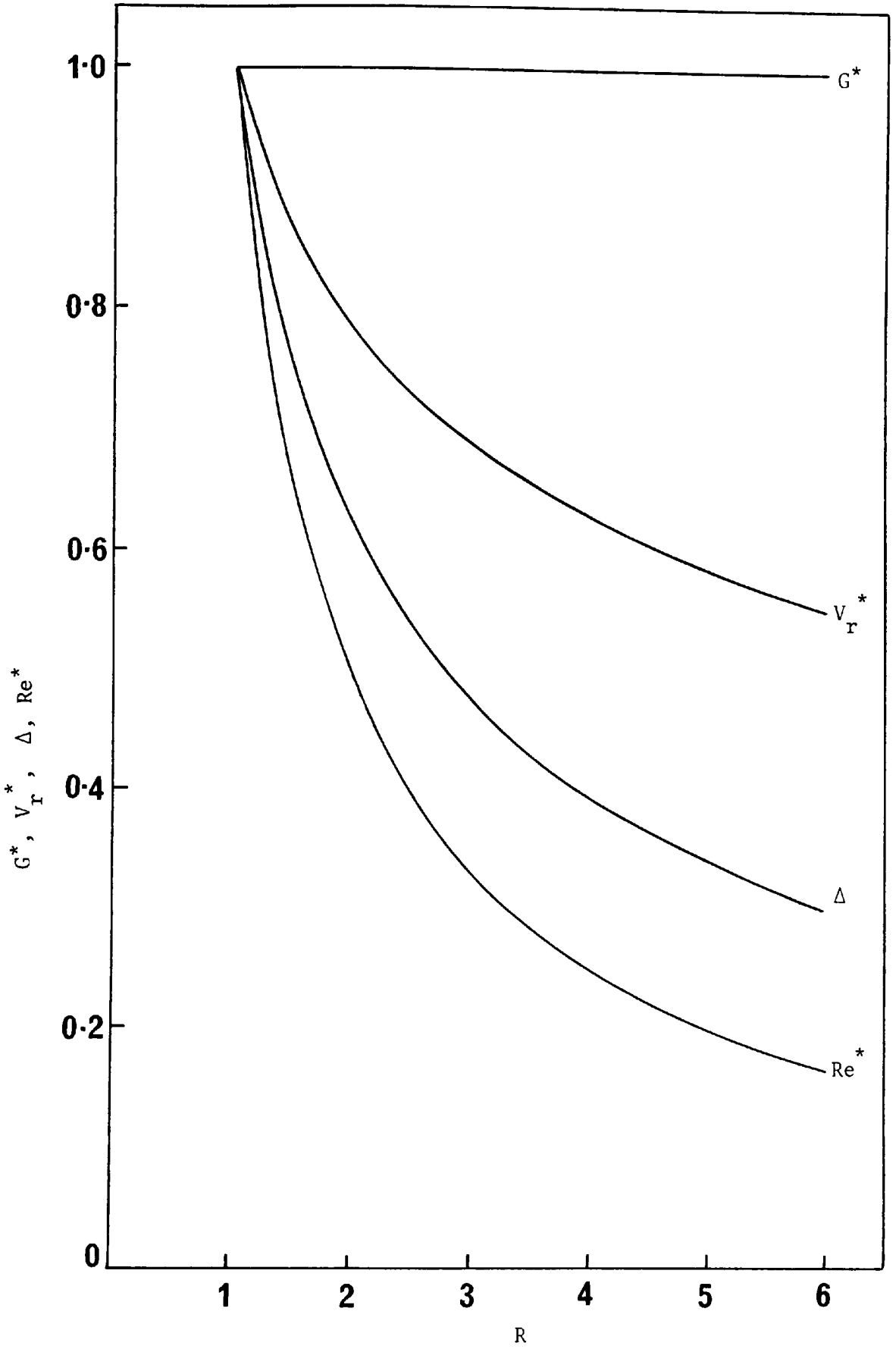

Figure 5.3 : Variation of dimensionless flow rate, velocity, film thickness and Reynolds number with dimensionless radial position.

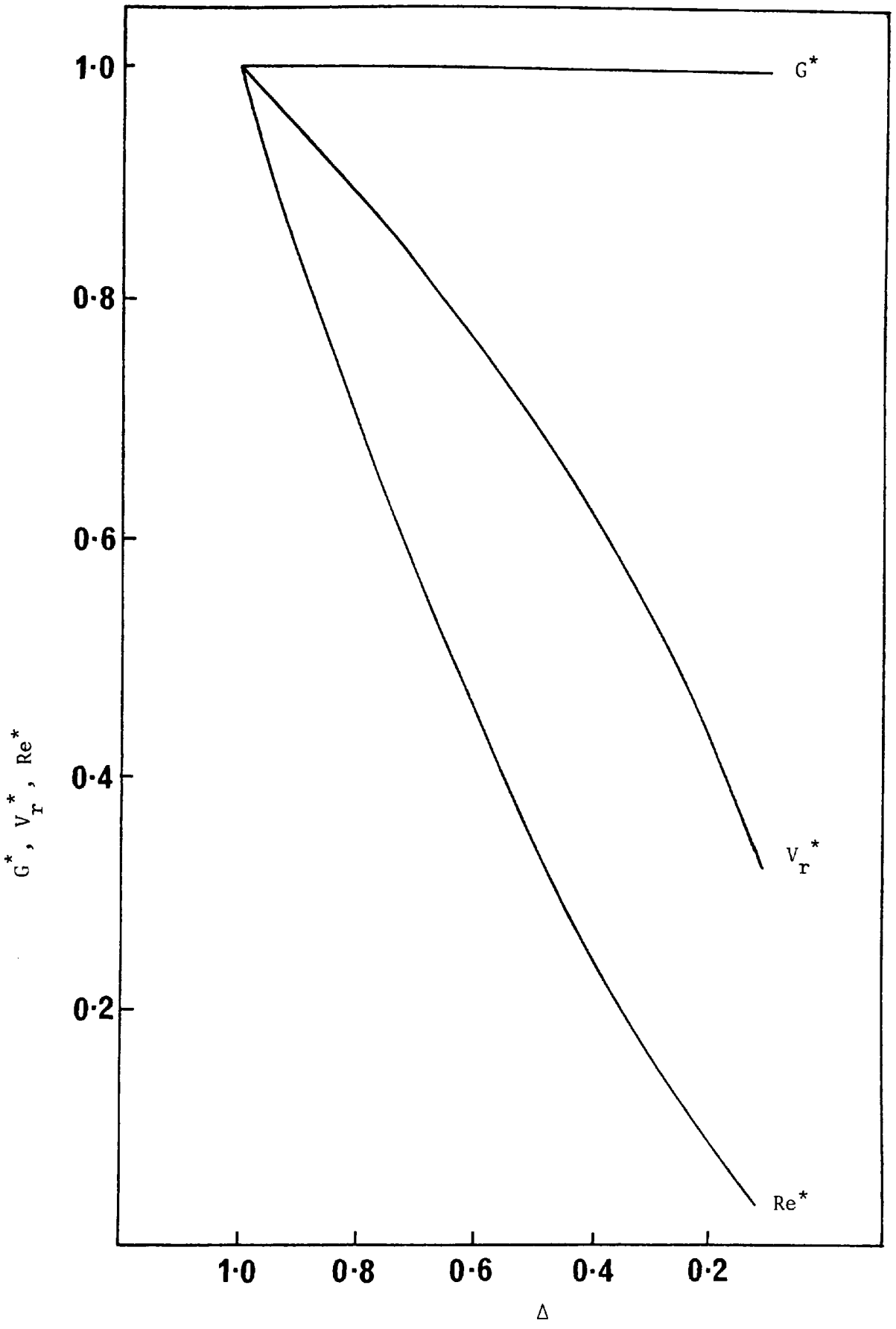

Figure 5.4 : Variation of dimensionless flow rate, velocity and Reynolds number with dimensionless film thickness.

The following assumptions are considered :

(1) The validity of Raoult's law.

(2) Rate of diffusion through the liquid film is greater than the rate of evaporation.

(3) Vapour flow has no effect on the liquid movement.

Figure 5.5. shows a small circumferential stripe of the rotor surface over which the distilland is flowing. During the residence time of the distilland on the stripe, a certain amount will be evaporated subject to the temperature and composition, and the rest will be moving onto the next stripe.

Let :

Mass flow rate of component 1 entering the stripe = G_{O1}

" " " " " 2 " " " = G_{O2}

" " " " " 1 leaving " " = G_1

" " " " " 2 " " " = G_2

Introducing the activity coefficient, γ , to take into account any deviation from Raoult's law and also to cover the evaporation cofficient, and applying equation (2.10) to each component separately, to obtain :

$$\frac{d\,w_1}{A\,dt} = 5.833 \times 10^{-2} \times P_1 \times \gamma_1 \sqrt{\frac{M_1}{T}} \times \frac{\frac{G_1}{M_1}}{\frac{G_1}{M_1} + \frac{G_2}{M_2}} = - \frac{d\,G_1}{A\,dt} \quad \ldots 5.48$$

$$\frac{d\,w_2}{A\,dt} = 5.833 \times 10^{-2} \times P_2 \times \gamma_2 \sqrt{\frac{M_2}{T}} \times \frac{\frac{G_2}{M_2}}{\frac{G_1}{M_1} + \frac{G_2}{M_2}} = - \frac{d\,G_2}{A\,dt} \quad \ldots 5.49$$

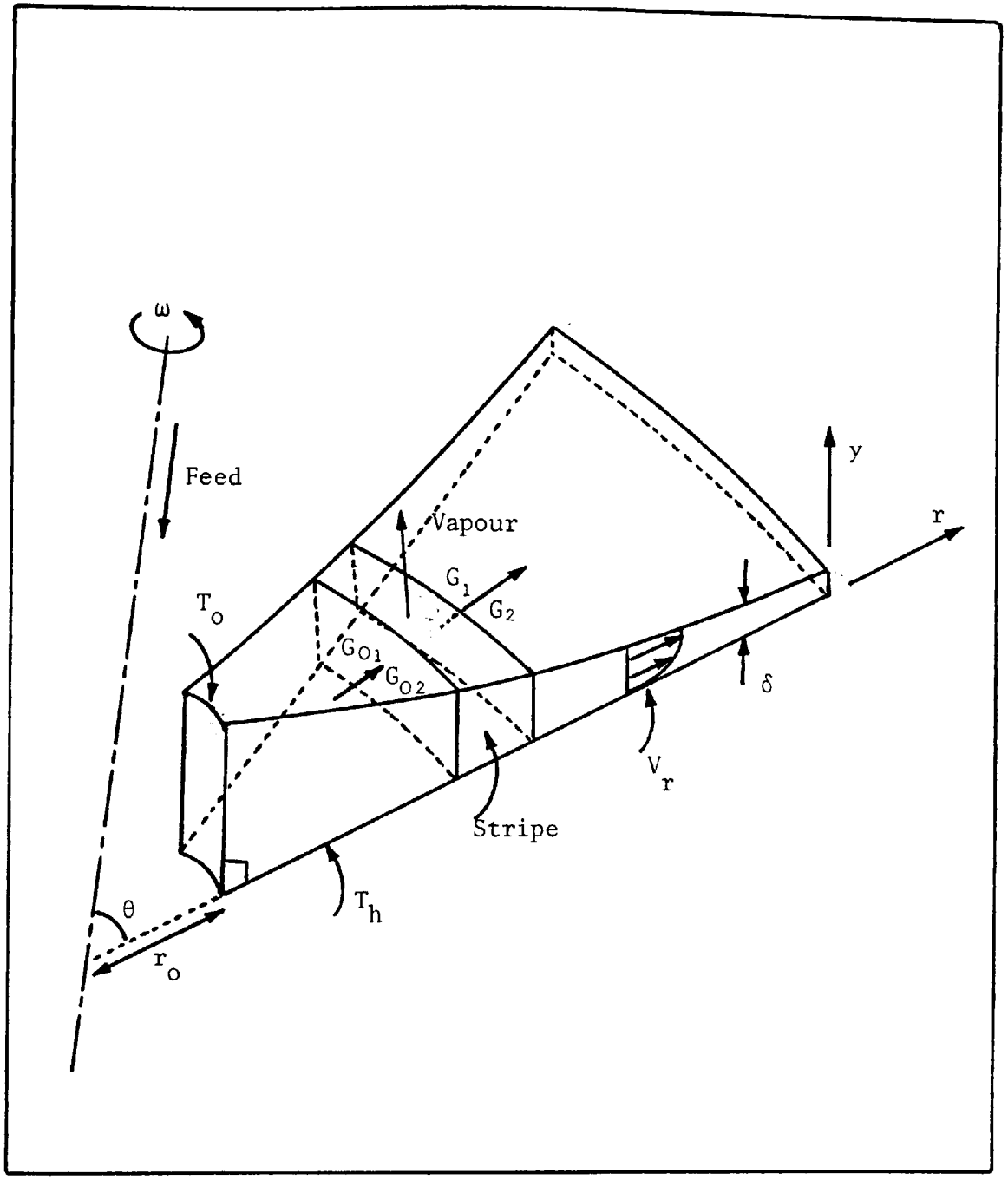

Figure 5.5 : Schematic diagram of a section of the liquid film on the rotor surface.

Dividing equation (5.48) by equation (5.49), gives :

$$\frac{d\,G_1}{d\,G_2} = \frac{\gamma_1}{\gamma_2}\,\frac{P_1}{P_2}\sqrt{\frac{M_2}{M_1}}\,\frac{G_1}{G_2} \qquad \ldots 5.50$$

The above equation can be integrated providing that the ratio $\frac{\gamma_1}{\gamma_2}$ can be considered to remain constant over the composition range. This has been experimentally proven to be true for the system EHP-EHS [61].

$\frac{\gamma_1}{\gamma_2}\,\frac{P_1}{P_2}\sqrt{\frac{M_2}{M_1}}$ represents the experimental relative volatility under conditions of molecular distillation, and will be denoted by α.

Upon integration over the limits,

$$G_{O1} \rightarrow G_1$$

$$G_{O2} \rightarrow G_2$$

equation (5.50) becomes :

$$\frac{G_1}{G_{O1}} = \left(\frac{G_2}{G_{O2}}\right)^{\alpha} \qquad \ldots 5.51$$

Introducing the following dimensionless parameters :

$$G_1^{*} = \frac{G_1}{G_{O1}} \qquad \ldots 5.52$$

$$G_2^{*} = \frac{G_2}{G_{O2}} \qquad \ldots 5.53$$

equation (5.51) becomes :

$$G_1^{*} = \left(G_2^{*}\right)^{\alpha} \qquad \ldots 5.54$$

Putting:

$$K_1 = -5.833 \times 10^{-2} \times P_1 \sqrt{\frac{M_1}{T}}$$

$$K_2 = -5.833 \times 10^{-2} \times P_2 \sqrt{\frac{M_2}{T}}$$

Introducing equations (5.52, 5.53, 5.54) into equation (5.48), and re-arranging to obtain :

$$\left[1 + \frac{G_{O2}}{G_{O1}^{1/\alpha}} \frac{M_1}{M_2} G_1^{\left(\frac{1-\alpha}{\alpha}\right)} \right] d G_1 = K_1 \gamma_1 A \, dt \quad \ldots 5.55$$

If γ_1 is a constant, the solution of the above equation is :

$$G_1 + \alpha \frac{G_{O2}}{G_{O1}^{1/\alpha}} \frac{M_1}{M_2} G_1^{1/\alpha} - G_{O1} - \alpha G_{O2} \frac{M_1}{M_2} = K_1 \gamma_1 A t \quad \ldots 5.56$$

since γ_1 is actually not a constant but a function of composition and temperature, the G_1 values at various t can only be calculated by constant iteration using the following equations :

$$G_1 + \alpha \frac{G_{O2}}{G_{O1}^{1/\alpha}} \frac{M_1}{M_2} G_1^{1/\alpha} - G_{O1} - \alpha G_{O2} \frac{M_1}{M_2} = K_1 \bar{\gamma}_1 A t \quad \ldots 5.57$$

$$\bar{\gamma}_1 = \frac{1}{G_1 - G_{O1}} \int_{G_{O1}}^{G_1} \gamma_1 \, d w_1 \quad \ldots 5.58$$

The mean value of G_1 can be expressed as :

$$\bar{G}_1 = \frac{1}{t} \int_0^t G_1 \, d t \quad \ldots 5.59$$

Substituting equation (5.55) into equation (5.59) and integrating and re-arranging to obtain :

$$\overline{G}_1 = \frac{\frac{G_{O1}^2}{2}\left(G_1^{*2} - 1\right) + G_{O1}\, G_{O2}\, \frac{M_1}{M_2}\, \frac{\alpha}{(1+\alpha)}\left(G_1^{*\left(\frac{1+\alpha}{\alpha}\right)} - 1\right)}{G_{O1}\left(G_1^* - 1\right) + \alpha\, G_{O2}\, \frac{M_1}{M_2}\left(G_1^{*1/\alpha} - 1\right)} \qquad \ldots 5.60$$

Exactly the same procedure has been followed to obtain $\overline{G}_2$:

$$\overline{G}_2 = \frac{\frac{G_{O2}^2}{2}\left(G_1^{*2/\alpha} - 1\right) + G_{O1}\, G_{O2}\, \frac{M_2}{M_1}\, \frac{1}{(1+\alpha)}\left(G_1^{*\left(\frac{1+\alpha}{\alpha}\right)} - 1\right)}{G_{O2}\left(G_1^{*1/\alpha} - 1\right) + \frac{1}{\alpha}\, G_{O1}\, \frac{M_2}{M_1}\left(G_1^* - 1\right)} \qquad \ldots 5.61$$

and hence, the total mean flow rate may be expressed as :

$$\overline{G} = \overline{G}_1 + \overline{G}_2 \qquad \ldots 5.62$$

Furthermore, during the evaporation process, equation (5.29) can be expressed as :

$$t = \frac{1}{C\,\overline{G}^{2/3}}\, \frac{[r - r_o]^2}{r^{2/3} - r_o^{2/3}} \qquad \ldots 5.63$$

The area of evaporation, A, can also be expressed in terms of radial position, r, as :

$$A = \pi\, \mathrm{Sin}\theta\, (r^2 - r_o^2) \qquad \ldots 5.64$$

Rewriting equation (5.57) :

$$t = \frac{G_{O1}\,(G_1^* - 1) + \alpha\, G_{O2}\,\frac{M_1}{M_2}\left(G_1^{*\,1/\alpha} - 1\right)}{\pi\,\mathrm{Sin}\,\theta\;K_1\;\overline{\gamma}_1\;(r^2 - r_o^{\,2})} \qquad \ldots 5.65$$

Thus, introducing equations (5.60, 5.61, 5.63, 5.65) into equation (5.62), and re-arranging to obtain an equation relating G_1^* and R for any particular set of $\overline{\gamma}_1$, α and K_1.

$$\left[\frac{\frac{G_{O1}^{\,2}}{2}\,(G_1^{*\,2} - 1) + G_{O1}\,G_{O2}\,\frac{M_1}{M_2}\,\frac{\alpha}{(1+\alpha)}\left(G_1^{*\,\left(\frac{1+\alpha}{\alpha}\right)} - 1\right)}{G_{O1}\,(G_1^* - 1) + \alpha\,G_{O2}\,\frac{M_1}{M_2}\left(G_1^{*\,1/\alpha} - 1\right)}\right.$$

$$\left. + \frac{\frac{G_{O2}^{\,2}}{2}\left(G_1^{*\,2/\alpha} - 1\right) + G_{O1}\,G_{O2}\,\frac{M_2}{M_1}\,\frac{1}{(1+\alpha)}\left(G_1^{*\,\left(\frac{1+\alpha}{\alpha}\right)} - 1\right)}{G_{O2}\left(G_1^{*\,1/\alpha} - 1\right) + \frac{1}{\alpha}\,G_{O1}\,\frac{M_2}{M_1}\,(G_1^* - 1)}\right]^{2/3}$$

$$\times \left[G_{O1}\,(G_1^* - 1) + \alpha\,G_{O2}\,\frac{M_1}{M_2}\left(G_1^{*\,1/\alpha} - 1\right)\right]$$

$$= \frac{K_1\,\overline{\gamma}_1\,\pi\,\mathrm{Sin}\,\theta}{C}\;r_o^{\,10/3}\left[R^{4/3} + R^{2/3} + 1\right]\,[R-1]^2 \qquad \ldots 5.66$$

5.3 HEAT TRANSFER

The heat needed for the evaporation of the liquid from the surface of the film is normally provided by an electrical heating element embedded beneath the surface of the rotor and capable of providing constant power output.

Prior to introducing the equation of energy [8], the following assumptions are made :

(1) The velocity profile is fully developed at any radial position.

(2) The feed enters at a constant temperature, T_o.

(3) The surface of the rotor is at a constant temperature, T_h.

(4) Viscous dissipation is negligible.

(5) Liquid physical properties are taken at a mean temperature.

With these and the previously stated assumptions governing the fluid flow, the energy equation reduces to :

$$\rho \, C_p \, V_r \, \frac{\partial T}{\partial r} = k \, \frac{\partial^2 T}{\partial y^2} \qquad \ldots 5.67$$

The above equation indicates that there is a temperature gradient from the centre of the rotor to the periphery, in addition to the temperature gradient across the thickness of the liquid film.

Since the molecular distillation process is a surface phenomenon, i.e. the evaporation rate is a function of the temperature and the composition of the specie at the surface; therefore the shape of the temperature profiles developed within the liquid

film are of no influence on the rate of evaporation. Hence, equation (5.67) can be approximated to :

$$\bar{V}_r \frac{\partial T}{\partial r} = \alpha' \frac{\partial^2 T}{\partial y^2} \qquad \ldots 5.68$$

where α' is a combination of the physical properties of the material defined as :

$$\alpha' = \frac{k}{\rho C_p}$$

This is known as the thermal diffusivity of the material.

Combining equations (5.23) and (5.25), gives :

$$\bar{V}_r = C_2 \, r^{-1/3} \qquad \ldots 5.69$$

where

$$C_2 = \frac{1}{3} \frac{\omega^2}{\nu} \left[\frac{3 \nu G}{2 \pi \rho \omega^2} \right]^{2/3}$$

Introducing equation (5.69) into equation (5.68), and re-arranging to obtain :

$$B \, r^{-1/3} \frac{\partial T}{\partial r} = \frac{\partial^2 T}{\partial y^2} \qquad \ldots 5.70$$

where

$$B = \frac{C_2}{\alpha'}$$

Equation (5.70) is only valid for predicting approximate values of liquid film surface temperature and not temperature profiles within the liquid film. It has the following boundary conditions :

$$y = 0 \quad , \quad r > r_o \quad ; \quad T = T_h$$

$$y = \delta_o \quad , \quad r = r_o \quad ; \quad T = T_o$$

5.3.1 Similarity Solution of the Energy Equation

Introducing the reduced variable :

$$\psi = \frac{T - T_o}{T_h - T_o} \qquad \ldots 5.71$$

and a new independent variable β defined by :

$$\beta = B^{1/2} r^{-2/3} y \qquad \ldots 5.72$$

Upon simplification and re-arrangement, equation (5.70) reduces to the following ordinary differential equation :

$$\frac{3}{2} \frac{d^2\psi}{d\beta^2} = - \beta \frac{d\psi}{d\beta} \qquad \ldots 5.73$$

and the boundary conditions reduce to :

$$\beta = 0 \quad ; \quad \psi = 1$$

$$\beta = B^{1/2} r_o^{-2/3} \delta_o \quad ; \quad \psi = 0$$

The solution of equation (5.73) is readily found to be :

$$\psi = - \frac{\int_{B^{1/2} r_o^{-2/3} \delta_o}^{\beta} e^{-\beta^2/3} \, d\beta}{\int_{0}^{B^{1/2} r_o^{-2/3} \delta_o} e^{-\beta^2/3} \, d\beta} \qquad \ldots 5.74$$

Equation (5.74) can be simplified further to :

$$\psi = \frac{\operatorname{erf}\left(\frac{B^{1/2}\, r_o^{-2/3}\, \delta_o}{\sqrt{3}}\right) - \operatorname{erf}\frac{\beta}{\sqrt{3}}}{\operatorname{erf}\left(\frac{B^{1/2}\, r_o^{-2/3}\, \delta_o}{\sqrt{3}}\right)} \qquad \ldots 5.75$$

The variation of the reduced film surface temperature ψ_s and the reduced film surface similarity variable β_s for several values of the mass flow rate G are computed using Simpson's Approximation. The numerical values are tabulated in Table 5.1. and the distribution of these variables is sketched in Figures 5.6 and 5.7. The following data have been used in the calculation :

$\alpha' = 0.00061 \text{ cm}^2/\text{sec}$;

$\nu = 0.0281 \text{ cm}^2/\text{sec}$;

$\rho = 0.98 \text{ gm/cm}^3$;

$\theta = 75^o$;

$r_o = 1.11125 \text{ cm}$;

$\omega = 140 \text{ sec}^{-1}$.

Table 5.1

G gm sec^{-1}	r cm	β_s	ψ_s
0.6	2	0.4492038113	0.5048207613
	3	0.2616104495	0.7073613500
	4	0.1782666507	0.7997797872
	5	0.1323904792	0.8510704819
	6	0.1038201757	0.8831224668
0.5	2	0.3977918995	0.5130216038
	3	0.2316688217	0.7131070158
	4	0.1578638200	0.8038820187
	5	0.1172382311	0.8541714872
	6	0.0919378328	0.8855745633
0.4	2	0.3428066670	0.5207368247
	3	0.1996461383	0.7184814907
	4	0.1360429160	0.8077131471
	5	0.1010328448	0.8570657692
	6	0.0792296225	0.8878625248
0.3	2	0.2829806687	0.5278661415
	3	0.1648042561	0.7234216434
	4	0.1123009528	0.8112295423
	5	0.0834007758	0.8597207734
	6	0.0654026124	0.8899607707
0.2	2	0.2159546681	0.5342612843
	3	0.1257691862	0.7278320266
	4	0.0857016668	0.8143647332
	5	0.0636467040	0.8620867472
	6	0.0499115346	0.8918301443

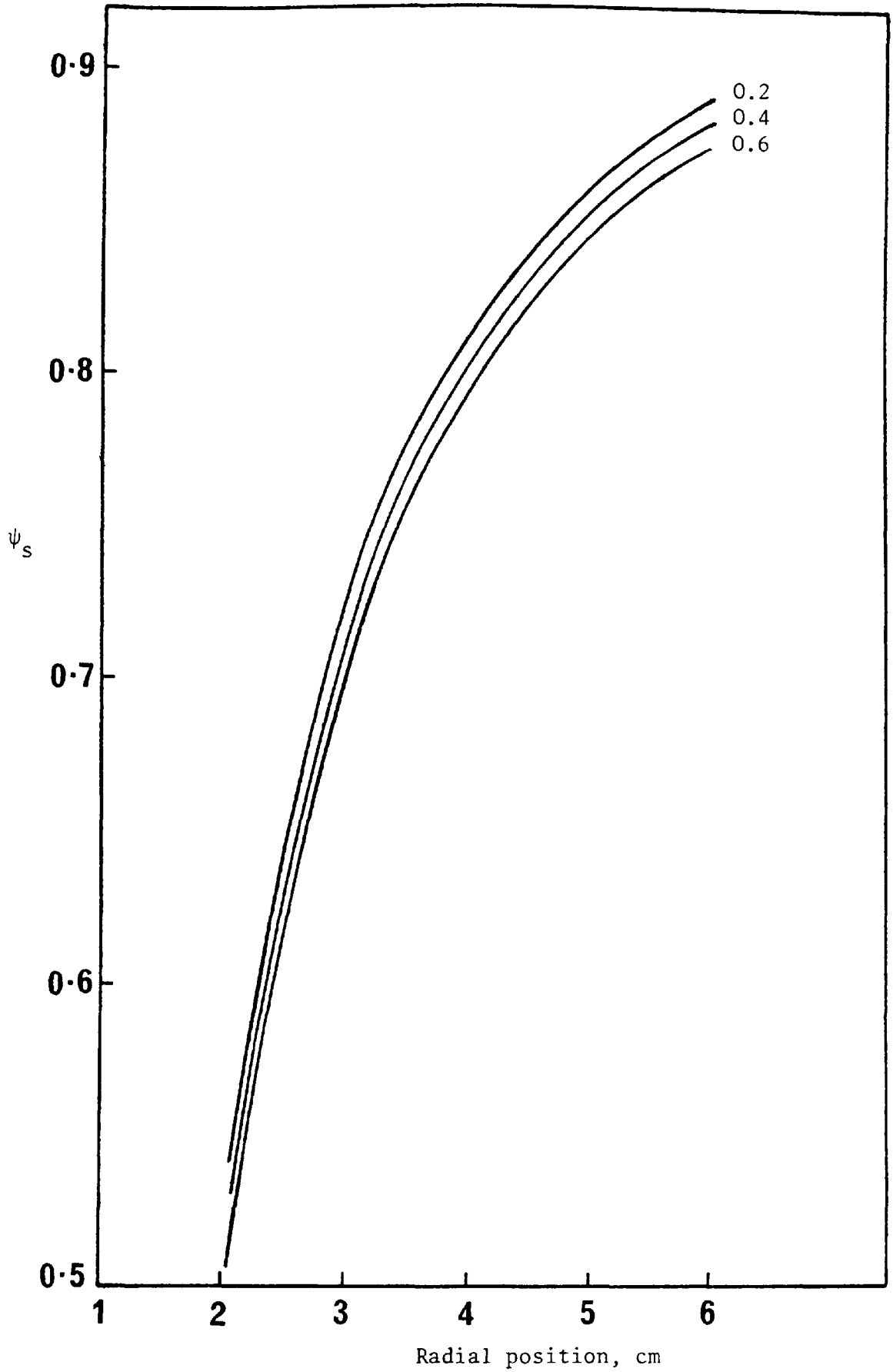

Figure 5.6 : Variation of reduced surface temperature with radial position for different values of mass flow rate.

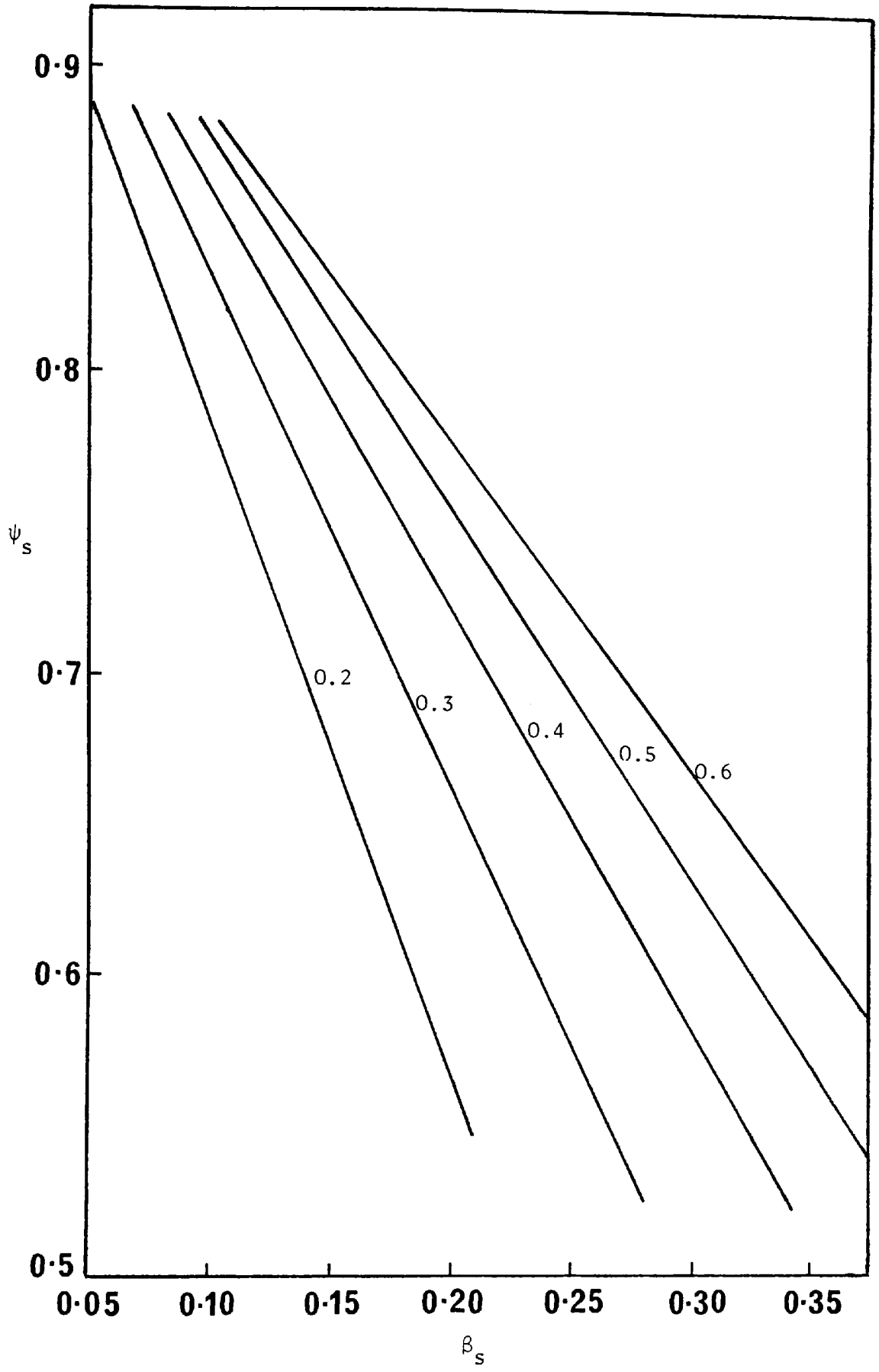

Figure 5.7 : Variation of reduced surface temperature with the reduced similarity variable for different values of mass flow rate.

CHAPTER VI

SOLUTION OF THE MATHEMATICAL MODEL

6.1 INTRODUCTION

Equations (5.66 and 5.74) represent a system relating indirectly the evaporation rate of a binary mixture and the radial position on the rotor surface for any particular set of C_p, G_{o1}, G_{o2}, k, K_1, M_1, M_2, r_o, T_o, T_h, α, $\bar{\gamma}_1$, θ, ν, ρ, and ω.

The solution of this system will provide an approximate analysis of the coupled phenomena of fluid dynamics, heat transfer, and surface evaporation of a binary mixture in the centrifugal molecular still.

6.2 PARAMETERS

6.2.1 Design Parameters

The CMS-5 is designed in such a way that the following parameters are fixed :

(1) Rotor face angle, $(90 - \theta) = 15^{o}$

(2) Initial radial position, $r_o = 1.15$ cm

(3) Final radial position, $r = 6.23$ cm

(4) Angular velocity of rotor, $\omega = 140\ sec^{-1}$

6.2.2 Experimental Parameters

In each experimental run made on the di-2-ethylhexyl phthalate-di-2-ethylhexyl sebacate system, the following parameters were kept

constant throughout the entire run :

(1) Rate of feed to rotor, G_o

(2) Composition of feed, x_o

(3) Temperature of feed, T_o

(4) Mean distilland temperature at the periphery, T_{mdp}

6.2.3 Test Mixture Parameters

Most of the physical property data of the binary mixture are functions of both temperature and composition, and although equations and graphs have been presented in Chapter IV relating a particular property to the temperature for a certain composition, and in order to solve the mathematical model, a general formula relating that property to the temperature and the composition is required. Accordingly the following expressions have been correlated for each property:

Specific heat:

$$C_{mix} = 8.467394 \times 10^{-4}\, t - 1.225941 \times 10^{-4}\, t\, x - 0.02524\, x + 0.4393 \quad (cal/gm\ ^{o}C) \qquad ...6.1$$

Viscosity:

$$\mu_{mix} = \left[x \times 10^{(0.82536 - 0.40577\, t^{0.25})} + (1 - x)\ 10^{(14.95492\, t^{-1} - 0.654215)} \right]^{3} \quad (poise) \qquad ...6.2$$

Density* :

$$\rho_{mix} = 0.0693\, x + 0.9103 \quad (gm/cm^3) \qquad ...6.3$$

---

*Thermal expansion is negligible.

Thermal conductivity :

$$k = 3.264409 \times 10^{-4} - 2.44 \times 10^{-7}\, t \quad \text{(cal/sec cm } ^{o}\text{C)} \quad \ldots 6.4$$

K_1 :

$$K_1 = -5.833 \times 10^{-5} \times \left(\frac{390.57}{t + 273.15}\right)^{0.5} \times 10^{\left(14.62 - \frac{5440}{t+273.15}\right)} \quad \ldots 6.5$$

α :

$$\alpha = 1.0452 \times 10^{\left(\frac{340}{t+273.15} - 0.28\right)} \quad \ldots 6.6$$

where

x = mole fraction of EHP ;

t = temperature (^{o}C).

6.3 THE SOLUTION

During the process of distillation, the composition and temperature of the distilland are changing, traversing from the centre of the rotor to the periphery. Since equation (5.66) contains parameters which are functions of temperature and composition, the composition, the mean bulk and surface temperatures of the distilland have to be known before this equation can be solved.

Unfortunately, equation (5.74) involves the rotor surface temperature, T_h, which is an unknown parameter. Therefore a solution technique has been devised where the experimental mean distilland temperature at the periphery, T_{mdp}, is used in an iterative method to confirm a correct guess value of T_h.

In general, the numerical solution of the mathematical model involves dividing the radial distance into small equal parts and assuming an initial guess value for T_h.

Starting at the feed position, values for the density, kinematic viscosity, film thickness, mean velocity, and Reynolds number can be calculated as functions of the feed temperature, T_o, and composition, x_o, from equations (6.3, 6.2, 5.27, 5.23, 5.31) respectively. For the first part of the radial distance, values for the mean bulk kinematic viscosity, thermal conductivity, and specific heat are also calculated as functions of the arithmetic mean bulk temperature and the initial composition using equations (6.2, 6.4, 6.1) respectively. The values for α and K_1 are calculated as functions of the initial surface temperature using equations (6.5 and 6.6) respectively.

With all parameters known, equation (5.66) can now be solved numerically using the Newton-Raphson method[30]. Upon convergence, $\overline{G}$, G_2^*, G_1, G_2, G^*, film thickness, mean velocity, and Reynolds number can be calculated using equations (5.62, 5.54, 5.52, 5.53, 5.34, 5.43, 5.44, 5.47) respectively.

In order to determine the surface temperature of the second part, equation (5.74) is also solved numerically by Simpson's Rule [30]. The limits of integration are calculated using equation (5.72).

These calculations proceed for each part of the radial distance in turn until the edge of the rotor is reached; then the mean distilland temperature at the periphery can be calculated

and compared to the experimental mean. If agreement is not attained, the entire iteration procedure is repeated, starting with an incremented value of T_h.

The listing of the computer program used in these computations is given in Appendix II.

The program was run to obtain :

(1) Mass flow rate, composition, film thickness, mean velocity, Reynolds number, surface temperature, and relative volatility as functions of radial position on the rotor surface.

(2) Mean values for distillation rate, composition of distillate, composition of distilland, relative volatility and surface temperature.

In this solution, the distillation process has been assumed as one obeying Raoult's Law, i.e. the activity coefficient equals unity. This seems to be a justifiable assumption, since it is known that the present experimental binary mixture conforms closely to ideal mixing and solution behaviour. In addition, the measured experimental distillation rate and the composition of distillate can now be considered as a measure of the extent to which molecular distillation process follows Raoult's Law when compared to the calculated values.

CHAPTER VII

RESULTS AND DISCUSSION

7.1 LIQUID PATHLINE

The stroboscopic photograph, Plate 3.7, is typical of either components of the binary mixture, showing di-2-ethylhexyl phthalate at the moment of impinging on the moving rotor surface at low feeding rate (50 teeth gear), and the temperature being 17°C. The radial streaks imply that the liquid has the same rotational speed as the rotor and the domination of the radial velocity over the tangential velocity, i.e. the path traversed by any liquid particle with respect to the rotor surface is straight and radial. Plate 3.8 shows the liquid film when it is fully developed, and the same behaviour has been observed when other feed gears were used.

Spiral pattern (Plates 3.9 and 3.10) has appeared at the centre of the rotor for both di-2-ethylhexyl phthalate and di-2-ethylhexyl sebacate when they were fed at 120°C using high feeding rate (30 teeth gear) and the phenomenon persisted for the other feed gears.

This phenomenon is attributed to the Coriolis effect [29,98]. The liquid at any point on a rotating disk is subject to two main forces: a centrifugal force acting in the positive radial direction and a Coriolis force acting in the plane of rotation and normal to the radius.

The condition for neglecting the Coriolis force requires that :

$$\frac{\text{Coriolis force}}{\text{Centrifugal force}} = \frac{m\ (2\ \omega\ V_r)}{m\ \omega^2\ r\ \sin^2\theta} \ll 1$$

where m is a unit mass

or

$$V_r \ll \omega\ r\ \sin^2\theta/2$$

Substituting equation (5.24) for V_r and rearranging to obtain :

$$\frac{\omega\ \delta^2}{\nu} \ll 1\ ,$$

this dimensionless ratio is denoted by N; in practice N means that the mathematical model is restricted to relatively thin layers of liquid of high kinematic viscosity for any particular value of the angular velocity.

The application of N to a typical experimental run is shown graphically in Figure 7.1 which illustrates that N varies across the rotor from approximately 0.2 to 0.05. However, as can be seen from the photographs, the feed tube discharges the feed liquid in a normal rather than tangential direction with respect to the rotational plane. This undoubtedly will add an additional radial component upon the centrifugally genrated radial velocity. Therefore it could be reasonably assumed that the Coriolis effect is not as high as it seems, and the mathematical model with regard to this point is still sound.

It was aimed, by taking a high speed film (500 fr./sec.), to have an estimate of the time required for a liquid particle to cross the rotor surface. Unfortunately, the high intensity of light required

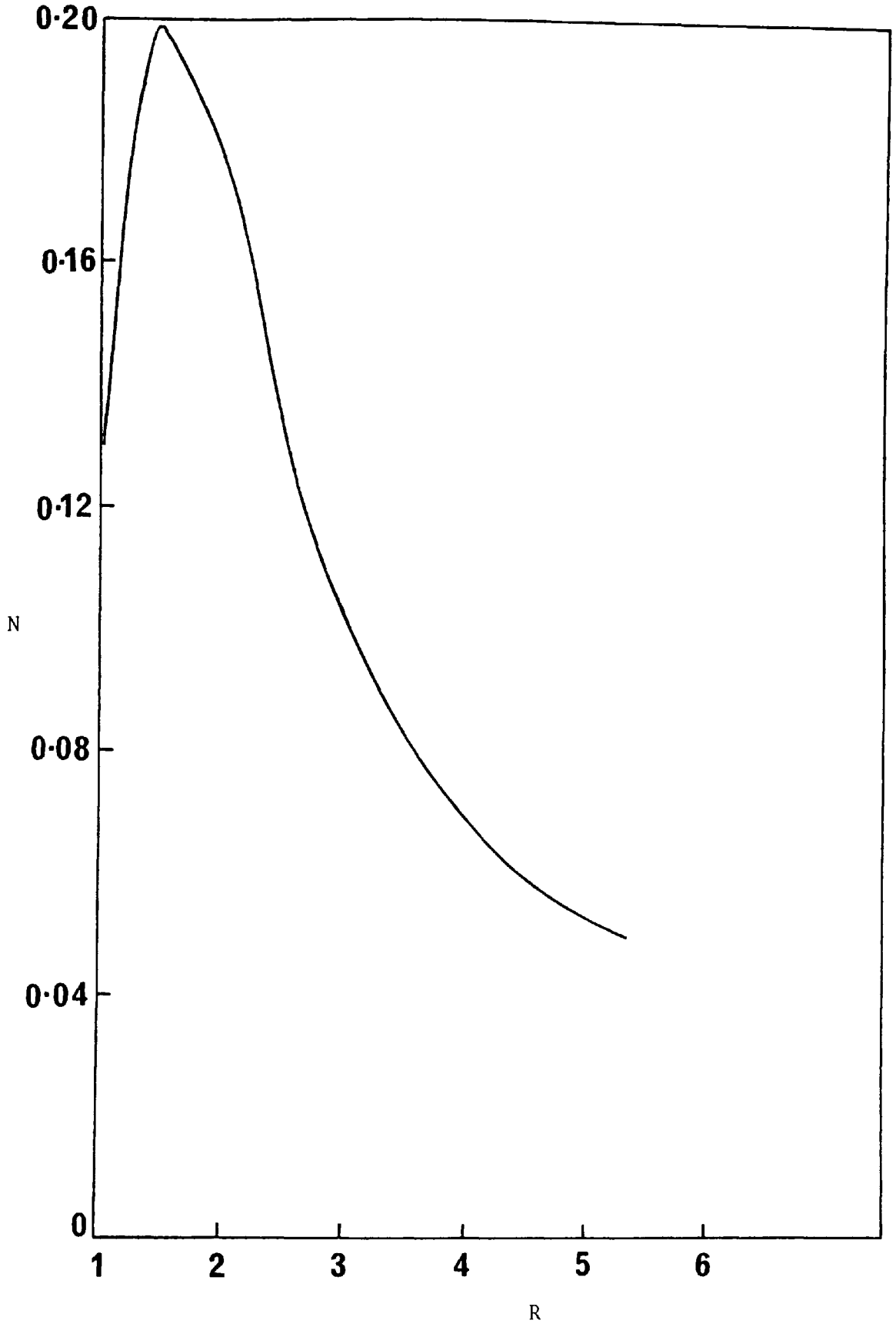

Figure 7.1 : Variation of the dimensionless Coriolis ratio, N, with the dimensionless radial position.

for such a film created a problem; due to the shining face of the rotor, as well as the thinness of the layer of the liquid film a high percentage of the light flux was reflected back to the lens of the camera. Upon examination of the developed film, it was noticed that the film had been over-exposed and, consequently, the task of tracing a particle was an extremely difficult one.

7.2 DEGASIFICATION TEMPERATURE OF MATERIALS

The procedure for determining a safe degasification temperature for the components is given in Chapter III. The properties of di-2-ethylhexyl sebacate were unaffected by the test despite increasing the temperature up to 95°C. At 70°C, the colour of di-2-ethylhexyl phthalate was slightly changing after three hours of continuous heating, but there was no change in the refractive index of the material. At 80°C, and after 1.5 hours of heating, the colour was nearly yellow and a slight change in the refractive index was observed.

Therefore, depending on these observations, the upper limit of the degasification temperature was set at 65°C.

7.3 EFFECT OF VACUUM IMPROVEMENT

The addition of the second diffusion pump, and the proper greasing and maintenance of the various joints in the CMS-5 proved to increase the rate of evacuation of the still and reduce the pressure down to approximately 10^{-5} mm Hg. The main purpose of such low pressure was not to improve the evaporation rate, but to ensure

that the vacuum was maintained at 10^{-3} mm Hg or below. This is known to be a satisfactory vacuum for molecular distillation processes [55].

7.4 EFFECT OF THE CONDENSING SURFACE TEMPERATURE

The condensing surface temperature was considered as one of the main parameters to be studied in this investigation. Upon the recommendation of Dr. G. Burrows*, the condenser thermocouple was fabricated and installed on the inside face of the Bell-jar opposite the evaporating rotor. This thermocouple failed to provide a satisfactory performance for two reasons:

(1) Insufficient distillate film to cover the thermocouple head and consequently fluctuating output.

(2) Even, when the distillation rate was increased as an atempt to increase the thickness of distillate film, channellings in the film were set up and this phenomenon is mainly due to the fact that di-2-ethylhexyl phthalate and di-2-ethylhexyl sebacate are non-wetting to glass [111].

However, a closer inspection of the literature regarding this problem revealed that it was unnecessary to know the condensing surface temperature as long as the condensing surface was kept cool enough to prevent any re-evaporation of the distillate molecules [34]. The optimum rate of cooling water to the condenser was found to be 250 cc/min. This value was arrived at by conducting rate studies on the pure components. Their experimental evaporation rates were improved by more than 15% compared to the rates when no cooling

---

* Private communications to Dr. G.J. Rees

water was used. Any further increase in the rate of cooling offered no improvement in the rate of evaporation. As a result of this optimum value, the outside temperature of the condenser was noted to be between 30 and 60°C depending on the distillation rate.

However, the condensing surface temperature in typical experimental runs may be approximately calculated as follows:

Maximum distillation rate	≃	0.1 gm/sec
Minimum distillation rate	≃	0.002 gm/sec
Condensation area	≃	100 cm^2
Latent heat	≃	60 cal/gm
Thermal conductivity of glass	≃	2×10^{-3} cal/sec cm^oC
Thickness of glass	≃	0.5 cm

Hence, the temperature difference across the glass for the maximum distillation rate is given by:

$$\Delta t = \frac{0.1 \times 60 \times 0.5}{100 \times 2 \times 10^{-3}}$$

$$= 15^oC$$

and, similarly for the minimum distillation rate:

$$\Delta t = 0.3^oC$$

Therefore, the condensing surface temperature is approximately between 31 and 75°C. In practice, however, these values will be increased somewhat by the heat radiated from the evaporator.

7.5 ANALYSIS OF THE EXPERIMENTAL RUNS

7.5.1 Introduction

A total of 120 experimental runs were carried out on five different compositions of the EHP-EHS system using the three available spur gears (30, 40, and 50 teeth) over a range of temperatures. The experimental parameters, together with the numerically calculated values for some runs are presented in Tables 1 through 75 in Appendix III. Mass flow rate, composition, film thickness, mean velocity, Reynolds number, surface temperature, and relative volatility, calculated as described in Chapter VI are tabulated for each run as a function of radial position on the rotor surface starting at the initial position (1.15 cm) and ending at the edge of rotor at 6.23 cm. In addition, the calculated and experimental mean values of distillation rate, distillate composition, relative volatility, surface temperature, and distilland temperature at the periphery are also tabulated. Also, the calculated mean distilland compositions for selected runs are given in Table 76. Figure III.1 shows some of the above-mentioned variables in normalized form as a function of the dimensionless radial position for a typical experimental run.

7.5.2 Mean Distillation Temperature

The problem of determining the exact temperature of distillation has been fully discussed in Chapters III and V. The relationship between the calculated mean surface temperature and the experimental mean distilland temperature at the periphery for the two extremes of the composition spectrum is shown

graphically in Figure 7.2. It can be seen from the graph that the mean surface temperature, i.e. the mean distillation temperature, is not just a function of the mean distilland temperature at the periphery, but also a function of feed rate and composition. When EHS is the dominating component, i.e. low evaporation rate, the relationship tends to be linear for the three different feed rates, but when EHP is dominating, i.e. higher evaporation rate at the same temperature, the rate of change of the distillation temperature decreases with increasing the mean distilland temperature.

In the experimental phase of his studies on the evaporation rates of EHP, EHS, and other pure materials in the centrifugal molecular still, Greenberg [38] pre-heated the feed to the same temperature as that of the mean distilland at the periphery and postulated a one-dimensional heat flow assuming that the heat flux across the liquid film is being the latent heat of vapourization of the material. Doing so, he avoided the complexity and the problems of deciding the true temperature of distillation. Unfortunately, in pre-heating the liquid, Greenberg had overlooked one of the main advantages of the centrifugal molecular still, i.e. the short exposure to heat in order to reduce the thermal hazard to a minimum.

However, as Figure 7.2 also shows, the difference between the two temperatures can reach as much as $40^{o}C$ taking into account that $10^{o}C$ could double the evaporation rate of either components. Therefore, before it is concluded that the mean distilland temperature at the periphery does in no way give the true temperature of

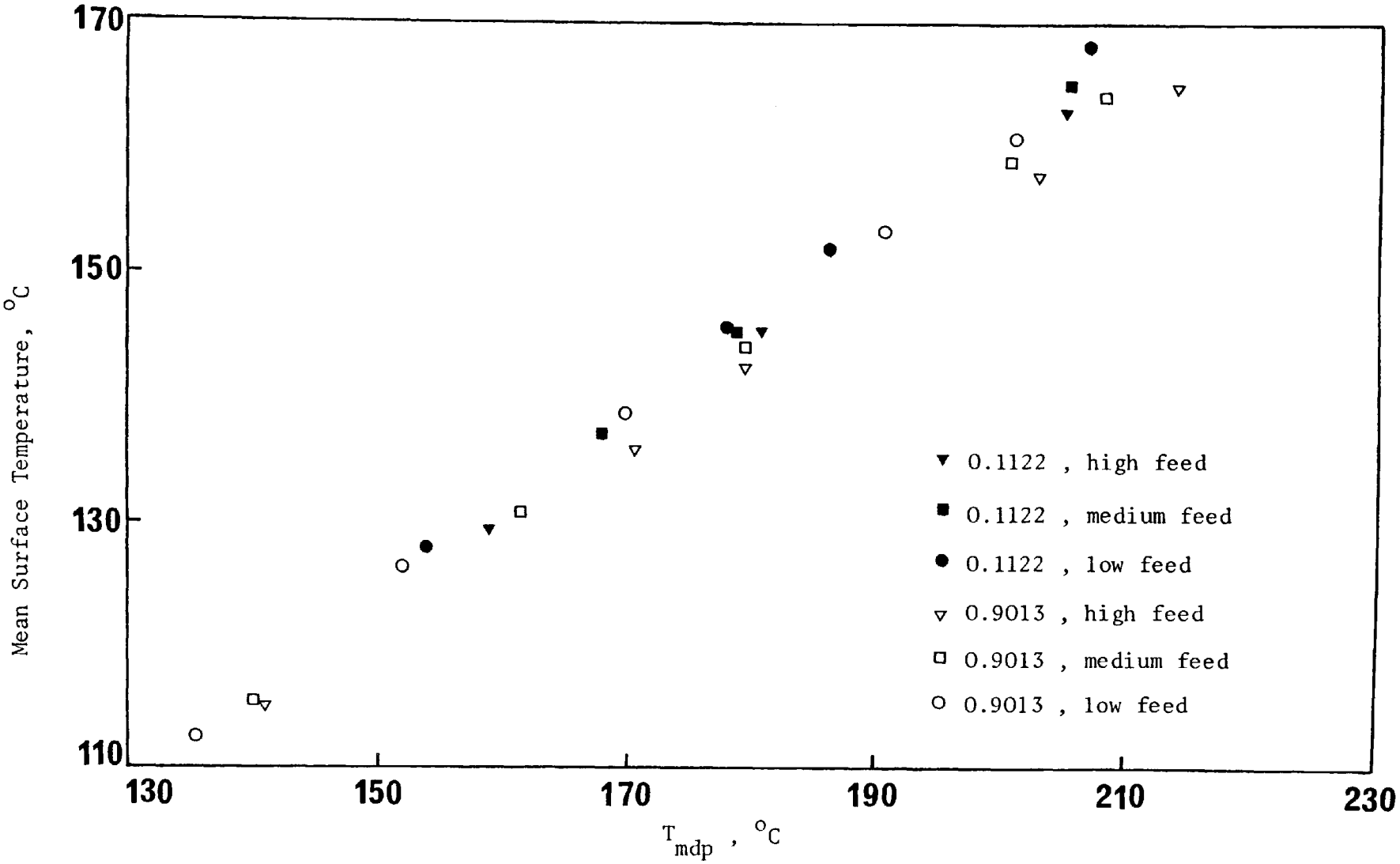

7.2 : Variation of mean surface temperature with the mean distilland temperature at the periphery

distillation, Figures 7.3, 7.4 and 7.5 illustrate the experimental distillation rates relative to the theoretically calculated values. Although these Figures only show the two extreme compositions, they are good representatives of all runs. The rate of change of the experimental values with the theoretically calculated varies from about 99 percent at low temperature to 92 percent at high temperature. These results, however, assert to a certain degree the validity of applying the mathematical model to this problem.

7.5.3 Relative Volatility

The experimental relative volatility for each run has been calculated according to equation (2.47), and the results are presented in Appendix III. Figure 7.6 shows the experimental relative volatility as a function of the mean surface temperature for different feed compositions and flow rates. The general trend of the experimental points starts falling steadily above 120°C and steeply above 160°C. These data are in good agreement with the data of Malyusov [72] and Trevoy [107] particularly above 140°C, and 150% better than those obtained by Cvengros [26] when evaluating the same binary mixture.

The Figure also shows that better relative volatilities are obtained in general for high feeds than for low feeds. This is mainly due to the shorter residence time of the distilland on the rotor surface, i.e. the mean distilland composition remains higher for high feed than low feed for the same feed composition. Consequently better distillate composition and slightly higher distillation rate.

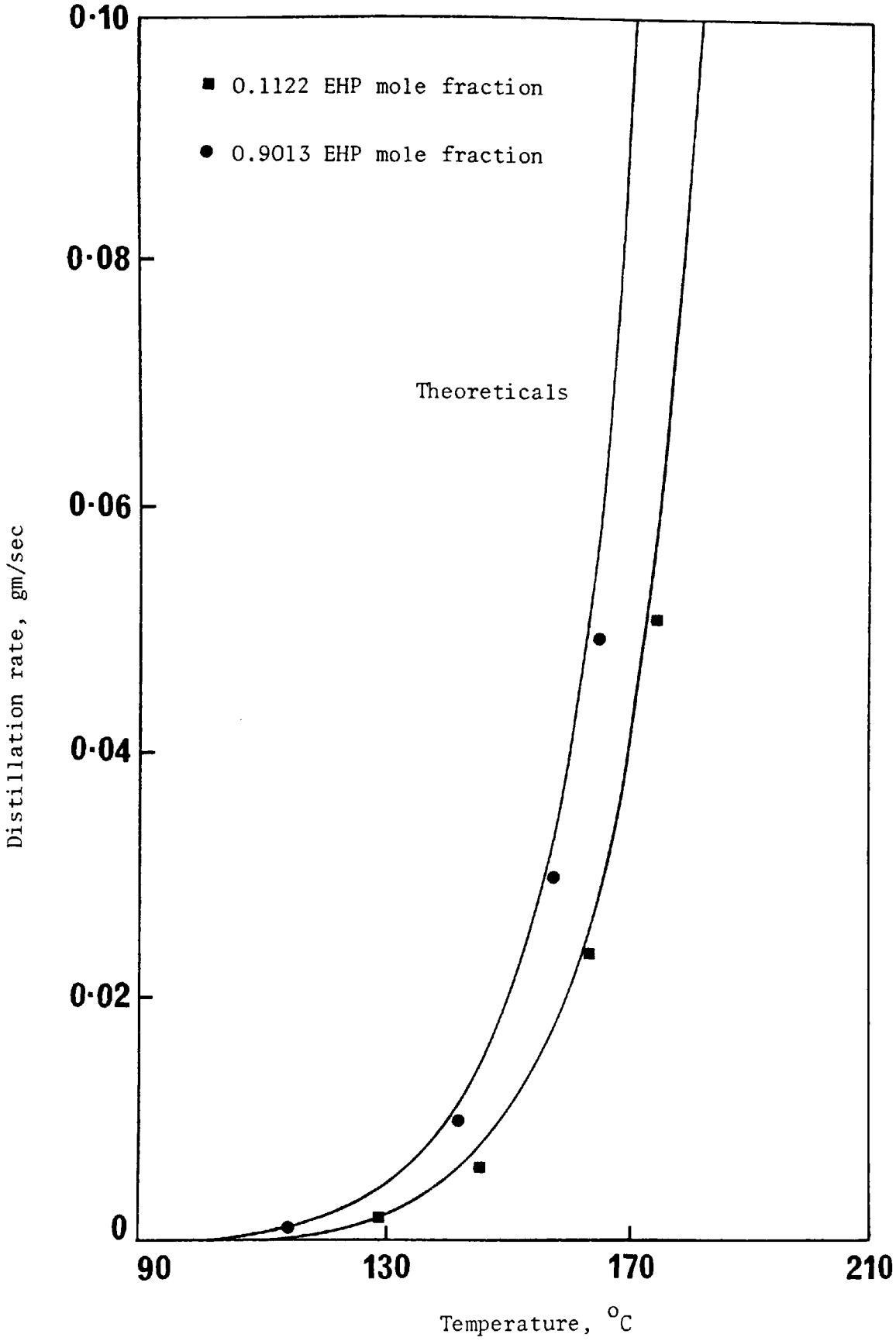

Figure 7.3 : Variation of experimental distillation rate with the mean surface temperature using high feed

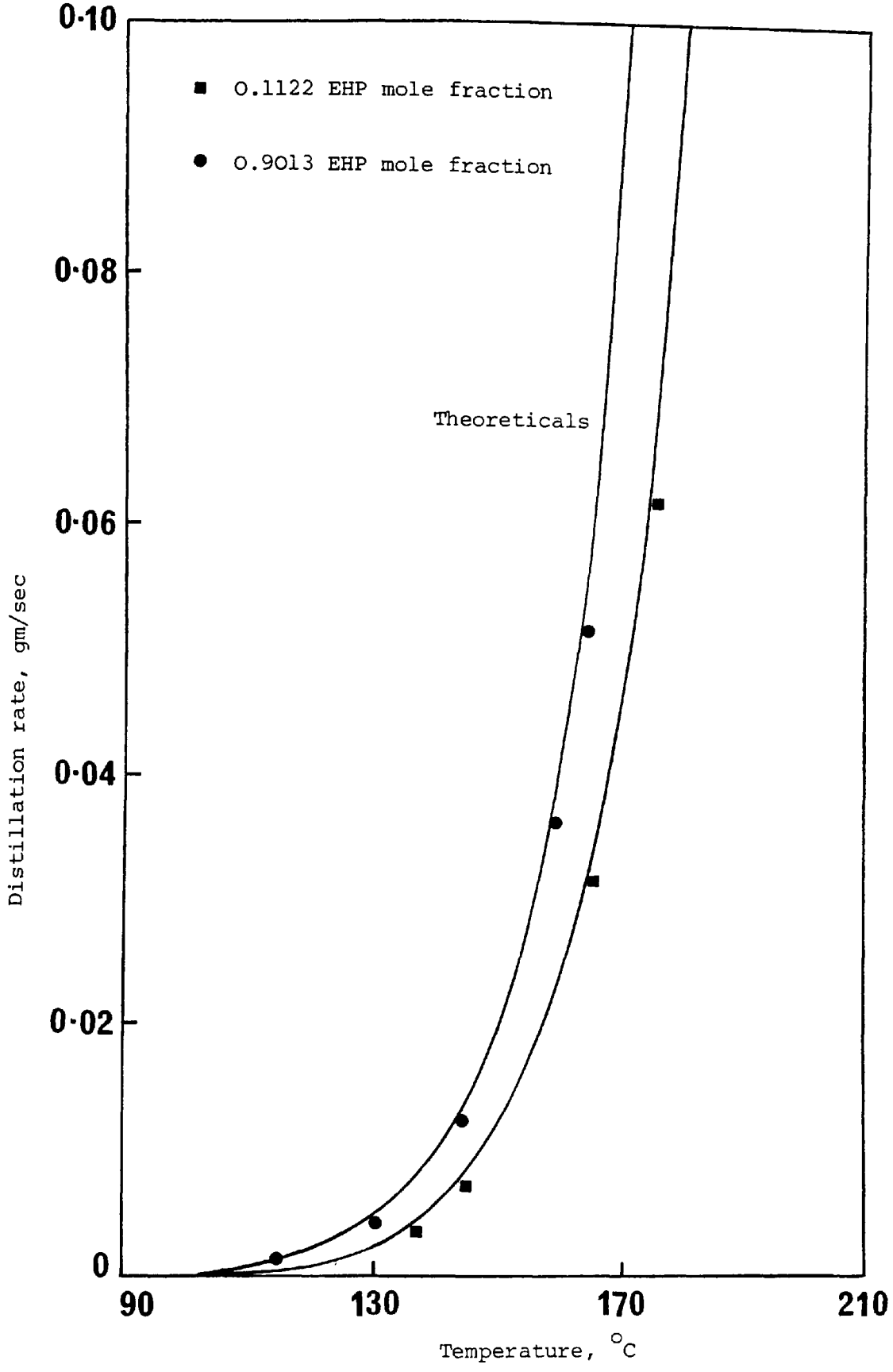

Figure 7.4 : Variation of experimental distillation rate with the mean surface temperature using medium feed

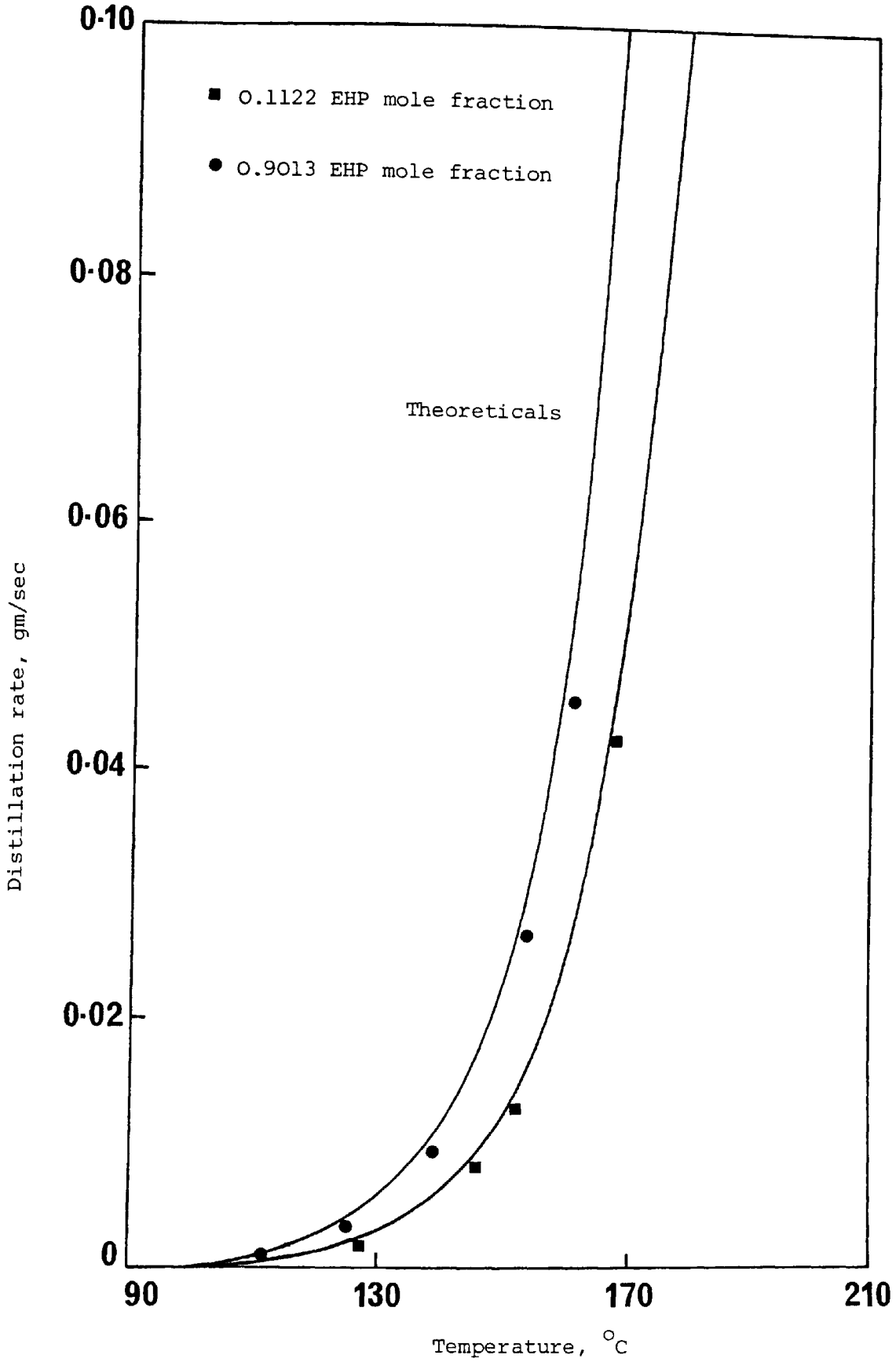

Figure 7.5 : Variation of experimental distillation rate with the mean surface temperature using low feed

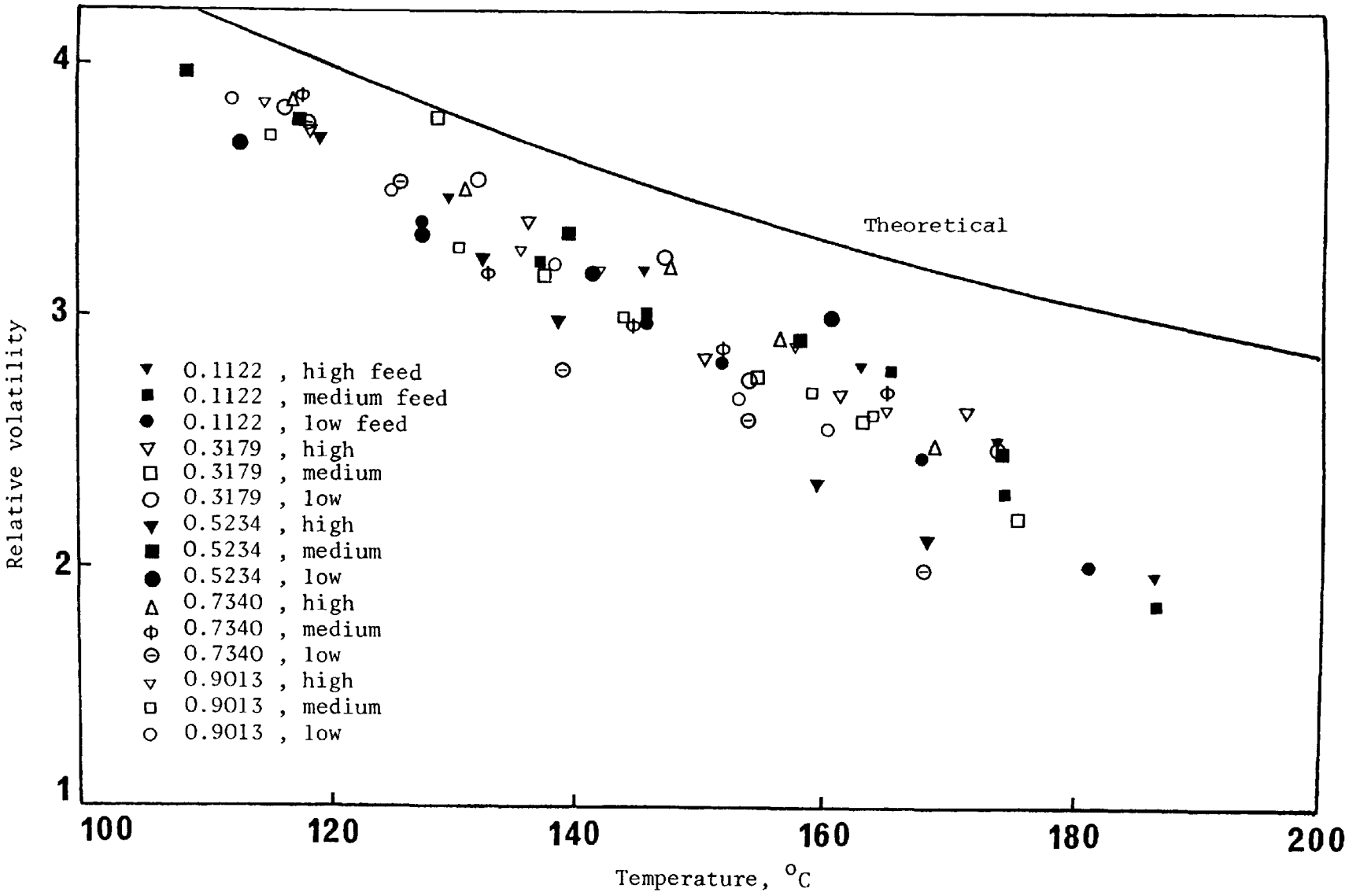

Figure 7.6 : Variation of the experimental relative volatility with the mean surface temperature for different feed compositions and flow rates.

In regard to the relationship between feed compositions and experimental relative volatility, no trends are apparent. This finding is also in agreement with Trevoy's conclusion regarding the distillation of this mixture in the falling-stream tensimeter.

Therefore, it could be concluded that the experimental relative volatility for the EHP-EHS system is virtually independent of the composition of the mixture and its dependency on temperature is not far from that of the theoretical providing that the distillation temperature is kept below 160°C.

7.5.4. Theoretical Molecular Plate

In estimating the number of theoretical plates in the CMS-5, use can be made of equation (2.53), where x_o is now the numerically calculated mean distilland composition; x_n is the experimental distillate composition; and α is the theoretically calculated mean relative volatility.

The calculated values of TMP for 74 experimental runs are presented in Figure 7.7 as functions of the mean surface temperature. Since the CMS-5 is a single stage distillation unit, theoretically speaking [7], it can only represent one TMP. Although the results for the experimental distillate compositions are given in Tables 1 through 75 and are self-explanatory when compared to the theoretically calculated values and feed compositions, expressing them in terms of the TMP will show the general trend of the efficiency of the CMS-5.

Figure 7.7 shows that the TMP can reach 0.96 at low temperature, i.e. low distillation rate, and gradually decreases to (0.8-0.9) at 160°C. Above 160°C falls sharply with increasing the

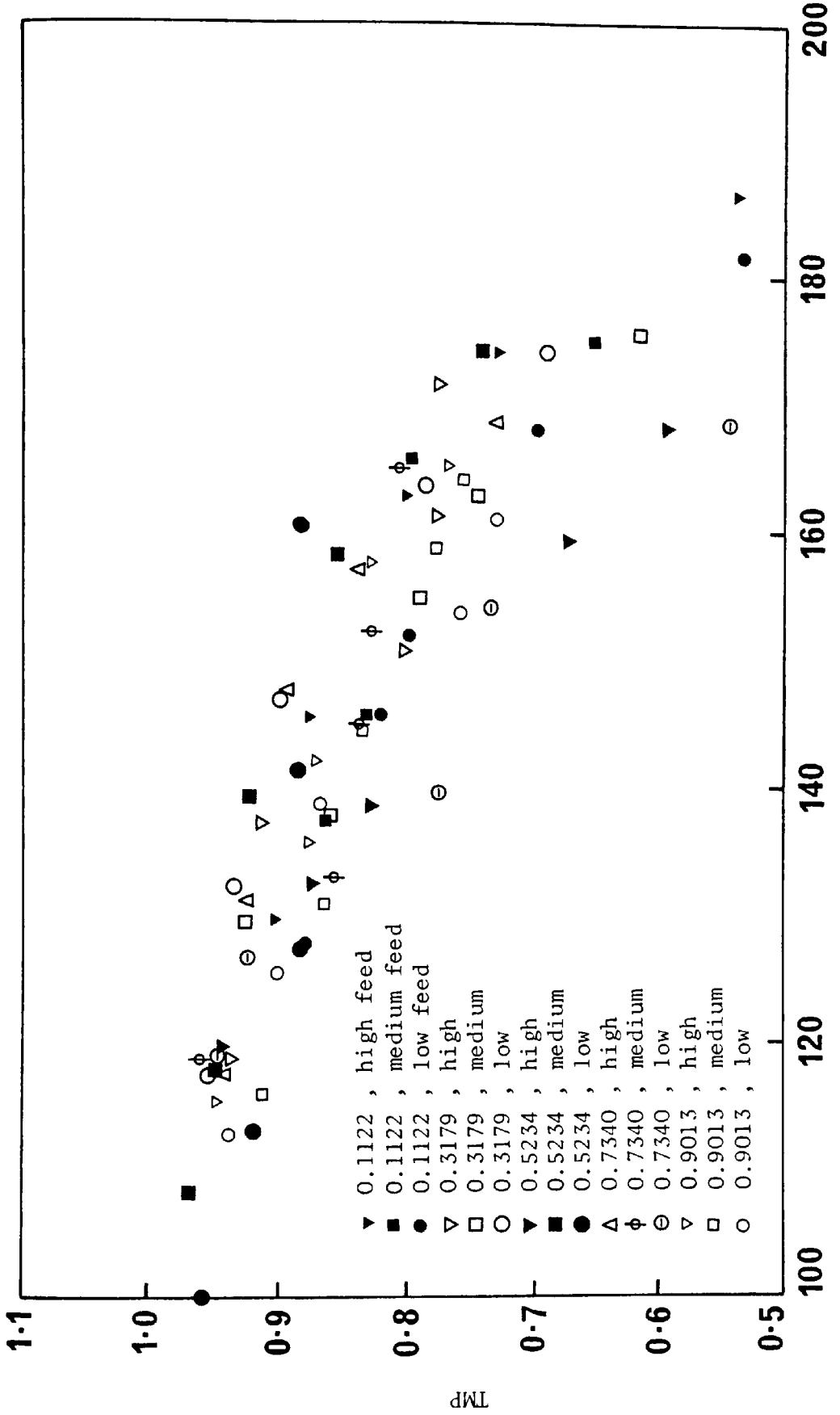

7.7 : Variation of the theoretical molecular plate, with the mean surface temperature for different feed compositions and flow rates

temperature to a value of 0.53 at (170^{o}-190^{o}C). The influence of the feed rate, which was evident in the variation of relative volatility with the mean surface temperature does not appear. The values obtained here are comparable to Trevoy's data and three times better than Cvengros'.

Since the evaluation of the TMP involved an experimentally measured value, the mean composition of distillate x_n, the numerical solution of the mathematical model applies directly to the physical problem when the CMS-5 is evaluated in terms of the TMP than the relative volatility.

CHAPTER VIII

CONCLUSIONS AND SUGGESTIONS FOR FURTHER WORK

8.1 CONCLUSIONS

One of the main achievements of this study is the mathematical model, where the equations of fluid dynamics, heat transfer, and surface evaporation under conditions of molecular distillation are directly applied to the centrifugal molecular still. Despite the limitations of this model, it offers good agreement between the experimental and calculated values, and without it, it was not possible to predict the true temperature of distillation which was found to differ by as much as 40^{o}C (depending on the rates of distillation and feed) from that claimed by the manufacturers of the CMS-5. The tabulated solutions for each experimental run provide comprehensive information regarding the transport behaviour of the fluid on the rotor surface during the process of molecular distillation.

This study has also provided new physical property data for the test mixture and confirmed that its relative volatility is independent of composition.

The separating efficiency of the still has been also improved by the various modifications, particularly the addition of a water-cooled condenser.

8.2 SUGGESTIONS FOR FURTHER WORK

This investigation can be extended to include the following areas:

(1) The application of the mathematical model to non-ideal binary mixtures.

(2) The application of the mathematical model to a CMS-15 centrifugal molecular still using the present binary mixture.

(3) A theoretical and experimental study of the separations attainable with ternary systems.

REFERENCES

1. Alty,T. "The Maximum Rate of Evaporation of Water".
   Phil.Mag., 15, p.82 (1933).

2. Alty,T. and Mackay,C.A. "The Accommodation Coefficient and the Evaporation Coefficient of Water".
   Proc.Roy.Soc. (London), A.149, p.104 (1935).

3. Alty,T. and Nicoll,F.H. "The Interchange of Molecules between a Liquid and its Vapor".
   Can.J.Research, 4, p.547 (1931).

4. Baranaev,M. "Relation between Surface Energy of Liquids and the Accommodation Coefficient".
   J.Phys.Chem. (U.S.S.R.), 13, p.1635 (1939).

5. Barclay,I.M. and Butler,J.A.V. "The Entropy of Solution".
   Trans.Far.Soc., 34, p.1445 (1938).

6. Bellingham and Stanley Ltd., Tunbridge Wells, England.
   Abbe 60 Refractometer Instruction Manual.

7. Biehler,R.M., Hickman,K.C.D. and Perry,E.S. "Small Laboratory Centrifugal Molecular Still".
   Anal.Chem., 21, p.638 (1949).

8. Bird,R.B., Stewart,W.E. and Lightfoot,E.N.
   Transport Phenomena. Wiley, New York (1960).

9. Birks,J. and Bradley,R.S. "The Rate of Evaporation of Droplets".
   Proc.Roy.Soc. (London), A.198, p.226 (1949).

10. Bromley,L.A. "Prediction of Performance Characteristics of Hickman-Badger Centrifugal Boiler Still".
    Ind.Eng.Chem., 50, p.233 (1958).

11. Bronsted,J.N. and von Hevesy,G. "Uber die Trennung der Isotopen des Quecksilbers".
    Z.Physik.Chem., 99, p.189 (1921).

12. Brush,S.G. Kinetic Theory, Vol.3.
Pergamon Press, Oxford (1972).

13. Bucka,H. "The Condensation Coefficient of Ethanol and a Procedure for Determining Condensation Coefficients".
Z.Physik.Chem., 195, p.260 (1950).

14. Burch,C. "Some Experiments on Vacuum Distillation".
Proc.Roy.Soc.(London), A.123, p.271 (1929).

15. Burch,C. and van Dijck,W. "The Theory and Development of High-Vacuum Distillation".
J.Soc.Chem.Ind., Trans. 58, p.39 (1939).

16. Burrows,G. "Determination of the Boiling Points of Liquids of Low Vapour Pressure".
J.Soc.Chem.Ind., 65, p.360 (1946).

17. Burrows,G. "Some Aspects of Molecular Distillation".
Trans.Inst.Chem.Eng., 32, p.23 (1954).

18. Burrows,G. "Evaporation at Low Pressures".
J.Appl.Chem., 7, p.375 (1957).

19. Burrows,G. Molecular Distillation.
Oxford University Press, Oxford (1960).

20. Burrows,G. "Evaporation in an Evacuated Container".
Vacuum, 15, p.389 (1965).

21. Buttrey,D.N. Plasticizers.
Cleaver-Home Press Ltd., London (1950).

22. Carman,P.C. "Molecular Distillation and Sublimation".
Trans.Far.Soc., 44, p.529 (1948).

23. Chalmers,B. and King.R. Progress in Metal Physics, 6.
Pergamon Press (1956).

24. Clausius,R. "Ueber die Mittlere Lange der Wege, Welch bei Molecularbewegung Gasformigen Korpor von den Einzelnen Moleculen Zurnckgelegt Werden, nebst Einigen Anderen Bemerkuugen Uber die Mechanischen Warmetheorie".
Ann.Phys., 105, p.239 (1858).

25. Consolidated Vacuum Corporation, Rochester, New York.
CMS-5 Instruction Manual.

26. Cvengros,J. and Tkac,A. "Continuous Processes in Wiped Films 2. Distilling Capacity and Separating Effficiency of a Molecular Evaporator with a Convex Evaporating Surface".
Ind.Eng.Chem.Process Des.Dev., 17, p.246 (1978).

27. Delaney,L.J., Houston,R.W. and Eagleton,L.C. "The Rate of Vaporization of Water and Ice".
Chem.Eng.Sci., 19, p.105 (1964).

28. Dieter,K. "Efficiency of Thin-Layer Evaporation, II. Distillation Mass-Transfer Coefficients".
Chem.Z., 94, p.445 (1970).

29. Dixon,B.E., Russell,A.A.W. and Swallow,J.E.L. "Liquid Films Formed by Means of Rotating Discs".
Br.J.Appl.Phys., 3, p.3 (1952).

30. Dorn,W.S. and McCracken,D.D. Numerical Methods with Fortran IV Case Studies.
John Wiley and Sons, New York (1972).

31. Dushman,S. Scientific Foundations of Vacuum Technique.
John Wiley and Sons, New York (1966).

32. Emslie,A.G., Bonner,F.T. and Peck,L.G. "Flow of a Viscous Liquid on a Rotating Disc".
J.Appl.Phys., 29, p.856 (1958).

33. Fallah,R., Hunter,T.G. and Nash,A.W. "The Application of Physico-Chemical Principles to the Design of Liquid-Liquid Contact Equipment, Part III : Isothermal Flow in Liquid Wetted-Wall Systems". J.Soc.Chem.Ind., 53, p.369 (1934).

34. Fawcett,E.W.M. "The General Technique of Molecular Distillation, I: The Characteristics and Scope of the Process". J.Soc.Chem.Ind.Trans., 58, p.43 (1939).

35. Friedman,S.J. and Miller,C.O. "Liquid Films in the Viscous Flow Region". Ind.Eng.Chem., 33, p.885 (1941).

36. Glasstone,S., Laidler,K.J. and Eyring,H. The Theory of Rate Processes. McGraw-Hill, New York (1941).

37. Gebruder Haake, Berlin, W.Germany. RV2 Instruction Manual.

38. Greenberg,D.B. High Vacuum Distillation. Ph.D.Dissertation. Louisiana St.Univ., Baton Rouge (1964).

39. Greenberg,D.B. "Theoretical and Experimental Study of the Centrifugal Molecular Still". A.I.Chem.Eng.J., 18, p.269 (1972).

40. Grimley,S.S. "Liquid-Flow Conditions in Packed Towers". Trans.Inst.Chem.Engrs. (London), 23, p.228 (1948).

41. Heideger,W.J. and Boudart,M. "Interfacial Resistance to Evaporation". Chem.Eng.Sci., 17, p.1 (1962).

42. Hertz,H. "On the Evaporation of Liquids: Especially Mercury, in Vacuo". Ann.Phys. (Leipzig), 17, p.177 (1882).

43. Herzfeld,K.K. Kinetische Theorie der Warme.
Brannschweig (1925).

44. Hickman,K.C.D. "Molecular Distillation Apparatus and Methods".
Ind.Eng.Chem., 29, p.968 (1937).

45. Hickman,K.C.D. U.S.Patent No.2210,928. 13 August (1940).

46. Hickman,K.C.D. "High Vacuum Short-Path Distillation : A Review".
Chem.Rev., 34, p.51 (1944).

47. Hickman,K.C.D. "Commercial Molecular Distillation".
Ind.Eng.Chem., 39, p.686 (1947).

48. Hickman,K.C.D. "Surface Behaviour in the Pot Still".
Ind.Eng.Chem., 44, p.1892 (1952).

49. Hickman,K.C.D. and Embree, N.D. "Decomposition Hazard of
Vacuum Stills".
Ind.Eng.Chem., 40, p.135 (1948).

50. Hickman,K.C.D., Hecker,J.C. and Embree,N. "Direct Determination
of Low Vapour Pressures".
Ind.Eng.Chem.Anal.Ed., 9, p.264 (1937).

51. Hickman,K.C.D. and Trevoy, D.J. "Studies in High Vacuum
Evaporation".
Ind.Eng.Chem., 44, p.1882 (1952).

52. Hickman,K.C.D. and Trevoy,D.J. "Comparison of High Vacuum
Stills and Tensimeters".
Ind.Eng.Chem., 44, p.1903 (1952).

53. Hinze,J.O. and Milborn,H. "Atomization of Liquids by Means of
a Rotating Cup".
J.Appl.Mech., 17, p.145 (1950).

54. Hirschfelder,J.O., Stevenson,D.P. and Eyring,H. "A Theory of
Liquid Structure".
J.Chem.Phys., 5, p.896 (1937).

55. Hollo,J., Kurucz,E. and Borodi,A.
The Applications of Molecular Distillation.
Akademiai Kiado, Budapest (1971).

56. Irving,J.B. and Barlow,A.J. "An Automatic High Pressure Viscometer".
J.Phys.E : Sci.Instrum., 4, p.232 (1971).

57. Ishii,H. "A Continuous Distillation Method for High Grade Diffusion Pump Fluids : Checking the Ultimate Vacuum of the Distillates".
Proc. 1st Int.Cong. on Vac.Tech., 2, p.186 (1958).

58. Jacobs,R.B. and Kapff,S.F. "Trajectories of Heavy Molecules in Air".
Ind.Eng.Chem., 40, p.842 (1948).

59. Jeans,J. An Introduction to the Kinetic Theory of Gases.
MacMillan Co., New York (1940).

60. Kapff,S.F. and Jacobs,R.B. "Determination of Vapor Pressures below 10^{-3} mm Hg".
Rev.Sci.Instrum., 18, p.581 (1947).

61. Kawala,Z. "A Dibutyl Phthalate-Dibutyl Sebacate Mixture as a System for Testing Molecular Distillation Columns".
Int.Chem.Eng., 14, p.536 (1974).

62. Kamiya,T. and Kayano,A. "Film-Type Disintegration by Rotating Disk".
J.Chem.Eng.Japan, 5, p.174 (1972).

63. Kincaid,J.F. and Eyring,H. "Free Volumes and Free Angle Ratios of Molecules in Liquids".
J.Chem.Phys., 6, p.620 (1938).

64. Knudsen,M. "Molecular Flow of Hydrogen through Tubes and the Hot-Wire Anemometer.
Ann.Phys. (Leipzig), 35, p.389 (1911).

65. Knudsen,M. "Maximum Velocity of Evaporation of Mercury". Ann.Phys. (Leipzig), 47, p.697 (1915).

66. Koch-Light Laboratories Ltd. Private Communication (1980).

67. Langmuir,I. "Chemical Reactions at Very Low Pressures, I : The Clean-up of Oxygen in a Tungsten Lamp". J.Am.Chem.Soc., 35, p.105 (1913).

68. Langmuir,I. "The Characteristics of Tungsten Filaments as Functions of Temperature". Phys.Rev., 7, p.302 (1916).

69. Loeb,L.B. Kinetic Theory of Gases. McGraw-Hill, New York (1934).

70. Lohwater,R.K. "Progress Report - Molecular Distillation". Res./Dev., 22, p.36 (1971).

71. Malafeev,N.A., Malyusov,V.A. and Podgornaya,I.V. "Determination of Coefficients of Separation of a Dibutyl Azelate-Bis(2-Ethylhexyl) Phthalate Mixture by Evaporation in High Vacuum". Zh.Prikl.Khim., 38, p.2066 (1965).

72. Malyusov,V.A. and Malafeev,N.A. "The Relative Volatilities of Mixtures in Evaporation under High Vacuum". Dokl.Akad.Nauk.SSSR., 16, p.660 (1957).

73. Malyusov,V.A., Malafeev,N.A. and Zhavoronkov,N.M. "Distillation Process in Molecular Stills of the Centrifugal Type". Khim.Prom., 33, p.31 (1958).

74. Malyusov,V.A., Malafeev,N.A. and Zhavoronkov,N.M. "Determination of the Separation Coefficient of Dibutyl Phthalate-Dibutyl Azelate Mixture by Vaporization in High Vacuum". Zhur.Fiz.Khim., 32, p.2403 (1958).

75. Maxwell,J.C. "Illustrations of the Dynamical Theory of Gases". Phil.Mag., 20, p.21 (1860).

76. Meyer,O.E. Kinetic Theory of Gases. Longmans, Green and Co., London (1899).

77. Nabavian,K. and Bromley,L.A. "Condensation Coefficient of Water". Chem.Eng.Sci., 18, p.651 (1953).

78. Neumann,K. "Comments on the Theory of Vaporization Velocity". Z.Physik.Chem., 196, p.16 (1950).

79. Nikolaev,V.S., Vachagin,K.D. and Baryshev,Y.N. "Film Flow of Viscous Liquids over Surfaces of Rapidly Rotating Conical Discs". Int.Chem.Eng., 7, p.595 (1967).

80. Norman,W.S. and Binns,D.T. "The Effect of Surface Tension Changes on the Minimum Wetting Rates in a Wetted-Rod Distillation Column". Trans.Inst.Chem.Eng., 38, p.294 (1960).

81. Penn,R.W. and Kearsley,E.A. "An Absolute Determination of Viscosity using Channel Flow". J.Res.Nat.Bur.Stad., A.75, 6, p.553 (1971).

82. Penner,S.S. "The Maximum Possible Rate of Evaporation of Liquids". J.Phys.Chem., 52, p.367 (1948).

83. Penner,S.S. "Melting and Evaporation as Rate Processes". J.Phys.Chem., 52, p.949 (1948).

84. Penner,S.S. "Additions to the Article - Melting and Evaporation as Rate Processes". J.Phys.Chem., 52, p.1262 (1948).

85. Penner,S.S. "On the Kinetics of Evaporation". J.Phys.Chem., 56, p.475 (1952).

86. Perkin-Elmer Corporation, Norwalk, Connecticut, U.S.A.
DSC-2 Instruction Manual.

87. Perry,E.S. and Cox,D.S. "High-Vacuum Still".
Ind.Eng.Chem., 48, p.1473 (1956).

88. Perry,E.S. and Fuguitt,R.E. "Liquid Vapour Equilibria in High Vacuum : Two Phthalate Sebacate Systems at .1 mm".
Ind.Eng.Chem., 39, p.782 (1947).

89. Perry,E.S. and Weber,W.H. "Vapour Pressures of Phlegmatic Liquids, II".
J.Am.Chem.Soc., 71, p.3726 (1949).

90. Polanyi,M. and Wigner,E. "The Interference of Characteristic Vibrations as the Cause of Energy Fluctuations and Chemical Change".
Z.Physik.Chem., 139, p.439 (1928).

91. Poltz,H. "The Thermal Conductivity of Dialky-phthalates".
Waerme-Stoffuebertrag, 3, p.247 (1970).

92. Ratchford,W.P. and Rehberg,C.E. "An Improved Tensimeter-Still".
Anal.Chem., 21, p.1417 (1949).

93. Ray,A.K. and Davies,E.J. "Determination of Ultra-Low Vapour Pressures by Submicron Droplet Evaporation",
J.Chem.Phys., 71, p.582,(1979).

94. Rayleigh,L. "On the Distillation of Binary Mixtures".
Phil.Mag., 4, p.521 (1902).

95. Rees,G.J., Scully,D.B. and Weldon,L.H.P. "Optimisation of Separating Efficiency in the Centrifugal Molecular Still".
Chem.Eng.Sci., 34, p.159 (1979).

96. Reid,R.C. and Shwerwood, T.K. The Properties of Gases and Liquids.
McGraw-Hill, New York (1966).

97. Rukenshtein,E. "Continuous Molecular Distillation".
Dokl.Akad.Nauk. SSSR., 108, p.518 (1956).

98. Schlichting,H. Boundary Layer Theory.
McGraw-Hill, New York (1968).

99. Schrage,R.W. A Theoretical Study of Interphase Mass Transfer.
Columbia Univ.Press, New York (1953).

100. Sherwood,T.K. and Cook,N.E. "Mass Transfer at Low Pressures".
Am.Inst.Chem.Eng., 3, p.37 (1957).

101. Sherwood,T.K. and Pigford,R.L. Absorption and Extraction.
McGraw-Hill, New York (1952).

102. Small,P.A., Small,K.W. and Cowley,P. "The Vapour Pressures of
Some High Boiling Esters".
Trans.Far.Soc., 44, p.810 (1948).

103. Sunier,A. and Rosenblum,C. "Physical Methods of Separating
Constant-Boiling Mixtures".
Ind.Eng.Chem.Anal.Ed., 2, p.109 (1930).

104. Taylor,J.H. "Systems Design for Centrifugal Molecular Distillation".
Chem.Eng., 26, p.109 (1968).

105. Tkac,A. and Cvengros,J. "Continuous Processes in Wiped Films, I :
Multistage Molecular Distillation in an Arrangement
with a Single Convex-Shaped Evaporator Body.
Ind.Eng.Chem.Process Des.Dev., 17, p.242 (1978).

106. Toei,R., Okazaki,M. and Asseda,H. "Some Considerations of
Mass Transfer under Vacuum".
J.Chem.Eng.Japan, 4, p.188 (1971).

107. Trevoy,D.J. "Projective and Equilibrium Vapour-Liquid Relationship
for Two Binary Systems over an Extended Range".
Ind.Eng.Chem., 44, p.1888 (1952).

108. Trevoy,D.J. "Rate of Evaporation of Glycerol in High Vacuum". Ind.Eng.Chem., 45, p.2366 (1953).

109. Uyeha,H., Kajiura,T. and Yoshikawa,O. "Evaporation from a Liquid Surface under a High and Medium Vacuum". Kagaku Kogaku, 24, p.274 (1960).

110. Washburn,E.W., Brunn,J.H. and Hicks,M.M. "Apparatus and Method for the Separation, Identification, and Determination of the Chemical Constituents of Petroleum". Bur.Stds.J.Res., 2, p.476 (1929).

111. Watt,P.R. Molecular Stills. Reinhold Publishing Co., New York (1963).

112. Werner, A.C. "Vapour Pressure of Phthalate Esters". Ind.Eng.Chem., 44, p.2736 (1952).

113. Williams,F.E. "A Binary Mixture for Evaluating Low Pressure Distillation Columns". Ind.Eng.Chem., 39, p.779 (1947).

114. Wyllie,G. and Wills,H.H. "Evaporation and the Surface Structure of Liquids". Proc.Roy.Soc. (London), A.197, p.383 (1949).

115. Yamada,I., Hiraoka,S., Inuzuka,M. and Yoshizane, H. "Characteristics of Liquid Film on a Rotating Spherical Surface". Kagaku Kogaku Ronbunshu, 3, p.96 (1977).

116. Yarwood,J. High Vacuum Techniques : Theory, Practice and Properties of Materials. Chapman and Hall, London (1967).

117. Ziolkowski,Z. and Kawala,Z. "Molecular Distillation Process in a Multistage Apparatus, I : Distillation Rate". Chem.Stos., 7, p.539 (1970).

APPENDICES

APPENDIX I

NOMENCLATURE

A	area
B	defined in page 149
C	defined in page 136
C_p	specific heat
C_2	defined in page 149
D	equivalent diameter of the fluid system
erf	error function
F	dimensionless pressure
g	gravitational constant
G	mass flow rate
k	thermal conductivity
K	defined in page 145
M	molecular weight
P	vapour pressure
Q	volumetric flow rate
r	radial distance in spherical coordinate
R	dimensionless radial distance
Re	Reynolds number based on flow rate
t	residence time
T	temperature
U,V,W	dimensionless velocities
U_ϕ	circumferential velocity
V_r, V_ϕ, V_θ	velocity components in the liquid film
w	total amount evaporated in time, t
y	coordinate system perpendicular to r

Greek symbols

α	relative volatility
α'	thermal diffusivity
β	similarity variable
γ	activity coefficient
δ	film thickness
Δ	dimensionless radial film thickness
η	dimensionless angular velocity
θ	angle in spherical coordinate
μ	viscosity
ν	kinematic viscosity
ξ	dimensionless distance from the surface of the rotor
ρ	density
ϕ	angle in spherical coordinate
ψ	reduced temperature
ω	angular velocity

Superscripts and subscripts

-	mean value
mx	maximum value
o	initial value
s	pertains to film surface
h	pertains to rotor surface
*	dimensionless variable
1,2	components in the binary system

APPENDIX II

COMPUTER PROGRAM FOR THE SOLUTION OF THE MATHEMATICAL MODEL

II.1 LIST OF SYMBOLS

Some symbols of the notation used for the equations in Chapters V and VI have been changed slightly in order to make the symbols more suitable for insertion in FORTRAN instructions.

Program symbol	Principal variable	Program symbol	Principal variable
GI	G_o	EHPTER	K_1
XI	$\mathbf{x}_o$	GAMMA1	$\overline{\gamma}_1$
TI	T_o	GMEAN	$\overline{G}$
TMDP	T_{mdp}	G1STAR	G_1^*
TH	T_h	G2STAR	G_2^*
RO	r_o	GSTAR	G^*
RR	r	DELTA	δ
ALFA	α	VMEAN	$\overline{V}_r$
RØ	ρ_{mix}	RE	Re
VISK	μ_{mix}/ρ_{mix}	BEE	B
COND	k	BETA	β
SPHT	C_{mix}	ZI	ψ

II.2 LISTING OF THE COMPUTER PROGRAM

```
C****      DISTILLATION OF A BINARY MIXTURE IN THE
C                  CENTRIFUGAL MOLECULAR STILL
C
C
C
C**    DEFINE A DUMMY VARIABLE FOR THE INTEGRAND
         F(Y)=EXP(-Y*Y/3.0)
         READ(5,11)Z,EPSI,N
    5    READ(5,10)GI,XI,TI,TMDP,TH
         IF(GI.EQ.0.0) GO TO 900
   11    FORMAT(F5.1,F10.7,I4)
   10    FORMAT(2F10.6,3F10.2)
  333    T0=TI
         G0=GI
         X0=XI
         R0=1.15
         RR=1.15
         G1STAR=0.999
         ALFA=0.0
         ALFSUM=0.0
         TSUM=0.0
         XSUM=0.0
         R0=0.0693*X0+0.9103
         VISK=(X0*10.0**(0.82536-0.40577*T0**0.25)+(1.0-X0)
        1 *10.0**(14.95492*T0**(-1.0)-0.654215))**3.0/R0
         DELTA0=(VISK*G0/36995.25/R0)**(1.0/3.0)*R0**(-2.0/3.0)
         VMEAN0=6095.683*R0*DELTA0**(2.0)/VISK
         RE0=4.0*DELTA0*VMEAN0/VISK
  101    WRITE(6,12)R0,G0,X0,DELTA0,VMEAN0,RE0,T0,ALFA
   12    FORMAT(10X,8(F10.6,3X))
         TM=(TH+T0)/2.0
         R0=0.0693*X0+0.9103
         VISK=(X0*10.0**(0.82536-0.40577*TM**0.25)+(1.0-X0)
        1 *10.0**(14.95492*TM**(-1.0)-0.654215))**3.0/R0
         COND=3.26441*10.0**(-4.0)-2.44*10.0**(-7.0)*TM
         SPHT=0.4393+(8.467394*10.0**(-4.0)*TM)-0.02524
        1 *X0-(1.225941*10.0**(-4.0)*TM*X0)
         ALFA=1.0452*10.0**(340.0/(T0+273.15)-0.28)
         EHPTER=-0.05833*(390.57/(T0+273.15))**0.5*
        1 0.001*10.0**(14.62-5440.0/(T0+273.15))
         C=12.35305/(VISK**(1.0/3.0))/(R0**(2.0/3.0))
         RR=RR+5.08/Z
         IF(RR.GT.6.24) GO TO 108
         R=RR/R0
         PI=3.1416
         GAMMA1=1.0
         G01=G0*X0*390.57/(X0*390.57+426.68*(1.0-X0))
         G02=G0-G01
         A=EHPTER*GAMMA1*PI*0.96593*R0**(10.0/3.0)*(R**(4.0/3.0)+
        1 R**(2.0/3.0)+1.0)*(R-1.0)**2.0/C
         ITER=1
```

```
  102   B=(G1STAR**2.0-1.0)*0.5*G01**2.0+(G1STAR**(1.0/ALFA+1.0)-1.0)
     1 *G01*G02*0.91537*ALFA/(1.0+ALFA)
        D=(G1STAR-1.0)*G01+(G1STAR**(1.0/ALFA)-1.0)*ALFA*G02*0.91537
        E=(G1STAR**(2.0/ALFA)-1.0)*0.5*G02**2.0+(G1STAR**(1.0/ALFA+1.0)-
     1 1.0)*G01*G02*1.09245/(1.0+ALFA)
        Q=(G1STAR**(1.0/ALFA)-1.0)*G02+(G1STAR-1.0)*G01*1.09245/ALFA
        DD=G01+G02*0.91537*G1STAR**(1.0/ALFA-1.0)
        BD=G01*G01*G1STAR+G01*G02*0.91537*G1STAR**(1.0/ALFA)
        ED=G02*G02/ALFA*G1STAR**(2.0/ALFA-1.0)+G01*G02/ALFA*1.09245*
     1 G1STAR**(1.0/ALFA)
        QD=G02/ALFA*G1STAR**(1.0/ALFA-1.0)+G01*1.09245/ALFA
C**     BEGINS NEWTON'S METHOD
        FK=(B/D+E/Q)**(2.0/3.0)*D-A
        FD=DD*(B/D+E/Q)**(2.0/3.0)+2.0/3.0*D*(B/D+E/Q)**(-1.0/3.0)*
     1 ((D*BD-B*DD)/D/D+(Q*ED-E*QD)/Q/Q)
        G1STNE=G1STAR-FK/FD
        WRITE(6,701)G1STNE
  701   FORMAT(50X,F10.7)
        ERR=ABS((G1STNE-G1STAR)/G1STAR)
        IF (EPSI.GT.ERR) GO TO 103
        IF(ITER.GT.30) GO TO 700
        IF(G1STNE.LE.0.0) GO TO 700
        ITER=ITER+1
        G1STAR=G1STNE
        GO TO 102
  103   G1STAR=ABS(G1STNE)
        B=(G1STAR**2.0-1.0)*0.5*G01**2.0+(G1STAR**(1.0/ALFA+1.0)-1.0)
     1 *G01*G02*0.91537*ALFA/(1.0+ALFA)
        D=(G1STAR-1.0)*G01+(G1STAR**(1.0/ALFA)-1.0)*ALFA*G02*0.91537
        E=(G1STAR**(2.0/ALFA)-1.0)*0.5*G02**2.0+(G1STAR**(1.0/ALFA+1.0)-
     1 1.0)*G01*G02*1.09245/(1.0+ALFA)
        Q=(G1STAR**(1.0/ALFA)-1.0)*G02+(G1STAR-1.0)*G01*1.09245/ALFA
C**     END OF NEWTON'S METHOD
        GMEAN=B/D+E/Q
        G2STAR=G1STAR**(1.0/ALFA)
        G1=G1STAR*G01
        G2=G2STAR*G02
        G=G1+G2
        X1=(G1/390.57)/(G1/390.57+G2/426.68)
        GSTAR=G/G0
        DELTA=DELTA0*GSTAR**(1.0/3.0)*R**(-2.0/3.0)
        VMEAN=VMEAN0*GSTAR**(2.0/3.0)*R**(-1.0/3.0)
        RE=RE0*GSTAR/R
C**     THE HEAT EQUATION
        BEE=5.49024*R0**(1.0/3.0)*SPHT*GMEAN**(2.0/3.0)/
     1 VISK**(1.0/3.0)/COND
        BETA0=BEE**(0.5)*DELTA0/R0**(2.0/3.0)
        BETA=BEE**(0.5)*DELTA/RR**(2.0/3.0)
C**     NUMERICAL INTEGRATION BY SIMPSON'S RULE
        V=BETA0
        W=BETA
        FN=N
        H=(W-V)/FN
        TWOH=H+H
        SUM4=0.0
        SUM2=0.0
        X=V+H
```

```
      I=1
200   SUM4=SUM4+F(X)
      SUM2=SUM2+F(X+H)
      IF (I.GE.N-3) GO TO 201
      I=I+2
      X=X+TWOH
      GO TO 200
201   ZI1=-H/3.0*(4.0*SUM4+2.0*SUM2+F(V)+4.0*F(W-H)+F(W))
      V=0.0
      W=BETAO
      FN=N
      H=(W-V)/FN
      TWOH=H+H
      SUM4=0.0
      SUM2=0.0
      X=V+H
      I=1
300   SUM4=SUM4+F(X)
      SUM2=SUM2+F(X+H)
      IF(I.GE.N-3) GO TO 301
      I=I+2
      X=X+TWOH
      GO TO 300
301   ZI2=H/3.0*(4.0*SUM4+2.0*SUM2+F(V)+4.0*F(W-H)+F(W) )
      ZI=ZI1/ZI2
      TS1=TO+ZI*(TH-TO)
      TO=TS1
      DELTAO=DELTA
      VMEANO=VMEAN
      REO=RE
      XO=X1
      GO1=G1
      GO2=G2
      GO=GO1+GO2
      RO=RR
      TSUM=TSUM+TO
      XSUM=XSUM+XO
      ALFSUM=ALFSUM+ALFA
      GO TO 101
108   ALFMEN=ALFSUM/Z
      TMEAN=TSUM/Z
      XMEAN=XSUM/Z
      WRITE(6,109)ALFMEN,TMEAN,XMEAN
109   FORMAT(//10X,F11.6//10X,F11.6//10X,F11.6)
      GE=GI-GO
      XE=(XI*GI-XO*GO)/GE
      WRITE(6,800)GE,XE
800   FORMAT(///10X,F10.6//10X,F10.6)
      TMNEW=(TO+TH)/2.0
      IF(TMNEW.GE.TMDP) GO TO 700
      TH=TH+0.1
      GO TO 333
700   GO TO 5
900   STOP
      END
```

APPENDIX III

NUMERICAL RESULTS OF EXPERIMENTAL RUNS

Table III.1 : Run 42

Mean distillation rate (gm/sec)		Distillate mole fraction (—)		Mean relative volatility (—)		Mean temperature (^{o}C)	
Theoretical	Experimental	Theoretical	Experimental	Theoretical	Experimental	Distilland	Surface
0.002016	0.001973	0.315581	0.301200	4.046155	3.383886	153.900000	127.808852
Radial position (cm)	Mass flow rate (gm/sec)	EHP mole fraction (—)	Film thickness (cm)	Mean velocity (cm/sec)	Reynolds number (—)	Surface temperature (^{o}C)	Relative volatility (—)
1.150	0.288200	0.112200	0.008810	5.104976	1.687822	49.000000	0.000000
1.658	0.288200	0.112200	0.006904	4.518887	1.170685	88.110679	5.302127
2.166	0.288198	0.112198	0.005777	4.133701	0.896113	108.774435	4.473016
2.674	0.288184	0.112187	0.005020	3.853287	0.725838	121.067208	4.108821
3.182	0.288143	0.112154	0.004470	3.636058	0.609871	129.056738	3.910005
3.690	0.288052	0.112086	0.004049	3.460533	0.525744	134.597047	3.786773
4.198	0.287890	0.111968	0.003715	3.314286	0.461865	138.630585	3.703769
4.706	0.287639	0.111787	0.003442	3.189533	0.411649	141.679829	3.644490
5.214	0.287281	0.111533	0.003213	3.081109	0.371079	144.054958	3.600271
5.722	0.286801	0.111196	0.003018	2.985422	0.337569	145.950505	3.566159
6.230	0.286184	0.110767	0.002850	2.899885	0.309377	147.494050	3.539130

Table III.2 : Run 44

Mean distillation rate (gm/sec)		Distillate mole fraction (—)		Mean relative volatility (—)		Mean temperature (°C)	
Theoretical	Experimental	Theoretical	Experimental	Theoretical	Experimental	Distilland	Surface
0.008772	0.008424	0.290815	0.271300	3.761364	2.985053	177.800000	145.724309
Radial position (cm)	Mass flow rate (gm/sec)	EHP mole fraction (—)	Film thickness (cm)	Mean velocity (cm/sec)	Reynolds number (—)	Surface temperature (°C)	Relative volatility (—)
1.150	0.287900	0.112200	0.008746	5.137197	1.721776	49.500000	0.000000
1.658	0.287900	0.112200	0.006853	4.547408	1.194235	97.045179	5.119999
2.166	0.287894	0.112195	0.005735	4.159775	0.914129	122.311836	4.199814
2.674	0.287851	0.112162	0.004983	3.877459	0.740354	137.383239	3.811127
3.182	0.287700	0.112054	0.004437	3.658403	0.621831	147.194823	3.603032
3.690	0.287346	0.111811	0.004018	3.480736	0.535564	154.008912	3.475477
4.198	0.286686	0.111372	0.003684	3.331705	0.469675	158.978821	3.390133
4.706	0.285623	0.110679	0.003410	3.203260	0.417421	162.744812	3.329410
5.214	0.284065	0.109682	0.003179	3.090013	0.374696	165.687207	3.284190
5.722	0.281926	0.108332	0.002980	2.988183	0.338860	168.044569	3.249302
6.230	0.279128	0.106587	0.002806	2.895010	0.308140	169.973374	3.221615

Table III.3 : Run 45

Mean distillation rate (gm/sec)		Distillate mole fraction (—)		Mean relative volatility (—)		Mean temperature (°C)	
Theoretical	Experimental	Theoretical	Experimental	Theoretical	Experimental	Distilland	Surface
0.014060	0.013382	0.281313	0.258700	3.671838	2.835656	185.800000	151.883890
Radial position (cm)	Mass flow rate (gm/sec)	EHP mole fraction (—)	Film thickness (cm)	Mean velocity (cm/sec)	Reynolds number (—)	Surface temperature (°C)	Relative volatility (—)
1.150	0.287500	0.112200	0.008659	5.181764	1.769435	50.200000	0.000000
1.658	0.287500	0.112200	0.006785	4.586859	1.227292	100.416885	5.047181
2.166	0.287492	0.112193	0.005677	4.195851	0.939425	127.111447	4.108791
2.674	0.287428	0.112146	0.004933	3.910992	0.760786	143.038645	3.717034
3.182	0.287197	0.111985	0.004392	3.689701	0.638815	153.411193	3.508443
3.690	0.286647	0.111618	0.003976	3.509712	0.549814	160.619700	3.380950
4.198	0.285610	0.110949	0.003644	3.357955	0.481533	165.883170	3.295759
4.706	0.283923	0.109885	0.003370	3.226121	0.427015	169.878324	3.235158
5.214	0.281430	0.108341	0.003139	3.108594	0.382027	173.007104	3.189992
5.722	0.277983	0.106239	0.002938	3.001380	0.343846	175.521653	3.155085
6.230	0.273440	0.103504	0.002761	2.901497	0.310648	177.587455	3.127307

Table III.4 : Run 46

Mean distillation rate (gm/sec)		Distillate mole fraction (—)		Mean relative volatility (—)		Mean temperature (^{o}C)	
Theoretical	Experimental	Theoretical	Experimental	Theoretical	Experimental	Distilland	Surface
0.046297	0.042672	0.247838	0.220000	3.457124	2.445781	206.800000	168.068551
Radial position (cm)	Mass flow rate (gm/sec)	EHP mole fraction (—)	Film thickness (cm)	Mean velocity (cm/sec)	Reynolds number (—)	Surface temperature (^{o}C)	Relative volatility (—)
1.150	0.286700	0.112200	0.008408	5.321811	1.922163	52.400000	0.000000
1.658	0.286700	0.112200	0.006588	4.710826	1.333224	109.434775	4.857378
2.166	0.286681	0.112185	0.005513	4.309195	1.020470	139.742370	3.885863
2.674	0.286509	0.112065	0.004789	4.016135	0.826108	157.833116	3.491516
3.182	0.285848	0.111636	0.004262	3.786991	0.692619	169.632608	3.284147
3.690	0.284206	0.110622	0.003853	3.597647	0.593838	177.861573	3.158080
4.198	0.281023	0.108725	0.003523	3.433332	0.516130	183.908516	3.073875
4.706	0.275706	0.105641	0.003244	3.284083	0.451704	188.545005	3.013722
5.214	0.267638	0.101062	0.003000	3.142498	0.395765	192.230975	2.968478
5.722	0.256140	0.094663	0.002778	3.002337	0.345136	195.258425	2.932976
6.230	0.240403	0.086079	0.002570	2.857371	0.297517	197.825546	2.904055

Table III.5 : Run 47

Mean distillation rate (gm/sec)		Distillate mole fraction (—)		Mean relative volatility (—)		Mean temperature (°C)	
Theoretical	Experimental	Theoretical	Experimental	Theoretical	Experimental	Distilland	Surface
0.130150	0.117916	0.191670	0.170300	3.305730	2.011171	225.400000	181.560223
Radial position (cm)	Mass flow rate (gm/sec)	EHP mole fraction (—)	Film thickness (cm)	Mean velocity (cm/sec)	Reynolds number (—)	Surface temperature (°C)	Relative volatility (—)
1.150	0.286500	0.112200	0.008364	5.345740	1.949568	52.800000	0.000000
1.658	0.286500	0.112200	0.006554	4.732007	1.352232	115.868272	4.744919
2.166	0.286464	0.112173	0.005484	4.328488	1.034960	149.496560	3.733885
2.674	0.286107	0.111936	0.004763	4.033243	0.837294	169.612574	3.333193
3.182	0.284645	0.111041	0.004235	3.799561	0.700028	182.779170	3.124609
3.690	0.280866	0.108848	0.003819	3.600448	0.595641	192.030003	2.998107
4.198	0.273273	0.104613	0.003473	3.417568	0.509409	198.923583	2.913190
4.706	0.260099	0.097489	0.003166	3.236146	0.432513	204.338717	2.851673
5.214	0.239087	0.086442	0.002875	3.040843	0.358837	208.825782	2.804122
5.722	0.206815	0.070051	0.002574	2.808948	0.282844	212.799251	2.764881
6.230	0.156350	0.046047	0.002216	2.487342	0.196391	216.751041	2.729537

Table III.6 : Run 49

Mean distillation rate (gm/sec)		Distillate mole fraction (—)		Mean relative volatility (—)		Mean temperature (^{o}C)	
Theoretical	Experimental	Theoretical	Experimental	Theoretical	Experimental	Distilland	Surface
0.003936	0.003803	0.303193	0.289600	3.897841	3.213907	167.800000	137.166213
Radial position (cm)	Mass flow rate (gm/sec)	EHP mole fraction (—)	Film thickness (cm)	Mean velocity (cm/sec)	Reynolds number (—)	Surface temperature (^{o}C)	Relative volatility (—)
1.150	0.365800	0.112200	0.009607	5.942033	2.097012	48.500000	0.000000
1.658	0.365800	0.112200	0.007528	5.259843	1.454502	91.167278	5.259803
2.166	0.365797	0.112198	0.006299	4.811499	1.113364	114.766222	4.358704
2.674	0.365778	0.112186	0.005474	4.485095	0.901801	129.055999	3.963345
3.182	0.365709	0.112146	0.004874	4.232188	0.757689	138.421758	3.748700
3.690	0.365550	0.112055	0.004415	4.027724	0.653093	144.946328	3.616316
4.198	0.365253	0.111893	0.004050	3.857181	0.573596	149.710023	3.527498
4.706	0.364774	0.111636	0.003752	3.711452	0.511008	153.318484	3.464256
5.214	0.364074	0.111266	0.003502	3.584478	0.460334	156.133697	3.417186
5.722	0.363115	0.110767	0.003288	3.472042	0.418361	158.383658	3.380932
6.230	0.361864	0.110122	0.003103	3.371104	0.382924	160.218325	3.352235

Table III.7 : Run 50

Mean distillation rate (gm/sec)		Distillate mole fraction (—)		Mean relative volatility (—)		Mean temperature (°C)	
Theoretical	Experimental	Theoretical	Experimental	Theoretical	Experimental	Distilland	Surface
0.007612	0.007469	0.292363	0.274500	3.772371	3.011032	178.800000	145.386724
Radial position (cm)	Mass flow rate (gm/sec)	EHP mole fraction (—)	Film thickness (cm)	Mean velocity (cm/sec)	Reynolds number (—)	Surface temperature (°C)	Relative volatility (—)
1.150	0.365300	0.112200	0.009548	5.970589	2.130303	48.900000	0.000000
1.658	0.365300	0.112200	0.007482	5.285120	1.477592	95.229796	5.175449
2.166	0.365296	0.112197	0.006261	4.834615	1.131034	120.926613	4.236649
2.674	0.365262	0.112177	0.005440	4.506587	0.916079	136.507126	3.831741
3.182	0.365141	0.112108	0.004844	4.252260	0.769572	146.726917	3.613802
3.690	0.364847	0.111949	0.004387	4.046329	0.663091	153.851391	3.480052
4.198	0.364288	0.111655	0.004024	3.874070	0.581959	159.057331	3.390586
4.706	0.363375	0.111187	0.003726	3.726211	0.517836	163.004956	3.326990
5.214	0.362021	0.110504	0.003475	3.596561	0.465642	166.089000	3.279692
5.722	0.360149	0.109574	0.003261	3.480793	0.422109	168.558109	3.243260
6.230	0.357688	0.108366	0.003074	3.375763	0.385040	170.575823	3.214403

Table III.8 : Run 52

Mean distillation rate (gm/sec)		Distillate mole fraction (—)		Mean relative volatility (—)		Mean temperature (°C)	
Theoretical	Experimental	Theoretical	Experimental	Theoretical	Experimental	Distilland	Surface
0.034189	0.032800	0.260807	0.248900	3.502774	2.786019	205.500000	165.330361
Radial position (cm)	Mass flow rate (gm/sec)	EHP mole fraction (—)	Film thickness (cm)	Mean velocity (cm/sec)	Reynolds number (—)	Surface temperature (°C)	Relative volatility (—)
1.150	0.364500	0.112200	0.009372	6.069936	2.243336	50.200000	0.000000
1.658	0.364500	0.112200	0.007343	5.373062	1.555993	105.219365	4.974213
2.166	0.364488	0.112193	0.006145	4.915027	1.191022	135.887367	3.965632
2.674	0.364376	0.112130	0.005339	4.581212	0.964458	154.530202	3.547000
3.182	0.363921	0.111894	0.004752	4.321354	0.809472	166.784778	3.325814
3.690	0.362751	0.111318	0.004301	4.108767	0.695787	175.352917	3.191391
4.198	0.360426	0.110216	0.003938	3.927435	0.607672	181.642782	3.101864
4.706	0.356490	0.108399	0.003636	3.766889	0.536155	186.445716	3.038228
5.214	0.350480	0.105685	0.003377	3.619774	0.475758	190.235486	2.990715
5.722	0.341921	0.101888	0.003148	3.480516	0.422934	193.311437	2.953824
6.230	0.330311	0.096818	0.002940	3.344484	0.375257	195.872095	2.924228

Table III.9 : Run 53

Mean distillation rate (gm/sec)		Distillate mole fraction (—)		Mean relative volatility (—)		Mean temperature (°C)	
Theoretical	Experimental	Theoretical	Experimental	Theoretical	Experimental	Distilland	Surface
0.068164	0.062370	0.238174	0.207500	3.389347	2.282893	218.400000	174.858112
Radial position (cm)	Mass flow rate (gm/sec)	EHP mole fraction (—)	Film thickness (cm)	Mean velocity (cm/sec)	Reynolds number (—)	Surface temperature (°C)	Relative volatility (—)
1.150	0.363800	0.112200	0.009279	6.118939	2.302530	50.900000	0.000000
1.658	0.363800	0.112200	0.007270	5.416438	1.597049	109.981605	4.882353
2.166	0.363781	0.112189	0.006084	4.954675	1.222426	142.967135	3.848852
2.674	0.363588	0.112084	0.005286	4.617822	0.989666	163.039481	3.427086
3.182	0.362771	0.111678	0.004703	4.354435	0.829798	176.252642	3.205950
3.690	0.360613	0.110661	0.004253	4.136433	0.711304	185.517335	3.071981
4.198	0.356240	0.108680	0.003886	3.946282	0.617648	192.354016	2.982722
4.706	0.348696	0.105362	0.003576	3.771836	0.539306	197.619306	2.919021
5.214	0.336934	0.100311	0.003302	3.603678	0.470343	201.829304	2.871060
5.722	0.319756	0.093085	0.003050	3.433296	0.406734	205.316264	2.833291
6.230	0.295636	0.083154	0.002807	3.251204	0.345390	208.312574	2.802288

Table III.10 : Run 55

Mean distillation rate (gm/sec)		Distillate mole fraction (—)		Mean relative volatility (—)		Mean temperature (^{o}C)	
Theoretical	Experimental	Theoretical	Experimental	Theoretical	Experimental	Distilland	Surface
0.169788	0.149668	0.187630	0.162300	3.260264	1.835927	235.300000	186.920039
Radial position (cm)	Mass flow rate (gm/sec)	EHP mole fraction (—)	Film thickness (cm)	Mean velocity (cm/sec)	Reynolds number (—)	Surface temperature (^{o}C)	Relative volatility (—)
1.150	0.363300	0.112200	0.009202	6.161230	2.353838	51.500000	0.000000
1.658	0.363300	0.112200	0.007211	5.453874	1.632636	115.629030	4.780839
2.166	0.363268	0.112181	0.006034	4.988858	1.249619	151.543695	3.717373
2.674	0.362902	0.111992	0.005241	4.648945	1.011201	173.439804	3.292043
3.182	0.361278	0.111224	0.004660	4.380519	0.845962	187.896716	3.070966
3.690	0.356842	0.109243	0.004205	4.152358	0.720541	198.099984	2.937308
4.198	0.347582	0.105281	0.003825	3.942907	0.616913	205.725909	2.847844
4.706	0.331053	0.098434	0.003487	3.734450	0.524148	211.734000	2.783152
5.214	0.304069	0.087568	0.003166	3.508154	0.434520	216.733839	2.733158
5.722	0.261694	0.071046	0.002830	3.235145	0.340765	221.197974	2.691790
6.230	0.193512	0.046018	0.002418	2.843708	0.231435	225.734905	2.654167

Table III.11 : Run 57

Mean distillation rate (gm/sec)		Distillate mole fraction (—)		Mean relative volatility (—)		Mean temperature (°C)	
Theoretical	Experimental	Theoretical	Experimental	Theoretical	Experimental	Distilland	Surface
0.001777	0.001754	0.312828	0.307900	4.021541	3.479263	158.800000	129.618211
Radial position (cm)	Mass flow rate (gm/sec)	EHP mole fraction (—)	Film thickness (cm)	Mean velocity (cm/sec)	Reynolds number (—)	Surface temperature (°C)	Relative volatility (—)
1.150	0.493000	0.112200	0.010464	7.352975	2.948370	49.500000	0.000000
1.658	0.493000	0.112200	0.008199	6.508799	2.045009	86.489153	5.354330
2.166	0.492999	0.112199	0.006861	5.954004	1.565381	108.215267	4.502574
2.674	0.492989	0.112195	0.005962	5.550160	1.267970	121.670906	4.107798
3.182	0.492958	0.112181	0.005309	5.237412	1.065474	130.582168	3.889013
3.690	0.492886	0.112149	0.004809	4.984865	0.918656	136.823434	3.752783
4.198	0.492752	0.112092	0.004413	4.774655	0.807269	141.393291	3.660936
4.706	0.492536	0.112003	0.004089	4.595597	0.719811	144.859845	3.595365
5.214	0.492219	0.111874	0.003818	4.440269	0.649263	147.565700	3.546500
5.722	0.491787	0.111699	0.003587	4.303512	0.591101	149.727914	3.508848
6.230	0.491223	0.111474	0.003388	4.181610	0.542280	151.489828	3.479052

Table III.12 : Run 59

Mean distillation rate (gm/sec)		Distillate mole fraction (—)		Mean relative volatility (—)		Mean temperature (°C)	
Theoretical	Experimental	Theoretical	Experimental	Theoretical	Experimental	Distilland	Surface
0.006545	0.006309	0.293086	0.286500	3.769227	3.173189	180.400000	145.548735
Radial position (cm)	Mass flow rate (gm/sec)	EHP mole fraction (—)	Film thickness (cm)	Mean velocity (cm/sec)	Reynolds number (—)	Surface temperature (°C)	Relative volatility (—)
1.150	0.492000	0.112200	0.010302	7.453414	3.077090	50.600000	0.000000
1.658	0.492000	0.112200	0.008072	6.597707	2.134290	94.207765	5.188940
2.166	0.491997	0.112198	0.006755	6.035327	1.633717	119.995111	4.261211
2.674	0.491971	0.112187	0.005869	5.625903	1.323279	136.015745	3.845041
3.182	0.491874	0.112146	0.005226	5.308650	1.111800	146.643937	3.618363
3.690	0.491633	0.112049	0.004734	5.052090	0.958270	154.096720	3.478672
4.198	0.491166	0.111867	0.004343	4.837950	0.841509	159.559759	3.385110
4.706	0.490389	0.111572	0.004022	4.654745	0.749484	163.709004	3.318600
5.214	0.489226	0.111138	0.003754	4.494819	0.674856	166.952554	3.269166
5.722	0.487603	0.110541	0.003524	4.352836	0.612902	169.549110	3.231131
6.230	0.485455	0.109761	0.003325	4.224932	0.560446	171.669559	3.201047

Table III.13 : Run 61

Mean distillation rate (gm/sec)		Distillate mole fraction (—)		Mean relative volatility (—)		Mean temperature (^{o}C)	
Theoretical	Experimental	Theoretical	Experimental	Theoretical	Experimental	Distilland	Surface
0.024867	0.023644	0.269423	0.255800	3.535490	2.795290	204.700000	162.999159
Radial position (cm)	Mass flow rate (gm/sec)	EHP mole fraction (—)	Film thickness (cm)	Mean velocity (cm/sec)	Reynolds number (—)	Surface temperature (^{o}C)	Relative volatility (—)
1.150	0.491500	0.112200	0.010244	7.487785	3.123030	51.000000	0.000000
1.658	0.491500	0.112200	0.008027	6.628131	2.166154	101.977269	5.043657
2.166	0.491493	0.112197	0.006717	6.063141	1.658094	132.466025	4.035957
2.674	0.491421	0.112166	0.005836	5.651653	1.342896	151.501728	3.598952
3.182	0.491115	0.112047	0.005196	5.332193	1.127804	164.166790	3.365152
3.690	0.490302	0.111747	0.004705	5.072522	0.970930	173.070180	3.222557
4.198	0.488648	0.111159	0.004313	4.853586	0.850558	179.616174	3.127607
4.706	0.485801	0.110175	0.003989	4.663160	0.754322	184.608061	3.060285
5.214	0.481411	0.108691	0.003714	4.492898	0.674677	188.531693	3.010242
5.722	0.475136	0.106605	0.003475	4.336787	0.606765	191.695459	2.971636
6.230	0.466633	0.103821	0.003264	4.190255	0.547315	194.303461	2.940939

Table III.14 : Run 62

Mean distillation rate (gm/sec)		Distillate mole fraction (—)		Mean relative volatility (—)		Mean temperature (^{o}C)	
Theoretical	Experimental	Theoretical	Experimental	Theoretical	Experimental	Distilland	Surface
0.054733	0.051449	0.250451	0.227900	3.405417	2.486544	219.800000	173.920730
Radial position (cm)	Mass flow rate (gm/sec)	EHP mole fraction (—)	Film thickness (cm)	Mean velocity (cm/sec)	Reynolds number (—)	Surface temperature (^{o}C)	Relative volatility (—)
1.150	0.491200	0.112200	0.010176	7.533488	3.182508	51.500000	0.000000
1.658	0.491200	0.112200	0.007973	6.668587	2.207408	106.948639	4.951192
2.166	0.491188	0.112194	0.006672	6.100129	1.689656	140.283002	3.905652
2.674	0.491055	0.112141	0.005797	5.685894	1.368288	161.146537	3.461071
3.182	0.490456	0.111918	0.005160	5.363430	1.148442	175.053008	3.225563
3.690	0.488804	0.111339	0.004670	5.099317	0.987000	184.852341	3.082657
4.198	0.485355	0.110178	0.004275	4.873207	0.861441	192.084493	2.987665
4.706	0.479291	0.108200	0.003945	4.671522	0.758851	197.632558	2.920225
5.214	0.469752	0.105161	0.003660	4.484444	0.671285	202.032137	2.869867
5.722	0.455821	0.100808	0.003405	4.304189	0.593547	205.625285	2.830696
6.230	0.436467	0.094863	0.003172	4.123795	0.522002	208.641941	2.799143

Table III.15 : Run 63

Mean distillation rate (gm/sec)		Distillate mole fraction (—)		Mean relative volatility (—)		Mean temperature (^{o}C)	
Theoretical	Experimental	Theoretical	Experimental	Theoretical	Experimental	Distilland	Surface
0.136914	0.124866	0.216237	0.180000	3.272060	1.950851	237.900000	186.571537
Radial position (cm)	Mass flow rate (gm/sec)	EHP mole fraction (—)	Film thickness (cm)	Mean velocity (cm/sec)	Reynolds number (—)	Surface temperature (^{o}C)	Relative volatility (—)
1.150	0.491200	0.112200	0.010176	7.533488	3.182508	51.500000	0.000000
1.658	0.491200	0.112200	0.007973	6.668587	2.207408	112.104862	4.866744
2.166	0.491180	0.112191	0.006672	6.100095	1.689628	148.864781	3.774615
2.674	0.490924	0.112092	0.005797	5.685389	1.367923	171.969189	3.320114
3.182	0.489690	0.111658	0.005158	5.360636	1.146648	187.421233	3.081949
3.690	0.486129	0.110481	0.004661	5.089997	0.981598	198.365139	2.938105
4.198	0.478432	0.108048	0.004255	4.849928	0.849155	206.514990	2.842411
4.706	0.464452	0.103776	0.003904	4.622805	0.735357	212.863227	2.773988
5.214	0.441622	0.096982	0.003585	4.393081	0.631086	218.024897	2.722100
5.722	0.406602	0.086803	0.003278	4.143333	0.529457	222.418934	2.680595
6.230	0.354286	0.071995	0.002958	3.846787	0.423717	226.388378	2.645452

Table III.16 : Run 64

Mean distillation rate (gm/sec)		Distillate mole fraction (—)		Mean relative volatility (—)		Mean temperature (^{o}C)	
Theoretical	Experimental	Theoretical	Experimental	Theoretical	Experimental	Distilland	Surface
0.001054	0.001009	0.650705	0.650100	4.255193	3.836922	139.400000	116.573999
Radial position (cm)	Mass flow rate (gm/sec)	EHP mole fraction (—)	Film thickness (cm)	Mean velocity (cm/sec)	Reynolds number (—)	Surface temperature (^{o}C)	Relative volatility (—)
1.150	0.292500	0.317900	0.009350	4.807286	1.410279	48.000000	0.000000
1.658	0.292500	0.317900	0.007327	4.255374	0.978179	81.923857	5.447575
2.166	0.292498	0.317898	0.006131	3.892652	0.748759	99.929727	4.675563
2.674	0.292490	0.317887	0.005327	3.628610	0.606493	110.664226	4.326462
3.182	0.292465	0.317857	0.004744	3.424115	0.509624	117.648300	4.133177
3.690	0.292413	0.317796	0.004298	3.258973	0.439387	122.493809	4.012399
4.198	0.292325	0.317694	0.003943	3.121513	0.386101	126.022121	3.930636
4.706	0.292192	0.317540	0.003654	3.004433	0.344265	128.689276	3.872045
5.214	0.292005	0.317328	0.003411	2.902888	0.310525	130.766292	3.828240
5.722	0.291758	0.317048	0.003206	2.813514	0.282717	132.423265	3.794396
6.230	0.291446	0.316696	0.003028	2.733887	0.259386	133.771810	3.767552

Table III.17 : Run 66

Mean distillation rate (gm/sec)		Distillate mole fraction (—)		Mean relative volatility (—)		Mean temperature (°C)	
Theoretical	Experimental	Theoretical	Experimental	Theoretical	Experimental	Distilland	Surface
0.003814	0.003800	0.628400	0.627800	3.975608	3.527469	159.400000	131.915196
Radial position (cm)	Mass flow rate (gm/sec)	EHP mole fraction (—)	Film thickness (cm)	Mean velocity (cm/sec)	Reynolds number (—)	Surface temperature (°C)	Relative volatility (—)
1.150	0.291300	0.317900	0.009146	4.894512	1.494579	49.500000	0.000000
1.658	0.291300	0.317900	0.007167	4.332585	1.036649	90.165504	5.255179
2.166	0.291296	0.317895	0.005997	3.963272	0.793509	111.823814	4.408303
2.674	0.291271	0.317865	0.005211	3.694371	0.642706	124.758104	4.037648
3.182	0.291193	0.317776	0.004640	3.485959	0.539955	133.182145	3.835784
3.690	0.291023	0.317585	0.004203	3.317381	0.465347	139.031571	3.710860
4.198	0.290719	0.317251	0.003855	3.176671	0.408609	143.294572	3.626803
4.706	0.290245	0.316736	0.003571	3.056326	0.363906	146.520353	3.566806
5.214	0.289568	0.316006	0.003332	2.951356	0.327684	149.035460	3.522061
5.722	0.288657	0.315030	0.003129	2.858292	0.297653	151.044881	3.487539
6.230	0.287486	0.313781	0.002952	2.774628	0.272273	152.683136	3.460174

Table III.18 : Run 67

Mean distillation rate (gm/sec)		Distillate mole fraction (—)		Mean relative volatility (—)		Mean temperature (°C)	
Theoretical	Experimental	Theoretical	Experimental	Theoretical	Experimental	Distilland	Surface
0.012229	0.011989	0.604659	0.601300	3.740834	3.231592	179.100000	146.848799
Radial position (cm)	Mass flow rate (gm/sec)	EHP mole fraction (—)	Film thickness (cm)	Mean velocity (cm/sec)	Reynolds number (—)	Surface temperature (°C)	Relative volatility (—)
1.150	0.290300	0.317900	0.008980	4.967906	1.568210	50.800000	0.000000
1.658	0.290300	0.317900	0.007037	4.397553	1.087720	98.059251	5.084601
2.166	0.290291	0.317889	0.005888	4.022679	0.832588	123.312536	4.177819
2.674	0.290227	0.317816	0.005116	3.749580	0.674267	138.420241	3.792615
3.182	0.290009	0.317576	0.004555	3.537481	0.566195	148.272598	3.585870
3.690	0.289505	0.317039	0.004124	3.365118	0.487399	155.123899	3.458960
4.198	0.288576	0.316068	0.003780	3.220054	0.427045	160.127085	3.373951
4.706	0.287089	0.314533	0.003497	3.094416	0.378983	163.923408	3.313398
5.214	0.284919	0.312307	0.003258	2.982911	0.339473	166.894221	3.268243
5.722	0.281949	0.309268	0.003051	2.881804	0.306110	169.278925	3.233351
6.230	0.278071	0.305289	0.002870	2.788342	0.277282	171.234671	3.205605

Table III.19 : Run 69

Mean distillation rate (gm/sec)		Distillate mole fraction (—)		Mean relative volatility (—)		Mean temperature (°C)	
Theoretical	Experimental	Theoretical	Experimental	Theoretical	Experimental	Distilland	Surface
0.041825	0.039986	0.567435	0.545900	3.519344	2.748596	201.400000	163.413420
Radial position (cm)	Mass flow rate (gm/sec)	EHP mole fraction (—)	Film thickness (cm)	Mean velocity (cm/sec)	Reynolds number (—)	Surface temperature (°C)	Relative volatility (—)
1.150	0.290200	0.317900	0.008933	4.992397	1.592066	51.200000	0.000000
1.658	0.290200	0.317900	0.007000	4.419231	1.104266	106.071484	4.934669
2.166	0.290180	0.317877	0.005857	4.042461	0.845222	135.586297	3.960391
2.674	0.290014	0.317694	0.005089	3.767573	0.684256	153.302735	3.559680
3.182	0.289389	0.317044	0.004528	3.552792	0.573777	164.889581	3.347898
3.690	0.287859	0.315503	0.004095	3.375675	0.492171	172.979707	3.218869
4.198	0.284922	0.312598	0.003745	3.222580	0.428198	178.925079	3.132627
4.706	0.280056	0.307820	0.003450	3.084420	0.375452	183.479475	3.071042
5.214	0.272729	0.300602	0.003194	2.954583	0.330006	187.092679	3.024784
5.722	0.262380	0.290257	0.002964	2.827725	0.289298	190.049482	2.988584
6.230	0.248375	0.275879	0.002750	2.698873	0.251525	192.541019	2.959231

Table III.20 : Run 70

Mean distillation rate (gm/sec)		Distillate mole fraction (—)		Mean relative volatility (—)		Mean temperature (°C)	
Theoretical	Experimental	Theoretical	Experimental	Theoretical	Experimental	Distilland	Surface
0.089662	0.081721	0.524678	0.497100	3.393572	2.456434	215.600000	173.904994
Radial position (cm)	Mass flow rate (gm/sec)	EHP mole fraction (—)	Film thickness (cm)	Mean velocity (cm/sec)	Reynolds number (—)	Surface temperature (°C)	Relative volatility (—)
1.150	0.290000	0.317900	0.008852	5.034506	1.633818	51.900000	0.000000
1.658	0.290000	0.317899	0.006936	4.456505	1.133225	111.297535	4.835745
2.166	0.289968	0.317863	0.005804	4.076499	0.867352	143.331119	3.833132
2.674	0.289672	0.317548	0.005042	3.798730	0.701857	162.591691	3.428138
3.182	0.288509	0.316375	0.004484	3.579946	0.587439	175.219349	3.215764
3.690	0.285575	0.313512	0.004048	3.395900	0.501416	184.079041	3.086677
4.198	0.279799	0.307959	0.003690	3.230911	0.431825	190.647361	3.000175
4.706	0.269989	0.298505	0.003379	3.073418	0.371705	195.752766	2.937901
5.214	0.254774	0.283535	0.003095	2.913297	0.316583	199.899007	2.890396
5.722	0.232414	0.260587	0.002821	2.739229	0.263159	203.424417	2.852214
6.230	0.200338	0.225355	0.002537	2.534049	0.208343	206.600421	2.819779

Table III.21 : Run 73

Mean distillation rate (gm/sec)		Distillate mole fraction (—)		Mean relative volatility (—)		Mean temperature (°C)	
Theoretical	Experimental	Theoretical	Experimental	Theoretical	Experimental	Distilland	Surface
0.002689	0.002528	0.632339	0.629000	4.027929	3.529336	157.000000	129.122613
Radial position (cm)	Mass flow rate (gm/sec)	EHP mole fraction (—)	Film thickness (cm)	Mean velocity (cm/sec)	Reynolds number (—)	Surface temperature (°C)	Relative volatility (—)
1.150	0.369800	0.317900	0.009985	5.691754	1.851410	48.900000	0.000000
1.658	0.369800	0.317900	0.007824	5.038298	1.284150	87.389814	5.330611
2.166	0.369797	0.317897	0.006547	4.608839	0.982967	108.761776	4.482838
2.674	0.369781	0.317882	0.005689	4.296196	0.796190	121.731531	4.101494
3.182	0.369728	0.317833	0.005066	4.054001	0.668984	130.242059	3.891916
3.690	0.369611	0.317729	0.004589	3.858299	0.576702	136.174360	3.761754
4.198	0.369400	0.317544	0.004210	3.695227	0.506626	140.506618	3.674051
4.706	0.369068	0.317257	0.003900	3.556104	0.451531	143.788136	3.611426
5.214	0.368590	0.316849	0.003641	3.435161	0.407010	146.347606	3.564730
5.722	0.367944	0.316300	0.003420	3.328391	0.370226	148.392233	3.528722
6.230	0.367111	0.315597	0.003229	3.232905	0.339268	150.058383	3.500202

Table III.22 : Run 74

Mean distillation rate (gm/sec)		Distillate mole fraction (—)		Mean relative volatility (—)		Mean temperature (°C)	
Theoretical	Experimental	Theoretical	Experimental	Theoretical	Experimental	Distilland	Surface
0.005153	0.004925	0.620727	0.600000	3.887243	3.155895	167.500000	137.370424
Radial position (cm)	Mass flow rate (gm/sec)	EHP mole fraction (—)	Film thickness (cm)	Mean velocity (cm/sec)	Reynolds number (—)	Surface temperature (°C)	Relative volatility (—)
1.150	0.368800	0.317900	0.009764	5.804630	1.969082	50.500000	0.000000
1.658	0.368800	0.317900	0.007651	5.138215	1.365768	92.193502	5.211432
2.166	0.368796	0.317896	0.006402	4.700232	1.045438	115.326234	4.340740
2.674	0.368767	0.317869	0.005563	4.381342	0.846762	129.363171	3.955115
3.182	0.368672	0.317784	0.004953	4.134187	0.711395	138.574809	3.744786
3.690	0.368455	0.317596	0.004487	3.934258	0.613096	144.997360	3.614719
4.198	0.368058	0.317258	0.004116	3.767341	0.538325	149.689553	3.527306
4.706	0.367427	0.316729	0.003812	3.624514	0.479391	153.245839	3.464985
5.214	0.366510	0.315967	0.003557	3.499843	0.431605	156.021866	3.418554
5.722	0.365264	0.314938	0.003339	3.389194	0.391949	158.241787	3.382758
6.230	0.363647	0.313609	0.003151	3.289582	0.358395	160.053095	3.354401

Table III.23 : Run 76

Mean distillation rate (gm/sec)		Distillate mole fraction (—)		Mean relative volatility (—)		Mean temperature (°C)	
Theoretical	Experimental	Theoretical	Experimental	Theoretical	Experimental	Distilland	Surface
0.019463	0.018937	0.592668	0.559800	3.635691	2.753155	191.100000	154.700706
Radial position (cm)	Mass flow rate (gm/sec)	EHP mole fraction (—)	Film thickness (cm)	Mean velocity (cm/sec)	Reynolds number (—)	Surface temperature (°C)	Relative volatility (—)
1.150	0.368500	0.317900	0.009698	5.839220	2.006126	51.000000	0.000000
1.658	0.368500	0.317900	0.007599	5.168833	1.391462	100.400302	5.051884
2.166	0.368490	0.317890	0.006359	4.728217	1.065089	128.071671	4.099449
2.674	0.368409	0.317819	0.005525	4.407220	0.862557	144.937225	3.691912
3.182	0.368109	0.317566	0.004919	3.157834	0.724261	156.035308	3.473518
3.690	0.367377	0.316968	0.004453	3.954911	0.623310	163.792449	3.339812
4.198	0.365974	0.315847	0.004081	3.783649	0.545791	169.476852	3.250452
4.706	0.363662	0.314026	0.003774	3.634604	0.483799	173.802459	3.186897
5.214	0.360214	0.311329	0.003514	3.501370	0.432521	177.196973	3.139536
5.722	0.355409	0.307576	0.003288	3.379366	0.388865	179.930215	3.102932
6.230	0.349037	0.302578	0.003088	3.265147	0.350753	182.179984	3.073792

Table III.24 : Run 77

Mean distillation rate (gm/sec)		Distillate mole fraction (—)		Mean relative volatility (—)		Mean temperature (°C)	
Theoretical	Experimental	Theoretical	Experimental	Theoretical	Experimental	Distilland	Surface
0.036018	0.034697	0.575246	0.537100	3.531990	2.576506	202.800000	162.980962
Radial position (cm)	Mass flow rate (gm/sec)	EHP mole fraction (—)	Film thickness (cm)	Mean velocity (cm/sec)	Reynolds number (—)	Surface temperature (°C)	Relative volatility (—)
1.150	0.368800	0.317900	0.009764	5.804630	1.969082	50.500000	0.000000
1.658	0.368800	0.317900	0.007651	5.138215	1.365768	103.754145	4.999966
2.166	0.368786	0.317887	0.006402	4.700191	1.045410	133.811697	4.002467
2.674	0.368659	0.317777	0.005562	4.380914	0.846515	152.194644	3.582564
3.182	0.368160	0.317367	0.004951	4.132273	0.710407	164.317872	3.359438
3.690	0.366896	0.316365	0.004480	3.928704	0.610503	172.810923	3.223450
4.198	0.364414	0.314441	0.004102	3.754866	0.532995	179.054073	3.132730
4.706	0.360241	0.311244	0.003787	3.600729	0.470015	183.826261	3.068174
5.214	0.353902	0.306405	0.003516	3.459243	0.416757	187.595073	3.019932
5.722	0.344919	0.299506	0.003276	3.325063	0.370118	190.656489	2.982447
6.230	0.332782	0.290047	0.003059	3.193749	0.327976	193.207039	2.952354

Table III.25 : Run 78

Mean distillation rate (gm/sec)		Distillate mole fraction (—)		Mean relative volatility (—)		Mean temperature (°C)	
Theoretical	Experimental	Theoretical	Experimental	Theoretical	Experimental	Distilland	Surface
0.086636	0.081999	0.537441	0.480600	3.383618	2.183210	219.600000	175.351587
Radial position (cm)	Mass flow rate (gm/sec)	EHP mole fraction (—)	Film thickness (cm)	Mean velocity (cm/sec)	Reynolds number (—)	Surface temperature (°C)	Relative volatility (—)
1.150	0.368300	0.317900	0.009635	5.874499	2.043816	51.500000	0.000000
1.658	0.368300	0.317900	0.007549	5.200061	1.417603	109.858382	4.881080
2.166	0.368275	0.317877	0.006317	4.756719	1.085055	142.911318	3.851144
2.674	0.368025	0.317667	0.005488	4.433105	0.878321	163.167459	3.426588
3.182	0.366983	0.316844	0.004883	4.179442	0.736011	176.557792	3.203155
3.690	0.364254	0.314763	0.004413	3.968219	0.629965	185.979049	3.067495
4.198	0.358744	0.310645	0.004028	3.781960	0.545356	192.957885	2.976900
4.706	0.349239	0.303575	0.003700	3.608222	0.473597	198.359870	2.912033
5.214	0.334389	0.292404	0.003406	3.436869	0.409278	202.710616	2.862949
5.722	0.312581	0.275522	0.003130	3.257923	0.348620	206.354297	2.823990
6.230	0.281664	0.250372	0.002856	3.058795	0.288523	209.542833	2.791594

Table III.26 : Run 80

Mean distillation rate (gm/sec)		Distillate mole fraction (—)		Mean relative volatility (—)		Mean temperature (°C)	
Theoretical	Experimental	Theoretical	Experimental	Theoretical	Experimental	Distilland	Surface
0.000970	0.000898	0.646016	0.644200	4.233279	3.740730	145.500000	118.524024
Radial position (cm)	Mass flow rate (gm/sec)	EHP mole fraction (—)	Film thickness (cm)	Mean velocity (cm/sec)	Reynolds number (—)	Surface temperature (°C)	Relative volatility (—)
1.150	0.506500	0.317900	0.011476	6.782847	2.287641	46.500000	0.000000
1.658	0.506500	0.317900	0.008992	6.004126	1.586723	79.119221	5.561697
2.166	0.506499	0.317899	0.007524	5.492350	1.214581	98.787922	4.731692
2.674	0.506493	0.317895	0.006538	5.119831	0.983826	111.103059	4.333707
3.182	0.506475	0.317882	0.005822	4.831376	0.826731	119.303281	4.109834
3.690	0.506493	0.317855	0.005275	4.598508	0.712857	125.063569	3.969348
4.198	0.506359	0.317805	0.004840	4.404773	0.626501	129.288470	3.874202
4.706	0.506240	0.317727	0.004485	4.239874	0.558741	132.496569	3.806085
5.214	0.506067	0.317615	0.004188	4.096981	0.504131	135.002102	3.755228
5.722	0.505833	0.317464	0.003936	3.971349	0.459162	137.004785	3.715995
6.230	0.505530	0.317271	0.003718	3.859561	0.421469	138.636800	3.684923

Table III.27 : Run 82

Mean distillation rate (gm/sec)		Distillate mole fraction (—)		Mean relative volatility (—)		Mean temperature (°C)	
Theoretical	Experimental	Theoretical	Experimental	Theoretical	Experimental	Distilland	Surface
0.004281	0.004191	0.620805	0.619200	3.926333	3.396096	169.900000	136.193178
Radial position (cm)	Mass flow rate (gm/sec)	EHP mole fraction (—)	Film thickness (cm)	Mean velocity (cm/sec)	Reynolds number (—)	Surface temperature (°C)	Relative volatility (—)
1.150	0.506200	0.317900	0.011307	6.880152	2.388928	47.500000	0.000000
1.658	0.506200	0.317900	0.008859	6.090259	1.656976	87.236986	5.380676
2.166	0.506198	0.317898	0.007414	5.571137	1.268354	111.536104	4.448979
2.674	0.506180	0.317886	0.006442	5.193233	1.027359	126.847169	4.017733
3.182	0.506115	0.317844	0.005736	4.900491	0.863232	137.076314	3.779957
3.690	0.505955	0.317742	0.005196	4.663928	0.744157	144.276549	3.632594
4.198	0.505648	0.317551	0.004767	4.466751	0.653708	149.565522	3.533610
4.706	0.505138	0.317240	0.004416	4.298425	0.582555	153.586898	3.463145
5.214	0.504377	0.316781	0.004123	4.151942	0.525004	156.731754	3.410740
5.722	0.503318	0.316148	0.003872	4.022425	0.477390	159.249053	3.370418
6.230	0.501919	0.315316	0.003655	3.906355	0.437244	161.303736	3.338537

Table III.28 : Run 84

Mean distillation rate (gm/sec)		Distillate mole fraction (—)		Mean relative volatility (—)		Mean temperature (°C)	
Theoretical	Experimental	Theoretical	Experimental	Theoretical	Experimental	Distilland	Surface
0.013130	0.011963	0.599624	0.570500	3.713233	2.825807	189.900000	150.569887
Radial position (cm)	Mass flow rate (gm/sec)	EHP mole fraction (—)	Film thickness (cm)	Mean velocity (cm/sec)	Reynolds number (—)	Surface temperature (°C)	Relative volatility (—)
1.150	0.505800	0.317900	0.011207	6.935573	2.449060	48.100000	0.000000
1.658	0.505800	0.317900	0.008782	6.139318	1.698684	93.585300	5.250380
2.166	0.505795	0.317897	0.007348	5.616006	1.300274	121.724888	4.247307
2.674	0.505754	0.317869	0.006385	5.234976	1.053165	139.550969	3.795362
3.182	0.505585	0.317763	0.005686	4.939541	0.884733	151.495423	3.549900
3.690	0.505142	0.317496	0.005149	4.700215	0.762264	159.920601	3.399156
4.198	0.504251	0.316973	0.004722	4.499769	0.668841	166.121576	3.298474
4.706	0.502731	0.316094	0.004372	4.327295	0.594842	170.847027	3.227038
5.214	0.500404	0.314766	0.004077	4.175468	0.534402	174.552785	3.173993
5.722	0.497103	0.312896	0.003823	4.039133	0.483745	177.529370	3.133179
6.230	0.492670	0.310392	0.003602	3.914515	0.440338	179.969398	3.100868

Table III.29 : Run 85

Mean distillation rate (gm/sec)		Distillate mole fraction (—)		Mean relative volatility (—)		Mean temperature (°C)	
Theoretical	Experimental	Theoretical	Experimental	Theoretical	Experimental	Distilland	Surface
0.028677	0.023274	0.581985	0.550000	3.567057	2.639400	204.600000	161.354629
Radial position (cm)	Mass flow rate (gm/sec)	EHP mole fraction (—)	Film thickness (cm)	Mean velocity (cm/sec)	Reynolds number (—)	Surface temperature (°C)	Relative volatility (—)
1.150	0.505000	0.317900	0.011017	7.044254	2.570069	49.300000	0.000000
1.658	0.505000	0.317900	0.008633	6.235521	1.782617	98.901029	5.134003
2.166	0.504992	0.317895	0.007224	5.703997	1.364513	129.669910	4.098558
2.674	0.504914	0.317845	0.006277	5.316869	1.105115	149.193112	3.640964
3.182	0.504578	0.317641	0.005588	5.016257	0.928067	162.290412	3.394871
3.690	0.503668	0.317112	0.005060	4.771737	0.798857	171.541843	3.244558
4.198	0.501795	0.316051	0.004637	4.565256	0.699576	178.365222	3.144434
4.706	0.498542	0.314241	0.004288	4.385177	0.620014	183.581232	3.073436
5.214	0.493490	0.311456	0.003991	4.223503	0.553934	187.689893	3.020648
5.722	0.486222	0.307462	0.003733	4.074423	0.497322	191.010168	2.979902
6.230	0.476323	0.302001	0.003503	3.933463	0.447471	193.753972	2.947472

Table III.30 : Run 86

Mean distillation rate (gm/sec)		Distillate mole fraction (—)		Mean relative volatility (—)		Mean temperature (°C)	
Theoretical	Experimental	Theoretical	Experimental	Theoretical	Experimental	Distilland	Surface
0.060009	0.049898	0.560072	0.540800	3.437848	2.623516	219.100000	171.877422
Radial position (cm)	Mass flow rate (gm/sec)	EHP mole fraction (—)	Film thickness (cm)	Mean velocity (cm/sec)	Reynolds number (—)	Surface temperature (°C)	Relative volatility (—)
1.150	0.504700	0.317900	0.010869	7.136154	2.673563	50.300000	0.000000
1.658	0.504700	0.317900	0.008516	6.316870	1.854401	103.883249	5.031816
2.166	0.504687	0.317891	0.007126	5.778393	1.419447	137.261261	3.966748
2.674	0.504548	0.317804	0.006192	5.385996	1.149465	158.483961	3.504389
3.182	0.503913	0.317433	0.005512	5.080475	0.964741	172.745195	3.257963
3.690	0.502143	0.316440	0.004988	4.830063	0.829003	182.842200	3.108130
4.198	0.498415	0.314403	0.004565	4.615323	0.723276	190.317775	3.008460
4.706	0.491817	0.310851	0.004212	4.423196	0.636658	196.067164	2.937668
5.214	0.481377	0.305253	0.003906	4.244149	0.562432	200.637482	2.884776
5.722	0.466058	0.296981	0.003631	4.070520	0.496190	204.380173	2.843592
6.230	0.444691	0.285220	0.003378	3.895315	0.434836	207.532942	2.810360

Table III.31 : Run 87

Mean distillation rate (gm/sec)		Distillate mole fraction (—)		Mean relative volatility (—)		Mean temperature (^{o}C)	
Theoretical	Experimental	Theoretical	Experimental	Theoretical	Experimental	Distilland	Surface
0.000281	0.000312	0.832451	0.825900	4.597303	4.095143	116.300000	99.909244
Radial position (cm)	Mass flow rate (gm/sec)	EHP mole fraction (—)	Film thickness (cm)	Mean velocity (cm/sec)	Reynolds number (—)	Surface temperature (^{o}C)	Relative volatility (—)
1.150	0.310000	0.523400	0.009579	4.898726	1.429560	50.500000	0.000000
1.658	0.310000	0.523400	0.007505	4.336315	0.991552	75.011568	5.559675
2.166	0.309999	0.523399	0.006281	3.966697	0.758997	87.971612	4.959601
2.674	0.309995	0.523395	0.005457	3.697655	0.614797	95.682739	4.673277
3.182	0.309986	0.523386	0.004860	3.489335	0.516632	100.694504	4.510248
3.690	0.309970	0.523369	0.004403	3.321185	0.445484	104.169368	4.406643
4.198	0.309945	0.523344	0.004040	3.181333	0.391544	106.698388	4.335719
4.706	0.309908	0.523307	0.003744	3.062355	0.349236	108.609315	4.284499
5.214	0.309859	0.523258	0.003496	2.959326	0.315160	110.096777	4.245989
5.722	0.309796	0.523196	0.003286	2.868829	0.287122	111.282870	4.216110
6.230	0.309719	0.523120	0.003104	2.788400	0.263644	112.247689	4.192336

Table III.32 : Run 89

Mean distillation rate (gm/sec)		Distillate mole fraction (—)		Mean relative volatility (—)		Mean temperature (^{o}C)	
Theoretical	Experimental	Theoretical	Experimental	Theoretical	Experimental	Distilland	Surface
0.000957	0.000996	0.819070	0.808300	4.319335	3.678095	134.700000	113.143615
Radial position (cm)	Mass flow rate (gm/sec)	EHP mole fraction (—)	Film thickness (cm)	Mean velocity (cm/sec)	Reynolds number (—)	Surface temperature (^{o}C)	Relative volatility (—)
1.150	0.311700	0.523400	0.009786	4.821125	1.355262	49.000000	0.000000
1.658	0.311700	0.523400	0.007668	4.267624	0.940018	80.529212	5.464350
2.166	0.311698	0.523398	0.006417	3.903858	0.719548	97.422593	4.732169
2.674	0.311689	0.523389	0.005576	3.639057	0.582833	107.533641	4.394882
3.182	0.311665	0.523365	0.004965	3.433982	0.489747	114.124901	4.206525
3.690	0.311616	0.523318	0.004498	3.268386	0.422258	118.702733	4.088268
4.198	0.311535	0.523239	0.004127	3.130570	0.371064	122.038181	4.007975
4.706	0.311413	0.523123	0.003824	3.013216	0.330879	124.560461	3.950328
5.214	0.311244	0.522962	0.003571	2.911468	0.298479	126.525070	3.907170
5.722	0.311022	0.522753	0.003355	2.821954	0.271786	128.092537	3.873793
6.230	0.310743	0.522489	0.003169	2.742246	0.249400	129.368282	3.847301

Table III.33 : Run 90

Mean distillation rate (gm/sec)		Distillate mole fraction (—)		Mean relative volatility (—)		Mean temperature (°C)	
Theoretical	Experimental	Theoretical	Experimental	Theoretical	Experimental	Distilland	Surface
0.003198	0.003240	0.805158	0.790100	4.036555	3.321567	153.200000	127.775668
Radial position (cm)	Mass flow rate (gm/sec)	EHP mole fraction (—)	Film thickness (cm)	Mean velocity (cm/sec)	Reynolds number (—)	Surface temperature (°C)	Relative volatility (—)
1.150	0.308300	0.523400	0.009382	4.973770	1.504521	52.000000	0.000000
1.658	0.308300	0.523400	0.007352	4.402744	1.043545	89.245863	5.239352
2.166	0.308295	0.523395	0.006152	4.027449	0.798787	109.193664	4.455325
2.674	0.308271	0.523371	0.005346	3.754201	0.646984	121.136296	4.104198
3.182	0.308199	0.523302	0.004760	3.542453	0.543568	128.924224	3.910852
3.690	0.308047	0.523158	0.004312	3.371249	0.468504	134.335393	3.790452
4.198	0.307785	0.522913	0.003955	3.228460	0.411460	138.280085	3.709125
4.706	0.307383	0.522541	0.003664	3.106488	0.366564	141.265092	3.650930
5.214	0.306816	0.522019	0.003420	3.000287	0.330240	143.592094	3.607456
5.722	0.306062	0.521327	0.003211	2.906349	0.300182	145.450627	3.573879
6.230	0.305102	0.520447	0.003031	2.822147	0.274840	146.965147	3.547246

Table III.34 : Run 92

Mean distillation rate (gm/sec)		Distillate mole fraction (—)		Mean relative volatility (—)		Mean temperature (°C)	
Theoretical	Experimental	Theoretical	Experimental	Theoretical	Experimental	Distilland	Surface
0.008506	0.008403	0.792688	0.780000	3.783705	3.167074	168.100000	141.457517
Radial position (cm)	Mass flow rate (gm/sec)	EHP mole fraction (—)	Film thickness (cm)	Mean velocity (cm/sec)	Reynolds number (—)	Surface temperature (°C)	Relative volatility (—)
1.150	0.302000	0.523400	0.008429	5.423287	1.991111	61.000000	0.000000
1.658	0.301999	0.523399	0.006605	4.800650	1.381045	100.934654	4.897863
2.166	0.301987	0.523387	0.005527	4.391399	1.057101	122.004462	4.166622
2.674	0.301920	0.523321	0.004802	4.093262	0.856084	134.545146	3.842809
3.182	0.301724	0.523136	0.004275	3.861855	0.718945	142.702499	3.665190
3.690	0.301315	0.522755	0.003872	3.674158	0.619129	148.365302	3.554729
4.198	0.300613	0.522109	0.003550	3.516803	0.542940	152.493916	3.480123
4.706	0.299543	0.521131	0.003286	3.381390	0.482607	155.620824	3.426700
5.214	0.298038	0.519759	0.003063	3.262320	0.433399	158.062149	3.386739
5.722	0.296040	0.517934	0.002873	3.155686	0.392274	160.016139	3.355816
6.230	0.293494	0.515595	0.002707	3.058650	0.357188	161.612814	3.331228

Table III.35 : Run 94

Mean distillation rate (gm/sec)		Distillate mole fraction (—)		Mean relative volatility (—)		Mean temperature (^{o}C)	
Theoretical	Experimental	Theoretical	Experimental	Theoretical	Experimental	Distilland	Surface
0.036404	0.031307	0.766298	0.764100	3.524004	3.020115	195.000000	160.775545
Radial position (cm)	Mass flow rate (gm/sec)	EHP mole fraction (—)	Film thickness (cm)	Mean velocity (cm/sec)	Reynolds number (—)	Surface temperature (^{o}C)	Relative volatility (—)
1.150	0.303300	0.523400	0.008608	5.333503	1.885732	59.100000	0.000000
1.658	0.303299	0.523399	0.006745	4.721173	1.307953	109.008924	4.785323
2.166	0.303272	0.523372	0.005644	4.318626	1.001104	135.709285	3.933996
2.674	0.303078	0.523192	0.004903	4.024872	0.810398	151.707540	5.572971
3.182	0.302428	0.522606	0.004363	3.795434	0.679558	162.161463	3.379199
3.690	0.300942	0.521297	0.003946	3.606672	0.583126	169.453656	3.260093
4.198	0.298219	0.518917	0.003610	3.444441	0.507924	174.804236	3.180073
4.706	0.293858	0.515099	0.003329	3.299510	0.446468	178.892367	3.122792
5.214	0.287462	0.509424	0.003087	3.165366	0.394198	182.122589	3.079761
5.722	0.278622	0.501378	0.002871	3.036992	0.348156	184.750036	3.046161
6.230	0.266896	0.490269	0.002674	2.910086	0.306309	186.944166	3.019054

Table III.36 : Run 96

Mean distillation rate (gm/sec)		Distillate mole fraction (—)		Mean relative volatility (—)		Mean temperature (^{o}C)	
Theoretical	Experimental	Theoretical	Experimental	Theoretical	Experimental	Distilland	Surface
0.000567	0.000572	0.823033	0.822100	4.414221	3.998818	129.700000	108.721820
Radial position (cm)	Mass flow rate (gm/sec)	EHP mole fraction (—)	Film thickness (cm)	Mean velocity (cm/sec)	Reynolds number (—)	Surface temperature (^{o}C)	Relative volatility (—)
1.150	0.397500	0.523400	0.010684	5.631613	1.693854	48.500000	0.000000
1.658	0.397500	0.523400	0.008372	4.985062	1.174869	77.264974	5.552127
2.166	0.397499	0.523399	0.007005	4.560147	0.899320	93.346833	4.840357
2.674	0.397494	0.523395	0.006087	4.250852	0.728459	103.128792	4.501177
3.182	0.397479	0.523384	0.005421	4.011355	0.612140	109.553838	4.309297
3.690	0.397450	0.523361	0.004911	3.818024	0.527829	114.034093	4.188094
4.198	0.397402	0.523325	0.004506	3.657203	0.463900	117.305912	4.105539
4.706	0.397330	0.523270	0.004175	3.520353	0.413748	119.783452	4.046159
5.214	0.397230	0.523194	0.003899	3.401810	0.373343	121.714798	4.001657
5.722	0.397099	0.523096	0.003665	3.297640	0.340085	123.256461	3.967220
6.230	0.396933	0.522972	0.003462	3.205010	0.312224	124.511510	3.939878

Table III.37 : Run 98

Mean distillation rate (gm/sec)		Distillate mole fraction (—)		Mean relative volatility (—)		Mean temperature (°C)	
Theoretical	Experimental	Theoretical	Experimental	Theoretical	Experimental	Distilland	Surface
0.001339	0.001351	0.813228	0.811700	4.249275	3.754432	143.900000	117.816729
Radial position (cm)	Mass flow rate (gm/sec)	EHP mole fraction (—)	Film thickness (cm)	Mean velocity (cm/sec)	Reynolds number (—)	Surface temperature (°C)	Relative volatility (—)
1.150	0.401700	0.523400	0.011268	5.396087	1.474517	45.000000	0.000000
1.658	0.401700	0.523400	0.008829	4.776576	1.022735	79.113381	5.574424
2.166	0.401698	0.523399	0.007388	4.369431	0.782866	98.708492	4.731326
2.674	0.401690	0.523392	0.006420	4.073060	0.634125	110.766166	4.338589
3.182	0.401663	0.523371	0.005717	3.843540	0.532853	118.731855	4.119649
3.690	0.401603	0.523327	0.005179	3.658204	0.459427	124.304476	3.982717
4.198	0.401497	0.523249	0.004752	3.503948	0.403725	128.382247	3.890098
4.706	0.401331	0.523128	0.004403	3.372573	0.359995	131.474357	3.823820
5.214	0.401094	0.522957	0.004111	3.258636	0.324729	133.887297	3.774338
5.722	0.400773	0.522726	0.003863	3.158358	0.295663	135.815038	3.736158
6.230	0.400361	0.522431	0.003649	3.069015	0.271275	137.385587	3.705913

Table III.38 : Run 100

Mean distillation rate (gm/sec)		Distillate mole fraction (—)		Mean relative volatility (—)		Mean temperature (°C)	
Theoretical	Experimental	Theoretical	Experimental	Theoretical	Experimental	Distilland	Surface
0.006738	0.006782	0.794198	0.791000	3.832510	3.350440	168.300000	139.486107
Radial position (cm)	Mass flow rate (gm/sec)	EHP mole fraction (—)	Film thickness (cm)	Mean velocity (cm/sec)	Reynolds number (—)	Surface temperature (°C)	Relative volatility (—)
1.150	0.388300	0.523400	0.009613	6.114377	2.219238	56.500000	0.000000
1.658	0.388300	0.523400	0.007532	5.412400	1.539277	96.286592	5.051150
2.166	0.388292	0.523394	0.006303	4.951033	1.178243	118.386338	4.259141
2.674	0.388248	0.523360	0.005477	4.615071	0.954295	131.808744	3.902270
3.182	0.388111	0.523258	0.004876	4.354592	0.801659	140.622785	3.705897
3.690	0.387810	0.523039	0.004417	4.143746	0.690759	146.771145	3.583819
4.198	0.387274	0.522656	0.004051	3.967538	0.606332	151.264934	3.501489
4.706	0.386438	0.522062	0.003751	3.816558	0.539713	154.672250	3.442643
5.214	0.385243	0.521216	0.003500	3.684541	0.485621	157.333133	3.398715
5.722	0.383633	0.520081	0.003285	3.567126	0.440659	159.461969	3.364795
6.230	0.381562	0.518618	0.003098	3.461157	0.402542	161.199861	3.337887

Table III.39 : Run 102

Mean distillation rate (gm/sec)		Distillate mole fraction (—)		Mean relative volatility (—)		Mean temperature (°C)	
Theoretical	Experimental	Theoretical	Experimental	Theoretical	Experimental	Distilland	Surface
0.025736	0.024192	0.773815	0.761200	3.550900	2.911820	191.800000	158.246621
Radial position (cm)	Mass flow rate (gm/sec)	EHP mole fraction (—)	Film thickness (cm)	Mean velocity (cm/sec)	Reynolds number (—)	Surface temperature (°C)	Relative volatility (—)
1.150	0.383300	0.523400	0.009080	6.389469	2.565489	61.500000	0.000000
1.658	0.383299	0.523399	0.007115	5.655907	1.779437	107.953504	4.782859
2.166	0.383279	0.523383	0.005954	5.173722	1.362026	133.661178	3.967009
2.674	0.383136	0.523278	0.005173	4.822235	1.102862	149.262964	3.609967
3.182	0.382664	0.522940	0.004605	4.548732	0.925650	159.512523	3.416153
3.690	0.381592	0.522188	0.004168	4.325556	0.795979	166.673336	3.296500
4.198	0.379633	0.520833	0.003818	4.136423	0.696067	171.921969	3.216051
4.706	0.376511	0.518682	0.003528	3.970937	0.615822	175.918803	3.158562
5.214	0.371961	0.515538	0.003282	3.822024	0.549106	179.058816	3.115551
5.722	0.365730	0.511187	0.003067	3.684586	0.491974	181.591033	3.082188
6.230	0.357564	0.505376	0.002876	3.554728	0.441769	183.679632	3.055533

Table III.40 : Run 103

Mean distillation rate (gm/sec)		Distillate mole fraction (—)		Mean relative volatility (—)		Mean temperature (°C)	
Theoretical	Experimental	Theoretical	Experimental	Theoretical	Experimental	Distilland	Surface
0.077337	0.065736	0.746368	0.718300	3.345795	2.463864	212.500000	174.348362
Radial position (cm)	Mass flow rate (gm/sec)	EHP mole fraction (—)	Film thickness (cm)	Mean velocity (cm/sec)	Reynolds number (—)	Surface temperature (°C)	Relative volatility (—)
1.150	0.380000	0.523400	0.008753	6.571169	2.814874	65.000000	0.000000
1.658	0.379999	0.523399	0.006859	5.816744	1.952410	117.39813	4.591470
2.166	0.379952	0.523363	0.005739	5.320724	1.494319	146.379403	3.754950
2.674	0.379597	0.523107	0.004985	4.958321	1.209303	163.980184	3.397399
3.182	0.378357	0.522246	0.004435	4.673921	1.012920	175.566904	3.205323
3.690	0.375442	0.520263	0.004007	4.437309	0.866742	183.697527	3.087202
4.198	0.369973	0.516565	0.003659	4.229835	0.750760	189.702927	3.007695
4.706	0.361031	0.510459	0.003363	4.038729	0.653530	194.331463	2.950537
5.214	0.347630	0.501056	0.003102	3.854158	0.567962	198.033723	2.907273
5.722	0.328647	0.487074	0.002861	3.667256	0.489277	201.099724	2.873073
6.230	0.302663	0.466427	0.002630	3.468204	0.413852	203.731860	2.844930

Table III.41 : Run 105

Mean distillation rate (gm/sec)		Distillate mole fraction (—)		Mean relative volatility (—)		Mean temperature (°C)	
Theoretical	Experimental	Theoretical	Experimental	Theoretical	Experimental	Distilland	Surface
0.001264	0.001257	0.811814	0.810000	4.197100	3.714092	146.000000	119.734316
Radial position (cm)	Mass flow rate (gm/sec)	EHP mole fraction (—)	Film thickness (cm)	Mean velocity (cm/sec)	Reynolds number (—)	Surface temperature (°C)	Relative volatility (—)
1.150	0.537500	0.523400	0.011582	7.024662	2.431155	50.000000	0.000000
1.658	0.537500	0.523400	0.009075	6.218179	1.686265	81.339275	5.459561
2.166	0.537498	0.523399	0.007594	5.688156	1.290776	100.426878	4.679524
2.674	0.537490	0.523394	0.006599	5.302349	1.045541	112.433742	4.299367
3.182	0.537465	0.523380	0.005876	5.003592	0.878581	120.448282	4.083866
3.690	0.537409	0.523349	0.005324	4.762388	0.757549	126.086129	3.948055
4.198	0.537309	0.523295	0.004885	4.561691	0.665754	130.224900	3.855833
4.706	0.537153	0.523210	0.004526	4.390837	0.593715	133.369466	3.789694
5.214	0.536929	0.523089	0.004226	4.242747	0.535646	135.826421	3.740254
5.722	0.536626	0.522928	0.003972	4.112506	0.487816	137.790906	3.702078
6.230	0.536236	0.522720	0.003752	3.996574	0.447713	139.392205	3.671822

Table III.42 : Run 107

Mean distillation rate (gm/sec)		Distillate mole fraction (—)		Mean relative volatility (—)		Mean temperature (°C)	
Theoretical	Experimental	Theoretical	Experimental	Theoretical	Experimental	Distilland	Surface
0.003572	0.003362	0.799724	0.785300	3.963232	3.226498	163.000000	132.618640
Radial position (cm)	Mass flow rate (gm/sec)	EHP mole fraction (—)	Film thickness (cm)	Mean velocity (cm/sec)	Reynolds number (—)	Surface temperature (°C)	Relative volatility (—)
1.150	0.534800	0.523400	0.011204	7.224840	2.658324	52.500000	0.000000
1.658	0.534800	0.523400	0.008779	6.395374	1.843831	88.452908	5.278374
2.166	0.534797	0.523398	0.007346	5.850242	1.411383	110.381661	4.451741
2.674	0.534778	0.523387	0.006384	5.453404	1.143211	124.192738	4.058528
3.182	0.534714	0.523352	0.005685	5.146011	0.960584	133.419207	3.838474
3.690	0.534566	0.523273	0.005150	4.897662	0.828113	139.913615	3.700862
4.198	0.534295	0.523129	0.004724	4.690761	0.727534	144.683862	3.607883
4.706	0.533860	0.522902	0.004377	4.514284	0.648470	148.310342	3.541425
5.214	0.533225	0.522572	0.004086	4.360908	0.584593	151.145716	3.491859
5.722	0.532358	0.522124	0.003838	4.225540	0.531827	153.414524	3.453644
6.230	0.531228	0.521542	0.003624	4.104511	0.487425	155.265552	3.423386

Table III.43 : Run 108

Mean distillation rate (gm/sec)		Distillate mole fraction (—)		Mean relative volatility (—)		Mean temperature (^{o}C)	
Theoretical	Experimental	Theoretical	Experimental	Theoretical	Experimental	Distilland	Surface
0.005689	0.005417	0.793995	0.770200	3.862563	2.977124	170.900000	138.682369
Radial position (cm)	Mass flow rate (gm/sec)	EHP mole fraction (—)	Film thickness (cm)	Mean velocity (cm/sec)	Reynolds number (—)	Surface temperature (^{o}C)	Relative volatility (—)
1.150	0.533300	0.523400	0.011034	7.316066	2.768063	53.700000	0.000000
1.658	0.533300	0.523400	0.008646	6.476127	1.919946	91.819072	5.196225
2.166	0.533296	0.523397	0.007235	5.924107	1.469643	115.075609	4.351551
2.674	0.533267	0.523382	0.006286	5.522227	1.190381	129.728839	3.954154
3.182	0.533170	0.523329	0.005598	5.210840	1.000156	139.521073	3.733023
3.690	0.532942	0.523208	0.005071	4.959117	0.862097	146.415819	3.595198
4.198	0.532517	0.522986	0.004652	4.749159	0.757170	151.481887	3.502269
4.706	0.531829	0.522631	0.004309	4.569757	0.674563	155.334936	3.435933
5.214	0.530818	0.522114	0.004022	4.413446	0.607682	158.349106	3.386497
5.722	0.529428	0.521406	0.003777	4.275032	0.552282	160.762626	3.348396
6.230	0.527611	0.520482	0.003564	4.150766	0.505508	162.733351	3.318228

Table III.44 : Run 109

Mean distillation rate (gm/sec)		Distillate mole fraction (—)		Mean relative volatility (—)		Mean temperature (°C)	
Theoretical	Experimental	Theoretical	Experimental	Theoretical	Experimental	Distilland	Surface
0.026374	0.025052	0.772087	0.718100	3.560985	2.324593	199.300000	159.614963
Radial position (cm)	Mass flow rate (gm/sec)	EHP mole fraction (—)	Film thickness (cm)	Mean velocity (cm/sec)	Reynolds number (—)	Surface temperature (°C)	Relative volatility (—)
1.150	0.530000	0.523400	0.010687	7.506850	3.008930	56.300000	0.000000
1.658	0.530000	0.523400	0.008374	6.645007	2.087013	102.262591	4.973540
2.166	0.529988	0.523393	0.007007	6.078565	1.597504	130.569395	4.056734
2.674	0.529892	0.523342	0.006088	5.665964	1.293780	148.492589	3.640680
3.182	0.529522	0.523150	0.005421	5.345556	1.086469	160.507586	3.413579
3.690	0.528588	0.522679	0.004908	5.085050	0.935243	168.990922	3.273605
4.198	0.526754	0.521771	0.004498	4.865419	0.819218	175.244552	3.179826
4.706	0.523675	0.520262	0.004160	4.674499	0.726514	180.021015	3.113080
5.214	0.519012	0.517981	0.003874	4.504022	0.649891	183.778487	3.063346
5.722	0.512437	0.514753	0.003626	4.348064	0.584691	186.809081	3.024923
6.230	0.503626	0.510377	0.003406	4.202152	0.527781	189.306694	2.994351

Table III.45 : Run 110

Mean distillation rate (gm/sec)		Distillate mole fraction (—)		Mean relative volatility (—)		Mean temperature (^{o}C)	
Theoretical	Experimental	Theoretical	Experimental	Theoretical	Experimental	Distilland	Surface
0.047213	0.043436	0.761251	0.691600	3.441738	2.077490	210.200000	168.463283
Radial position (cm)	Mass flow rate (gm/sec)	EHP mole fraction (—)	Film thickness (cm)	Mean velocity (cm/sec)	Reynolds number (—)	Surface temperature (^{o}C)	Relative volatility (—)
1.150	0.527500	0.523400	0.010341	7.721494	3.290002	59.200000	0.000000
1.658	0.527500	0.523400	0.008103	6.835007	2.281966	107.994357	4.836975
2.166	0.527481	0.523389	0.006780	6.252339	1.746706	137.857680	3.923999
2.674	0.527317	0.523302	0.005891	5.827693	1.414432	156.726356	3.515138
3.182	0.526676	0.522976	0.005244	5.497193	1.187176	169.368554	3.293211
3.690	0.525048	0.522171	0.004746	5.226977	1.020573	178.300877	3.156752
4.198	0.521830	0.520604	0.004346	4.996762	0.891575	184.898450	3.065357
4.706	0.516392	0.517973	0.004013	4.793312	0.787044	189.954984	3.000216
5.214	0.508096	0.513943	0.003728	4.607352	0.698951	193.953534	2.951519
5.722	0.496291	0.508123	0.003477	4.431894	0.622100	197.202560	2.913698
6.230	0.480287	0.500019	0.003249	4.261187	0.552948	199.907987	2.883368

Table III.46 : Run 112

Mean distillation rate (gm/sec)		Distillate mole fraction (—)		Mean relative volatility (—)		Mean temperature (°C)	
Theoretical	Experimental	Theoretical	Experimental	Theoretical	Experimental	Distilland	Surface
0.001897	0.002004	0.915400	0.914500	4.220757	3.747175	143.500000	118.721426
Radial position (cm)	Mass flow rate (gm/sec)	EHP mole fraction (—)	Film thickness (cm)	Mean velocity (cm/sec)	Reynolds number (—)	Surface temperature (°C)	Relative volatility (—)
1.150	0.330800	0.734000	0.010638	4.635340	1.152495	47.000000	0.000000
1.658	0.330800	0.734000	0.008336	4.103168	0.799378	81.619526	5.477393
2.166	0.330797	0.733998	0.006975	3.753417	0.611892	100.656155	4.669131
2.674	0.330783	0.733990	0.006061	3.498804	0.495625	112.179668	4.299464
3.182	0.330740	0.733966	0.005397	3.301577	0.416446	119.734852	4.094272
3.690	0.330651	0.733915	0.004889	3.142246	0.359017	124.999295	3.966032
4.198	0.330495	0.733829	0.004486	3.009540	0.315424	128.842935	3.879260
4.706	0.330257	0.733697	0.004156	2.896404	0.281172	131.753722	3.817119
5.214	0.329921	0.733512	0.003880	2.798156	0.253519	134.023485	3.770687
5.722	0.329473	0.733266	0.003645	2.711543	0.230698	135.836152	3.734830
6.230	0.328903	0.732954	0.003442	2.634221	0.211520	137.312759	3.706399

Table III.47 ; Run 113

Mean distillation rate (gm/sec)		Distillate mole fraction (—)		Mean relative volatility (—)		Mean temperature (°C)	
Theoretical	Experimental	Theoretical	Experimental	Theoretical	Experimental	Distilland	Surface
0.003371	0.003539	0.912056	0.909300	4.065366	3.532511	152.000000	126.332698
Radial position (cm)	Mass flow rate (gm/sec)	EHP mole fraction (—)	Film thickness (cm)	Mean velocity (cm/sec)	Reynolds number (—)	Surface temperature (°C)	Relative volatility (—)
1.150	0.325800	0.734000	0.010010	4.851620	1.341742	51.300000	0.000000
1.658	0.325800	0.734000	0.007844	4.294617	0.930641	87.769378	5.282517
2.166	0.325795	0.733997	0.006563	3.928539	0.712364	107.618380	4.494511
2.674	0.325769	0.733982	0.005703	3.662003	0.576985	119.585642	4.137771
3.182	0.325694	0.733939	0.005078	3.455457	0.484758	127.417319	3.940550
3.690	0.325534	0.733850	0.004600	3.288460	0.417817	132.869651	3.817523
4.198	0.325258	0.733696	0.004220	3.149181	0.366945	136.849087	3.734353
4.706	0.324835	0.733462	0.003909	3.030209	0.326909	139.862681	3.674815
5.214	0.324237	0.733133	0.003648	2.926621	0.294515	142.213172	3.630329
5.722	0.323443	0.732696	0.003426	2.834994	0.267710	144.091138	3.595967
6.230	0.322429	0.732139	0.003234	2.752863	0.245111	145.621894	3.568710

Table III.48 : Run 115

Mean distillation rate (gm/sec)		Distillate mole fraction (—)		Mean relative volatility (—)		Mean temperature (^{o}C)	
Theoretical	Experimental	Theoretical	Experimental	Theoretical	Experimental	Distilland	Surface
0.009463	0.009275	0.905063	0.886900	3.866254	2.813833	170.5000000	139.113221
Radial position (cm)	Mass flow rate (gm/sec)	EHP mole fraction (—)	Film thickness (cm)	Mean velocity (cm/sec)	Reynolds number (—)	Surface temperature (^{o}C)	Relative volatility (—)
1.150	0.328700	0.734000	0.010337	4.740021	1.240226	49.000000	0.000000
1.658	0.328700	0.734000	0.008100	4.195831	0.860229	92.184326	5.232444
2.166	0.328692	0.733995	0.006778	3.838162	0.658461	116.148531	4.329965
2.674	0.328640	0.733966	0.005889	3.577664	0.533284	130.725259	3.933180
3.182	0.328467	0.733871	0.005244	3.375543	0.447910	140.310109	3.717378
3.690	0.328072	0.733657	0.004749	3.211643	0.385782	147.003991	3.584112
4.198	0.327348	0.733269	0.004354	3.074224	0.338350	151.902394	3.494600
4.706	0.326194	0.732654	0.004030	2.955886	0.300762	155.621672	3.430775
5.214	0.324514	0.731760	0.003757	2.851679	0.270061	158.531082	3.383188
5.722	0.322223	0.730536	0.003523	2.758136	0.244347	160.863577	3.346454
6.230	0.319237	0.728929	0.003319	2.672727	0.222343	162.772564	3.317296

Table III.49 : Run 116

Mean distillation rate (gm/sec)		Distillate mole fraction (—)		Mean relative volatility (—)		Mean temperature (^{o}C)	
Theoretical	Experimental	Theoretical	Experimental	Theoretical	Experimental	Distilland	Surface
0.028811	0.026218	0.895582	0.875300	3.654914	2.576930	191.400000	154.034191
Radial position (cm)	Mass flow rate (gm/sec)	EHP mole fraction (—)	Film thickness (cm)	Mean velocity (cm/sec)	Reynolds number (—)	Surface temperature (^{o}C)	Relative volatility (—)
1.150	0.329000	0.734000	0.010394	4.718203	1.222063	48.600000	0.000000
1.658	0.329000	0.734000	0.008145	4.176517	0.847630	98.546317	5.119684
2.166	0.328985	0.733992	0.006815	3.820469	0.648804	126.667355	4.134037
2.674	0.328868	0.733927	0.005922	3.560934	0.525358	143.892450	3.712828
3.182	0.328431	0.733694	0.005271	3.358860	0.440900	155.267772	3.487136
3.690	0.327366	0.733135	0.004770	3.193592	0.378968	163.242983	3.348922
4.198	0.325322	0.732072	0.004368	3.052817	0.331029	169.106148	3.256461
4.706	0.321942	0.730314	0.004034	2.928549	0.292228	173.585392	3.190574
5.214	0.316871	0.727646	0.003747	2.815233	0.259601	177.118362	3.141325
5.722	0.309747	0.723815	0.003495	2.708718	0.231236	179.982249	3.103083
6.230	0.300189	0.718492	0.003268	2.605630	0.205827	182.360963	3.072436

Table III.50 : Run 117

Mean distillation rate (gm/sec)		Distillate mole fraction (—)		Mean relative volatility (—)		Mean temperature (^{o}C)	
Theoretical	Experimental	Theoretical	Experimental	Theoretical	Experimental	Distilland	Surface
0.076495	0.069173	0.882197	0.837800	3.460024	1.984130	209.400000	168.312239
Radial position (cm)	Mass flow rate (gm/sec)	EHP mole fraction (—)	Film thickness (cm)	Mean velocity (cm/sec)	Reynolds number (—)	Surface temperature (^{o}C)	Relative volatility (—)
1.150	0.325000	0.734000	0.009856	4.915327	1.398729	52.500000	0.000000
1.658	0.324999	0.734000	0.007723	4.351009	0.970166	107.440999	4.905482
2.166	0.324968	0.733982	0.006462	3.980017	0.742559	138.199049	3.921574
2.674	0.324697	0.733835	0.005614	3.709052	0.600987	157.011739	3.509633
3.182	0.323659	0.733289	0.004994	3.496389	0.503426	169.447232	3.290723
3.690	0.321076	0.731951	0.004512	3.319082	0.430656	178.199311	3.156981
4.198	0.316033	0.729340	0.004119	3.162677	0.372598	184.683289	3.067300
4.706	0.307533	0.724850	0.003782	3.016967	0.323436	189.700846	3.002920
5.214	0.294445	0.717638	0.003482	2.873658	0.279500	193.738883	2.954133
5.722	0.275399	0.706338	0.003200	2.724555	0.238212	197.116563	2.915387
6.230	0.248505	0.688382	0.002922	2.559214	0.197422	200.068051	2.883171

Table III.51 : Run 118

Mean distillation rate (gm/sec)		Distillate mole fraction (—)		Mean relative volatility (—)		Mean temperature (°C)	
Theoretical	Experimental	Theoretical	Experimental	Theoretical	Experimental	Distilland	Surface
0.001560	0.001936	0.915543	0.917200	4.238248	3.869942	143.800000	117.998014
Radial position (cm)	Mass flow rate (gm/sec)	EHP mole fraction (—)	Film thickness (cm)	Mean velocity (cm/sec)	Reynolds number (—)	Surface temperature (°C)	Relative volatility (—)
1.150	0.428300	0.734000	0.011579	5.513908	1.498270	47.100000	0.000000
1.658	0.428300	0.734000	0.009073	4.880870	1.039210	79.976417	5.524685
2.166	0.428298	0.733999	0.007592	4.464834	0.795477	99.126487	4.714766
2.674	0.428287	0.733994	0.006597	4.161987	0.644338	110.982435	4.331491
3.182	0.428255	0.733980	0.005875	3.927444	0.541429	118.839547	4.116344
3.690	0.428184	0.733949	0.005322	3.738041	0.466814	124.346081	3.981298
4.198	0.428059	0.733895	0.004883	3.580386	0.410205	128.379947	3.889762
4.706	0.427865	0.733813	0.004524	3.446099	0.365759	131.440983	3.824171
5.214	0.427588	0.733695	0.004225	3.329617	0.329909	133.830878	3.775157
5.722	0.427217	0.733538	0.003969	3.227079	0.300359	135.740910	3.737315
6.230	0.426740	0.733336	0.003749	3.135701	0.275559	137.297470	3.707322

Table III.52 : Run 120

Mean distillation rate (gm/sec)		Distillate mole fraction (—)		Mean relative volatility (—)		Mean temperature (^{o}C)	
Theoretical	Experimental	Theoretical	Experimental	Theoretical	Experimental	Distilland	Surface
0.005035	0.005000	0.908436	0.899900	3.971771	3.186598	163.200000	132.674006
Radial position (cm)	Mass flow rate (gm/sec)	EHP mole fraction (—)	Film thickness (cm)	Mean velocity (cm/sec)	Reynolds number (—)	Surface temperature (^{o}C)	Relative volatility (—)
1.150	0.425000	0.734000	0.011218	5.647564	1.622386	49.300000	0.000000
1.658	0.425000	0.734000	0.008790	4.999181	1.125298	87.799541	5.329207
2.166	0.424996	0.733998	0.007355	4.573052	0.861369	110.336895	4.458102
2.674	0.424968	0.733986	0.006391	4.262808	0.697683	124.331413	4.057042
3.182	0.424876	0.733946	0.005691	4.022397	0.586173	133.622382	3.835161
3.690	0.424667	0.733857	0.005155	3.827996	0.505225	140.142075	3.697100
4.198	0.424282	0.733696	0.004729	3.665796	0.443686	144.923419	3.604044
4.706	0.423667	0.733440	0.004380	3.527133	0.395218	148.555777	3.537608
5.214	0.422773	0.733070	0.004088	3.406247	0.355958	151.395326	3.488079
5.722	0.421552	0.732565	0.003839	3.299124	0.323420	153.668059	3.449891
6.230	0.419965	0.731909	0.003622	3.202869	0.295930	155.523377	3.419642

Table III.53 : Run 122

Mean distillation rate (gm/sec)		Distillate mole fraction (—)		Mean relative volatility (—)		Mean temperature (°C)	
Theoretical	Experimental	Theoretical	Experimental	Theoretical	Experimental	Distilland	Surface
0.013020	0.012290	0.901780	0.893000	3.791457	2.988309	181.000000	144.799380
Radial position (cm)	Mass flow rate (gm/sec)	EHP mole fraction (—)	Film thickness (cm)	Mean velocity (cm/sec)	Reynolds number (—)	Surface temperature (°C)	Relative volatility (—)
1.150	0.426700	0.734000	0.011395	5.581787	1.560116	48.200000	0.000000
1.658	0.426700	0.734000	0.008929	4.940956	1.082107	92.071344	5.267196
2.166	0.426693	0.733997	0.007472	4.519782	0.828303	118.315992	4.305466
2.674	0.426640	0.733974	0.006492	4.213069	0.670861	134.773756	3.872267
3.182	0.426444	0.733892	0.005781	3.975138	0.563500	145.758295	3.635779
3.690	0.425961	0.733693	0.005235	3.782215	0.485373	153.493289	3.489873
4.198	0.425030	0.733315	0.004800	3.620407	0.425706	159.182179	3.392064
4.706	0.423488	0.732692	0.004443	3.480926	0.378374	163.516410	3.322461
5.214	0.421179	0.731763	0.004142	3.357868	0.339647	166.915584	3.270653
5.722	0.417956	0.730461	0.003883	3.247078	0.307125	169.646631	3.230709
6.230	0.413680	0.728719	0.003656	3.145505	0.279195	171.886351	3.199028

Table III.54 : Run 123

Mean distillation rate (gm/sec)		Distillate mole fraction (—)		Mean relative volatility (—)		Mean temperature (^{o}C)	
Theoretical	Experimental	Theoretical	Experimental	Theoretical	Experimental	Distilland	Surface
0.021829	0.020870	0.897653	0.889100	3.687067	2.898156	190.700000	151.988265
Radial position (cm)	Mass flow rate (gm/sec)	EHP mole fraction (—)	Film thickness (cm)	Mean velocity (cm/sec)	Reynolds number (—)	Surface temperature (^{o}C)	Relative volatility (—)
1.150	0.426200	0.734000	0.011257	5.643563	1.614382	49.100000	0.000000
1.658	0.426200	0.734000	0.008821	4.995639	1.119746	95.675906	5.185847
2.166	0.426190	0.733996	0.007381	4.569794	0.857109	123.639616	4.201504
2.674	0.426111	0.733962	0.006414	4.259597	0.694147	141.209747	3.763314
3.182	0.425802	0.733834	0.005710	4.018686	0.582906	152.952093	3.525563
3.690	0.425027	0.733519	0.005170	3.822771	0.501743	161.231178	3.379380
4.198	0.423508	0.732910	0.004738	3.657530	0.439450	167.329942	3.281552
4.706	0.420960	0.731894	0.004382	3.513805	0.389654	171.986545	3.211964
5.214	0.417102	0.730353	0.004080	3.385364	0.348468	175.649313	3.160124
5.722	0.411663	0.728159	0.003818	3.267731	0.313390	178.603694	3.120077
6.230	0.404371	0.725166	0.003586	3.157515	0.282737	181.039039	3.088208

Table III.55 : Run 124

Mean distillation rate (gm/sec)		Distillate mole fraction (—)		Mean relative volatility (—)		Mean temperature (°C)	
Theoretical	Experimental	Theoretical	Experimental	Theoretical	Experimental	Distilland	Surface
0.055820	0.052997	0.887944	0.880300	3.524279	2.747678	209.700000	164.975197
Radial position (cm)	Mass flow rate (gm/sec)	EHP mole fraction (—)	Film thickness (cm)	Mean velocity (cm/sec)	Reynolds number (—)	Surface temperature (°C)	Relative volatility (—)
1.150	0.426500	0.734000	0.011319	5.616867	1.590461	48.700000	0.000000
1.658	0.426500	0.734000	0.008869	4.972008	1.103154	100.504825	5.107715
2.166	0.426485	0.733993	0.007422	4.548156	0.844397	132.201471	4.053819
2.674	0.426331	0.733929	0.006448	4.239185	0.683735	152.293749	3.594203
3.182	0.425680	0.733666	0.005739	3.998357	0.573701	165.794255	3.347776
3.690	0.423940	0.732979	0.005193	3.800550	0.492697	175.359302	3.197263
4.198	0.420375	0.731584	0.004751	3.630379	0.429434	182.448061	3.096795
4.706	0.414178	0.729153	0.004381	3.477488	0.377431	187.906554	3.025234
5.214	0.404488	0.725284	0.004060	3.334253	0.332687	192.252217	2.971630
5.722	0.390358	0.719439	0.003771	3.194420	0.292561	195.818364	2.929782
6.230	0.370680	0.710818	0.003502	3.052045	0.255161	198.832042	2.895906

Table III.56 : Run 125

Mean distillation rate (gm/sec)		Distillate mole fraction (—)		Mean relative volatility (—)		Mean temperature (°C)	
Theoretical	Experimental	Theoretical	Experimental	Theoretical	Experimental	Distilland	Surface
0.001241	0.001924	0.915754	0.915900	4.247255	3.806823	143.800000	117.321715
Radial position (cm)	Mass flow rate (gm/sec)	EHP mole fraction (—)	Film thickness (cm)	Mean velocity (cm/sec)	Reynolds number (—)	Surface temperature (°C)	Relative volatility (—)
1.150	0.570500	0.734000	0.012359	6.881228	2.186260	49.400000	0.000000
1.658	0.570500	0.734000	0.009684	6.091211	1.516404	79.185978	5.521022
2.166	0.570499	0.733999	0.008103	5.572011	1.160754	97.925383	4.746124
2.674	0.570490	0.733997	0.007041	5.194084	0.940223	109.874101	4.359480
3.182	0.570466	0.733989	0.006270	4.901433	0.790084	117.904504	4.138313
3.690	0.570411	0.733971	0.005681	4.665167	0.681249	123.575191	3.998356
4.198	0.570314	0.733939	0.005212	4.468590	0.598709	127.747719	3.903121
4.706	0.570161	0.733890	0.004830	4.301254	0.533936	130.922630	3.834744
5.214	0.569940	0.733820	0.004510	4.156229	0.481728	133.405745	3.783599
5.722	0.569463	0.733725	0.004238	4.028699	0.438731	135.392500	3.744094
6.230	0.569259	0.733604	0.004004	3.915199	0.402685	137.012729	3.712779

Table III.57 : Run 126

Mean distillation rate (gm/sec)		Distillate mole fraction (—)		Mean relative volatility (—)		Mean temperature (°C)	
Theoretical	Experimental	Theoretical	Experimental	Theoretical	Experimental	Distilland	Surface
0.003789	0.003493	0.909051	0.908500	4.007700	3.493433	162.900000	130.791492
Radial position (cm)	Mass flow rate (gm/sec)	EHP mole fraction (—)	Film thickness (cm)	Mean velocity (cm/sec)	Reynolds number (—)	Surface temperature (°C)	Relative volatility (—)
1.150	0.569600	0.734000	0.012258	6.927004	2.233707	50.000000	0.000000
1.658	0.569600	0.734000	0.009605	6.131733	1.549314	84.892121	5.399236
2.166	0.569597	0.733999	0.008037	5.609075	1.185942	107.267958	4.537855
2.674	0.569579	0.733993	0.006984	5.228604	0.960609	121.662718	4.117844
3.182	0.569517	0.733973	0.006219	4.933899	0.807162	131.383196	3.881063
3.690	0.569369	0.733926	0.005634	4.695812	0.695860	138.266971	3.732656
4.198	0.569091	0.733839	0.005169	4.497465	0.611354	143.341912	3.632336
4.706	0.568636	0.733697	0.004788	4.328281	0.544924	147.209252	3.560645
5.214	0.567962	0.733489	0.004470	4.181231	0.491250	150.237869	3.507200
5.722	0.567032	0.733203	0.004199	4.051427	0.446904	152.664130	3.466015
6.230	0.565811	0.732828	0.003965	3.935343	0.409579	154.645346	3.433421

Table III.58 : Run 130

Mean distillation rate (gm/sec)		Distillate mole fraction (—)		Mean relative volatility (—)		Mean temperature (°C)	
Theoretical	Experimental	Theoretical	Experimental	Theoretical	Experimental	Distilland	Surface
0.013204	0.0131150	0.900692	0.899500	3.747291	3.187902	185.700000	147.330766
Radial position (cm)	Mass flow rate (gm/sec)	EHP mole fraction (—)	Film thickness (cm)	Mean velocity (cm/sec)	Reynolds number (—)	Surface temperature (°C)	Relative volatility (—)
1.150	0.566700	0.734000	0.011921	7.086365	2.403682	52.100000	0.000000
1.658	0.566700	0.734000	0.009341	6.272797	1.667210	92.806386	5.217083
2.166	0.566694	0.733998	0.007816	5.738105	1.276180	119.226413	4.289453
2.674	0.566647	0.733983	0.006792	5.348789	1.033649	136.328422	3.849278
3.182	0.566465	0.733925	0.006048	5.046954	0.868349	147.918830	3.604974
3.690	0.566002	0.733783	0.005477	4.802519	0.748193	156.147701	3.453317
4.198	0.565089	0.733505	0.005023	4.597939	0.656593	162.227934	3.351424
4.706	0.563548	0.733042	0.004651	4.422129	0.584118	166.872424	3.278879
5.214	0.561208	0.732341	0.004338	4.267656	0.525019	170.519800	3.224902
5.722	0.557908	0.731352	0.004069	4.129303	0.475594	173.451596	3.183325
6.230	0.553496	0.730023	0.003834	4.003260	0.433359	175.855396	3.150392

Table III.59 : Run 132

Mean distillation rate (gm/sec)		Distillate mole fraction (—)		Mean relative volatility (—)		Mean temperature (°C)	
Theoretical	Experimental	Theoretical	Experimental	Theoretical	Experimental	Distilland	Surface
0.026315	0.023720	0.895237	0.889700	3.623832	2.906965	199.700000	156.653692
Radial position (cm)	Mass flow rate (gm/sec)	EHP mole fraction (—)	Film thickness (cm)	Mean velocity (cm/sec)	Reynolds number (—)	Surface temperature (°C)	Relative volatility (—)
1.150	0.567000	0.734000	0.011952	7.071573	2.387398	51.900000	0.000000
1.658	0.567000	0.734000	0.009365	6.259704	1.655915	96.015012	5.166152
2.166	0.566992	0.733997	0.007837	5.726120	1.267529	125.167065	4.183431
2.674	0.566917	0.733973	0.006810	5.337528	1.026591	144.190997	3.723199
3.182	0.566601	0.733876	0.006063	5.035935	0.862218	157.142024	3.470038
3.690	0.565760	0.733622	0.005490	4.790963	0.742412	166.365708	3.313790
4.198	0.564036	0.733109	0.005033	4.584680	0.650584	173.200480	3.209180
4.706	0.561048	0.732228	0.004655	4.405586	0.577282	178.438079	3.134824
5.214	0.556413	0.730861	0.004336	4.245835	0.516733	182.567526	3.079499
5.722	0.549752	0.728884	0.004059	4.099781	0.465220	185.903573	3.036813
6.230	0.540685	0.726152	0.003814	3.963142	0.420238	188.656535	3.002888

Table III.60 : Run 133

Mean distillation rate (gm/sec)		Distillate mole fraction (—)		Mean relative volatility (—)		Mean temperature (°C)	
Theoretical	Experimental	Theoretical	Experimental	Theoretical	Experimental	Distilland	Surface
0.062445	0.059338	0.886644	0.870000	3.474662	2.482281	217.800000	168.883861
Radial position (cm)	Mass flow rate (gm/sec)	EHP mole fraction (—)	Film thickness (cm)	Mean velocity (cm/sec)	Reynolds number (—)	Surface temperature (°C)	Relative volatility (—)
1.150	0.566300	0.734000	0.011904	7.091660	2.410776	52.200000	0.000000
1.658	0.566300	0.734000	0.009327	6.277484	1.672130	100.530854	5.086711
2.166	0.566287	0.733996	0.007805	5.742369	1.279930	133.073942	4.047863
2.674	0.566150	0.733953	0.006782	5.352479	1.036521	154.496213	3.569344
3.182	0.565523	0.733763	0.006037	5.049112	0.870078	169.155805	3.308910
3.690	0.563750	0.733241	0.005464	4.800852	0.747942	179.642178	3.149186
4.198	0.559968	0.732142	0.005002	4.588511	0.653023	187.453030	3.042547
4.706	0.553197	0.730179	0.004617	4.399207	0.575488	193.481572	2.966707
5.214	0.542383	0.727008	0.004283	4.223542	0.509265	198.283181	2.910042
5.722	0.526375	0.722186	0.003986	4.053972	0.450356	202.218739	2.865952
6.230	0.503855	0.715082	0.003712	3.883627	0.395937	205.534305	2.830419

Table III.61 : Run 135

Mean distillation rate (gm/sec)		Distillate mole fraction (—)		Mean relative volatility (—)		Mean temperature (°C)	
Theoretical	Experimental	Theoretical	Experimental	Theoretical	Experimental	Distilland	Surface
0.001318	0.001286	0.973266	0.9730	4.331667	3.883076	135.400000	112.898533
Radial position (cm)	Mass flow rate (gm/sec)	EHP mole fraction (—)	Film thickness (cm)	Mean velocity (cm/sec)	Reynolds number (—)	Surface temperature (°C)	Relative volatility (—)
1.150	0.332000	0.901300	0.010875	4.496509	1.060853	47.500000	0.000000
1.658	0.332000	0.901300	0.008521	3.980276	0.735815	79.115798	5.523223
2.166	0.331998	0.901299	0.007131	3.641002	0.563237	96.461704	4.765683
2.674	0.331986	0.901297	0.006196	3.394023	0.456219	106.953023	4.413380
3.182	0.331954	0.901290	0.005518	3.202736	0.383347	113.828813	4.216084
3.690	0.331888	0.901275	0.004998	3.048249	0.330507	118.618706	4.092116
4.198	0.331777	0.901251	0.004586	2.919645	0.290415	122.115159	4.007939
4.706	0.331610	0.901214	0.004249	2.810092	0.258935	124.762456	3.947512
5.214	0.331377	0.901164	0.003967	2.715058	0.233543	126.826250	3.902283
5.722	0.331070	0.901097	0.003728	2.631396	0.212612	128.473950	3.867312
6.230	0.330682	0.901013	0.003521	2.556838	0.195047	129.815720	3.839561

Table III.62 : Run 137

Mean distillation rate (gm/sec)		Distillate mole fraction (—)		Mean relative volatility (—)		Mean temperature (°C)	
Theoretical	Experimental	Theoretical	Experimental	Theoretical	Experimental	Distilland	Surface
0.003620	0.003479	0.971229	0.970100	4.099904	3.514717	152.000000	125.169156
Radial position (cm)	Mass flow rate (gm/sec)	EHP mole fraction (—)	Film thickness (cm)	Mean velocity (cm/sec)	Reynolds number (—)	Surface temperature (°C)	Relative volatility (—)
1.150	0.331700	0.901300	0.010801	4.523193	1.080828	48.000000	0.000000
1.658	0.331700	0.901300	0.008463	4.003896	0.749669	85.036110	5.391368
2.166	0.331696	0.901299	0.007082	3.662601	0.573839	105.554542	4.555762
2.674	0.331670	0.901293	0.006154	3.414111	0.464788	118.024660	4.176805
3.182	0.331594	0.901277	0.005480	3.221548	0.390495	126.219028	3.967448
3.690	0.331429	0.901241	0.004964	3.065847	0.336568	131.937204	3.836996
4.198	0.331138	0.901179	0.004553	2.935969	0.295580	136.116710	3.748901
4.706	0.330687	0.901083	0.004218	2.824994	0.263314	139.284887	3.685893
5.214	0.330045	0.900946	0.003936	2.728327	0.237198	141.757689	3.638850
5.722	0.329184	0.900763	0.003697	2.642771	0.215576	143.734473	3.602533
6.230	0.328080	0.900528	0.003489	2.566019	0.197334	145.346536	3.573739

Table III.63 : Run 138

Mean distillation rate (gm/sec)		Distillate mole fraction (—)		Mean relative volatility (—)		Mean temperature (°C)	
Theoretical	Experimental	Theoretical	Experimental	Theoretical	Experimental	Distilland	Surface
0.010087	0.009613	0.968892	0.967200	3.875856	3.223354	169.900000	138.508396
Radial position (cm)	Mass flow rate (gm/sec)	EHP mole fraction (—)	Film thickness (cm)	Mean velocity (cm/sec)	Reynolds number (—)	Surface temperature (°C)	Relative volatility (—)
1.150	0.330500	0.901300	0.010637	4.576525	1.123578	49.100000	0.000000
1.658	0.330500	0.901300	0.008335	4.051105	0.779320	91.738884	5.241256
2.166	0.330491	0.901298	0.006974	3.705771	0.596529	115.550960	4.342856
2.674	0.330435	0.901286	0.006060	3.454244	0.483120	130.083914	3.945428
3.182	0.330249	0.901246	0.005395	3.259057	0.405762	139.658117	3.728694
3.690	0.329827	0.901156	0.004886	3.100733	0.349453	146.352357	3.594670
4.198	0.329054	0.900994	0.004480	2.967925	0.306446	151.254892	3.504575
4.706	0.327824	0.900737	0.004146	2.853475	0.272344	154.979537	3.440301
5.214	0.326035	0.900362	0.003865	2.752594	0.244468	157.894625	3.392359
5.722	0.323594	0.899849	0.003624	2.661923	0.221097	160.232790	3.355336
6.230	0.320413	0.899172	0.003413	2.579005	0.201072	162.147367	3.325938

Table III.64 : Run 139

Mean distillation rate (gm/sec)		Distillate mole fraction (—)		Mean relative volatility (—)		Mean temperature (°C)	
Theoretical	Experimental	Theoretical	Experimental	Theoretical	Experimental	Distilland	Surface
0.029642	0.027478	0.965769	0.959900	3.661948	2.674553	190.200000	153.258315
Radial position (cm)	Mass flow rate (gm/sec)	EHP mole fraction (—)	Film thickness (cm)	Mean velocity (cm/sec)	Reynolds number (—)	Surface temperature (°C)	Relative volatility (—)
1.150	0.330000	0.901300	0.010564	4.600969	1.143407	49.600000	0.000000
1.658	0.330000	0.901300	0.008278	4.072742	0.793074	98.548913	5.106631
2.166	0.329984	0.901296	0.006927	3.725535	0.607042	126.211513	4.139801
2.674	0.329857	0.901269	0.006018	3.472418	0.491529	143.197986	3.723131
3.182	0.329396	0.901172	0.005357	3.275292	0.412480	154.433101	3.498955
3.690	0.328284	0.900943	0.004848	3.113999	0.354494	162.317994	3.361352
4.198	0.326167	0.900508	0.004439	2.976528	0.309587	168.118905	3.269165
4.706	0.322684	0.899789	0.004098	2.855085	0.273219	172.553045	3.203409
5.214	0.317472	0.898699	0.003807	2.744241	0.242616	176.052135	3.154218
5.722	0.310163	0.897129	0.003551	2.639923	0.215987	178.889968	3.115997
6.230	0.300358	0.894938	0.003319	2.538795	0.192104	181.248486	3.085346

Table III.65 : Run 140

Mean distillation rate (gm/sec)		Distillate mole fraction (—)		Mean relative volatility (—)		Mean temperature (^{o}C)	
Theoretical	Experimental	Theoretical	Experimental	Theoretical	Experimental	Distilland	Surface
0.050645	0.045732	0.963646	0.957300	3.562487	2.554672	200.700000	160.822403
Radial position (cm)	Mass flow rate (gm/sec)	EHP mole fraction (—)	Film thickness (cm)	Mean velocity (cm/sec)	Reynolds number (—)	Surface temperature (^{o}C)	Relative volatility (—)
1.150	0.329700	0.901300	0.010508	4.621364	1.159735	50.000000	0.000000
1.658	0.329700	0.901300	0.008234	4.090796	0.804399	102.060486	5.037942
2.166	0.329678	0.901295	0.006890	3.742026	0.615699	131.643133	4.043087
2.674	0.329489	0.901255	0.005986	3.487570	0.498445	149.862352	3.619580
3.182	0.328773	0.901106	0.005327	3.288733	0.417959	161.940118	3.393108
3.690	0.327000	0.900744	0.004817	3.124667	0.358475	170.439692	3.254487
4.198	0.323555	0.900041	0.004405	2.982624	0.311777	176.718236	3.161642
4.706	0.317784	0.898849	0.004057	2.854016	0.273160	181.546795	3.095264
5.214	0.308991	0.896979	0.003754	2.732466	0.239724	185.391628	3.045348
5.722	0.296397	0.894167	0.003480	2.612595	0.209539	188.551689	3.006215
6.230	0.279055	0.889985	0.003222	2.489032	0.181192	191.231372	2.974377

Table III.66 : Run 142

Mean distillation rate (gm/sec)		Distillate mole fraction (—)		Mean relative volatility (—)		Mean temperature (°C)	
Theoretical	Experimental	Theoretical	Experimental	Theoretical	Experimental	Distilland	Surface
0.001411	0.001507	0.972786	0.9718	4.282966	3.717373	140.000000	115.457793
Radial position (cm)	Mass flow rate (gm/sec)	EHP mole fraction (—)	Film thickness (cm)	Mean velocity (cm/sec)	Reynolds number (—)	Surface temperature (°C)	Relative volatility (—)
1.150	0.433200	0.901300	0.011791	5.411325	1.417063	48.100000	0.000000
1.658	0.433200	0.901300	0.009239	4.790064	0.982885	79.307790	5.522906
2.166	0.433198	0.901300	0.007731	4.381768	0.752361	97.503255	4.748688
2.674	0.433187	0.901298	0.006718	4.084555	0.609415	108.776256	4.377988
3.182	0.433156	0.901292	0.005982	3.854382	0.512086	I16.250496	4.168600
3.690	0.433090	0.901281	0.005420	3.668517	0.441520	121.490211	4.036677
4.198	0.432974	0.901262	0.004973	3.513824	0.387988	125.329286	3.947041
4.706	0.432798	0.901233	0.004607	3.382084	0.345965	128.242791	3.882704
5.214	0.432548	0.901191	0.004302	3.267842	0.312077	130.517599	3.834570
5.722	0.432214	0.901136	0.004043	3.167309	0.284151	132.335650	3.797374
6.230	0.431789	0.901066	0.003818	3.077758	0.260725	133.817202	3.767874

Table III.67 : Run 143

Mean distillation rate (gm/sec)		Distillate mole fraction (—)		Mean relative volatility (—)		Mean temperature (°C)	
Theoretical	Experimental	Theoretical	Experimental	Theoretical	Experimental	Distilland	Surface
0.004956	0.004874	0.970194	0.967900	4.005376	3.272988	161.500000	130.883209
Radial position (cm)	Mass flow rate (gm/sec)	EHP mole fraction (—)	Film thickness (cm)	Mean velocity (cm/sec)	Reynolds number (—)	Surface temperature (°C)	Relative volatility (—)
1.150	0.432000	0.901300	0.011705	5.436274	1.440745	48.600000	0.000000
1.658	0.432000	0.901300	0.009171	4.812149	0.999310	86.200779	5.375431
2.166	0.431996	0.901299	0.007674	4.401963	0.764931	108.517998	4.502176
2.674	0.431969	0.901295	0.006669	4.103329	0.619572	122.464641	4.095857
3.182	0.431879	0.901280	0.005938	3.871922	0.520550	131.755312	3.870122
3.690	0.431673	0.901246	0.005379	3.684814	0.448673	138.287561	3.729391
4.198	0.431295	0.901185	0.004934	3.528716	0.394034	143.083844	3.634441
4.706	0.430691	0.901087	0.004570	3.395292	0.351006	146.730330	3.566619
5.214	0.429810	0.900945	0.004266	3.278998	0.316160	149.582346	3.516044
5.722	0.428608	0.900752	0.004005	3.175973	0.287285	151.865809	3.477044
6.230	0.427044	0.900500	0.003780	3.083430	0.262897	153.730288	3.446151

Table III.68 : Run 145

Mean distillation rate (gm/sec)		Distillate mole fraction (—)		Mean relative volatility (—)		Mean temperature (°C)	
Theoretical	Experimental	Theoretical	Experimental	Theoretical	Experimental	Distilland	Surface
0.013337	0.012924	0.967867	0.965000	3.790676	3.018529	179.400000	144.215925
Radial position (cm)	Mass flow rate (gm/sec)	EHP mole fraction (—)	Film thickness (cm)	Mean velocity (cm/sec)	Reynolds number (—)	Surface temperature (°C)	Relative volatility (—)
1.150	0.429700	0.901300	0.011407	5.548519	1.540043	50.500000	0.000000
1.658	0.429700	0.901300	0.008938	4.911507	1.068184	93.072595	5.213272
2.166	0.429692	0.901299	0.007479	4.492839	0.817644	118.514551	4.292672
2.674	0.429632	0.901289	0.006499	4.187933	0.662218	134.475827	3.873732
3.182	0.429418	0.901254	0.005786	3.951373	0.556219	145.134450	3.643716
3.690	0.428906	0.901171	0.005240	3.759526	0.479072	152.642990	3.501308
4.198	0.427933	0.901016	0.004805	3.598591	0.420145	158.166964	3.405623
4.706	0.426341	0.900764	0.004447	3.459842	0.373397	162.376414	3.337426
5.214	0.423976	0.900388	0.004145	3.337425	0.335148	165.678157	3.286605
5.722	0.420696	0.899865	0.003886	3.227216	0.303030	168.331106	3.247390
6.230	0.416363	0.899168	0.003659	3.126194	0.275454	170.506814	3.216268

Table III.69 : Run 146

Mean distillation rate (gm/sec)		Distillate mole fraction (—)		Mean relative volatility (—)		Mean temperature (°C)	
Theoretical	Experimental	Theoretical	Experimental	Theoretical	Experimental	Distilland	Surface
0.038665	0.036848	0.964690	0.960400	3.587938	2.712311	200.400000	159.051334
Radial position (cm)	Mass flow rate (gm/sec)	EHP mole fraction (—)	Film thickness (cm)	Mean velocity (cm/sec)	Reynolds number (—)	Surface temperature (°C)	Relative volatility (—)
1.150	0.428700	0.901300	0.011328	5.574281	1.565237	51.000000	0.000000
1.658	0.428700	0.901300	0.008876	4.934311	1.085658	99.392197	5.092913
2.166	0.428685	0.901297	0.007427	4.513675	0.831006	128.803012	4.103764
2.674	0.428555	0.901276	0.006453	4.207123	0.672929	147.408961	3.663997
3.182	0.428040	0.901194	0.005744	3.968548	0.564818	159.897686	3.425685
3.690	0.426725	0.900987	0.005199	3.773498	0.485563	168.734077	3.279244
4.198	0.424116	0.900580	0.004761	3.607317	0.424196	175.267565	3.181204
4.706	0.419690	0.899889	0.004396	3.460423	0.374456	180.278953	3.111346
5.214	0.412913	0.898816	0.004084	3.326081	0.332516	184.244513	3.059133
5.722	0.403230	0.897245	0.003808	3.199179	0.295889	187.469038	3.018584
6.230	0.390035	0.895016	0.003558	3.075452	0.262870	190.156567	2.986059

Table III.70 ; Run 147

Mean distillation rate (gm/sec)		Distillate mole fraction (—)		Mean relative volatility (—)		Mean temperature (°C)	
Theoretical	Experimental	Theoretical	Experimental	Theoretical	Experimental	Distilland	Surface
0.055495	0.051727	0.963287	0.958700	3.524915	2.628662	207.900000	164.178700
Radial position (cm)	Mass flow rate (gm/sec)	EHP mole fraction (—)	Film thickness (cm)	Mean velocity (cm/sec)	Reynolds number (—)	Surface temperature (°C)	Relative volatility (—)
1.150	0.428700	0.901300	0.011328	5.574281	1.565237	51.000000	0.000000
1.658	0.428700	0.901300	0.008876	4.934311	1.085658	101.371089	5.059300
2.166	0.428682	0.901297	0.007427	4.513664	0.831000	132.204398	4.046019
2.674	0.428514	0.901270	0.006453	4.206992	0.672866	151.777992	3.598868
3.182	0.427830	0.901161	0.005743	3.967900	0.564541	164.945567	3.357588
3.690	0.426041	0.900882	0.005196	3.771482	0.484786	174.282360	3.209658
4.198	0.422432	0.900323	0.004755	3.602537	0.422512	181.205282	3.110679
4.706	0.416223	0.899355	0.004384	3.450868	0.371363	186.536938	3.040072
5.214	0.406584	0.897820	0.004063	3.309001	0.327419	190.780952	2.987137
5.722	0.392603	0.895503	0.003774	3.170826	0.288092	194.261951	2.945797
6.230	0.373205	0.892083	0.003507	3.030565	0.251527	197.201082	2.912338

Table III.71 : Run 149

Mean distillation rate (gm/sec)		Distillate mole fraction (—)		Mean relative volatility (—)		Mean temperature (^{o}C)	
Theoretical	Experimental	Theoretical	Experimental	Theoretical	Experimental	Distilland	Surface
0.001162	0.001098	0.972788	0.972900	4.288563	3.865838	140.900000	115.082623
Radial position (cm)	Mass flow rate (gm/sec)	EHP mole fraction (—)	Film thickness (cm)	Mean velocity (cm/sec)	Reynolds number (—)	Surface temperature (^{o}C)	Relative volatility (—)
1.150	0.575200	0.901300	0.012666	6.688964	2.015694	49.900000	0.000000
1.658	0.575200	0.901300	0.009924	5.921021	1.398099	78.375466	5.530413
2.166	0.575198	0.901300	0.008305	5.416327	1.070195	96.374784	4.781114
2.674	0.575190	0.901299	0.007216	5.048960	0.866870	107.878624	4.402942
3.182	0.575166	0.901296	0.006426	4.764488	0.728445	115.620326	4.185337
3.690	0.575114	0.901289	0.005822	4.534830	0.628103	121.091512	4.047159
4.198	0.575021	0.901277	0.005342	4.343758	0.552008	125.119260	3.952928
4.706	0.574877	0.901259	0.004950	4.181122	0.492296	128.184998	3.885172
5.214	0.574671	0.901234	0.004622	4.040185	0.444173	130.583235	3.834439
5.722	0.574394	0.901199	0.004344	3.916269	0.404544	132.502342	3.795222
6.230	0.574038	0.901155	0.004103	3.806006	0.371327	134.067537	3.764117

Table III.72 : Run 151

Mean distillation rate (gm/sec)		Distillate mole fraction (—)		Mean relative volatility (—)		Mean temperature (°C)	
Theoretical	Experimental	Theoretical	Experimental	Theoretical	Experimental	Distilland	Surface
0.006283	0.006198	0.969267	0.967900	3.923770	3.272403	170.400000	135.877763
Radial position (cm)	Mass flow rate (gm/sec)	EHP mole fraction (—)	Film thickness (cm)	Mean velocity (cm/sec)	Reynolds number (—)	Surface temperature (°C)	Relative volatility (—)
1.150	0.574200	0.901300	0.012502	6.764877	2.088736	50.900000	0.000000
1.658	0.574200	0.901300	0.009796	5.988219	1.448761	87.032680	5.347032
2.166	0.574196	0.901299	0.008197	5.477790	1.108970	110.645634	4.466638
2.674	0.574169	0.901296	0.007123	5.106198	0.898249	125.976387	4.036505
3.182	0.574072	0.901284	0.006343	4.818298	0.754718	136.382030	3.794207
3.690	0.573837	0.901255	0.005746	4.585558	0.650550	143.774211	3.642520
4.198	0.573385	0.901201	0.005271	4.391432	0.571376	149.235661	3.540091
4.706	0.572639	0.901111	0.004882	4.225529	0.509034	153.404382	3.466951
5.214	0.571523	0.900978	0.004557	4.080929	0.458544	156.673637	3.412453
5.722	0.569970	0.900793	0.004279	3.952813	0.416699	159.296195	3.370465
6.230	0.567917	0.900548	0.004038	3.837695	0.381342	161.440638	3.337233

Table III.73 : Run 152

Mean distillation rate (gm/sec)		Distillate mole fraction (—)		Mean relative volatility (—)		Mean temperature (°C)	
Theoretical	Experimental	Theoretical	Experimental	Theoretical	Experimental	Distilland	Surface
0.010180	0.010000	0.968144	0.967200	3.824066	3.209577	179.500000	142.302804
Radial position (cm)	Mass flow rate (gm/sec)	EHP mole fraction (—)	Film thickness (cm)	Mean velocity (cm/sec)	Reynolds number (—)	Surface temperature (°C)	Relative volatility (—)
1.150	0.573300	0.901300	0.012404	6.807773	2.132064	51.500000	0.000000
1.658	0.573300	0.901300	0.009719	6.026190	1.478814	89.854746	5.285308
2.166	0.573295	0.901299	0.008133	5.512521	1.131972	115.116685	4.375097
2.674	0.573256	0.901294	0.007067	5.138538	0.916861	131.581111	3.934602
3.182	0.573111	0.901277	0.006293	4.848678	0.770291	142.780656	3.687928
3.690	0.572748	0.901233	0.005700	4.614127	0.663825	150.748421	3.534086
4.198	0.572037	0.901148	0.005228	4.418120	0.582770	156.642089	3.430457
4.706	0.570843	0.901006	0.004841	4.250094	0.518777	161.145920	3.356574
5.214	0.569038	0.900793	0.004517	4.102989	0.466752	164.682466	3.301567
5.722	0.566501	0.900493	0.004239	3.971867	0.423418	167.523631	3.259195
6.230	0.563120	0.900092	0.003997	3.853139	0.386571	169.850902	3.225649

Table III.74 : Run 154

Mean distillation rate (gm/sec)		Distillate mole fraction (—)		Mean relative volatility (—)		Mean temperature (°C)	
Theoretical	Experimental	Theoretical	Experimental	Theoretical	Experimental	Distilland	Surface
0.031576	0.030389	0.965087	0.963200	3.614358	2.891334	202.600000	157.749631
Radial position (cm)	Mass flow rate (gm/sec)	EHP mole fraction (—)	Film thickness (cm)	Mean velocity (cm/sec)	Reynolds number (—)	Surface temperature (°C)	Relative volatility (—)
1.150	0.573200	0.901300	0.012388	6.815295	2.139512	51.600000	0.000000
1.658	0.573200	0.901300	0.009707	6.032848	1.483980	95.277319	5.191526
2.166	0.573191	0.901299	0.008122	5.518600	1.135920	124.948612	4.194771
2.674	0.573109	0.901289	0.007058	5.144072	0.919987	144.565206	3.721706
3.182	0.572753	0.901246	0.006284	4.853305	0.772834	158.016877	3.460444
3.690	0.571784	0.901132	0.005690	4.616899	0.665138	167.640384	3.298986
4.198	0.569768	0.900898	0.005215	4.417404	0.582589	174.794210	3.190835
4.706	0.566233	0.900489	0.004822	4.243553	0.516476	180.290803	3.113932
5.214	0.560694	0.899847	0.004489	4.087585	0.461595	184.635543	3.056676
5.722	0.552659	0.898904	0.004199	3.943831	0.414587	188.155281	3.012452
6.230	0.541624	0.897581	0.003941	3.807896	0.373178	191.069788	2.977243

Table III.75 : Run 155

Mean distillation rate (gm/sec)		Distillate mole fraction (—)		Mean relative volatility (—)		Mean temperature (°C)	
Theoretical	Experimental	Theoretical	Experimental	Theoretical	Experimental	Distilland	Surface
0.052646	0.049556	0.963371	0.959200	3.523150	2.629796	213.600000	165.090054
Radial position (cm)	Mass flow rate (gm/sec)	EHP mole fraction (—)	Film thickness (cm)	Mean velocity (cm/sec)	Reynolds number (—)	Surface temperature (°C)	Relative volatility (—)
1.150	0.572800	0.901300	0.012325	6.845328	2.169436	52.000000	0.000000
1.658	0.572800	0.901300	0.009657	6.059433	1.504735	98.036019	5.139418
2.166	0.572789	0.901299	0.008081	5.542910	1.151801	129.685023	4.111663
2.674	0.572671	0.901284	0.007022	5.166626	0.932793	150.726978	3.628164
3.182	0.572137	0.901221	0.006251	4.874078	0.783143	165.204935	3.362716
3.690	0.570632	0.901046	0.005658	4.635207	0.673552	175.591538	3.199256
4.198	0.567426	0.900678	0.005182	4.431814	0.588719	183.337145	3.089940
4.706	0.561694	0.900020	0.004786	4.251823	0.519864	189.313848	3.012184
5.214	0.552553	0.898960	0.004446	3.086582	0.461577	194.066433	2.954154
5.722	0.539058	0.897357	0.004144	3.929359	0.410326	197.949344	2.909113
6.230	0.520154	0.895018	0.003869	3.774334	0.363651	201.203209	2.872965

TABLE III.76

Run No.	Mean distilland composition	Run No.	Mean distilland composition
42	0.111846	98	0.523164
44	0.110860	103	0.510976
45	0.110143	105	0.523235
46	0.106202	109	0.520468
47	0.097918	110	0.518234
50	0.111296	113	0.733540
52	0.108695	115	0.732802
55	0.098365	118	0.733838
59	0.111632	122	0.732795
62	0.108376	125	0.733904
64	0.317597	130	0.733104
67	0.314912	133	0.730081
70	0.298499	137	0.901112
74	0.316871	139	0.899879
77	0.311658	142	0.901242
82	0.317301	145	0.900810
84	0.316210	147	0.899355
86	0.310921	151	0.901127
89	0.523168	154	0.900501
94	0.515804	155	0.899993

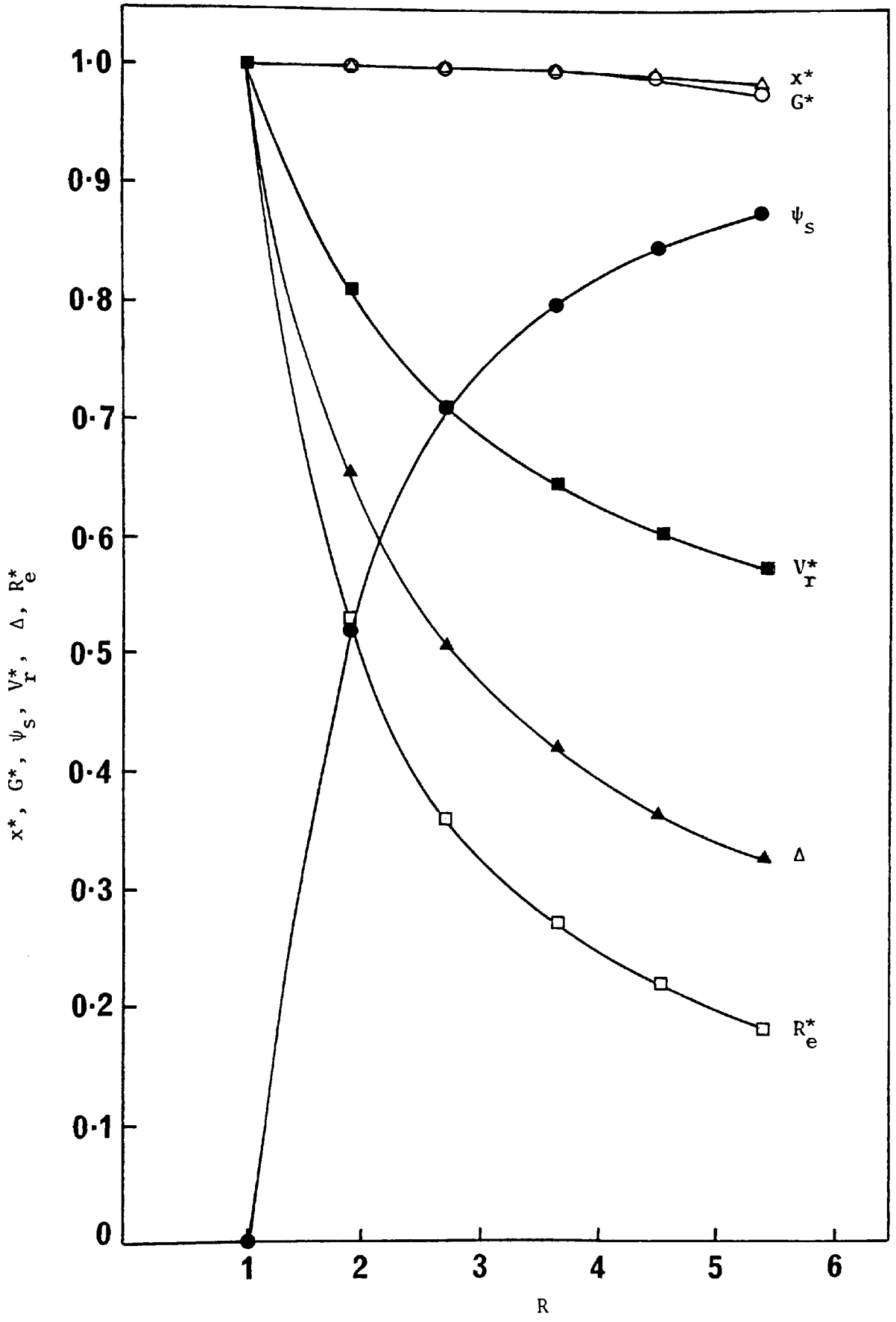

Figure III.1 : Normalized graph; Run No. 100